# Covariant Radiative Transfer in Dynamical Spacetime: a 5 Dimensional Formulation


**Yichao Hu**

University College London

Mullard Space Science Laboratory

Department of Space and Climate Physics


Submitted to University College London (UCL) in partial fulfilment of the requirements for the award of the degree of Doctor of Philosophy.

Principal supervisor: Prof Kinwah Wu

April 3, 2024

# Declaration

I, Yichao Hu, confirm that the work presented in this thesis is my own. Where information has been derived from other sources, I confirm that this has been indicated in the thesis.

# Abstract

We propose a novel approach for constructing a covariant formulation of radiative transfer in dynamical spacetimes, which overcomes limitations of previous methods when they are applied in the strong-field regime, by promoting the 3+1 numerical relativity (NR) decomposition via an embedding of a 4 dimensional spacetime into a 5 dimensional non-flat pseudo-Riemannian manifold. This new formulation uses a 4+1 approach: one is able to calculate, in a physically-consistent way, the null geodesics emitted from gravitational wave (GW) sources, e.g., from black hole and neutron star coalescence. Chapters 1–3 introduce the fundamental knowledge for this work and review previous studies of the general relativistic radiative transfer formulation in stationary spacetimes (e.g., Kerr). Chapter 4 introduces the level set method, which is applied to evolving the 4 dimensional spacetime (and null geodesics) in higher dimensional manifolds. Chapter 5 discusses the causal structure of a generic spacetime and studies the embedding of a 4 dimensional spacetime in a 5 dimensional flat and a non-flat manifold. We recover the Lorentz structure by choosing a specific isometric embedding and by defining an appropriately-chosen form of the 5 dimensional metric (e.g., the Schwarzschild and Oppenheimer-Snyder metrics). Chapter 6 discusses the embedding of the 3+1 numerical representation of the Kerr black hole and a 4 dimensional Brill-Lindquist spacetime. In Chapter 7, we present the proof that the isometric embedding of a 4 dimensional Lorentzian manifold in a 5 dimensional manifold with chosen metric, where the Lorentz structure is enforced, exists and is non-unique. Chapter 8 looks at the construction of a covariant radiative transfer formulation for a binary black hole system. We apply the embedding method for an equal mass non-spinning black hole merger using 3+1 numerical relativity and find the evolution equation of the geometric flow (spacetime flow). A summary of the work presented in this thesis, together with discussions and additional remarks, is presented in Chapter 9. Finally, directions for future work are presented in Chapter 10.

# Impact Statement

## Impact on general relativistic astrophysics

This article constructs mathematical applications of geometry and numerical computation to the astrophysical problem, and we also propose a theoretical foundation for calculation photons propagation in highly dynamical spacetime. Once the outcome is ready, researchers such as those in the EHT (Event Horizon Telescope) Consortium would be the first organisation that can apply the result and make more tests on the validation of general relativity in the strong field regime. Furthermore, the computation provides a reliable framework for the theoretical and observational studies of gravitational wave sources, especially those to be detected by LISA (Laser Interferometer Space Antenna).

## Impact on mathematical physics

The embedding of Lorentz structure studied in this thesis might be motivated the interest of mathematicians and mathematical physicists, although not completed yet. Further investigation can be dedicated to this area and complement the unfinished proof.

## Impact on a broader community

This article contributes to the human endeavour of formulating the physical world of our universe from the very beginning to its present time. It applies the general theory of relativity which proposed by A. Einstein more than 100 years ago, to the propagation of photons in the highly curved and dynamical spacetime. Once the full evolution of the light ray travelling through the intervening environment of dynamical spacetime, there would be more educational opportunities for undergraduate and postgraduate students to participate and conduct relevant research of gravitational waves in the future.

# Acknowledgements

I would like to express appreciation to my supervisor, Professor Kinwah Wu, who has dedicated a plenty of his time in supporting me with my research and scientific career. His constant help has a significant influence on my PhD study over the last few years.

I also want to thank Doctor Ziri Younsi and Professor Ignacio Ferreras, who provide a lot help and advice in my PhD research.

I would like to express my gratitude for Professor Martin Man-Chun Li and Doctor Lap-Ming Lin, who made my research visit at CUHK a fascinating trip. Their outstanding knowledge on geometry and relativity has an important influence on my thesis research.

I would like to thank my father, who continually support me throughout my entire postgraduate study, and the last 30 years. He means tremendously to me.

I appreciate, in particular, the love and help from my mother, Ms Jun Wu, who is not only a great mother but also a great woman for me. Her dedication to my life, study, research etc. is priceless and incomparable. Her persistence in her professional field has a considerable influence on me, which is one of the critical reasons that lead me to the world of science.

I want to thank my friends, Jennifer Chan, Ellis Owen, Joana Teixeira, Luke Pratley, Tom Kimpson, Kaye Li, Qin Han, Brian Yu and Paul Lai in Office 158, you made my research and life in MSSL a great journey.

Finally, I want to express my appreciation to a person who plays an important (maybe the most) role in my life, without you I won't achieve what I got now. And without you I won't become a better man. To you, I am forever indebted. Words cannot describe how much you means to me. Thanks.

# Preface

*"For every principle and methodology, it is essential to thoroughly understand the underlying reasons. Following its branches, tracing back to its origin and reaching its core. Not only should it encompass the culmination of astronomical knowledge, but also serve as the foundation for everything."*

*— Hsü Kuang-Ch'i (1562-1633), former Chinese scientist and politician, Introduction of Chongzhen Calendar.*

# Contents

# Table of Acronyms

| Notation | Description |
|---|---|
| aka | Also known as. |
| BBH | Binary Black Hole. |
| BH | Black Hole. |
| BNS | Binary Neutron Star. |
| CMC | Constant mean curvature. |
| CTS | Conformal thin sandwich. |
| CTT | Conformal transverse traceless. |
| DG | Differential geometry. |
| DOF | Degree of freedom. |
| EM | Electromagnetic. |
| ENO | Essentially non-oscillatory. |
| GR | General relativity. |
| GRRT | General relativistic radiative transfer. |
| GW | Gravitational wave. |
| HJ | Hanmilton-Jacobi. |
| iff | If and only if. |
| IMRI | Intermediate mass ratio inspiral. |
| MBH | Massive black hole. |
| NB | Nota bene. |
| NR | Numerical relativity. |
| NS | Neutron star. |
| ODE | Ordinary differential equation. |
| PDE | Partial differential equation. |
| QFT | Quantum field theory. |
| RK | Runge-Kutta. |
| SR | Special relativity. |
| TVD | Total variation diminishing. |
| wrt | With respect to. |
| XCTS | Extended conformal thin sandwich. |

# List of Figures

# List of Tables

# Chapter 1

# Introduction

We have found hundreds of events of the ripples of spacetime (i.e., gravitational wave) [1] since 2015. The covariant radiation transport formulation in stationary spacetime (e.g., Kerr) has also been constructed in the previous research [2], for which the radiative transfer equation is solved along the derived null geodesics, satisfying the invariance of particle number and the conservation of phase space density of the particles. Due to the recent detections of gravitational waves from a binary black hole (BBH) coalescence [1] and the receiving of both the electromagnetic (EM) and gravitational signals from a binary neutron star (BNS) merger [3], it is necessary to construct a covariant formulation of radiation transport in dynamical spacetime, which will benefit for a lot of scientific collaborations and consortium, e.g., the LISA and ngEHT [4, 5]. However, we encounter certain difficulties in generalizing the current covariant radiative transfer formulation in dynamical spacetime, there are 5 problems prohibit the progress: 3 numerical difficulties (time-symmetry problem, scattering problem and frame changing problem) and 2 physical difficulties (caustic problem and Lorentz structure problem). And in this research, we combine 2 mathematical frameworks, level set approach and embedding, to fix these drawbacks.

In general relativity (GR), spacetime is a four dimensional smooth pseudo-Riemannian manifold, consisting of events in the universe, cf., A for further information. The metric $g_{ab}$ of a spacetime is indefinite and symmetric between the two indices. This property leads to a consequence that all observers' and massive particles' motion are time-like, and all massless (e.g., photons) particles' motion are light-like (also known as (aka) null), and none could travel along a space-like worldline. The geometric structure of spacetime is governed by the Einstein (gravitational) equation. Roughly speaking, there exists two analogues of spacetime, called the stationary and the dynamical spacetimes, which are introduced in the following Chapter.

The trajectories of a free-falling particle (massless or massive) in curved spacetime are described by geodesics derived in a 4 dimensional manner via the Lagrangian formulation, i.e., using the geodesic equation

$$T^a \nabla_a T^b = 0\,, \tag{1.0.1}$$

where $T^a$ is the tangent to the curve and $\nabla_a$ is the Levi-Civita connection associated with the spacetime metric $g_{ab}$, satisfying $\nabla_a g_{bc} = 0$.

The geodesic equation can in general be solved numerically for analytical spacetimes with explicit metric function expressions, such as the Schwarzschild and Kerr spacetimes [2]. For a general dynamical spacetime, one could in principle apply the method of 3+1 numerical relativity to construct numerical spacetime metrics [6], by splitting the 4 dimensional spacetime into a family of 3 dimensional space-like hypersurfaces by virtue of a global scalar function $t$, to calculate an arbitrary geodesic numerically [7].

However, as was mentioned in the previous context, neither of these two methods is applicable to radiative transfer in dynamical spacetimes. On the one hand, explicit analytical metric functions are in general not available for solving equation (4.2.1) since there are no analytical solutions to the Einstein equation for most dynamical spacetimes, including binary black hole mergers. On the other hand, although numerical relativity has proven to be a powerful tool to obtain dynamical spacetime solutions to the Einstein equations, applying 3+1 methods to calculate (in particular, null) geodesics in dynamical spacetimes is physically problematic. First, the current radiative transfer equation is constructed with the affine parameter $\tau$ of the photon along the derived geodesic. In the 3+1 numerical relativity, spacetime is indexed with the coordinate time $t$ rather than the affine parameter $\tau$ and we need to convert from the coordinate frame to comoving frame pointwisely. In a desirable numerical algorithm, we need to overcome this inefficiency.

It is well-known that scattering is a non-local phenomenon [8]. The non-local nature of scattering problems, particularly their non-uniform and inhomogeneous properties, render the ray-tracing technique ill-suited to their solution. In dynamical spacetimes close to merger, the binary pair is in relativistic motion and both companions can orbit at a significant fraction of the speed of light. The effect of these relativistic motions convolved with the dispersive properties of the increasingly powerful gravitational waves being generated in-situ, give rise to a regime where emergent radiation is strongly scattered by the rapidly-varying and dynamical gravitational field therein. Consequently, ray-tracing is poorly suited to the solution of the radiative transfer equation in highly dynamical spacetimes.

Another example of studying null geodesics in numerical relativity is related to the method of finding the event horizon of a black hole (BH) in dynamical simulations (see [9] for a review). The event horizon is a global three dimensional hypersurface in spacetime which can be determined only in a post-processing analysis when the spacetime has settled down to a quasi stationary state, which is known as that the event horizon is teleological. Making use of the definition that the event horizon is the boundary of the causal past of future null infinity $\mathcal{J}^+$ (J), the event horizon can be found approximately from the numerically reconstructed 3+1 spacetime by integrating null geodesics backwards in time. While this reverse ray-tracing method has been demonstrated to work well for particular applications, it cannot be applied to ray-tracing for general radiative transfer problems. Furthermore, the key assumption underpinning the ray-tracing technique and subsequent observer-to-emitter approach is the condition of time symmetry of the spacetime (i.e., a time-like Killing field

exists). However, this assumption is invalid in a dynamical spacetime, which lacks of time-like Killing field and time-symmetry is violated, i.e., there is no time reversibility for a general relativistic radiative transfer formulation.

There are unphysical consequences which arise when using the 3+1 decomposition to calculate the transport of radiation within a 3+1 foliated spacetime. Whilst one can obtain a single null geodesic using the formulation given in [10], one encounters issues when considering bundles of photons, which define a definite (and invariant) phase space volume (Liouville's theorem). Such a consideration is integral to establishing a covariant formulation of radiative transfer, regardless of whether the spacetime is stationary or dynamical. Although this approach has the immediate advantage of simplifying the numerical calculations for the geodesics and subsequently the radiative transfer atop these geodesics, the reduction in dimensionality of the phase space (usually from 8D $\rightarrow$ 6D) will lead to the formation of caustic structures (pinching of the bundle's phase space volume) due to the projection of the "true" bundle into this artificial lower dimensional phase space [11, 12, 13]. As a consequence of this, the convergence and divergence of bundles of photons, i.e., the gravitational lensing and resulting focusing and de-focusing effects caused by the modulations of the highly dynamical spacetime geometry cannot be properly calculated. This is a fundamental physical limitation inherent to solving the radiative transfer problem in foliated spacetimes. This limitation is not to be conflated with the well-established principle of 3+1 foliation for the purposes of numerically evolving a dynamical spacetime.

Each ray is a null geodesic and its 4-momentum, $k^a$ with components $k^\mu$, must therefore satisfy the condition $k_\mu k^\mu = 0$, which is the vacuum dispersion relation of photons. Since the numerical 3+1 formalism foliates spacetime into a discrete series of spatial hypersurfaces, every point along the geodesic integration must necessarily interpolate for the metric parameters, e.g., the lapse function, shift vector, and 3 dimensional metric tensor, together with their corresponding spatial derivatives, between pairs of neighbouring foliations. This procedure introduces small secular errors in $k^\mu$, and therefore in $p_i(t)$, along a given geodesic. As the geodesic progressively samples the more strongly curved and dynamical gravitational field near both event horizons, this accumulated error grows rapidly. One could naively enforce $k_\mu k^\mu = 0$ by, for example, exploiting $k_t = -E$ (as is done in the 3+1 formulation of geodesic motion via the 6D Hamiltonian). However, in enforcing the null condition in this manner, one is essentially altering $k_\varphi = L_\mathrm{z}$ of the geodesic (itself a conserved quantity), thereby changing its trajectory by introducing a secular external force which drives its path away from a null geodesic to a timelike geodesic (i.e., causing artificial spatial dispersion). Conversely, since (in vacuum) null geodesic paths do not depend on the energy of the photon, one could instead fix the angular momentum ($p_\varphi$) of the geodesic and obtain a constraint equation for $k_t$ such that $k_\mu k^\mu = 0$, i.e., one could continually "correct" the energy of the geodesic to enforce the geodesic to be null. However, this approach would mean that the frequencies of photons would become increasingly erroneous as the rays evolve (i.e.,

causing artificial temporal dispersion). This destroys the solution of the radiative transfer equations and prohibits general relativistic radiative transfer (GRRT) calculations altogether.

In order to circumvent these aforementioned issues, a Hamilton-Jacobi (HJ) method is employed in this work, wherein a 4 dimensional spacetime is embedded into a generic 5 dimensional pseudo-Riemannian manifold, requiring that the 4 dimensional foliation evolves along an extra coordinate $w$ instead of the original temporal coordinate $t$ and the geodesic equation is solved using a new 4+1 formulation. This method is in part motivated by the level set approach [14, 15], where the essential steps are given as follows: (i) Embed the original 4 dimensional dynamical spacetime into a 5 dimensional spacetime, via a series of isometric embedding maps $\phi_w$ [16], (ii) construct the Hamilton-Jacobi equations and solve them numerically to carry out the evolution of 4 dimensional spacetime slices, and (iii) slicing all 4 dimensional spacetime foliations by light cones to calculate null geodesics which evolve along the additional fifth coordinate. This approach is shown to naturally maintains the causal structure of the 4 dimensional spacetime.

In this thesis, I will quickly discuss the basic knowledge of spacetime in general relativity in the second Chapter, the previous work on geodesics construction in stationary spacetime (Kerr black hole) and a covariant formulation of radiative transfer equation is briefly reviewed in the third Chapter. Firstly, the structure of a Kerr black hole along with ray-tracing in the background spacetime are introduced, and the GRRT equations for massless and massive particles propagating in Kerr spacetime are described in details. The level set method is introduced in Chapter 4 and will be used to reconstruct the 4 dimensional null geodesics in the 5 dimensional manifold in the fourth Chapter. In the next Chapter, I proposed the 4+1 formulation by embedding the 4 dimensional manifold in a 5 dimensional manifold. The isometric and conformal embeddings for a 4 dimensional manifold in a 5 dimensional flat or non-flat pseudo-Riemannian manifold are discussed. We will apply a non-flat 5 dimensional manifold for our problem, where the cases of embedding the Schwarzschild and Oppenheimer-Snyder spacetimes are demonstrated. The local Lorentz structure is maintained by choosing an appropriate metric form on the 5 dimensional manifold. In the sixth Chapter, I generalize the 4+1 method constructed in Chapter 5 to a 3+1 numerical representation of Kerr black hole and to a 4 dimensional fake evolution generated from the Brill-Lindquist initial data. It is shown that the 4+1 method can be generalized to any 3+1 numerical data. In Chapter 7, we provide a proof for the embedding process, which indicates that a 4 dimensional Lorentzian manifold can be isometrically embedded in a 5 dimensional manifold with a given metric form, where the Lorentz structure correlating two adjacent foliations is maintained. Finally, in Chapter 8, I investigate the application of the 4+1 formulation to a real numerical spacetime, where an equal mass, non-spinning binary black hole merger is considered. The 3+1 data is generated from the Einstein toolkit [17] and is embedded in a 5 dimensional manifold, where a 5 dimensional metric is given after the embedding. Chapter 9 and 10 conclude the whole thesis and discuss the future work.

# Chapter 2

# Foundations of Spacetime in General Relativity

## 2.1 Overview

We will review the foundations of general relativity and the background knowledge for this research in this Chapter. Relevant astrophysical detection is discussed. We also review the background knowledge for gravitational wave physics and compare with its electromagnetic counterpart. The recent reception for GW and EM radiations from the same source (binary neutron stars) are the dominant astrophysical motivations for this research.

Chapter 2 introduces the foundational knowledge and critical astrophysical motivations of the research.

## 2.2 Stationary Spacetime

We, throughout this work, adopt the natural unit system, in which $c = G = h = 1$, where $c$ is the speed of light, unless otherwise stated, and $G$ is the gravitational constant. Also, a $(-,+,+,+)$ signature is adopted for the metric tensor in the 4 dimensional spacetime manifold. Hereafter, we apply the convention of Penrose abstract index notation [18, 19], where the Latin letters $a\,,\ b\,,\ldots$ denote the coordinate-independent non-numerical indices of the tensors for all dimensional manifolds, and the Greek letters $\mu\,,\ \nu\,,\ldots$ denote the coordinate-dependent indices of tensors for all dimensional manifolds in this study.

A spacetime $(\mathcal{M}, g_{ab})$ is said to be stationary, if there exists a vector field $\xi^a$, which is a time-like Killing field when it is approaching the infinity, see appendices A and J for further reference. Assume $(\mathcal{M}, g_{ab})$ has such a vector field. Let the parameter of $\xi^a$'s integral curve be $t$, such that $\xi^a = (\partial/\partial t)^a$. In the adapted coordinate system $(t, x^i)$ of $\xi^a$, we have

$$\frac{\partial g_{\mu\nu}}{\partial t}|_{\text{inf}} = \mathcal{L}_\xi g_{\mu\nu} = 0\,, \tag{2.2.1}$$

which implies that components of $g_{ab}$ are independent of $t$, i.e., the metric is invariant under time translation, as the name 'stationary', and the index 'inf' denotes infinity, herein we denote the 3 dimensional coordinates by $x^i$.

| | Non-spinning ($J = 0$) | Spinning ($J \neq 0$) |
|---|---|---|
| Uncharged ($Q = 0$) | Schwarzschild | Kerr |
| Charged ($Q \neq 0$) | Reissner-Nordström | Kerr-Newman |

Table 2.1: Black Hole Category. These are the vacuum solutions to the Einstein equation. The black holes are parameterized by three physical quantities: the mass $M$, the spin $J$ and the electric charge $Q$.

Contrarily, if there exists a coordinate system $(t, x^i)$ in $(\mathcal{M}, g_{ab})$, such that

$$\frac{\partial g_{\mu\nu}}{\partial t}|_{\text{inf}} = 0\,, \tag{2.2.2}$$

and $(t, x^i)$ is adapted coordinate system to the time-like (at infinity) vector field $\xi^a \equiv (\partial/\partial t)^a$. Then

$$\mathcal{L}_\xi g_{ab}|_{\text{inf}} = 0\,, \tag{2.2.3}$$

indicating that $\xi^a$ is a time-like (at infinity) Killing vector field on $\mathcal{M}$, i.e., spacetime is stationary. Moreover, if (2.2.2) is true only in a local coordinate patch $\mathcal{O}$, then $(\mathcal{O}, g_{ab})$ is said to be stationary locally.

It should be noted that stationary is the intrinsic property of spacetime, which never changes under a coordinate transformation.

One example for stationary spacetime (also the first) was derived by Schwarzschild in 1916 [20], the metric is given by

$$\mathrm{d}s^2 = -\left(1 - \frac{2M}{r}\right)\mathrm{d}t^2 + \left(1 - \frac{2M}{r}\right)^{-1}\mathrm{d}r^2 + r^2(\mathrm{d}\theta^2 + \sin^2\theta\mathrm{d}\varphi^2)\,. \tag{2.2.4}$$

This is a spherically symmetric vacuum solution to Einstein equation. $M$ is the star mass, $(t, r, \theta, \varphi)$ are the Schwarzschild coordinates.

Later in 1965, Newman and his collaborators derived a new solution [21, 22], given as

$$\begin{aligned}\mathrm{d}s^2 = &-[1 - \widetilde{\Sigma}^{-1}(2Mr - Q^2)]\mathrm{d}t^2 + \widetilde{\Sigma}\Delta^{-1}\mathrm{d}r^2 + \widetilde{\Sigma}\mathrm{d}\theta^2 \\ &+ \widetilde{\Sigma}^{-1}[(r^2 + a^2)^2 - \Delta a^2\sin^2\theta]\sin^2\theta\mathrm{d}\varphi^2 \\ &- 2\widetilde{\Sigma}^{-1}a(2Mr - Q^2)\sin^2\theta\mathrm{d}t\mathrm{d}\varphi\,,\end{aligned} \tag{2.2.5}$$

where the explanation of the physical quantities ($M$, $\widetilde{\Sigma}$ and $\Delta$) are given in the next Chapter. This is an axisymmetrically (possessed by spinning stars) electromagnetic vacuum solution to the Einstein gravitational equation, generalizing the solution found by Kerr in 1963 by considering a charged star solution, which regards the Maxwell tensor $F_{ab}$ as the source of the energy-momentum tensor (Reissner-Nordström metric, a solution to the Einstein-Maxwell equation [23, 24, 25, 26]). These four related solutions are summarized in 2.1. In Chapter 3, we will investigate the structure of Kerr spacetime and derive the photons trajectories around a Kerr black hole.

All the above solutions are actually the spacetimes of black hole, for which spacetime singularities present and are enclosed within boundary regions, called the event horizons. The existence of such spacetime deficit predicted by general relativity was proven to be true first by Roger Penrose in the 1960s [27], and later by both Hawking [28, 29] and Penrose

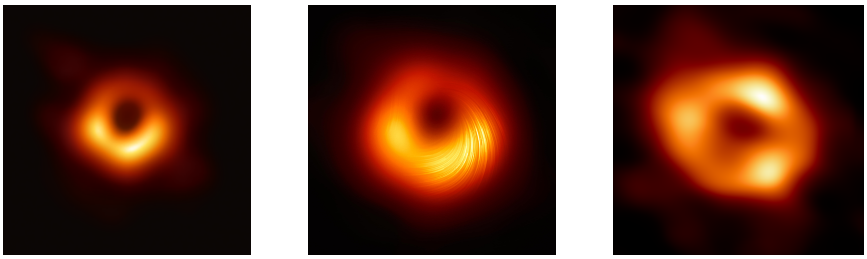

Figure 2.1: These are the figures of black hole imaged by EHT collaboration. The first on the left is the image of M87. The second in the middle show its polarization. The third on the right is the image of the black hole in the centre of the milky way (i.e., the Sgr A*).

in the 1970s [30, 31, 32]. In the year of 2019, the EHT collaboration pictured the first image of black hole [33, 34, 35, 36, 37, 38]. Following their first celebrated imaging, EHT has carried out more figures of black hole in 2021 [39, 40]. And in the year of 2022, the figure of the massive compact object locating in the centre of our galaxy, i.e., the Milky Way, was firstly brought to the world [41, 42, 43, 44, 45, 46], cf., Fig.2.1. An enhanced image of the 2019 black hole is pictured in [47]. The ngEHT will present more detailed and advanced figures in the future [5].

## 2.3 Dynamical Spacetime

Stationary spacetime is an ideal physical model, which is actually not common in the universe. It is more frequent to encounter dynamical spacetime, where the mathematical form of the metric is more complex and it is hardly possible to find an analytical solution for a highly dynamical spacetime due to the high-order and non-linear structure of the Einstein equation. Nevertheless, physicists have developed a powerful 3+1 numerical formalism of GR, which has been applied to various dynamical models, including the gravitational wave. Among them, binary stars (neutron star-neutron star (NS-NS), NS-BH, BH-BH) are fascinating and deeply studied systems.

Binary black hole mergers are primary targets for GW interferometers (e.g., LIGO) which has been and is currently constructed on the earth. According to GR, the orbit of a binary system decays in three phases due to the loss of energy and momentum carried away by gravitational waves [48, 49, 50]. By emitting gravitational radiations, two compact stars orbiting each other move closer and evolve into a quasi-circular inspiral phase, where post-Newtonian techniques are applied. Following the inspiral stage, two black holes meet in the plunge and merger phase, and the amplitude of gravitational waves peak at this time. It is proven that post-Newtonian and perturbation methods break down at this stage, the numerical relativity algorithms [51] must be employed. Eventually, two black holes coalesce into one compact object (a dynamical black hole), damping to a stable black hole by emitting less GW, which is called the ringdown phase.

Recent detected gravitational waves are very important hints for binary stars as instances of dynamical spacetime. Gravitational wave is one of the most exciting conclusions and the final prediction from the gen-

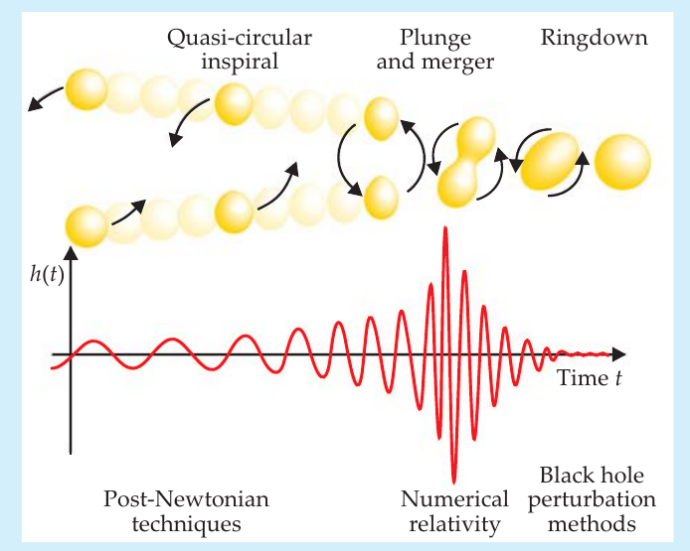


Figure 2.2: Three stages of two merging black holes with the corresponding gravitational wave magnitude shown below, from inspiral to ringdown phases. Credit: T. W. Baumgarte and S. L. Shapiro, 2011.

eral theory of relativity. These phenomena are considered as spacetime ripples have been detected from LIGO in 2015 and 2017, and by Virgo in 2017 [1, 52, 53, 54, 3, 55]. And more observations have been confirmed their existence by the subsequent detections of LIGO and Virgo, one of them unveils the existence of an intermediate-mass black hole ($10^2$ to $10^5$ $M_\odot$) which are formed from two smaller stellar-mass black holes [56, 57, 58, 59, 60]. They also detected gravitational wave signal emitted from a black hole and a neutron star (NS) coalescences, although this time there was no reception of EM radiation reported [61]. A most recent report on the GW event is given in [62]. Except the aforementioned LIGO and Virgo observatories, there are a series of advanced GW detectors, either ground-based or space-based, have been launched or in process, e.g., the GEO, KAGRA, Taiji, AIGO, TianQin, DECIGO, ET, LISA etc. [63, 64, 65, 66, 67, 68, 69, 70, 71, 72, 73, 74, 4], eagerly to reveal the mystery of the strong field characters and dynamical properties of gravitation.

In 1916, Albert Einstein found the wave solution to his gravitational field equation in the linearized weak-field limit [75, 76], cf., appendix E for detail. He believed that the amplitude of gravitational wave is remarkably small [77]. Nevertheless, it was a significantly controversial topic about the physical reality of gravitational waves until 1957 [78].

Also in 1916, Schwarzschild published his result for Einstein's equation [20], later in 1963 Kerr generalized this solution [79] to include spinning effect. Currently, it enables physicists to model the binary black hole evolution and its accurate waveforms, due to the breakthrough in both analytical and numerical studies of GR in the past four decades [80, 81, 82, 83, 84, 85, 86, 87].

The detection of gravitational waves began with Weber and his resonant mass detectors in the 1960s [88]. Later the interferometer detectors were suggested in the 1960s [89] and in the 1970s [90] (this idea was also considered by Weiss). By the early 2000s, a series detectors, including LIGO and Virgo were completed and started their work. In 2015, the

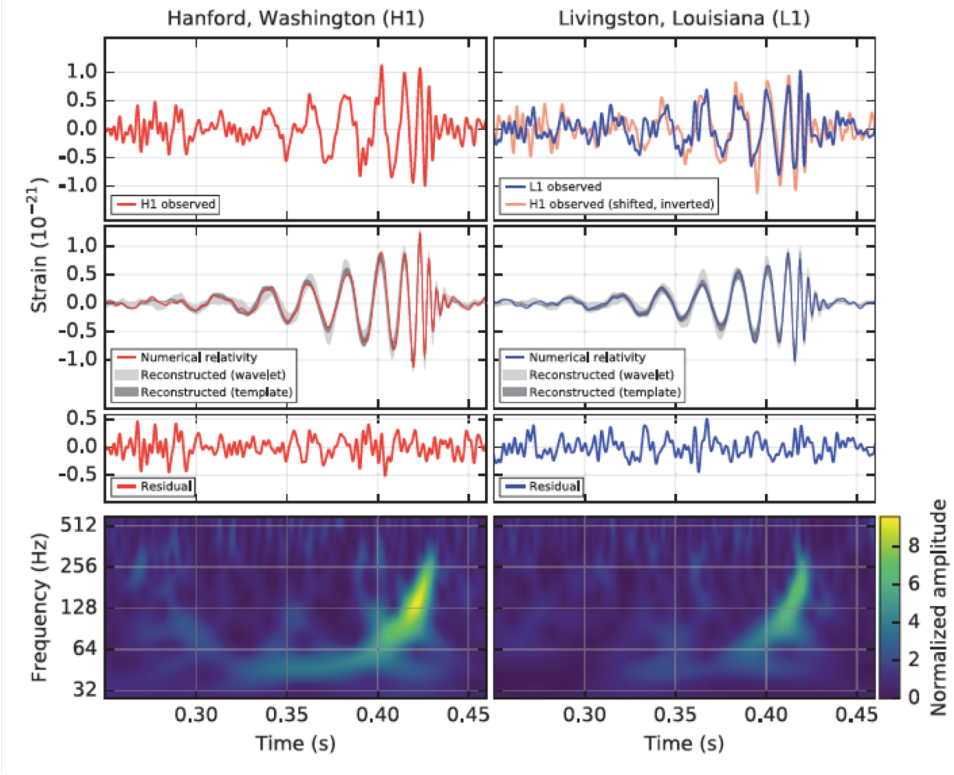


Figure 2.3: The first GW event, GW150914 detected by the LIGO in Hanford (H1, left panels) and the LIGO in Livingston (L1, right panels). Credit: B. P. Abbot et al., 2016.

advanced LIGO was initiated and eventually detected the gravitational radiation signals from two merging black holes after a century since the prediction of Einstein [91, 92, 93, 66]. Future space-based detector, e.g., LISA, is under construction and part of them will be launched during the 2030s to start their work [94, 95]. The emerging research area brings a fruitful results in developing relevant studies, including the detection of primordial gravitational waves, the multi-messenger astronomy and the gravitational wave cosmology [96, 97, 98].

As was first proposed by Henri Poincaré in 1905 [99] and subsequently by Einstein in 1916 from the GR, gravitational waves were once believed to be the oscillation of coordinate systems [100]. Bondi and other physicists then proved in a coordinate-independent way that these waveforms are not the behaviour of coordinates and do carry energy [101]. Whereas it is distortion of the fabric of spacetime (i.e., metric) and caused by the changes of shape and position of massive bodies (or energy). GWs, moving at the speed of light, take away energy and momentum from the source objects. It is then natural to compare GWs with electromagnetic waves which propagate at the same speed. Nevertheless, these two physical phenomena are very different. Electromagnetic waves are propagation of oscillations of electromagnetic fields in the background spacetime, whereas GWs are ripples of spacetime, i.e., spacetime itself. In addition, EM waves experience strong absorption and scattering while GWs have essentially not affected by these processes.

Furthermore, the quantum properties of GW and EM waves are different. The fundamental gauge particles (hypothetical) that mediate

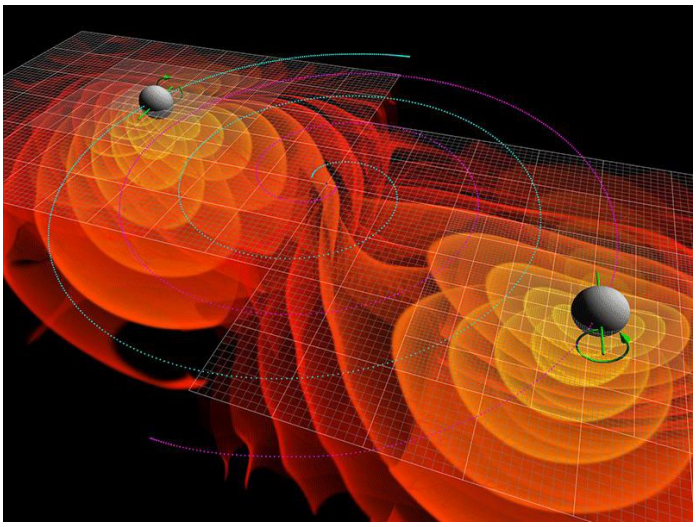

Figure 2.4: Two coalescing black holes, strongly warp the surrounding spacetime dynamically. Credit: NASA/Ames Research Center/C. Henze.

gravity are gravitons, possessing spin 2. While those for EM radiation are photons with spin 1. The dominating term is quadrapolar in GW, whereas it is dipole term in EM wave. Hence the GW is weaker than EM radiation with similar conditions. It is widely acknowledged that the strong gravitational radiations are normally generated in fierce astrophysical activities, such as the coalescence of two black holes, merging neutron stars, and the events during the formation of early universe, e.g., the inflation [102, 103].

One of the simplest GW solutions is derived in the limit of linearized gravity, where the field equation becomes

$$\partial^c \partial_c \gamma_{ab} = 0\,. \tag{2.3.1}$$

Solve this equation under the radiation gauge, yields

$$\gamma_{ab} = H_{ab} \cos(K_\mu x^\mu)\,, \tag{2.3.2}$$

where $H_{ab}$ is a symmetric constant field, satisfying $\partial_c H_{ab} = 0$, called the amplitude. This is the plane-wave solution of GR. $K^\mu$ denotes components of the constant 4 dimensional wavevector, such that

$$K^\mu K_\mu = 0\,, \tag{2.3.3}$$

which implies that $K^a$ is a null vector field, i.e., the wave speed is the speed of light. Rewrite $K^a$ in a 3+1 form as $K^a = \omega(\partial/\partial t)^a + \vec{K}^a$, it follows that

$$\omega^2 = \vec{K}^a \vec{K}_a = \vec{K}^2\,, \tag{2.3.4}$$

where $\omega$ represents for angular frequency and $\vec{K}^a$ for 3 dimensional wavevector. Equation (2.3.1) together with Lorentz condition yield

$$H_{\mu\nu} K^\nu = 0\,, \tag{2.3.5}$$

which implies that the propagation direction of GW is orthogonal to $H_{ab}$.

## 2.4 Electromagnetic Counterparts of Gravitational Wave

Apart from GW, the detection of its electromagnetic counterpart has brought a new observational area for the multi-messenger astronomy [104].

On the one hand, upon the completion of previous general relativistic radiative transfer formalism in stationary Kerr spacetime, it is necessary to generalize the current formulation to a covariant formulation in dynamical spacetime upon the detection of GW, particular the signals detected by LIGO and Virgo in 2017 from two coalescing neutron stars, for which can be the source of the EM radiation[1]. The 2017 detection is the first time that a gravitational wave source was confirmed by a non-gravitational signal, which is just 1.7 seconds later than the reception of the GW radiation [105, 106, 107]. On the other hand, the research of gravitational waves has not developed enough at the time, it is difficult for astrophysicists to study the properties of the source stars from the information carried by GW. Nevertheless, one can study its electromagnetic counterpart to fill the gap, hence a covariant formulation of radiative transfer may help us to understand various astrophysical phenomena via multi-messenger astronomy [108].

Accordingly, the next task is to reformulate the covariant formulation of radiative transfer in a dynamical spacetime, which is the work I am currently doing. Consider the case of the dynamical spacetime, more specifically, I will investigate the covariant radiative transfer formulation in a binary black hole merger system.

[1] In principle, one of the two compact stars must be a neutron star which can be a source of the EM signals, provided the quantum effect is negligible.

# Chapter 3

# General Relativistic Radiative Transfer in Kerr Spacetime

## 3.1 Overview

The construction of general relativistic radiative transfer formulation in Kerr spacetime has been carried out in the previous research by several people [2, 107, 109]. The covariant formulation of radiation transport is the key framework for either a stationary astrophysical context or a highly dynamical one. The violation of the covariance in the conventional approach largely motivates the embedding level set method. In this Chapter, I review the previous covariant formulation of radiative transfer, based on the Kerr spacetime. It gives the basic idea that how one constructs a covariant formalism for the radiative transfer in a black hole spacetime from the first principle and calculate the radiation transport equation. Furthermore, the ray-tracing in Kerr spacetime is discussed in details. Nevertheless, for a dynamical case the calculation algorithm needs considerable modification and a new numerical method which can be applied is introduced in the next Chapter.

In this Chapter, I derive the trajectories of photons and code it to make geodesics plots, using Runge-Kutta (RK, Cash-Karp) method. The results are given in section 3.3, where two figures are given therein and illustrate the null geodesics propagating in the Kerr spacetime.

## 3.2 The Structure of Kerr Spacetime

It is widely acknowledged that all astrophysical stellar objects undergoing gravitational collapse evolves to black holes, when their masses satisfy certain condition (reach the Tolman-Oppenheimer-Volkoff limit) [110, 111]. The first exact solution to the Einstein equation derived by Schwarzschild in 1916 describes the properties of a spherically symmetric stationary black hole (Schwarzschild black hole). Later, in 1963, Kerr assumed that the collapsed star possesses another parameter, the angular momentum $J$, inherited form its progenitor, in which case the spacetime of the compact object is stationary as the Schwarzschild metric. However, it is axisymmetric instead of spherically symmetric. Due to the 'no-hair conjecture', an astrophysical black hole can be wholly characterized by three

parameters, its mass, spin angular momentum and charge. Nevertheless, a charged black hole can be neutralized by the surrounding medium and accretion flow. An uncharged spinning black hole (Kerr black hole) is therefore assumed throughout this thesis.

The Kerr solution of the Einstein equation written in the Boyer-Lindquist coordinate system is given by

$$\mathrm{d}s^2 = g_{tt}\mathrm{d}t^2 + 2g_{t\varphi}\mathrm{d}t\mathrm{d}\varphi + g_{rr}\mathrm{d}r^2 + g_{\theta\theta}\mathrm{d}\theta^2 + g_{\varphi\varphi}\mathrm{d}\varphi^2\,, \tag{3.2.1}$$

where the coefficients of the metric are given by

$$g_{tt} = -\left(1 - \frac{2Mr}{\tilde{\Sigma}}\right)\,, \tag{3.2.2}$$

$$g_{t\varphi} = -\frac{2aMr\sin^2\theta}{\tilde{\Sigma}}\,, \tag{3.2.3}$$

$$g_{rr} = \frac{\tilde{\Sigma}}{\Delta}\,, \tag{3.2.4}$$

$$g_{\theta\theta} = \tilde{\Sigma}\,, \tag{3.2.5}$$

$$g_{\varphi\varphi} = \frac{\sin^2\theta}{\tilde{\Sigma}}[(r^2+a^2)^2 - \tilde{\Sigma}a^2\sin^2\theta]\,, \tag{3.2.6}$$

and

$$\tilde{\Sigma} = r^2 + a^2\cos^2\theta\,, \tag{3.2.7}$$

$$a = \frac{J}{M}\,, \tag{3.2.8}$$

$$\Delta = r^2 - 2Mr + a^2\,, \tag{3.2.9}$$

where $(\theta, \varphi)$ are spherical polar zenith and azimuthal coordinates, $r$ is modified radial coordinate, $M$ and $J$ are mass and total spin angular momentum of the black hole respectively, $a$ is defined as the spin parameter. Note that the components $g_{\mu\nu}$ which do not depend on $t$ and $\varphi$ implies that the metric is stationary and axisymmetric. It reduces to the Schwarzschild metric when $a = 0$. The transformation between a Cartesian coordinate and the Boyer-Lindquist coordinate is given by

$$x = \sqrt{r^2+a^2}\sin\theta\cos\varphi\,, \tag{3.2.10}$$

$$y = \sqrt{r^2+a^2}\sin\theta\sin\varphi\,, \tag{3.2.11}$$

$$z = r\cos\theta\,. \tag{3.2.12}$$

By observing equations (3.2.2)-(3.2.6), it is clear that there exist two singularities for Kerr metric, one at $\tilde{\Sigma} = 0$ and the other at $\Delta = 0$. Changing from Boyer-Lindquist coordinate system to the Cartesian coordinate, the $\tilde{\Sigma} = 0$ singularity becomes a ring of radius $a$, located in the equatorial plane of the black hole. The $\Delta = 0$ singularity leads to $(r - r_+)(r - r_-) = 0$, where

$$r_\pm = M \pm \sqrt{M^2 - a^2}\,, \tag{3.2.13}$$

which results in two singularity regions, one is at $r_+$, corresponding to 'Event Horizon' of the black hole, the other is at $r_-$, corresponding to

'Cauchy Horizon'. The Cauchy Horizon has physical significant and a mathematical resultant, and is hidden inside Event Horizon as $r_- < r_+$. The existence of a Cauchy Horizon implies that the global causality breaks down, for which the events beyond the Horizon are unpredictable, i.e., there is no Cauchy surface. The Event Horizon is a 3 dimensional null hypersurface, from which photons cannot escape but maintain effective stationary motion on the surface. Any particle, massless or massive, passing through $r = r_+$ falls along geodesic with decreasing $r$, which indicates that all objects passing the surface will never escape, hence the name 'Event Horizon'. This region can be treated as the boundary of the black hole. Note that the Event Horizon reduces to $r = 2M$ when $a = 0$, which is the Event horizon of a Schwarzschild black hole. It is assumed that a 'naked singularity', a singularity without an Event Horizon, is not allowed in general relativity due to the weak Cosmic Censorship hypothesis (Penrose 1969). Correspondingly, the magnitude of $a$ is required to be less than 1.

In general relativity, there are two types of singularities, one is the spacetime singularity (aka true singularity, physical singularity), the other is the coordinate singularity. A spacetime singularity is one which cannot be eliminated by coordinate transformation, whereas a coordinate singularity can be removed by appropriate coordinate transformation. In the case of a Kerr black hole, the ring singularity at $\tilde{\Sigma} = 0$ is a true singularity at which there is a scalar polynomial curvature singularity[2] . The Event Horizon, as well as the Cauchy Horizon, can be removed by changing to the Kerr-Schild (1963) coordinate system from the Boyer-Lindquist coordinate, given by

$$\begin{aligned} \mathrm{d}t' &= \mathrm{d}t \pm \frac{r^2 + a^2}{\Delta}\mathrm{d}r\,, \\ \mathrm{d}\varphi' &= \mathrm{d}\varphi \pm \frac{a}{\Delta}\mathrm{d}r\,. \end{aligned} \tag{3.2.14}$$

Another region of physical interest of the Kerr black hole is called the ergo region. In order to define the region, one must introduce a new concept, the 'Static Limit', which is obtained by solving $g_{tt} = 0$, yielding

$$r_{SL\pm} = M \pm \sqrt{M^2 - a^2\cos^2\theta}\,. \tag{3.2.15}$$

The ergo region is bounded by the Event Horizon and $r = r_{SL+}$ Static Limit. Note that the Schwarzschild black hole has no ergo region since the Event Horizon and the Static Limit coincide when $a = 0$. $r_{SL-}$ is called the 'inner Static Limit'. It is clear that $g_{tt}$ changes sign as follows

$$\begin{aligned} &r > r_{SL+}\,,\ g_{tt} < 0\,, \\ &r_{SL-} < r < r_{SL+}\,,\ g_{tt} > 0\,, \\ &r < r_{SL-}\,,\ g_{tt} < 0\,. \end{aligned}$$

A static observer's worldline is defined as a time-like geodesic with a 4 dimensional velocity proportional to $U^\mu = (1, 0, 0, 0)$. This is precisely a time-like vector when $r > r_{SL+}$ due to $g_{\mu\nu}U^\mu U^\nu < 0$. However, when

[2] A Kretschmann scalar singularity is defined as $R_{[\mathrm{cs}]} = R^{\mu\nu\sigma\gamma}R_{\mu\nu\sigma\gamma}$ diverges, where $R_{\mu\nu\sigma\gamma}$ is the Riemann curvature.

the observer passes the Static Limit, $U^\mu$ becomes space-like as $g_{\mu\nu}U^\mu U^\nu$ becomes greater than zero, accordingly the observer must move with the rotating black hole to remain time-like, which implies a static observer cannot exist in the region where $r_{SL-} < r < r_{SL+}$.

A significant consequence by the rotation of a Kerr black hole is the inertial frame dragging [19], i.e., particles and observers have the trend to co-rotate with the compact star. Specifically, this phenomenon is caused by the cross component $g_{t\varphi}$ in the metric. To understand this, consider a stationary particle's (or an observer's) motion, with zero initial angular momentum $L_z = U_\varphi = 0$. In the Schwarzchild spacetime, the geodesic of this particle is orthogonal to hypersurfaces with constant time (Schwarzschild time), where the 4 dimensional velocity reads $U^\mu = (u^t, 0, 0, 0)$. Nevertheless, in the Kerr spacetime, even the stationary particle cannot remain zero angular velocity and its worldlines are not orthogonal to the hypersurfaces with constant Boyer-Lindquist time, since

$$U^\varphi = g^{t\varphi}U_t + g^{\varphi\varphi}U_\varphi \,. \tag{3.2.16}$$

By observing this equation, we know that $U^\varphi$ does not vanish even when $U_\varphi = 0$. As a result, the non-zero angular velocity is given by

$$\begin{aligned} \omega &= \frac{\mathrm{d}\varphi}{\mathrm{d}t} \\ &= \frac{\mathrm{d}\varphi}{\mathrm{d}\lambda} \Big/ \left(\frac{\mathrm{d}t}{\mathrm{d}\lambda}\right) \\ &= \frac{U^\varphi}{U^t} \,, \end{aligned} \tag{3.2.17}$$

where we use the definition of the 4 dimensional velocity and $\lambda$ is an affine parameter. In addition, from the relation $U_\varphi = 0 = g_{t\varphi}U^t + g_{\varphi\varphi}U^\varphi$, it follows that

$$\begin{aligned} \omega &= -\frac{g_{t\varphi}}{g_{\varphi\varphi}} \\ &= \frac{2aMr}{(r^2+a^2) - \Delta a^2 \sin^2\theta} \,, \end{aligned} \tag{3.2.18}$$

where $\omega/aM > 0$, which implies that the particle's angular velocity has the same sign as that of the black hole, i.e., it is co-rotating with the black hole. Then the particle's 4 dimensional velocity can be written as

$$U^\mu = (U^t, 0, 0, U^\varphi) = U^t(1, 0, 0, \omega) \,. \tag{3.2.19}$$

In order to calculate $U^t$, consider $U_t = g_{tt}U^t + g_{t\varphi}U^\varphi$, upon inserting (3.2.16), we get

$$U_t = \left[ g_{tt} - \frac{g_{t\varphi}^2}{g_{\varphi\varphi}} \right] U^t \,. \tag{3.2.20}$$

Note that we require $U^\mu U_\mu = -1$, (3.2.20) becomes

$$\begin{aligned} (U^t)^2 &= \frac{g_{\varphi\varphi}}{g_{t\varphi}^2 - g_{tt}g_{\varphi\varphi}} \\ &= \frac{g_{\varphi\varphi}}{\Delta \sin^2\theta} \,, \end{aligned} \tag{3.2.21}$$

hence the 4 dimensional velocity reads

$$U^{\mu} = \sqrt{\frac{g_{\varphi\varphi}}{\Delta \sin^2\theta}}(1, 0, 0, \omega)\,. \tag{3.2.22}$$

The regions of physical interest are shown in Fig.3.1.

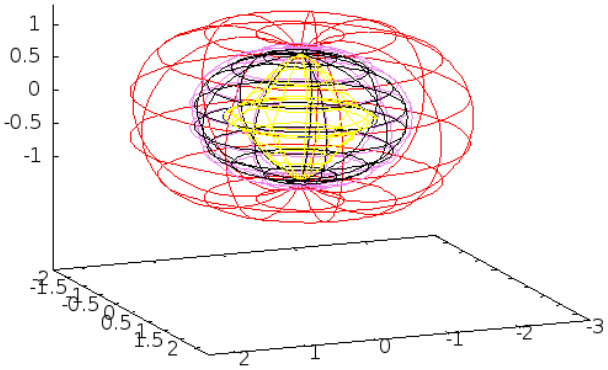


Figure 3.1: This is the Kerr black hole with its physical significant region boundary plotted in a three dimensional Cartesian coordinate system. The red grid sphere is Static Limit, the violet and black spheres are Event Horizon and Cauchy Horizon respectively, which are close to each other. The yellow inner most sphere is the inner Static Limit. The Ring Singularity coincides with the inner Static Limit on the equatorial plan.

## 3.3 Covariant Radiative Transfer

Radiative transfer is the study of how photons propagate through the medium. EM radiation could transmit information about physical properties of source object to remote receivers. The fundamental processes of radiative transfer are absorption, emission and scattering.

In the absence of gravity, i.e., a flat spacetime, the radiative transfer equation for which the medium is at rest can be expressed as

$$\frac{\partial I_\nu}{\partial \lambda} = -\chi I_\nu + \eta + \iint \sigma(\nu, \nu') I'_\nu(\tilde{\Omega}) \mathrm{d}\tilde{\Omega} \mathrm{d}\nu'\,, \tag{3.3.1}$$

where $I_\nu$ is the intensity, $\lambda$ is affine parameter, $\chi$ is the absorption coefficient, $\eta$ is the emission coefficient, and $\sigma$ is the scattering kernel. In general, it is difficult to obtain an analytical solution, unless there are numerous symmetries. Assume that we have enough symmetry, yields

$$\frac{\partial I_\nu}{\partial t} + \mu \frac{\partial I_\nu}{\partial t} = -\chi I_\nu + \eta\,, \tag{3.3.2}$$

for the plane-parallel symmetry, and

$$\frac{I_\nu}{\partial t} + \mu \frac{\partial I_\nu}{\partial r} + \frac{(1-\mu^2)}{r} \frac{\partial I_\nu}{\partial \mu} = -\chi I_\nu + \eta\,, \tag{3.3.3}$$

for the spherical symmetry, where $\mu = \cos\theta$. If scattering can be ignored, we can solve the above equation

$$I_\nu(\lambda) = I_\nu(\lambda_0)\exp\left(-\int_{\lambda_0}^{\lambda}\chi(\lambda',\nu)\mathrm{d}\lambda'\right) - \int_{\lambda_0}^{\lambda}\exp\left(-\int_{\lambda'}^{\lambda}\chi(\lambda'',\nu)\mathrm{d}\lambda''\right)\eta(\lambda',\nu)\mathrm{d}\lambda' . \tag{3.3.4}$$

In the presence of gravity, the background spacetime is curved and all equations must be covariant. The above radiative transfer equation needs to be modified into a covariant formalism. Current general relativistic radiative transfer equation is built in the Kerr spacetime, satisfying conservation of particle numbers and invariance of phase space [8].

The general relativistic radiative transfer formulation can be constructed once the geodesics near a Kerr black hole are calculated [112]. The evolution of photons intensity $I_\nu$ is computed through the material they traverses between the emission source and the observer. This can be achieved by solving the radiative transfer equation, given the absorption and emission coefficients from point to point. And the whole process must be performed in a covariant manner due to the general covariance principle.

The classical radiative transfer equation, in vacuum, given the emission and absorption properties and in the absence of scattering, can be written as

$$\frac{\mathrm{d}I_\nu}{\mathrm{d}s} = -\alpha_\nu I_\nu + j_\nu , \tag{3.3.5}$$

where $I_\nu$ is a function of $s$, denoting the intensity of the ray, $\nu$ is the frequency of the photon, $\alpha_\nu$ and $j_\nu$ are absorption and emission coefficients respectively, $\mathrm{d}s$ is the length that photons traverse in (Chandrasekhar 1960 [113]; Rybicki and Lightman 1979 [114]). Defining the optical depth as follow

$$\tau_\nu(s) = \int_{s_0}^{s}\mathrm{d}s'\alpha_\nu(s') , \tag{3.3.6}$$

then the radiative transfer equation can also be expressed as

$$\frac{\mathrm{d}I_\nu}{\mathrm{d}\tau_\nu} = -I_\nu + \frac{j_\nu}{\alpha_\nu} . \tag{3.3.7}$$

A direct integration of this equation leads to

$$I_\nu(s) = I_\nu(s_0)e^{-\tau_\nu} + \int_{s_0}^{s}\mathrm{d}s' j_\nu(s')e^{-(\tau_\nu(s)-\tau_\nu(s'))} , \tag{3.3.8}$$

where $I_\nu(s_0)$ represents the initial value of the specific intensity. If we introduce the source function $S_\nu = j_\nu/\alpha_\nu$, equations (3.3.6) and (3.3.8) can be rewritten as

$$\frac{\mathrm{d}I_\nu}{\mathrm{d}\tau_\nu} = -I_\nu + S_\nu , \tag{3.3.9}$$

$$I_\nu(s) = I_\nu(0)e^{-\tau_\nu} + \int_0^{\tau_\nu}\mathrm{d}\tau'_\nu S_\nu(\tau'_\nu)e^{-(\tau_\nu-\tau'_\nu)} . \tag{3.3.10}$$

Note that $I_\nu(s_0) = I_\nu(0)$, and these equations are not invariant under Lorentz transformations.

We now prove that the covariant formulation of radiative transfer can be constructed from the conservation of phase space and the conservation of particle number. Consider a phase space volume $\mathcal{V}$ full of particles, in the comoving frame, it is given by

$$\mathrm{d}\mathcal{V} \equiv \mathrm{d}x\mathrm{d}y\mathrm{d}z\mathrm{d}p^x\mathrm{d}p^y\mathrm{d}p^z\,, \tag{3.3.11}$$

where $\mathrm{d}^3x = \mathrm{d}x\mathrm{d}y\mathrm{d}z$ represents the 3 dimensional volume element, and $\mathrm{d}^3p = \mathrm{d}p^x\mathrm{d}p^y\mathrm{d}p^z$ represents the 3 dimensional momentum volume element. Liouville's theorem states the following expression

$$\frac{\mathrm{d}\mathcal{V}}{\mathrm{d}\lambda} = 0\,, \tag{3.3.12}$$

where $\lambda$ is the affine parameter [115]. The volume element $\mathrm{d}\mathcal{V}$ is thus a Lorentz scalar. Consider a new function

$$f(x^i, p^i) = \frac{\mathrm{d}N}{\mathrm{d}\mathcal{V}}\,, \tag{3.3.13}$$

where $\mathrm{d}N$ is the number of particles within the phase space volume. It is shown that $f(x^i, p^i)$ is Lorentz invariant, note that we have used the fact that $\mathrm{d}N$ is invariant under Lorentz transformations.

For relativistic massless particles, $|\vec{p}| = E$, and the 3 dimensional momentum volume element can be rewritten as $\mathrm{d}p^x\mathrm{d}p^y\mathrm{d}p^z = p^2\mathrm{d}p\mathrm{d}\Omega$. Taking these into consideration, we get

$$f(x^i, p^i) = \frac{\mathrm{d}N}{E^2\mathrm{d}E\mathrm{d}\Omega\mathrm{d}x\mathrm{d}y\mathrm{d}z}\,. \tag{3.3.14}$$

Moreover, the particle number in the three dimensional spatial volume $\mathrm{d}V = \mathrm{d}x\mathrm{d}y\mathrm{d}z$ is equivalent to that traverses through an area $\mathrm{d}A$ in a time interval $\mathrm{d}t$, which leads to

$$f(x^i, p^i) = \frac{\mathrm{d}N}{E^2\mathrm{d}E\mathrm{d}\Omega\mathrm{d}A\mathrm{d}t}\,. \tag{3.3.15}$$

The specific intensity of photons is

$$I_E = \frac{E\mathrm{d}N}{\mathrm{d}A\mathrm{d}t\mathrm{d}E\mathrm{d}\Omega}\,, \tag{3.3.16}$$

(Rybicki and Lightman 1979). Hence we get

$$\mathcal{I} \equiv \frac{I_\nu}{\nu^3} = \frac{I_E}{E^3}\,, \tag{3.3.17}$$

is a Lorentz scalar.

It is shown that $\chi = \nu\alpha_\nu$ is an invariant absorption coefficient under Lorentz transformations. In order to find a Lorentz invariant emission coefficient, note that $S_\nu/\nu^3$ is a Lorentz invariant quantity, thereof $\eta = j_\nu/\nu^2 = \alpha_\nu S_\nu/\nu^2$ is a Lorentz invariant emission coefficient. Reformulate (3.3.7) with Lorentz scalars

$$\frac{\mathcal{I}}{\tau_\nu} = -\mathcal{I} + \frac{\eta}{\chi}\,, \tag{3.3.18}$$

which is Lorentz covariant. Note that this equation holds only when the phase space volume is invariant for the light ray bundles with respect to the affine parameter. While in the 3+1 numerical relativity, artificial caustic arisen in the dimensional reduction will destroy the phase space, and hence violates the Liouville's theorem, which leads to the invalid of the covariance of the formulation.

For massless particles, including photons, the 4 dimensional momentum $k^a$ satisfies $k_a k^a = 0$ (cf., appendix A). Consider the hypersurface orthogonal to photon's 4 dimensional velocity $U^a$, the spatial component of $k^a$ is given by

$$\begin{aligned} v^a &= P^{ab} k_b \\ &= k^a + k_b u^b u^a \,, \end{aligned} \tag{3.3.19}$$

where projection operator is $P^{ab} = g^{ab} + u^a u^b$. Given the affine parameter $\lambda$, the variation in length $s$ with respect to (wrt) $\lambda$ is given by

$$\begin{aligned} \frac{\mathrm{d}s}{\mathrm{d}\lambda} &= -|v^a|\Big|_{\lambda_{\rm obs}} \\ &= -\sqrt{g_{ab}(k^a + k_c u^c u^a)(k^b + k_d u^d u^b)}\Big|_{\lambda_{\rm obs}} \\ &= -\sqrt{k_b k^b + 2(k_a u^a)^2 + (k_b u^b)^2 u_b k^b}\Big|_{\lambda_{\rm obs}} \\ &= -k_a u^a|_{\lambda_{\rm obs}} \,, \end{aligned} \tag{3.3.20}$$

where the subscript 'obs' stands for the observer. For a stationary located at infinity, $k_a u^a = -E_{\rm obs}$. Therefore, the relative energy shift between observer's frame and the comoving frame is given by

$$\tilde{\gamma} = \frac{\nu}{\nu_0} = \frac{E_{\rm obs}}{-k_a u^a|_\lambda} = \frac{k_a u^a|_{\lambda_{\rm obs}}}{k_b u^b|_\lambda} \,. \tag{3.3.21}$$

Since $\mathrm{d}\tau_\nu = \alpha_\nu \mathrm{d}s$, (3.3.18) becomes

$$\frac{\mathrm{d}\mathcal{I}}{\mathrm{d}s} = -\alpha_\nu \mathcal{I} + \frac{j_\nu}{\nu^3} \,, \tag{3.3.22}$$

substituting (3.3.20) into (3.3.22), yielding

$$\frac{\mathrm{d}\mathcal{I}}{\mathrm{d}\lambda} = -k_a u^a|_\lambda \left( -\alpha_{0,\nu} \mathcal{I} + \frac{j_{0,\nu}}{{\nu_0}^3} \right) \,, \tag{3.3.23}$$

where indices '0' denote the values in the local rest frame. Solving equation (3.3.23) leads to

$$\begin{aligned} \mathcal{I}(\lambda) = \;& \mathcal{I}(\lambda_0) e^{-\tau_\nu(\lambda)} \\ & - \int_{\lambda_0}^{\lambda} \mathrm{d}\lambda'' \frac{j_{0,\nu}(\lambda'')}{{\nu_0}^3} \exp\left( - \int_{\lambda''}^{\lambda} \mathrm{d}\lambda' \alpha_{0,\nu}(\lambda') k_a u^a|_{\lambda'} \right) k_b u^b|_{\lambda''} \,, \end{aligned} \tag{3.3.24}$$

where the optical depth is given by

$$\tau_\nu(\lambda) = - \int_{\lambda_0}^{\lambda} \mathrm{d}\lambda' \alpha_{0,\nu}(\lambda') k_a u^a|_{\lambda'} \,, \tag{3.3.25}$$

hence

$$\mathcal{I}(\tau_\nu) = \mathcal{I}(\tau_0)e^{-\tau_\nu} + \int_{\tau_0}^{\tau_\nu} \mathrm{d}\tau'_\nu \mathcal{S}(\tau'_\nu)e^{-(\tau_\nu - \tau'_\nu)}\,, \tag{3.3.26}$$

where $\mathcal{S}$ denotes the Lorentz invariant source function

$$\mathcal{S} = \frac{\eta}{\chi}\,. \tag{3.3.27}$$

If $-k_a u^a|_{\lambda_{\rm obs}} = E$ for an observer sitting at infinity, the radiative transfer equation can be decoupled to the following equations

$$\frac{\mathrm{d}\tau_\nu}{\mathrm{d}\lambda} = \frac{\alpha_{0,\nu}}{\tilde{\gamma}}\,, \tag{3.3.28}$$

$$\frac{\mathrm{d}\mathcal{I}}{\mathrm{d}\lambda} = \frac{j_{0,\nu}e^{-\tau_\nu}\tilde{\gamma}^{-1}}{{\nu_0}^3}\,. \tag{3.3.29}$$

For massive particle, the 4 dimensional momentum satisfies $p_a p^a = -m^2$. Therefore, equations (3.3.23) and (3.3.24) are not applicable. These equations need to be modified by the effect of a mass term. The variation of $s$ with respect to $\lambda$ is given by

$$\begin{aligned}\frac{\mathrm{d}s}{\mathrm{d}\lambda} &= -\sqrt{g_{ab}(p^a + p_c u^c u^a)(p^b + p_d u^d u^b)}\Big|_{\lambda_{\rm obs}} \\ &= -\sqrt{p_a p^a + 2(p_a u^a)^2 + (p_a u^a)^2 u_b u^b}\Big|_{\lambda_{\rm obs}} \\ &= -\sqrt{p_a p^a + (p_a u^a)^2}\Big|_{\lambda_{\rm obs}} \\ &= -\sqrt{-m^2 + (p_a u^a)^2}\Big|_{\lambda_{\rm obs}}\,.\end{aligned} \tag{3.3.30}$$

The covariant radiative transfer equation for massive particles is given by

$$\frac{\mathrm{d}\mathcal{I}}{\mathrm{d}\lambda} = -\sqrt{1 - \left(\frac{m}{p_a u^a|_{\lambda_{\rm obs}}}\right)^2}\, p_b u^b|_\lambda \left(-\alpha_{0,\nu}\mathcal{I} + \frac{j_{0,\nu}}{\nu^3}\right)\,. \tag{3.3.31}$$

$p_a u^a = -E$ for a stationary observer located at infinity, which leads to a $\sqrt{1-(m/E)^2}$ term. Apparently, the radiative transfer equation (3.3.31) reduces to equation (3.3.23) in the $m = 0$ limit.

## 3.4 Covariant Ray-Tracing

The equation of motion of a non-spinning free-falling massless particle in Kerr black hole spacetime is the mathematical formalism of a geodesic motion. It can be derived via the Lagrangian formulation

$$\mathcal{L} = \frac{1}{2}(g_{tt}\dot{t}^2 + 2g_{t\varphi}\dot{t}\dot{\varphi} + g_{rr}\dot{r}^2 + g_{\theta\theta}\dot{\theta}^2 + g_{\varphi\varphi}\dot{\varphi}^2)\,, \tag{3.4.1}$$

where $\dot{x}^\mu$ denotes the derivative of $x^\mu$ with respect to the affine parameter $\lambda$ [19] for the geodesic. By applying the Euler-Lagrange equation

$$\frac{\partial\mathcal{L}}{\partial x^\mu} - \frac{\mathrm{d}}{\mathrm{d}\lambda}\frac{\partial\mathcal{L}}{\partial\dot{x}^\mu} = 0\,,^3 \tag{3.4.2}$$

yielding the following equations

$$\dot{t} = E + \frac{2Mr}{\tilde{\Sigma}\Delta}[(r^2+a^2)E - aL_z]\,, \tag{3.4.3}$$

$$\dot{r}^2 = \frac{\Delta}{\tilde{\Sigma}}(E\dot{t} - L_z\dot{\varphi} - \tilde{\Sigma}\dot{\theta}^2)\,, \tag{3.4.4}$$

$$\dot{\theta}^2 = \frac{1}{\tilde{\Sigma}^2}[\mathcal{Q} + E^2a^2\cos^2\theta - L_z^2\cot^2\theta]\,, \tag{3.4.5}$$

$$\dot{\varphi} = \frac{2aMrE + (\tilde{\Sigma} - 2Mr)L_z\csc^2\theta}{\tilde{\Sigma}\Delta}\,, \tag{3.4.6}$$

where $E$ and $L_z$ are two constants on the geodesic of photon, defined as the total energy and projection of the particle's angular momentum along the black hole spin axis respectively, given by

$$\frac{\partial\mathcal{L}}{\partial\dot{t}} = -E\,, \tag{3.4.7}$$

$$\frac{\partial\mathcal{L}}{\partial\dot{\varphi}} = \quad L_z\,. \tag{3.4.8}$$

$\mathcal{Q}$ is a third constant of motion obtained by Carter in 1968 [116]. With these equations, (3.4.3) - (3.4.6) can be further simplified. Since equations (3.4.4) and (3.4.5) contain the square of $\dot{r}$ and $\dot{\theta}$, we must circumvent this problem by calculating the second derivatives, yielding

$$\begin{aligned}\ddot{r} = \ & \frac{\Delta}{\tilde{\Sigma}}\Bigg\{\frac{M(\tilde{\Sigma}-2r^2)}{\tilde{\Sigma}^2}\dot{t}^2 + \frac{(r-M)\tilde{\Sigma} - r\Delta}{\Delta^2}\dot{r}^2 \\ & + r\dot{\theta}^2 + \left[r + \left(\frac{\tilde{\Sigma}-2r^2}{\tilde{\Sigma}^2}\right)a^2M\sin^2\theta\right]\sin^2\theta\dot{\varphi}^2 \\ & - 2aM\sin^2\theta\left(\frac{\tilde{\Sigma}-2r^2}{\tilde{\Sigma}^2}\right)\dot{t}\dot{\varphi} + \frac{a^2\sin 2\theta}{\Delta}\dot{r}\dot{\theta}\Bigg\}\,,\end{aligned} \tag{3.4.9}$$

$$\begin{aligned}\ddot{\theta} = \ & \frac{1}{2\tilde{\Sigma}}\Bigg(\sin 2\theta\Bigg\{\frac{2a^2Mr}{\tilde{\Sigma}^2}\dot{t}^2 - \frac{4aMr(r^2+a^2)}{\tilde{\Sigma}^2}\dot{t}\dot{\varphi} - \frac{a^2}{\Delta}\dot{r}^2 \\ & + a^2\dot{\theta}^2 + \left[\Delta + \frac{2Mr(r^2+a^2)^2}{\tilde{\Sigma}^2}\right]\dot{\varphi}^2\Bigg\} - 4r\dot{r}\dot{\theta}\Bigg)\,.\end{aligned} \tag{3.4.10}$$

Equations (3.4.3), (3.4.6), (3.4.9), and (3.4.10) form a group of six coupled equations, solving them with appropriate initial conditions gives rise to solutions $(t, r, \dot{r}, \theta, \dot{\theta}, \varphi)$ of the geodesics. Fig.3.2 and Fig.3.3 illustrate the images of the trajectories of massless particles in Kerr spacetime. We need to solve the radiative transfer equation (3.3.18) along these derived null geodesics (colourful lines in the figures).

[3]More explicitly, the geodesic equation reads as $\mathrm{d}^2x^\mu/\mathrm{d}\tau^2 + \Gamma_{\nu\sigma}{}^\mu(\mathrm{d}x^\nu/\mathrm{d}\tau)(\mathrm{d}x^\sigma/\mathrm{d}\tau) = 0$, where $\tau$ is the affine parameter, cf., appendix B.

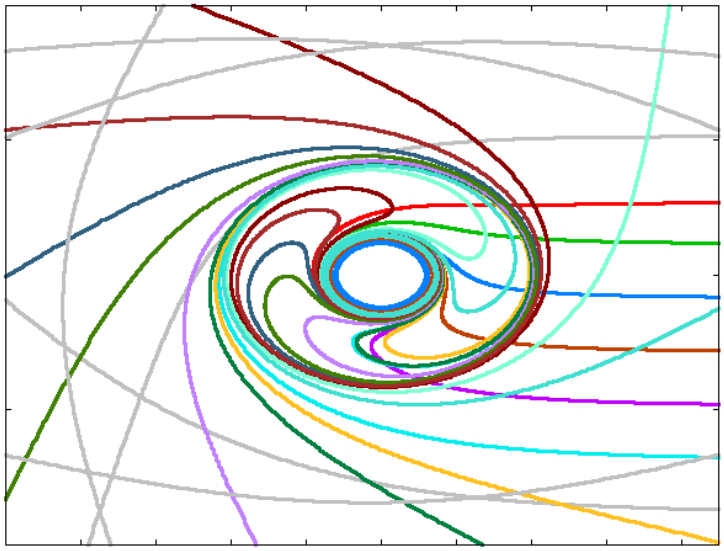

Figure 3.2: This image is the geodesics of photons around a Kerr black hole in the $(x, y)$ plane of a Cartesian coordinate. We use the backward ray-tracing, i.e. ray-traced with observer-to-emitter method. The grey lines indicate the escaping geodesics. The coloured lines indicate geodesics falling into the black hole, rotating with it anticlockwise (frame dragging). The inner blue circle indicates the Event Horizon of the Kerr black hole. The distant observer located on the far right, not shown in the plot.

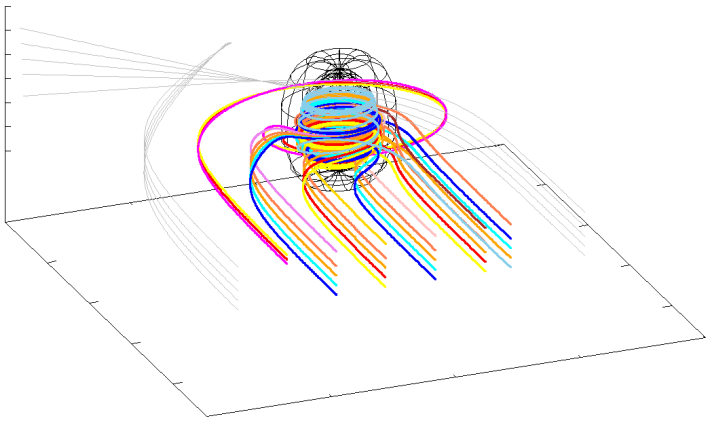

Figure 3.3: This image illustrates the geodesics of photons around a Kerr spacetime together with the black hole in a Cartesian coordinate system. Again, we apply the observer-to-emitter approach. The two black grid spheres indicate the black hole region, with the outer and inner ones correspond to Static Limit and Event Horizon respectively. The grey lines indicate the photons which are not captured by the black hole. Coloured lines indicate that the geodesics falling into the black hole. The observer located on the far bottom right which is not shown in the plot.

# Chapter 4

# Geodesic Calculation Using the Level Set Method

## 4.1 Overview

As was mentioned in the previous context, we demand a new embedding formalism to help us recover Lorentz structure and covariance of a radiative transfer formulation in dynamical spacetime, where a level set approach can be applied and allows a lower dimensional manifold propagating in a higher dimensional manifold. The fourth Chapter largely considered the new method which enables one to reconstruct null geodesics in dynamical spacetime. We have successfully calculated the numerical solutions to level set equations (4.4.2) with first-order finite difference method and third-order accurate essentially non-oscillatory (ENO) method. Both methods aim to increase the accuracy of spatial discretization. The temporal precision increased by total variation diminishing Runge-Kutta (TVD RK) is under consideration and will be added to numerically calculate the final geodesic equation. Level set method allows one to reconstruct the shortest paths in higher dimensional spaces. We have discussed specific level set equations and find non-constrained shortest geodesics in some case. In the case of a dynamical spacetime, as will be mentioned in the following context of this Chapter, one cannot derive the geodesic within the regime of a 4 dimensional spacetime, where both analytical and numerical methods are unavailable. In this Chapter we review the level set method and the associated numerical algorithm.

## 4.2 Motivation of Applying the Level Set Method

In general relativity the trajectory of a non-spinning free-falling particle in gravitational field is described by a geodesic, derived in a 4 dimensional manner, using geodesic equation [115]

$$\frac{\mathrm{d}^2 x^\mu}{\mathrm{d}\lambda^2} + \Gamma_{\nu\sigma}{}^{\mu} \frac{\mathrm{d}x^\nu}{\mathrm{d}\lambda} \frac{\mathrm{d}x^\sigma}{\mathrm{d}\lambda} = 0\,, \tag{4.2.1}$$

where $\Gamma_{\nu\sigma}{}^{\mu}$ is the Christoffel symbol appendix B, $\lambda$ is the affine parameter of the geodesic. This analytical method works for stationary spacetime[15], including Schwarzschild and Kerr spacetimes. For the dynamical case, one could, in general, apply the numerical relativity, in which a 4 dimensional spacetime is split into infinitely many 3 dimensional hypersurfaces by virtue of a global time function $t$ to calculate the geodesics numerically.

However, neither of these two methods is applicable in this project. On the one hand, the analytical computation method using equation (4.2.1) is not applicable to most of the the dynamical spacetime, including binary black hole mergers, whose metric cannot be solved analytically. On the other hand, the 3+1 numerical relativity foliation method can help to calculate most cases of geodesics in dynamical spacetime. By choosing an affine parameter of photons as the global function, one can foliate the whole manifold into many three dimensional surfaces, then cutting the hypersurfaces with null surfaces to derive the trajectories of photons. However, taking radiative transfer into account, one must select the specific photon rays that may approach the observers. One way to achieve this is to calculate all hypersurfaces under certain conditions and store all data on each slices, then cutting them by specific null surfaces. Nevertheless, one immediately realizes that infinite data must be stored in this scheme and it is clear that these huge numbers of data beyond the capacity of any current computer.

Physicists have constructed other ways to build up null geodesic. In [127], a back-trace 3+1 numerical method is applied to find the event and apparent horizon of a black hole. The author just decomposes the spacetime into time slices and trace from a future point backward to black hole and let the ray marginally approach the initial region of event horizon to recover the full 4 dimensional boundary of a black hole. Nevertheless, this back-trace method is invalid in the ray-tracing of radiative transfer, because radiative transfer deal with the absorption, emission and scattering processes of light when interacted with the intermediate matter point by point through its path. A back-trace method hence leads to a completely different results from that derived from the propagating forward method.

The current covariant formulation of radiative transfer in dynamical spacetime is only carried out in the far regime where the gravitational field is weak. In the strong field regime, where the spacetime is significantly curved by the compact binary system and the gravitational radiations present, using 3+1 numerical relativity to derive null geodesics may result in chaos on the photon trajectories. This is because all spacetime structure remain unchanged while doing the numerical calculation, however, the Lorentz structure in between any two adjacent time slices is deteriorated. In order to maintain causality, one needs to introduce extra parameter in the numerical process which breaks the null geodesic structure and brings chaos to the photon's path [128, 129]. We have to

[15]Geodesic equation (4.2.1) can be applied to some specific dynamical cases, the most famous one is the Friedmann-Lemaître-Robertson-Walker metric, which describes a homogeneous and isotropic cosmos [117, 118, 119, 120, 121, 122, 123, 124, 125, 126].

find other way to fix the defect.

Mathematically speaking, 3+1 numerical relativity is a formulation based on the ADM formalism [6], which is derived in the smooth 4 dimensional manifold background. In principle, the fundamental formulation is well-defined. However, when physicists try to carry this out practically, the smooth structure of a manifold is broken down to a group of 3 dimensional time slices and physical and numerical problems will occur in a practical calculation. Losing Lorentz structure is one of them.

One way to circumvent these problems is to apply the level set method [14, 15] and embed a four dimensional spacetime into a five dimensional manifold requiring that null geodesics evolve along the extra coordinate $w$ instead of the original temporal coordinate $t$. The fundamental steps are: Embedding the original four dimensional dynamical curved spacetime into the five dimensional manifold, via many embedding maps $\phi_w$. Subsequently, applying the level set method and solving level set equations to find the evolution of the four dimensional slices. Ultimately, cutting the four dimensional foliations by null surfaces (zero level set) to obtain the geodesics evolving along the fifth coordinate. This computational method is very similar to the 3+1 numerical relativity, but implemented in a 4+1 manner instead.

One of the advantages of level set method is shown in Fig.4.1. We demonstrates how one can manage to resolve the aforementioned backward ray-tracing problem. With the help of level set approach, one is able to propagate the wave-front of light rays (blue/dashed curves) forwardly, i.e. in the emitter-to-observer approach, where we don not need to worry about the backward tracing problem.

Nevertheless, there is a problem arising when one embeds the four dimensional spacetime into a five dimensional space, local Lorentz structure is not carried with the embedding maps to the new 5 dimensional space outside each single spacetime foliation. This has to be circumvented before proceeding, which has been given a mathematical proof in the next Chapter. We find a particular way to embed the 4 dimensional spacetime in a generic 5 dimensional manifold and by choosing a good metric on the ambient space to recover the Lorentz structure and show that it works for all types of spacetime, including stationary and dynamical ones. This reconstruction together with the cutting technique used by level set method guarantees how we can maintain the Lorentz structure for ray-tracing in radiative transfer in dynamical spacetime.

As we mentioned before, the usual analytical geodesic equation is derived within the Lagrangian formulation of general relativity, and a 3+1 formulation is based on the Hamiltonian formulation. A level set method employs an equation which is a Hamilton-Jacobi type. Hence, we might be able to apply new numerical algorithms (eg. the symplectic integrator [130], cf., appendix G) which contribute to a more efficient computation.

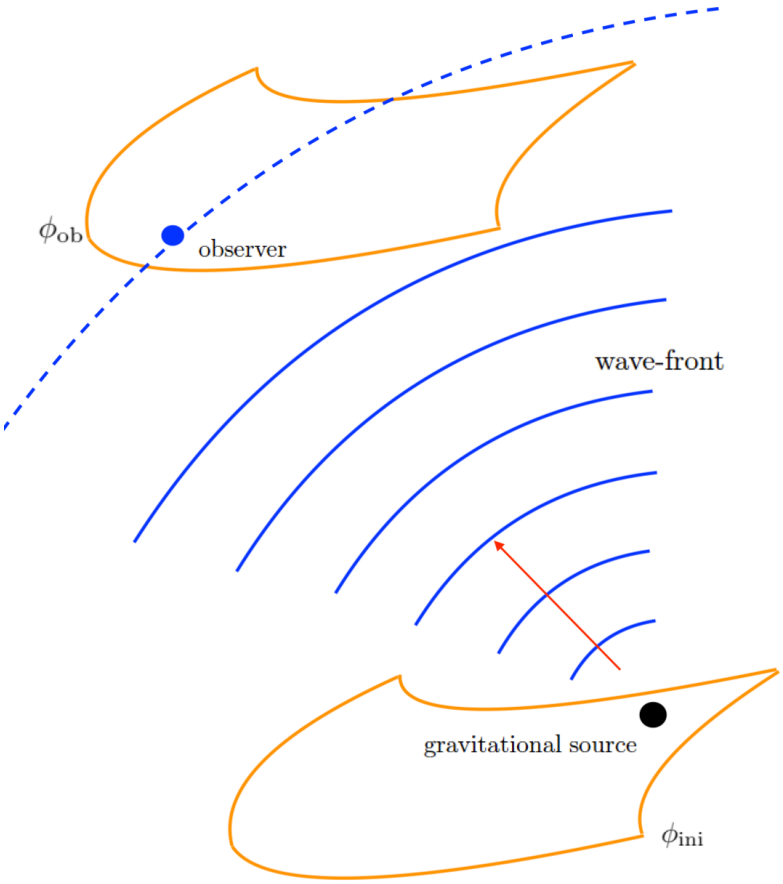


Figure 4.1: The figure illustrates the wave-front propagation in higher dimensional ambient manifold. $\phi_{\text{ini}}$ and $\phi_{\text{ob}}$ denote the initial slice and the slice where the wave-front cut the observer respectively. The black dot denotes the gravitational source and the blue dot denotes the observer. Curved blue lines denote the propagating wave-fronts, and the dotted curved blue line denotes the wave-front which hits the observer. The red arrow represents the light ray propagation direction. From the plot we can clearly find that the wave-front can always hit the observer while it is propagating forwardly.

## 4.3 Bases for the 3+1 Formalism of General Relativity

Since we need to reconstruct the geodesics in 5 dimensional space in a 4+1 manner, it is necessary to introduce the bases of formalism of the 3+1 numerical relativity.

Given a global function $t$ on spacetime $(\mathcal{M}, g_{ab})$ such that the hypersurfaces $\mathcal{W}_t$ is defined as level surfaces of $t$, given by

$$t(p) = con \iff \forall\, p \in \mathcal{W}_t \subset \mathcal{M}\,, \quad \forall\, con \in \mathbb{R}\,, \tag{4.3.1}$$

where the gradient of $t$ is given by $\nabla_a t$ which never vanishes. Note that from now on we apply $t$ instead of the $f$ for the global time function. It is assumed that any two $\mathcal{W}_{t_1}$ , $\mathcal{W}_{t_2} \in \{\mathcal{W}_t\}$ in this continuous set of level surfaces will not intersect one other, i.e.

$$\mathcal{W}_{t_1} \cap \mathcal{W}_{t_2} = \varnothing\,, \ \forall\, t_1 \neq t_2\,. \tag{4.3.2}$$

In this sense

$$\mathcal{M} = \bigcup_{t\in\mathbb{R}} \mathcal{W}_t \,. \tag{4.3.3}$$

If all hypersurfaces $\mathcal{W}_t$ are space-like surfaces (actually Cauchy surface [19]), then spacetime $(\mathcal{M}, g)$ is a globally hyperbolic manifold[16]. Accordingly, the topological structure of a globally hyperbolic spacetime is necessarily $\mathcal{W}_t \times \mathbb{R}$. Scalar field $t$ can be considered as 'time' in this sense, $\mathcal{W}_t$ can be considered as 'space' at time $t = con$, where $con$ is a constant for each $\mathcal{W}_t$. This is called a foliation of $\mathcal{M}$.

Given a foliation $\mathcal{W}_t \times \mathbb{R}$ of spacetime $(\mathcal{M}, g)$, a specific and critical normal covector is given by

$$n_a = -N\nabla_a t \,,\ \forall\ t \in \mathbb{R} \,. \tag{4.3.4}$$

The normal vector associated with $n$ is then given by

$$n^a = -N g^{ab}\nabla_b t \,. \tag{4.3.5}$$

Factor $N$ is called the lapse function, coined by Wheeler in 1964, given by

$$N := (-g^{ab}\nabla_a t \nabla_b t)^{-1/2} \,. \tag{4.3.6}$$

It is apparently that $n^a$ is a unit vector such that

$$\begin{aligned} g_{ab}n^a n^b &= n_a n^a \\ &= N^2 g^{ab}\nabla_b t \nabla_a t \\ &= (-g^{cd}\nabla_c t \nabla_d t)^{-1} g^{ab}\nabla_a t \nabla_b t \\ &= -1 \,, \end{aligned} \tag{4.3.7}$$

where we have used equations (4.3.4) and (4.3.5) in the third equality, and used equation (4.3.6) in the fourth equality.

There are three types of hypersurface, i.e., if

$$n^a n_a > 0 \iff \mathcal{W} \text{ is time-like,} \tag{4.3.8}$$
$$n^a n_a = 0 \iff \mathcal{W} \text{ is null,} \tag{4.3.9}$$
$$n^a n_a < 0 \iff \mathcal{W} \text{ is space-like.} \tag{4.3.10}$$

And if $n^a n_a \neq 0$ then the normal vector is supposed to be normalized, i.e.

$$n^a n_a = \pm 1 \,. \tag{4.3.11}$$

Defining the time-like normal evolution vector $m^a$ to $\mathcal{W}_t$, such that

$$m^a := N n^a \,. \tag{4.3.12}$$

The length of $m$ is $g_{ab}m^a m^b = -N^2$, the inner product of $\nabla^a t$ and $m^b$ is given as

$$g(\vec{\nabla}t, m) = g_{ab}m^b\nabla^a t = m^b\nabla_b t = N n^b \nabla_b t = 1 \,, \tag{4.3.13}$$

[16] A stably causal spacetime also admits such global function. Nevertheless, we still use a globally hyperbolic spacetime instead throughout this thesis.

where we have used (4.3.6) and (4.3.5), $\vec{\nabla} = \nabla^a = g^{ab}\nabla_b$. A geometrical consequence of this relation is that any point $p$ of $\mathcal{W}_t$ can be dragged to another point $p'$ of $\mathcal{W}_{t+\delta t}$ by a displacement $m\delta t$ (the index of $m^a$ is ignored here). For the scalar field $t$, we have

$$t(p') = t(p + m\delta t) = t(p) + \delta t m^a \nabla_a t = t(p) + \delta t\,, \tag{4.3.14}$$

where in the third equality we used (4.3.13). The result shows that $p' \in \mathcal{W}_{t+\delta t}$.

We choose, in general, tangent $(\partial_t)^a$ as the tangent to the zeroth coordinate line, which implies that this coordinate curve is parameterized by $t$. Since we know that $(\partial_t)^a(\mathrm{d}t)_a = 1$ and $(\mathrm{d}t)_a = \nabla_a t$, tangent vector $(\partial_t)^a$ obeys the same property as the normal evolution vector $m^a$, i.e., it drags hypersurfaces $\mathcal{W}_t$ to other slices. These two vectors $(\partial_t)^a$ and $m^a$ differ by a shift vector $\beta^a$, given by

$$\beta^a := (\partial_t)^a - m^a\,. \tag{4.3.15}$$

The name shift vector has been coined by Wheeler (1964). By combining equations (4.3.15) and (4.3.13), we get

$$(\mathrm{d}t)_a\beta^a = (\mathrm{d}t)_a(\partial_t)^a - (\mathrm{d}t)_a m^a = 1 - 1 = 0\,. \tag{4.3.16}$$

Equivalently, $n_a\beta^a = 0$ due to $(\mathrm{d}t)_a = \nabla_a t = -N^{-1}n_a$, i.e., vector $\beta^a$ is tangent to $\mathcal{W}_t$. Rewrite (4.3.15) as

$$(\partial_t)^a = Nn^a + \beta^a\,, \tag{4.3.17}$$

this expression will be used frequently in numerical relativity. Furthermore, $(\partial_t)^a$ satisfies

$$(\partial_t)^a(\partial_t)^b g_{ab} = -N^2 + g_{ab}\beta^a\beta^b\,. \tag{4.3.18}$$

Note that $(\partial_t)^a$ is not necessarily time-like, whereas

$$\begin{array}{lcl} (\partial_t)^a \text{ is time-like} & \Longleftrightarrow & g_{ab}\beta^a\beta^b < N^2\ , \\ (\partial_t)^a \text{ is null} & \Longleftrightarrow & g_{ab}\beta^a\beta^b = N^2\ , \\ (\partial_t)^a \text{ is space-like} & \Longleftrightarrow & g_{ab}\beta^a\beta^b > N^2\ . \end{array}$$

## 4.4 Foundations of the Level Set Method

Level set method [14, 15] is an effective computational algorithm to transform surfaces (as well as the interfaces) in higher dimensions (from $n$ to $n+1$), which is allowed to work for arbitrary dimensional space. One example is that the surfaces are described by the signed-distance-function, where given a point returns the distance to the surface. Hence a surface separates the inside and outside of a region, and the interface can be obtained by requiring the signed-distance-function equals to zero, i.e., the zero level set. Nevertheless, specific functions, which are not signed-distance-functions in general, are selected in different physics problems. This technique approximates the solutions of an initial value partial differential equation, requiring an adaptive methodology to obtain computational efficiency. In [14], Sethian and Osher demonstrate that the

solutions of level set equations resemble those of Hamilton-Jacobi equations, whose numerical algorithm may borrow from the technology developed for the equations of hyperbolic conservation laws [131]. In [131], higher-order accurate schemes are developed for solving Hamilton-Jacobi equations, nevertheless, this thesis is focusing on the first-order accurate solutions based on the finite difference techniques and 3rd-order accurate method (ENO). In addition to physics problems, level set method is of great significance in deposition in semi-conductor manufacturing, robotic navigation and path planning, image segmentation in medical imaging scans, computation of seismic travel times, and other aspects of computational geometry and computer science.

The most trivial case is that, in one spatial dimension, suppose one can separate the real coordinate line into three distinct pieces by two points, $x = -1$ and $x = 1$. More explicitly, these three regions are written as $(-\infty, -1)$, $(-1, 1)$ and $(1, \infty)$. We refer to the first and the third subdomains as the outside portion, and the second subdomain as the inside portion, denoted by $O^+ = (-\infty, -1) \cup (1, \infty)$ and $O^- = (-1, 1)$ respectively. The boundary between inside and outside portions consists of two points $\partial O = \{-1, 1\}$, and is called the interface (or zero level). This is an explicit representation of the interface. Nevertheless, one can construct an implicit representation by introducing an extra spatial dimension and define a level function $\phi(x) = x^2 - 1$, the zero level of $\phi(x)$ is the set of all points where $\phi(x) = 0$, which is exactly the boundary $\partial O$. This simplest one dimensional case can be readily generalized to arbitrarily higher dimensions and to non-Euclidean coordinates.

Consider a 3 dimensional implicit surface $\phi(\vec{x})$ moving under the speed field $\vec{V}(x, y, z)$, one can derive the evolution of all points on the surface by solving the following equation

$$\frac{\mathrm{d}\vec{x}}{\mathrm{d}t} = \vec{V}\,, \tag{4.4.1}$$

given the initial conditions of $\vec{V}(x, y, z)$ at $\vec{x}$ when $\phi(\vec{x}) = 0$, the evolution process of the surface can be computed using the above equation. This is known as the Lagrangian formulation of interface evolution [15]. One can then use the numerical discretization if the surface elements are not distorted too much. However, even the most trivial velocity field can cause a large distortion and the accuracy of the method can deteriorate quickly unless one modify the numerical scheme periodically to account for the deformations by smoothing and regularizing inaccurate surface elements. Moreover, one must deal with topological changes in addition to smoothing the surface deformation. The regularizing, smoothing and surgical modification would largely increase the complexity of the computational procedure [132]. The ability of handling spacetime defects, e.g., topological changes, enables the level set approach to tackle the scattering problem happens in constructing a radiative transfer formulation in dynamical spacetime, cf., Fig.4.2 for an example.

In order to avoid the instability and complexity arising in the Lagrangian formulation, we use the level set method instead to construct an implicit function, and solve the equations that govern the transformation of the surface where the velocity fields $F$ depend on externally

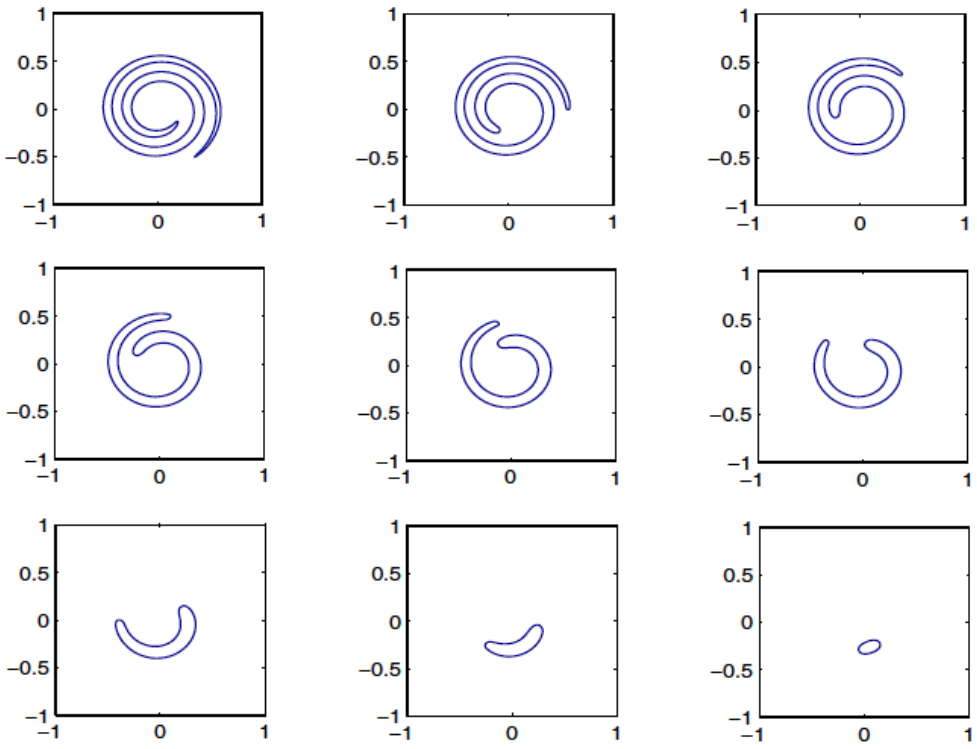

Figure 4.2: Evolution of a wound spiral in a curvature-driven flow. The high curvature part move faster than the elongated part. This figures demonstrates that the level set approach is well-behaved in manipulating sharp corner for an evolving interface (cf., the first plot at top left), which implies that this method can alleviate the aforementioned scattering problem encountered in the dynamical spacetime. Credit: S. Osher and R. Fedkiw, 2002.

generated velocity or mean curvature $\kappa$, where the equations are given as

$$\begin{aligned} &\phi_t + \vec{V} \cdot \nabla\phi = 0\,, \\ &\phi_t + F(\kappa) \cdot |\nabla\phi| = 0\,, \end{aligned} \tag{4.4.2}$$

the evolution of interfaces can be tracked with these equations. Specifically, the equation for non-constrained geodesics is given by [133]

$$\phi_t = \sqrt{a(x,y)\phi_x^2 + b(x,y)\phi_y^2 - c(x,y)\phi_x\phi_y}\,, \tag{4.4.3}$$

for which causal structure is not defined, where the recovery of the causality has been solved in the next Chapter.

## 4.5 Numerical Integrators for Level Set Equations

It follows last section that there exist two types of level set equation, corresponding to different evolution styles. The evolution of a surface which propagates under the externally generated velocity, which is independent of curvature $\kappa$, is determined by the following equation

$$\phi_t + \vec{V} \cdot \nabla\phi = 0\,. \tag{4.5.1}$$

Recall that $\nabla$ is the gradient operator (see following context), which satisfies

$$\vec{V} \cdot \nabla\phi = u_1\phi_x + u_2\phi_y + u_3\phi_z \,, \tag{4.5.2}$$

where $u_1$ , $u_2$ and $u_3$ are the three spatial components of $\vec{V}$. This partial differential equation defines the motion of surface as well as the interface $\phi = 0$, and is know as the Eulerian formulation of interface evolution, for which the interface is captured by the implicit function $\phi$ as opposed to being tracked by front elements in the Lagrangian formulation.

Finite difference is an effective first-order accurate method to calculate the numerical solutions of partial differential equations, for example the Hamilton-Jacobi equation

$$\phi_t + F \cdot H(\nabla\phi) = 0 \,, \tag{4.5.3}$$

where subscript $t$ denotes the temporal partial derivative $\partial/\partial t$, $\nabla$ denotes the $n$ dimensional gradient of function $\phi$, given by

$$\nabla\phi = \left(\frac{\partial\phi}{\partial x}, \frac{\partial\phi}{\partial y}, \frac{\partial\phi}{\partial z}, \cdots\right) . \tag{4.5.4}$$

In a Cartesian grid, the first-order forward difference is given by

$$\frac{\partial\phi}{\partial x} \approx \frac{\phi_{i+1} - \phi_i}{\Delta x} \,, \tag{4.5.5}$$

abbreviated as $D^+\phi$, where $\Delta x$ is the increment in the $x$ direction, denoted by $x_{i+1} - x_i$. The first-order backward difference is given by

$$\frac{\partial\phi}{\partial x} \approx \frac{\phi_i - \phi_{i-1}}{\Delta x} \,, \tag{4.5.6}$$

abbreviated as $D^-\phi$. The central difference is given by

$$\frac{\partial\phi}{\partial x} \approx \frac{\phi_{i+1} - \phi_{i-1}}{2\Delta x} \,, \tag{4.5.7}$$

abbreviated as $D^0\phi$. In this formulation, subscript $i$ denotes the position on the grid at the $i$-th point, i.e., at $x_i$, and $\phi_i$ is $\phi(x_i)$. It is assumed that the other dimensions have been suppressed and we are working in 1 dimensional space.

For second-order derivatives, it is convenient to express them using previous notations

$$\frac{\partial^2\phi}{\partial x^2} \approx \frac{\phi_{i+1} - 2\phi_i + \phi_{i-1}}{\Delta x^2} \,, \tag{4.5.8}$$

abbreviated as $D_x^+ D_x^-\phi$ or $D_x^- D_x^+\phi$. For the derivative on $y$ direction, one just substitutes $x$ with $y$ in equation (4.5.8), abbreviated as $D_y^+ D_y^-\phi$ or $D_y^- D_y^+\phi$. For $\phi_{xy}$, the finite difference formula is given by

$$\frac{\partial^2\phi}{\partial x\partial y} \approx \frac{\phi_{i+1,j+1} - \phi_{i-1,j+1} - \phi_{i+1,j-1} + \phi_{i-1,j-1}}{4\Delta x\Delta y} \,, \tag{4.5.9}$$

abbreviated as $D_x^0 D_y^0\phi$ or $D_y^0 D_x^0\phi$. Subscripts $i$ and $j$ denote the values of $\phi$ at $x_i$ and $y_j$ in a 2 dimensional space, respectively.

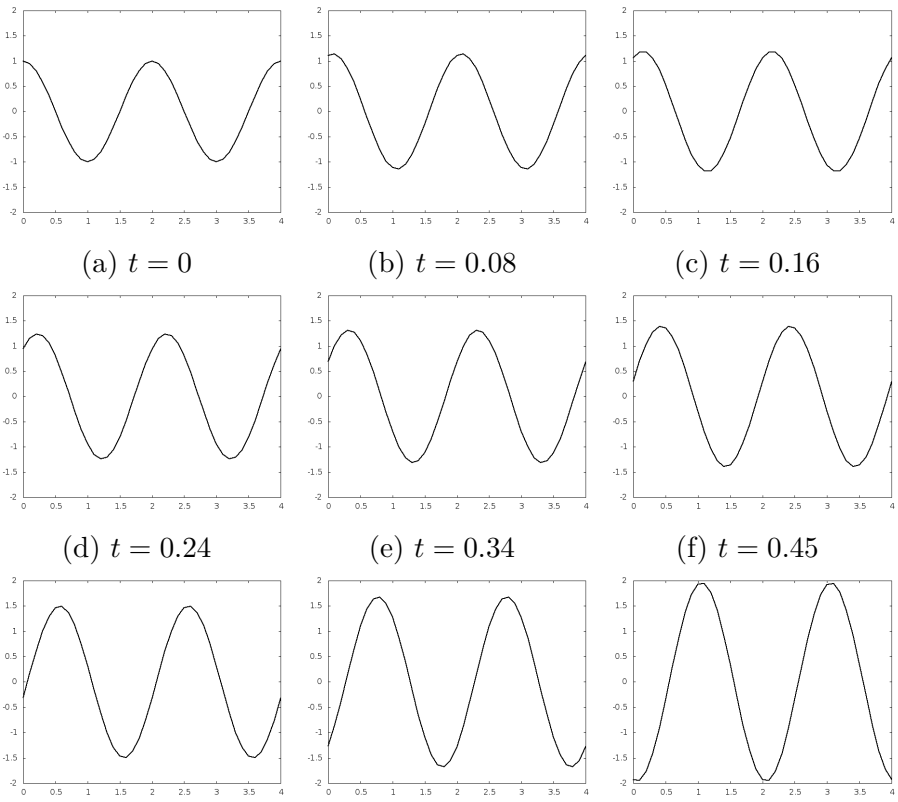

(a) $t = 0$ (b) $t = 0.08$ (c) $t = 0.16$

(d) $t = 0.24$ (e) $t = 0.34$ (f) $t = 0.45$

(g) $t = 0.59$ (h) $t = 0.80$ (i) $t = 1.09$

Figure 4.3: This group of figures illustrates the transforming surfaces at different points of time, under the external field $F = 1$ and initial surface is given by $\cos(\pi x)$. The value of the parameter $t$ is shown under each panel.

In addition, the curvature of an implicit function is of great significance in level set equation. A curvature is the reciprocal of the local radius of a function, in a 2 dimensional space it is given by

$$\kappa = \frac{\phi_x^2\phi_{yy} - 2\phi_x\phi_y\phi_{xy} + \phi_y^2\phi_{xx}}{|\nabla\phi|^3}\,, \tag{4.5.10}$$

where $\phi_x$ denotes the first-order partial derivative with respect to $x$, $|\nabla\phi| = \sqrt{\phi_x^2 + \phi_y^2}$. Same for the other expressions. Curvature in 3 dimensional space is given by

$$\begin{aligned}\kappa = \; & (\phi_x^2\phi_{yy} - 2\phi_x\phi_y\phi_{xy} + \phi_y^2\phi_{xx} + \phi_x^2\phi_{zz} - 2\phi_x\phi_z\phi_{zx} + \phi_z^2\phi_{xx} \\ & + \phi_y^2\phi_{zz} - 2\phi_y\phi_z\phi_{yz} + \phi_z^2\phi_{yy})/|\nabla\phi|^3\,.\end{aligned} \tag{4.5.11}$$

Curvatures in other dimensions can be derived in a similar manner.

The velocity field in equation (4.5.1) can come from numerous external sources, depending on the physical contexts. Fig.4.3 and Fig.4.4 illustrate an interface evolving under a constant velocity.

The numerical method used to solve equation (4.5.1) is called the upwind difference, which is first-order accurate and combines the finite difference and forward Euler method, given by

$$\frac{\phi^{n+1} - \phi^n}{\Delta t} + \vec{V}^n \cdot \nabla\phi^n = 0\,, \tag{4.5.12}$$

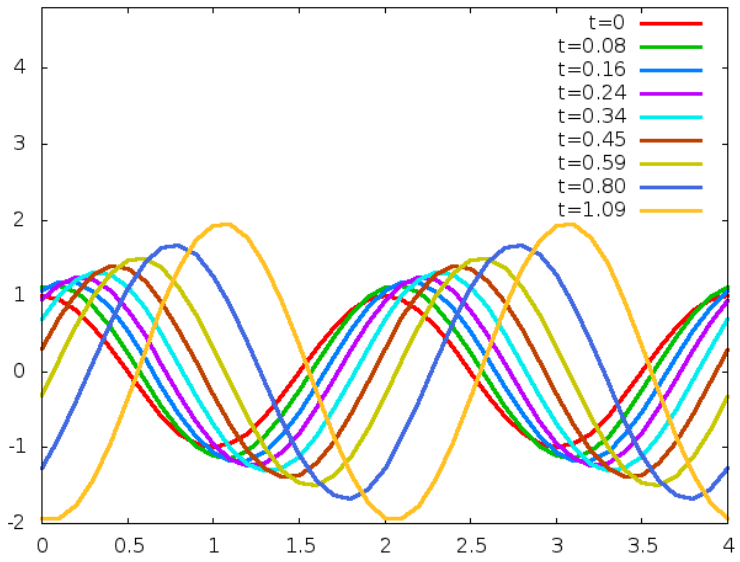


Figure 4.4: This figure illustrates all the nine curves in one graph, with the time-colour correspondence on the top right corner.

where superscripts $n$ denote the value at the time point $t^n$, for example, $\phi^n = \phi(t^n)$, $\Delta t$ is the increment in time parameter $t$. Expanding equation (4.5.12) yields

$$\frac{\phi^{n+1} - \phi^n}{\Delta t} + u^n \phi_x^n = 0\,, \tag{4.5.13}$$

where the equation is suppressed to one dimension. It is clear that the sign of $u$ determines whether the values of $\phi$ change to the right or the left. The upwind difference indicates that, at each grid point, if $u_i^n > 0$, approximate $\phi_x$ with $D_x^- \phi$, if $u_i^n < 0$, approximate $\phi_x$ with $D_x^+ \phi$.

The combination of forward Euler time discretization and upwind difference scheme is a consistent finite difference approximation due to the numerical error converges to zero as $\Delta x \to 0$ and $\Delta t \to 0$. Stability of the solutions is guaranteed by Courant-Friedreichs-Lewy condition (CFL condition), which claims that numerical waves cannot propagate slower than physical waves, implying

$$\Delta t = \frac{\Delta x}{\max\{|u|\}}\,, \tag{4.5.14}$$

where $\max\{|u|\}$ is chosen over the entire Cartesian grid. Equation (4.5.14) is usually enforced by choosing a CFL number $\tilde{\alpha}$ with

$$\Delta t \left( \frac{\max\{|u|\}}{\Delta x} \right) = \tilde{\alpha}\,, \tag{4.5.15}$$

given that $0 < \tilde{\alpha} < 1$. A common near-optimal choice is $\tilde{\alpha} = 0.9$, and a common conservative choice is $\tilde{\alpha} = 0.5$. A multi-dimensional version is given by

$$\Delta t \left( \frac{\max\{|u|\}}{\Delta x} \right) = \tilde{\alpha}\,. \tag{4.5.16}$$

Upwind difference is a rather simple first-order accurate numerical method. People have developed higher-order accurate techniques to

study the solutions of Hamilton-Jacobi equations. The essentially non-oscillatory polynomial interpolation of data has been applied to numerical computation and this initial idea has been improved considerably, generalizing the first-order technique to higher-order spatial accuracy by choosing more accurate $\phi_i^+$ and $\phi_i^-$ [14, 134, 10]. Moreover, one can use total variation diminishing Runge-Kutta method to increase the accuracy in temporal discretization [135]. See appendix C for more details.

Equipped with high-order numerical schemes, one can now discuss the solution to Hamilton-Jacobi (HJ) equation

$$\phi_t + H(\Delta\phi) = 0\,. \tag{4.5.17}$$

In three dimension, (4.5.17) can be rewritten as

$$\phi_t + H(\phi_x, \phi_y, \phi_z) = 0\,. \tag{4.5.18}$$

Note that the level set equation (4.4.3) is an example of HJ equation.

Consider the first-order accurate Euler forward time discretization of Hamilton-Jacobi equation, given as

$$\frac{\phi^{n+1} - \phi^n}{\Delta t} + H(\phi_x, \phi_y, \phi_z) = 0\,, \tag{4.5.19}$$

introducing a new function $\hat{H}(\phi_x^+, \phi_x^-, \phi_y^+, \phi_y^-, \phi_z^+, \phi_z^+)$ called the numerical Hamiltonian (appendix D), rewriting equation (4.5.19) with $\hat{H}$

$$\frac{\phi^{n+1} - \phi^n}{\Delta t} + \hat{H}(\phi_x^+, \phi_x^-, \phi_y^+, \phi_y^-, \phi_z^+, \phi_z^-) = 0\,. \tag{4.5.20}$$

The numerical Hamiltonian is required to be consistent with $H$ such that $\hat{H}(\phi_x, \phi_x, \phi_y, \phi_y, \phi_z, \phi_z) = H(\phi_x, \phi_y, \phi_z)$. It is apparently that one can apply ENO to improve the spatial accuracy of $\hat{H}(\phi_x^+, \phi_x^-, \phi_y^+, \phi_y^-, \phi_z^+, \phi_z^-)$ by substituting third-order accurate $\phi^\pm$ into $\hat{H}$ and to improve the accurate of numerical solutions. The temporal discretization can be generalized straightforwardly to higher-order TVD RK, cf., appendix C.

The CFL condition for equation (4.5.20) is given by

$$\Delta t \max\left\{\frac{H_1}{\Delta x} + \frac{H_2}{\Delta y} + \frac{H_3}{\Delta z}\right\} < 1\,, \tag{4.5.21}$$

where $H_1$, $H_2$, and $H_3$ are derivatives of $H$ with respect to $\phi_x$, $\phi_y$ and $\phi_z$ respectively. The numerical approximation scheme for $\hat{H}$ is given in appendix D.

## 4.6 Construction of Geodesics Using Level Set Equation

As we discussed in the previous context, deriving the photon trajectories in dynamical spacetime in a sensible way is critical before proceeding to formulate the radiative transfer. Since we have proven that we cannot achieve this goal in a four dimensional spacetime and the level set approach is introduced in this Chapter. We will focus on how to implement

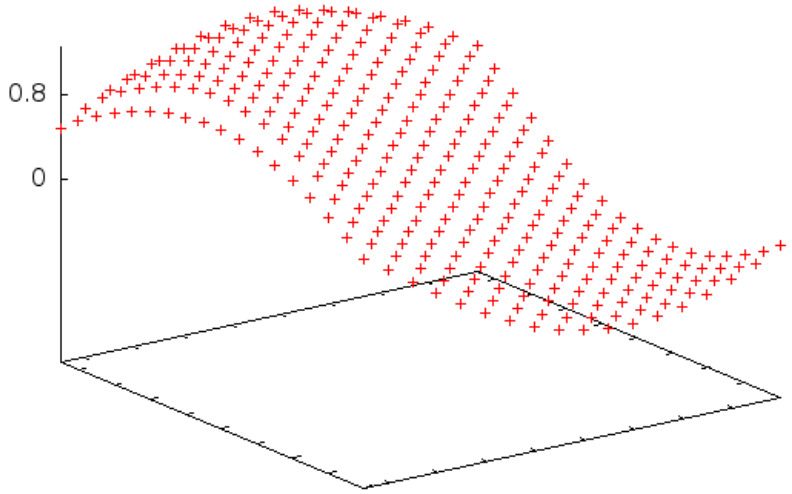


Figure 4.5: This image illustrates the solutions of a 2 dimensional equation $\phi_t + \phi \cdot H(\phi_x, \phi_y) = 0$ at time $t = 0.02$, where $H(u, v) = u + v$, under the initial condition $\phi(0, x, y) = 1/4 + \sin(\pi(x + y)/2)$, given on a grid mesh of $20 \times 20$ points. This equation is solved with 3rd-order accurate ENO method in spatial coordinates and 1st-order accurate TVD RK in temporal coordinate (appendix C).

the specific level set equation (4.4.3) (which is mentioned in the introductory Chapter) to work out the non-constrained geodesics in this section, and in the following context we generalize this method to carry out the geodesics in the Schwarzschild spacetime, Kerr spacetime, ultimately a binary black hole system.

The $n$ dimensional non-constrained geodesics, for which the causal structure is not defined, are generalization of the straight lines in $n$ dimensional Euclidean space. It is also known as the shortest paths between two source regions in an $n$ dimensional surface (where the metric is positive definite). There are several different methods, including analytical and numerical ones to derive shortest paths, nevertheless we will deal with the problem of finding paths of minimal lengths by solving level set equations [133].

The main step is to calculate the equal distance map from the source area (a region or a point). We use the level set method to compute the propagation of equal distance curve on the surface. For simplicity, we consider the geodesics on a 3 dimensional surface without loss of generality.

Let the equal distance curves be denoted by $C'(t)$[17], and the 2 dimensional projected curve $C(t)$, given by

$$C(t) = \tilde{\phi} \circ C'(t) = \{(x, y) \mid (x, y, z) \in C'(t)\}, \tag{4.6.1}$$

[17] $C'$ is actually a function of two parameters $t$ (time) and $u$. For one distance curve, $t$ is a constant and $u$ is variable, while for one geodesic $t$ is a variable and $u$ is a constant.

where $\tilde{\phi}$ is a projection map from 3 dimensional space to 2 dimensional space, $z$ is a function of the surface with arguments $(x, y)$.

From a general theory consequence, we know that the trace of a planar curve propagation can be determined by its normal velocity $V_{\mathrm{N}}$ [136]. Using the planar normal component of the 2 dimensional projected velocity [137], one can construct a differential equation describing the evolution of projected equal distance curve

$$\frac{\partial}{\partial t} C = V_{\mathrm{N}} \vec{n} \,, \tag{4.6.2}$$

the initial conditions are given by

$$C(0) = \{(x, y) \mid (x, y, z) = \partial \mathbf{W}\} \,, \tag{4.6.3}$$

where $\mathbf{W}$ represents the source area and $\partial \mathbf{W}$ represents its boundary, $\vec{n}$ is the planar normal with components $(n_1, n_2)$. $V_{\mathrm{N}}$ depends on the surface gradient ($p = \partial z/\partial x$ , $q = \partial z/\partial y$) and $\vec{n}$, given by

$$V_{\mathrm{N}} = \sqrt{\frac{(1+q^2)n_1^2 + (1+p^2)n_2^2 - 2pqn_1n_2}{1+p^2+q^2}} \,. \tag{4.6.4}$$

Then we can apply the level set method to calculate the propagation of equal distance curves. Let $C(t)$ be represented by the zero level sets of a level set function $\phi(x, y, t)$, such that $\phi$ is positive in the exterior of zero level set and negative in the interior of zero level set. The zero level set is defined as

$$X(t) = \{(x, y) \mid \phi(X(t), t) = 0\} \,. \tag{4.6.5}$$

We can find the evolution rule of $X(t)$, namely the equal distance curve $C(t)$, by finding the evolution rule of level set function $\phi$, i.e., solving the level set equation. Since from (4.6.5) we know that $\phi(X(t), t) = 0$, upon differentiation we get

$$\nabla \phi(X, t) \cdot X_t + \phi_t(X, t) = 0 \,, \tag{4.6.6}$$

substituting relation (4.6.2) and $C(t) = X(t)$ to equation (4.6.6), we obtain

$$\phi_t = -\nabla \phi \cdot V_{\mathrm{N}} \vec{n} \,, \tag{4.6.7}$$

note that the planar normal can be written as $\vec{n} = \phi/|\phi|$ in level set formulation. Take this into consideration, equation (4.6.7) becomes

$$\phi_t = -V_{\mathrm{N}} |\phi| \,. \tag{4.6.8}$$

The initial conditions are set to be

$$\phi(C, 0) = \pm d \,, \tag{4.6.9}$$

where $d$ is the distance from $(x, y)$ on the 2 dimensional plane to $C(0)$, and sign $+$ is taken for exterior region, sign $-$ is taken for interior region.

Using the normal components of velocity $V_{\mathrm{N}}$ (4.6.4), equation (4.6.8) reads

$$\phi_t = \sqrt{\frac{(1+q^2)\phi_x^2 + (1+p^2)\phi_y^2 - 2pq\phi_x\phi_y}{1+p^2+q^2}} \,, \tag{4.6.10}$$

which coincides with equation (4.4.3), where $a = (1+q^2)/(1+p^2+q^2)$, $b = (1+p^2)/(1+p^2+q^2)$ and $c = 2pq/(1+p^2+q^2)$. Parameters $a$, $b$ and $c$ can be determined once at the initialization step. This equation describes the propagation rule of $\phi$ and equal distance curve $C(t)$ can be computed as zero level set.

After solving equation (4.6.10), each grid point on the Cartesian mesh can be assigned a value of distance. To achieve this goal, check if

$$\phi_{i,j}^{n} \cdot \phi_{i,j}^{n-1} < 0\,, \tag{4.6.11}$$

then the distance from source region $\mathbf{R}$ to the point located at $(x_i, y_j)$ at time $t$ is given by

$$d_{i,j} = \mathrm{d}t\left(n - \frac{\phi_{i,j}^{n}}{\phi_{i,j}^{n} - \phi_{i,j}^{n-1}}\right). \tag{4.6.12}$$

It is guaranteed that all points in (4.6.12) are on equal distance contours, i.e., the zero level sets, due to equation (4.6.11).

Let $\mathcal{E}_{\mathbf{W}}(x, y)$ denote the set of equal distance maps from $(x, y)$ to source region $\mathbf{W}$, the shortest paths between regions $\mathbf{W}$ and $\mathbf{A}$ are given by

$$G = \{(x, y) \mid \mathcal{E}_{\mathbf{W}}(x, y) + \mathcal{E}_{\mathbf{A}}(x, y) = g_{\mathrm{m}}\}\,, \tag{4.6.13}$$

where $g_{\mathrm{m}} = \min(\mathcal{E}_{\mathbf{W}} + \mathcal{E}_{\mathbf{A}})$ is the global minimum of the sum of the distance maps from source and destination regions [133].

Nevertheless, this geodesic computation method is based on the fact that the curve has the globally shortest path in the Euclidean space or Riemannian space (locally shortest). Whilst in special relativity result is reversed where the time-like geodesics are globally longest and in general relativity this consequence is uncertain. We need to find new technique to generalize the method to more generic case, inclusive of the 4 dimensional pseudo-Riemannian manifold. Other ways of solving for geodesics by level set method may see reference [138].

# Chapter 5

# Embedding a Four Dimensional Curved Spacetime in a Five Dimensional Manifold

## 5.1 Overview

Chapter 5 looks at the embedding of a 4 dimensional spacetime in the 5 dimensional flat space $\mathbb{R}^5$ and the 5 dimensional non-flat space[4]. We try to solve specific problems arising as consequences of embedding manifolds with causal structure. It is proven that embedding a black hole spacetime does requires extra conditions in addition to diffeomorphism. One needs to analyze the property of manifold after being embedded in an ambient space, and causal structure within the same spacetime is preserved via isometric or conformal embedding maps.

The other problem is more subtle and complicated, which needs careful consideration and advanced geometry knowledge other than those presented in this thesis. It should be noted that the local causal structure within one 4 dimensional manifold is preserved by a conformal or isometric maps. Nevertheless, the metric has no definition between two different 4 dimensional manifolds in the 5 dimensional ambient manifold, as there is no well-defined correlation between two adjacent spacetime foliations. This leads to a problem that local causal structure (aka the local Lorentz structure) is not guaranteed and we might need to recover this before proceeding to derive geodesics using level set method due to numerical reason and theoretical justification. The possible ways have been taken into consideration, including causal set theory [139, 140, 141, 142], where the smooth structure of spacetime is discretized with the causal structure preserved by certain process. Geometric flow will have a consideration in the research. Actually, the propagation of the 4 dimensional manifold in the 5 dimensional manifold is one type of geometrical flow. Moreover, it is expected that this problem can be resolved with purely classically geometrical techniques, where all necessary tools have

[4]This notation is not rigorous enough when an indefinite metric is assigned to the manifold. Actually, this can be type of $\mathbb{R}^{1,4}$, or $\mathbb{R}^{2,3}$ etc., and a final choice would be made in due course.

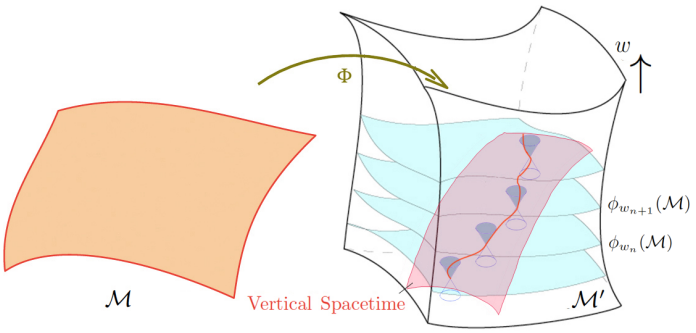


Figure 5.1: This image illustrates the fundamental procedure of construction of a null geodesic of a 4 dimensional spacetime in a 5 dimensional space, two dimensions are suppressed herein. $\mathcal{M}$ stands for the original spacetime, and $\mathcal{M}'$ stands for 5 dimensional ambient space, where $\phi_{w_n}(\mathcal{M})$ represents different spacetime foliations. $w$ denotes the extra dimension. The inclined pink rectangle surface illustrates the vertical spacetime, intersection between hypersurfaces via null surfaces (light cone) and null geodesic.

been introduced in this thesis. The way that we reconstruct Lorentz structure will affect the evolution type of foliation as well as that of null geodesic, which means that we need to develop a new computational technique to construct the geodesics.

The equivalence principle could be recovered once the local causal structure is reconstructed. As we can always find a coordinate system such that in a sufficiently small region, the recovered metric reduces to the Minkowskian metric $\eta_{ab}$.

We will investigate the embedding properties of a 4 dimensional manifold in 5 dimensional flat and non-flat manifolds. We show that the non-flat manifold is a desired target, and we recover the Lorentz structure of two adjacent 4 dimensional foliations for Schwarzschild, dynamical Schwarzschild and Oppenheimer-Snyder spacetimes.

## 5.2 Embedding Basics

Equipped with the level set method, it is rather natural to push-forward the original four dimensional spacetime in a five dimensional space and apply the level set equation to find the evolution of level set surface, i.e., the 4 dimensional foliation and hence to derive the null geodesics. In order to embed a 4 dimensional manifold into a 5 dimensional manifold, we have to use the induced maps introduced in appendix A.

Consider the case of a four dimensional spacetime $\mathcal{M}$, we embed it in a five dimensional real space with distinct diffeomorphism maps $\phi_w$, where $w \in \mathbb{R}$. Using level set method, one cuts the hypersurfaces with null surfaces, on which photons moving, leading to null geodesics. Note that in this formulation, massless particles are travelling through all the horizontal hypersurfaces instead of staying inside any specific surface Fig.5.1. However, one immediately realizes that the geodesics intersect with different coordinate systems in different manifolds $\phi_w(\mathcal{M})$ and a Lorentzian metric cannot be constructed with different hypersurfaces, which means that local causal structure is not carried into the new 5 dimensional space automatically. This problem has to be circumvented with other

techniques. Fig.5.1 illustrates how one achieves this goal graphically. In order to complete this, we need to impose certain further conditions on the embeddings $\phi$, which has a careful reconsideration in section 5.5.

## 5.3 Causal Structure of Spacetime

Causal structure in pseudo-Riemannian manifolds is a consequence of the presence of Lorentz metrics. This is reflected in the phenomena that the motion of all particles and observers have to be light-like (null) or time-like. The causal structure, or local Lorentz structure, cane be well-defined in a 4 dimensional spacetime. Nevertheless, it cannot be carried to a higher dimensional space (between two adjacent foliations) spontaneously after embedding in a 5 dimensional real space unless specific conditions are set with the embedding and the ambient manifold. In order to recover this one needs to study the causal structure of spacetime, which can also be employed to other problem in this project.

In GR, all time-like and null vectors (except zero vector) in the vector space $\mathcal{T}_p$ at any point $p$ in a spacetime can be split into two set portions, one is denoted to be the future part (denoted by $\tilde{F}_p$) and the other is denoted to be the past part (denoted by $\tilde{P}_p$). Elements in $\tilde{F}_p$ are called the future directed time-like (or null) vectors, those in $\tilde{P}_p$ are called the past directed time-like (or null) vectors.

Spacetime $(\mathcal{M}, g_{ab})$ is said to be time orientable if the light cone can be continuously defined, such that there exists a $C^0$ time-like vector field $t^a$, where the value of $t^a|_p$ at each point $p$ on $\mathcal{M}$ lies in the future part of $\mathcal{T}_p$. In general relativity, only the time orientable spacetime is considered as a physical spacetime.

On a light-like (null) hypersurface $\mathcal{W}_n$, there is only one null direction at each point $p \in \mathcal{W}_n$, i.e., ${v_p}^a = k{u_p}^a$, where ${v_p}^a$ and ${y_p}^a$ are tangent vectors at $p$, $k \in \mathbb{R}$. This direction is the same as that of the normal vector $n^a$.

A $C^1$ curve $\gamma$ is called a future (past) directed time-like curve, if the tangents of every point on $\gamma$ are future (past) time-like vectors. A $C^1$ curve $\gamma$ is called a future (past) directed causal curve, if the tangents of every point on $\gamma$ are future (past) null vectors. An observer's worldline is always future directed and time-like.

A light cone at $p$ is defined as a subset of $\mathcal{T}_p$, such that $\{v^a \in \mathcal{T}_p \mid g_{ab}v^a v^b = 0\}$.

Chronological (time-like) future (past) $\mathrm{I}^+(p)$ ($\mathrm{I}^-(p)$) of $p \in \mathcal{M}$ is a subset of manifold $\mathcal{M}$, satisfying

$$\mathrm{I}^+(p) := \{q \in \mathcal{M} \mid \exists \text{ Future directed time-like curve from } p \text{ to } q\}^5. \tag{5.3.1}$$

The chronological future (past) $\mathrm{I}^+(p, Nei)$ ($\mathrm{I}^-(p, Nei)$) of $p$ relative to a neighbourhood $Nei$ is defined as

$$\mathrm{I}^+(p, N) := \{q \in Nei \mid \exists \text{ Future directed time-like curve from } p \text{ to } q \text{ within region } Nei\}. \tag{5.3.2}$$

[5]Herein, a curve $\gamma$ from $p$ to $q$ is an image of $[a, b] \in \mathbb{R}$, where $p = \gamma(a)$ and $q = \gamma(b)$.

Note that $\mathrm{I}^+(p)$=$\mathrm{I}^+(p,\mathcal{M})$. $\mathrm{I}^+(p,Nei)$ is not necessarily equal to $\mathrm{I}^+(p)\cap N$. The minus sign is chosen for the 'past'.

The causal future (past) $\mathrm{J}^+(p)$ ($\mathrm{J}^-(p)$) of $p\in\mathcal{M}$ is a subset of manifold $\mathcal{M}$, satisfying

$$\mathrm{J}^+(p) := \{q\in\mathcal{M} \mid \exists \text{ Future directed causal curve from } p \text{ to } q\}. \quad (5.3.3)$$

The causal future (past) $\mathrm{J}^+(p,Nei)$ ($\mathrm{J}^-(p,Nei)$) of $p$ relative to a neighbourhood $Nei$ is defined as

$$\mathrm{J}^+(p,Nei) := \{q\in Nei \mid \exists \text{ Future directed causal curve from } p \text{ to } q \text{ within region } Nei\}. \quad (5.3.4)$$

$\mathrm{J}^-(p)$ and $\mathrm{J}^-(p,Nei)$ can be defined dually. $\mathrm{I}^+(p)$, $\mathrm{I}^-(p)$, $\mathrm{J}^+(p)$ and $\mathrm{J}^-(p)$ are collectively called the causal structure of $\mathcal{M}$.

We then have the following propositions derived from the above definitions

$$r\in\mathrm{I}^+(p),\ q\in\mathrm{I}^+(r)\Rightarrow q\in\mathrm{I}^+(p),\ \text{i.e. } \mathrm{I}+\mathrm{I}=\mathrm{I}, \quad (5.3.5)$$
$$r\in\mathrm{J}^+(p),\ q\in\mathrm{I}^+(r)\Rightarrow q\in\mathrm{I}^+(p),\ \text{i.e. } \mathrm{J}+\mathrm{I}=\mathrm{I}, \quad (5.3.6)$$
$$r\in\mathrm{I}^+(p),\ q\in\mathrm{J}^+(r)\Rightarrow q\in\mathrm{I}^+(p),\ \text{i.e. } \mathrm{I}+\mathrm{J}=\mathrm{I}. \quad (5.3.7)$$

A neighbourhood $Nei$ of $p\in\mathcal{M}$ is called a normal neighbourhood, if there exists an open set $\hat{\mathcal{T}}_p$ of the vector space $\mathcal{T}_p$ where $\mathbf{0}\in\hat{\mathcal{T}}$, such that the exponential map $\exp_p:\ \hat{\mathcal{T}}_p\to Nei$ is a diffeomorphism.

A neighbourhood $Nei$ of $p\in\mathcal{M}$ is called a convex neighbourhood, if $\forall\ q,\ r\in Nei$, there exists a unique geodesic connecting $q$ and $r$. Note that not all neighbourhoods are convex neighbourhoods, even in the cases of Minkowskian and Euclidean manifolds. Given a convex neighbourhood, such that it is a normal neighbourhood, then $Nei$ of $p$ is called a convex normal neighbourhood.

From its definition we know that a convex normal neighbourhood is an open set. Every point in any spacetime must have a convex normal neighbourhood. If $Nei$ is a normal neighbourhood of $p\in\mathcal{M}$, $Nei$ needs not to be a normal neighbourhood for the other points $q\in Nei$, $q\neq p$. Whereas the statement is true when $Nei$ is a convex normal neighbourhood, see Hicks (1965) for proofs of the second and third corollaries.

Given a convex normal neighbourhood $Nei$ and $p$, $q\in Nei$, there exists only one geodesic connecting $p$ and $q$, in addition, we have the following propositions

(a) If $q\in\mathrm{I}^+(p,Nei)$, then the geodesic from $p$ to $q$ must be time-like in $Nei$.

(b) If $q\in\mathrm{J}^+(p,Nei)-\mathrm{I}^+(p,Nei)$, $p\neq q$, then the geodesic from $p$ to $q$ must be null in $Nei$.

(c) If $q\in\mathrm{J}^+(p,Nei)-\mathrm{I}^+(p,Nei)$, $p\neq q$, then the future directed causal curve from $p$ to $q$ must be a null geodesic in $Nei$.

The above results imply that the causal properties of an arbitrary spacetime within convex normal neighbourhoods are very similar to that of a Minkowskian spacetime. And it becomes more complicated outside a convex normal neighbourhood. Nevertheless, the third proposition is not restricted by this situation, given in the following statement.

In any spacetime, if $q \in \mathrm{J}^+(p) - \mathrm{I}^+(p)$, then the future directed causal curve from $p$ to $q$ must be a null geodesic. And it should be noted that the statement: If there exists a future directed null geodesic from $p$ to $q$, then $q \in \mathrm{J}^+p - \mathrm{I}^+(p)$, is a false proposition.

The chronological future of a subset $\mathcal{W} \subset \mathcal{M}$ is defined as

$$\mathrm{I}^+(\mathcal{W}) := \bigcup_{p\in\mathcal{W}} \mathrm{I}^+(p)\,. \tag{5.3.8}$$

Note that

$$\begin{aligned} \mathrm{I}^+[\mathrm{I}^+(\mathcal{W})] &= \mathrm{I}^+(\mathcal{W})\,, \\ \mathrm{I}^-[\mathrm{I}^-(\mathcal{W})] &= \mathrm{I}^+(\mathcal{W})\,, \\ \mathrm{J}^+[\mathrm{J}^+(\mathcal{W})] &= \mathrm{J}^+(\mathcal{W})\,, \\ \mathrm{J}^-[\mathrm{J}^-(\mathcal{W})] &= \mathrm{J}^-(\mathcal{W})\,. \end{aligned} \tag{5.3.9}$$

The causal future of subset $\mathcal{W} \subset \mathcal{M}$ is defined as

$$\mathrm{J}^+(\mathcal{W}) := \bigcup_{p\in\mathcal{W}} \mathrm{J}^+(p)\,. \tag{5.3.10}$$

The chronological and causal past of subset $\mathcal{W}$, denoted by $\mathrm{I}^-(\mathcal{W})$ and $\mathrm{J}^-(\mathcal{W})$, can be dually defined.

The subset $\mathcal{W} \subset \mathcal{M}$ is called an achronal set, if there does not exist $p\,,\ q \in \mathcal{W}$, such that $q \in \mathrm{I}^+(p)$, i.e., $\mathrm{I}^+(\mathcal{W}) \cap \mathcal{W} = \varnothing$.

All time-like curves and time-like hypersurfaces are obviously not achronal set. Some of the space-like curves and hypersurfaces are not achronal set.

Suppose $I$ is an interval in $\mathbb{R}\,,\ \gamma :\ I \to \mathcal{M}$ is a future directed causal curve. $p \in \mathcal{M}$ is called the future endpoint of $\gamma$, if for any neighbourhoods $Nei$ of $p$, there exists $t_0 \in I$ such that $\gamma(t) \in Nei\,,\ \forall\ t \in I\,,\ t \geq t_0$. The past endpoint of $\lambda$ can be dually defined.

In Schwarzschild spacetime, the future directed causal curves that fall into singularity have no future endpoint. Intuitively, the endpoint is locating at $r = 0$ in the Schwarzschild coordinate system, which is not belonging to the spacetime.

A curve without a future endpoint is called future inextendible. Past inextendible property can be dually defined.

Spacetime is said to satisfy the chronological condition if it does not have closed time-like curve. Spacetime which is not chronological is considered as a causally violated spacetime and possesses the worst causality. However, a chronological spacetime admits closed null (causal) curves for photons or any massless particles is considered as possessing a rather weak causal condition. One can improve the situation by introducing more restrictions.

Spacetime is said to satisfy the causality condition if there is no closed causal curves (except isolated-point line), which is called a causal spacetime.

The causal condition of spacetime can be enhanced by introducing further restrictions. A spacetime $(\mathcal{M}, g_{ab})$ is said to satisfy the strong causality condition, if $\forall\ p \in \mathcal{M}$, and its neighbourhood $p \in Nei\,,\ \exists$ $Nei' \subset Nei$ such that there is no causal curves passing through $Nei'$

more than once, where $Nei'$ is a neighbourhood. Such spacetime is called a strong causal spacetime.

The causality of a strongly causal spacetime is stronger than that of a causal spacetime. Nevertheless, the stability of a strongly causal spacetime is not as elegant as what physicists expect. One substitution of this is to introduce the stably causal spacetime.

A spacetime $(\mathcal{M}, g_{ab})$ is said to satisfy the stably causal condition, if there exists a $C^0$ time-like vector field $t^a$, such that spacetime $(\mathcal{M}, \tilde{g}_{ab})$ satisfies the chronological condition, where $\tilde{g}_{ab} = g_{ab} - t_a t_b$ , $t_a = g_{ab}t^b$. A stably causal spacetime allows an infinitesimal perturbation to the metric $g_{ab}$ without violating the causal structure of $(\mathcal{M}, g_{ab})$. To explain this, we introduce the following lemma. Let $p$ be a point in $(\mathcal{M}, g_{ab})$ , $t^a \in \mathcal{T}_p$ be a time-like vector, then at point $p$, for the Lorentzian metric $\tilde{g}_{ab} = g_{ab} - t_a t_b$, if

$$g_{ab}v^a v^b \leq 0 \Rightarrow \tilde{g}_{ab}v^a v^b < 0\,, \tag{5.3.11}$$

which implies that the light cone encoded by perturbing the old metric to $\tilde{g}_{ab}$ is 'wider' than that of $g_{ab}$. If the spacetime satisfies stably causal condition, then the causal structure of the perturbed spacetime $(\mathcal{M}, \tilde{g}_{ab})$ is not violated, indicating that spacetime is stable under an infinitesimal perturbation.

A spacetime $\mathcal{M}$ has stable causality, if and only if (iff) there exists a differentiable function $f$ on $\mathcal{M}$ such that

$$\nabla^a f = g^{ab}\nabla_b f\,, \tag{5.3.12}$$

is a time-like vector field. $f$ is called the global time function. See Wald (1984) or Hawking and Ellis (1973) for proofs.

The existence of a global time function $f$ implies that the spacetime possesses a favourable causal structure. Since a time-like $\nabla^a f$ leads to a space-like hypersurface with equal value of $f$. The whole spacetime can be decomposed with respect to the one parameter space-like hypersurface congruence $\{\Sigma_f\}$, each $\Sigma_f$ is equivalent to the whole 'space' at time $f$. Accordingly, one can define $f$ to be the 'time' $t$ and the value of $f$ represents the instant time at each spacetime point. In addition, the future directed property of $\nabla^a f$ is satisfied by choosing the sign of $f$. This freedom guarantees that any possibility of causality violation is forbidden.

A stably causal spacetime must be strongly causal. There are more stronger conditions, e.g., causally simple, than stable causality which we will not discuss them here.

A complete hierarchy of the causality of a spacetime, from weakest to strongest, is listed as follow

$$\text{chronological} < \text{causal} < \text{strong causality} < \text{stably causal}\,. \tag{5.3.13}$$

Other detailed conditions can be inserted to reflect more delicate hierarchy, aka the causal ladder.

The future domain of influence of $\mathcal{W} \subset \mathcal{M}$ is defined as the chronological future $\mathrm{I}^+(\mathcal{W})$ (or causal future $\mathrm{J}^+(\mathcal{W})$) of $\mathcal{W}$.

Suppose $\mathcal{W}$ is a closed[6] achronal subset, the future domain of dependence of $\mathcal{W}$ is defined as

$$\mathrm{D}^+(\mathcal{W}) := \{p \in \mathcal{M} \mid \text{Any past inextendible causal curve starting from } p \text{ has no intersection with } \mathcal{W}\}. \tag{5.3.14}$$

The past domain of dependence $\mathrm{D}^-(\mathcal{W})$ of $\mathcal{W}$ can be defined dually. The (whole) domain of dependence of $\mathcal{W}$ is given as

$$\mathrm{D}(\mathcal{W}) := \mathrm{D}^+(\mathcal{W}) \bigcup \mathrm{D}^-(\mathcal{W}) . \tag{5.3.15}$$

$\mathrm{D}^+(\mathcal{W}) \cap \mathrm{I}^-(\mathcal{W}) = \varnothing$.

Suppose $\gamma'$ is a past inextendible causal curve of $p$, then $\forall\ p' \in \mathrm{I}^+(p)$, there exist past inextendible time-like curves $\gamma$ passing through $p'$, such that $\gamma \subset \mathrm{I}^+(\gamma')$.

An achronal closed set $\mathcal{W}$ is called a Cauchy surface, if $D(\mathcal{W}) = \mathcal{M}$. Note that not all spacetime has Cauchy surface.

Suppose $\mathcal{W}$ is a Cauchy surface, then

$$\mathcal{M} = \mathcal{W} \bigcup \mathrm{I}^+(\mathcal{W}) \bigcup \mathrm{I}^-(\mathcal{W}) . \tag{5.3.16}$$

If $\mathcal{W}$ is a Cauchy surface, then any two-way inextendible causal curve must pass through all of $\mathcal{W}$, $\mathrm{I}^+(\mathcal{W})$ and $\mathrm{I}^-(\mathcal{W})$.

The edge of a closed achronal subset $\mathcal{W}$ is defined as

$$\begin{aligned} edge(\mathcal{W}) := \{p \in \mathcal{W} \mid & \text{For any neighbourhood } Nei \text{ of } p, \text{ such that } q \in \\ & \mathrm{I}^+(p, Nei),\ r \in \mathrm{I}^-(p, Nei), \exists \text{ future directed time-} \\ & \text{like curve } \gamma \text{ from } r \text{ to } q, \text{ with } \gamma \subset Nei \\ & \text{and } \gamma \cap \mathcal{W} = \varnothing\}. \end{aligned} \tag{5.3.17}$$

$edge(\mathcal{W}) = \varnothing$ if $\mathcal{W}$ is a Cauchy surface. This is also know as Cauchy surface has no edge.

A spacetime is said to be globally hyperbolic, if it has a Cauchy surface. Globally hyperbolic condition is stronger than stably causal condition and is the strongest causal condition. Globally hyperbolic spacetime is of physical significance in GR, and its Cauchy surface is in general explained as the whole space at certain temporal point due to achronal property. The definition of Cauchy surface shows that everything happens in spacetime is determined by the initial data on the Cauchy surface. On the contrary, a non-globally hyperbolic spacetime violated determinism, since the whole history of spacetime cannot be determined by all data at the initial time. Throughout this thesis, thereof, all physical spacetimes are globally hyperbolic, unless otherwise specified.

## 5.4 Isometric and Conformal Embedding

In differential geometry (DG), diffeomorphism maps are critical tools in transferring differential structure from one manifold to another. Nevertheless, this type of map does not impose strong conditions on transformation for which sometimes are necessary in specific problems. In

[6] See Wald (1984) for a complete explanation of a closed subset.

Riemannian and pseudo-Riemannian geometries, an isometric embedding mapping occurs frequently, which preserves the metric (distance) while the rank-two tensor is carried into different manifold.

Isometry, or isometric embedding, is a diffeomorphism between two pseudo-Riemannian manifolds $(\mathcal{M}, g_{ab})$ and $(\mathcal{N}, \tilde{g}_{ab})$, $\phi : \mathcal{M} \to \mathcal{N}$, such that

$$\tilde{g}_{ab} = (\phi_* g)_{ab} \,. \tag{5.4.1}$$

Herein, no extra restriction is imposed on the two manifolds, i.e., $\mathcal{M}$ and $\mathcal{N}$ could be any type of pseudo-Riemannian manifold with an indefinite metric, where a 4 dimensional spacetime with a Lorentzian metric and a 5 dimensional pseudo-Euclidean space $\mathbb{R}^{2,3}$ are inclusive.

Nevertheless, isometric embedding is a rather strong condition which might require the ambient manifold to satisfy certain conditions. This can be cured by releasing the constraints to enlarge the scope of the class of mappings, among which is to introduce the notion of conformal transformation.

Suppose there are two metric fields $g_{ab}$ and $\tilde{g}_{ab}$ with arbitrary but same signatures, on manifold $\mathcal{M}$. If there exists a $C^\infty$ function $\Omega$ which is positive everywhere on manifold, such that

$$\tilde{g}_{ab} = \Omega^2 g_{ab} \,, \tag{5.4.2}$$

$\tilde{g}_{ab}$ is called conformally transformed from $g_{ab}$, scalar field $\Omega$ is called the conformal factor. It is easy to prove that $\tilde{g}^{ab} = \Omega^{-2} g^{ab}$. Since there exist two metric fields on $\mathcal{M}$, it should be specified when raising and lowering the indices of tensors.

Suppose we have two covariant derivatives $\nabla_a$ and $\tilde{\nabla}_a$ which are compatible with $g_{ab}$ and $\tilde{g}_{ab}$ respectively. We then have the relation

$$\tilde{\nabla}_a w_b = \nabla_a w_b - C^c{}_{ab} w_c \,, \tag{5.4.3}$$

where $\forall\, w_a \in \mathcal{T}(0,1)$. Consider (E.0.14) and the metric adapted covariant derivatives $\tilde{\nabla}_a$, $\nabla_a$, we have

$$C^c{}_{ab} = \frac{1}{2}\tilde{g}^{cd}(\nabla_a \tilde{g}_{bd} + \nabla_b \tilde{g}_{ad} - \nabla_d \tilde{g}_{ab}) \,. \tag{5.4.4}$$

On the other hand, using (5.4.2), yields

$$\nabla_a \tilde{g}_{bd} = \nabla_a(\Omega^2 g_{bd}) = 2\Omega g_{bd} \nabla_a \Omega \,. \tag{5.4.5}$$

Substituting (5.4.5) to (5.4.4), we get

$$\begin{aligned} C^c{}_{ab} &= \Omega^{-1} g^{cd}(g_{bd}\nabla_a \Omega + g_{ad}\nabla_b \Omega - g_{ab}\nabla_d \Omega) \\ &= \delta^c{}_{(a}\nabla_{b)} \ln \Omega - g_{ab} g^{cd} \nabla_d \ln \Omega \,. \end{aligned} \tag{5.4.6}$$

Given a spacetime $(\mathcal{M}, g_{ab})$, $\tilde{g}_{ab}$ and $g_{ab}$ are conformal metrics, $v^a$ is an arbitrary vector field. Then the following facts are satisfied

$$\begin{aligned} g_{ab}v^a v^b > 0 &\Rightarrow \tilde{g}_{ab}v^a v^b > 0 \,, \\ g_{ab}v^a v^b = 0 &\Rightarrow \tilde{g}_{ab}v^a v^b = 0 \,, \\ g_{ab}v^a v^b < 0 &\Rightarrow \tilde{g}_{ab}v^a v^b < 0 \,. \end{aligned} \tag{5.4.7}$$

These relations imply that Lorentzian structure is not changed under a conformal transformation. Nevertheless, these properties are not applicable to geodesics in general, except for specific class.

Suppose $\gamma(\lambda)$ is a null geodesic with respect to $g_{ab}$ , $\lambda$ is an affine parameter, such that $T^a\nabla_a T^b = 0$ where $T^a$ is the tangent vector. Consider a conformal metric $\tilde{g}_{ab}$, we have $\tilde{\nabla}_a T^b = \nabla_a T^b + C^b{}_{ac}T^c$. Accordingly,

$$\begin{aligned} T^a\tilde{\nabla}_a T^b &= T^a\nabla_a T^b + C^b{}_{ac}T^aT^c \\ &= C^b{}_{ac}T^aT^c \\ &= 2T^aT^c\delta^b{}_{(a}\nabla_{c)}\ln\Omega - T^aT^c g_{ac}g^{bd}\nabla_d\ln\Omega \\ &= 2T^c\nabla_c\ln\Omega T^b - T^aT^c g_{ac}g^{bd}\nabla_d\ln\Omega\,. \end{aligned} \tag{5.4.8}$$

Note that $\gamma$ is a null geodesic, with $T^cT^a g_{ac} = 0$. Equation (5.4.8) becomes

$$T^a\tilde{\nabla}_a T^b = 2T^c\nabla_c\ln\Omega T^b = \alpha' T^b\,, \tag{5.4.9}$$

where $\alpha' \equiv 2T^c\nabla_c\ln\Omega$ is a function on $\gamma(\lambda)$. One can always reparameterize $\gamma$ such that $\gamma(\tilde{\lambda})$ is a null geodesic with respect to $\tilde{g}_{ab}$ by selecting appropriate $\tilde{\lambda}$. The relation between two parameters is given by

$$\frac{\mathrm{d}\tilde{\lambda}}{\mathrm{d}\lambda} = c\Omega^2\,, \tag{5.4.10}$$

where $c$ is a non-zero constant. Thereof, null geodesic is invariant under a conformal transformation. Nevertheless, in general, time-like and space-like geodesics do not possess such property.

Suppose $(\mathcal{M}, g_{ab})$ and $(\tilde{\mathcal{M}}, \tilde{g}_{ab})$ are pseudo-Riemannian manifolds, a diffeomorphism $\phi : \mathcal{M} \to \tilde{\mathcal{M}}$ is called a conformal diffeomorphism, if there exists a $C^\infty$ function $\Omega$ which is positive everywhere on $\tilde{\mathcal{M}}$, such that $\tilde{g}_{ab} = \Omega^2(\phi_* g)_{ab}$. If the dimension of $\tilde{\mathcal{M}}$ is greater than the dimension of $\mathcal{M}$, then $\phi$ is called a conformal embedding.

The Riemann curvature $R_{abc}{}^d$ of $\nabla_a$ and the Riemann curvature $\tilde{R}_{abc}{}^d$ of $\tilde{\nabla}_a$ have the following relation

$$\begin{aligned} \tilde{R}_{abc}{}^d = \;& R_{abc}{}^d + 2\delta^d_{[a}\nabla_{b]}\nabla_c\ln\Omega - 2g^{de}g_{c[a}\nabla_{b]}\nabla_e\ln\Omega + 2(\nabla_{[a}\ln\Omega)\delta^d_{b]}\nabla_c\ln\Omega \\ & - 2(\nabla_{[a}\ln\Omega)g_{b]c}g^{de}\nabla_e\ln\Omega - 2g_{c[a}\delta^d_{b]}g^{ge}(\nabla_e\ln\Omega)\nabla_g\ln\Omega\,. \end{aligned} \tag{5.4.11}$$

The Weyl tensor is conformally invariant, i.e., $C_{abcd} = \tilde{C}_{abcd}$.

An $n$ dimensional pseudo-Riemannian manifold $(\mathcal{M}, g_{ab})$ is said to be conformally flat, iff $g_{ab}$ is conformal to an $n$ dimensional flat metric $\hat{\eta}_{ab}$, i.e.

$$g_{ab} = \Omega^2\hat{\eta}_{ab}\,. \tag{5.4.12}$$

A corollary resulting from this definition states that any 2 dimensional pseudo-Riemannian manifold is conformally flat.

## 5.5 Embedding a 4 Dimensional Manifold with a Lorentzian Metric

We investigate the embedding map, with certain conditions, from a 4 dimensional manifold into a higher dimensional flat manifold in this section. It is apparently that specific conditions should be imposed on the

embedded metric when the 4 dimensional spacetime is embedded into the higher dimensional metric space. Nevertheless, a natural choice is an isometry, or a conformal embedding, as it is not expected to have two different metrics defined on the same manifold, $\mathbb{R}^5$. Accordingly, the geometric properties might be maintained, including the local Lorentz relation for both isometric and conformal embeddings[7].

We will demonstrate that how one can embed a spacetime around a black hole into a 5 dimensional manifold. Consider a local coordinate system $(\mathcal{O}, \psi_x)$ in the original manifold $\mathcal{M}$. We embed $\mathcal{M}$ to $\mathbb{R}^5$ by a diffeomorphism $\phi$. For simplicity, we want to assume that one coordinate for $\phi(\mathcal{O}) \in \mathbb{R}^5$ is fixed to be constant (this guarantees that $\phi(\mathcal{O})$ is a 4 dimensional patch). Nevertheless, this situation is satisfied only for a flat or a conformally flat spacetime, i.e., when the Weyl curvature vanishes, which turns out to be not the case for a more general curved spacetime, for example a Schwarzschild or a Kerr black hole. Consider this effect, the embedding manifold is supposed to be more flexible which is a hypersurface of a 5 dimensional Euclidean space, denoted by $w$[8]. Moreover, $\mathcal{O}$ is carried into $\mathbb{R}^5$ in the following manner

$$\phi_w : \mathcal{O} \to \mathcal{R}, \quad \mathcal{R} \subsetneq \mathbb{R}^5, \tag{5.5.1}$$

where $\mathcal{R}$ is a real subset of $\mathbb{R}^5$. Let $(\mathcal{R}', \psi_y)$ denotes the local coordinate patch such that $\mathcal{R} \subset \mathcal{R}'$, for which

$$\psi_y : \mathcal{R} \to \mathcal{O}'_y \subset \mathbb{R}^5, \tag{5.5.2}$$

is a diffeomorphism. For these two given coordinate systems, one can obtain the diffeomorphic transition function. For $(\mathcal{O}, \psi_x)$, we have

$$\psi_x : \mathcal{O} \to \mathcal{O}'_x \subset \mathbb{R}^4, \quad \mathcal{O}'_x = \{x^\mu \mid (x^0, x^1, x^2, x^3) \in \mathbb{R}^4\}. \tag{5.5.3}$$

Similar for $(\mathcal{R}, \psi_y)$

$$\psi_y : \mathcal{R} \to \mathcal{O}'_y \subset \mathbb{R}^5, \quad \mathcal{O}'_y = \{y^\mu \mid (y^0, y^1, y^2, y^3, y^4) \in \mathbb{R}^5\}. \tag{5.5.4}$$

The transition function between them is given by

$$\psi_y \circ \phi_w \circ \psi_x^{-1} \begin{cases} \mathcal{O}'_x \to \mathcal{O}'_y, \\ x^\mu \to y^\nu(x^\nu). \end{cases} \tag{5.5.5}$$

Consider the metric $g_{ab} = g_{\mu\nu}(\mathrm{d}x^\mu)_a(\mathrm{d}x^\nu)_b$ in $\mathcal{O}'_x$. It is pushed-forward by an induced map

$$\phi_{w*} \begin{cases} g_{ab}(x) \to \tilde{g}_{ab}(y), \\ g_{\mu\nu} \to \tilde{g}_{\mu\nu}, \end{cases} \tag{5.5.6}$$

where the explicit coordinate transformation is given by

$$\tilde{g}_{\sigma\rho} = \frac{\partial x^\mu}{\partial y^\sigma}\frac{\partial x^\nu}{\partial y^\rho} g_{\mu\nu} = A_\sigma{}^\mu A_\rho{}^\nu g_{\mu\nu}, \tag{5.5.7}$$

[7] In fact, the isometry preserves the whole geometry, while the conformal embedding only maintains the null geodesic.

[8] Herein, actually, $w$ is a global smooth function defined on $\mathbb{R}^5$ and is a constant for a 4 dimensional hypersurface spacetime.

where we have used $A_{\sigma}{}^{\mu}$ to represent transformation matrix.

The metric $\det g = \det(g_{\mu\nu})$ is degenerate (a zero-determinant matrix) at the singularity. Then for the induced metric $\tilde{g}_{\sigma\rho}$ we have

$$\begin{aligned}\det g' &= \det(g'_{\ \sigma\rho}) \\ &= \det(A_{\sigma}{}^{\mu} A_{\rho}{}^{\nu} g_{\mu\nu}) \\ &= \det(A_{\sigma}{}^{\mu}) \det(A_{\rho}{}^{\nu}) \det(g_{\mu\nu}) \\ &= (\det A)^2 \det g \,. \end{aligned} \tag{5.5.8}$$

We used that the determinant of matrices product is equal to the product of matrices determinant. Requiring that $\det(A)$ is finite and non-vanishing at all points in $(\mathcal{O}, \psi_x)$, and recall that for a diffeomorphism its inverse map is a smooth map, which guarantees that $\det(A)$ is finite and $A$ is invertible. It is proven that $\det g'$ is degenerate, which implies a singularity remains a singularity.

For a coordinate singularity, consider another coordinate patch $(\mathcal{O}', \psi_{x'})$, such that $\det g'$ is non-degenerate, then $\det \tilde{g}$ satisfies

$$\det \tilde{g} = \det(A')^2 \det g' \,, \tag{5.5.9}$$

is non-degenerate. Implying that a coordinate singularity remains a coordinate singularity. In this sense, the properties of singularities have not been changed after being pushed-forward by a diffeomorphism embedding, i.e., coordinate singularities remain spacetime points whilst spacetime singularities remain ideal points (not spacetime points).

Nevertheless a diffeomorphism is not a good choice to push-forward a spacetime, even when there exist singularities on the original spacetime. As we want to preserve the local geometric properties of the 4 dimensional manifold, hence an isometric or a conformal embedding would be more appropriate. For example, the most trivial case is to embed the 4 dimensional Minkowskian spacetime in the 5 dimensional Euclidean space $\mathbb{R}^{1,4}$. This can be done in the following procedure

$$\phi_w \begin{cases} \mathbb{L}^4 \to \mathbb{R}^5 \,, \\ x^{\mu} \mapsto u^{\rho} \,, \end{cases} \tag{5.5.10}$$

with explicit coordinate transformation

$$\begin{aligned} &u^{\mu} = x^{\mu} \,, \ i = 0 \,, \ 1 \,, \ 2 \,, \ 3 \,, \\ &u^4 = con \,, \end{aligned} \tag{5.5.11}$$

where *con* is a constant. This is actually the $u^4 = con$ plane in $\mathbb{R}^{1,4}$. Alternatively, we can also interpret the embedded spacetime as a hypersurface (level surface) $\phi_w(\mathbb{L}^4) \to w - con = 0$ in $\mathbb{R}^{1,4}$ by a constant function $w$ defined on the 5 dimensional space. In this special case, $w = u^4 = con$.

However in the case of a black hole system, where the manifold is highly curved due to the strong gravitational field, one cannot simply embed everything to a 5 dimensional flat manifold without extra conditions as an isometric embedding may never exist for the case we are considering. We will have to consider the isometric embedding of a 4

dimensional manifold in a 5 dimensional flat manifold $\mathbb{R}^5$ first and if this cannot be carried out, we then have to apply the conformal embedding. And we will introduce a conformal factor $\Omega$ for both isometric and conformal embedding, where the factor is set to be 1 for isometric map. Let us consider the simplest case first, Schwarzschild spacetime.

The metric components of Schwarzschild metric in Schwarzschild coordinate system $x^\mu \sim (t, r, \varphi, \theta)$ are given by

$$g_{\mu\nu} = \begin{bmatrix} -(1-\frac{2M}{r}) & 0 & 0 & 0 \\ 0 & (1-\frac{2M}{r})^{-1} & 0 & 0 \\ 0 & 0 & r^2\sin^2\theta & 0 \\ 0 & 0 & 0 & r^2 \end{bmatrix}. \tag{5.5.12}$$

Suppose that the whole isolated system is pushed-forward in a coordinate system $u^\gamma$ of a 5 dimensional Euclidean manifold. The transformation for the metric is given as

$$g_{\mu\nu} = \frac{\partial u^\gamma}{\partial x^\mu}\frac{\partial u^\rho}{\partial x^\nu}\delta_{\gamma\rho}\,. \tag{5.5.13}$$

The components of Euclidean metric is given by

$$\delta_{\gamma\rho} = \begin{bmatrix} 1 & 0 & 0 & 0 & 0 \\ 0 & 1 & 0 & 0 & 0 \\ 0 & 0 & 1 & 0 & 0 \\ 0 & 0 & 0 & 1 & 0 \\ 0 & 0 & 0 & 0 & 1 \end{bmatrix}, \tag{5.5.14}$$

where we have demanded that the coordinate is a Cartesian coordinate. Substitute (5.5.12) and (5.5.14) into (5.5.13) we obtain

$$\left(\frac{\partial u^0}{\partial t}\right)^2 + \left(\frac{\partial u^1}{\partial t}\right)^2 + \left(\frac{\partial u^2}{\partial t}\right)^2 + \left(\frac{\partial u^3}{\partial t}\right)^2 + \left(\frac{\partial u^4}{\partial t}\right)^2 = -\Omega^2\left(1-\frac{2M}{r}\right), \tag{5.5.15}$$

$$\left(\frac{\partial u^0}{\partial r}\right)^2 + \left(\frac{\partial u^1}{\partial r}\right)^2 + \left(\frac{\partial u^2}{\partial r}\right)^2 + \left(\frac{\partial u^3}{\partial r}\right)^2 + \left(\frac{\partial u^4}{\partial r}\right)^2 = \Omega^2\left(1-\frac{2M}{r}\right)^{-1}, \tag{5.5.16}$$

$$\left(\frac{\partial u^0}{\partial \varphi}\right)^2 + \left(\frac{\partial u^1}{\partial \varphi}\right)^2 + \left(\frac{\partial u^2}{\partial \varphi}\right)^2 + \left(\frac{\partial u^3}{\partial \varphi}\right)^2 + \left(\frac{\partial u^4}{\partial \varphi}\right)^2 = \Omega^2 r^2\sin^2\theta\,, \tag{5.5.17}$$

$$\left(\frac{\partial u^0}{\partial \theta}\right)^2 + \left(\frac{\partial u^1}{\partial \theta}\right)^2 + \left(\frac{\partial u^2}{\partial \theta}\right)^2 + \left(\frac{\partial u^3}{\partial \theta}\right)^2 + \left(\frac{\partial u^4}{\partial \theta}\right)^2 = \Omega^2 r^2\,, \tag{5.5.18}$$

$$\sum_{i=0}^{4}\left(\frac{\partial u^i}{\partial x^\mu}\right)\left(\frac{\partial u^i}{\partial x^\nu}\right) = 0\,, \tag{5.5.19}$$

for $\mu, \nu = 0, 1, 2, 3$ and $\mu < \nu$. Solutions to the equation set and other $n$ dimensional Schwarzschild solutions to Einstein's equation have not been carried out by researchers in an isometric way. Instead, several isometric embedding maps have been made into a 6 dimensional Minkowskian space [143, 144], which means that the conformal embedding into the 6 dimensional Minkowskian space must exist as a conformal

condition is weaker than an isometric condition. In addition to embedding the full Schwarzschild spacetime into a 5 dimensional Euclidean space, mathematicians have successfully proven that space-like hypersurface of Schwarzschild solution can be isometrically embedded into a 5 dimensional Euclidean space [145, 146].

A Kerr spacetime is more complicated than the Schwarzschild case as the spherically symmetric property reduces to axisymmetry, leading to the presence of a cross term in the components of Kerr spacetime metric. Taking this into consideration, we may obtain the following equations

$$\left(\frac{\partial u^0}{\partial t}\right)^2+\left(\frac{\partial u^1}{\partial t}\right)^2+\left(\frac{\partial u^2}{\partial t}\right)^2+\left(\frac{\partial u^3}{\partial t}\right)^2+\left(\frac{\partial u^4}{\partial t}\right)^2=-\Omega^2\left(1-\frac{2Mr}{\tilde{\Sigma}}\right), \tag{5.5.20}$$

$$\left(\frac{\partial u^0}{\partial r}\right)^2+\left(\frac{\partial u^1}{\partial r}\right)^2+\left(\frac{\partial u^2}{\partial r}\right)^2+\left(\frac{\partial u^3}{\partial r}\right)^2+\left(\frac{\partial u^4}{\partial r}\right)^2=\Omega^2\left(1-\frac{\tilde{\Sigma}}{\Delta}\right), \tag{5.5.21}$$

$$\left(\frac{\partial u^0}{\partial \varphi}\right)^2+\left(\frac{\partial u^1}{\partial \varphi}\right)^2+\left(\frac{\partial u^2}{\partial \varphi}\right)^2+\left(\frac{\partial u^3}{\partial \varphi}\right)^2+\left(\frac{\partial u^4}{\partial \varphi}\right)^2= \Omega^2\frac{\sin^2\theta}{\tilde{\Sigma}}[(r^2+a^2)^2-\tilde{\Sigma}a^2\sin^2\theta], \tag{5.5.22}$$

$$\left(\frac{\partial u^0}{\partial \theta}\right)^2+\left(\frac{\partial u^1}{\partial \theta}\right)^2+\left(\frac{\partial u^2}{\partial \theta}\right)^2+\left(\frac{\partial u^3}{\partial \theta}\right)^2+\left(\frac{\partial u^4}{\partial \theta}\right)^2=\Omega^2\tilde{\Sigma}, \tag{5.5.23}$$

$$\left(\frac{\partial u^0}{\partial t}\right)\left(\frac{\partial u^0}{\partial \varphi}\right)+\left(\frac{\partial u^1}{\partial t}\right)\left(\frac{\partial u^1}{\partial \varphi}\right)+\left(\frac{\partial u^2}{\partial t}\right)\left(\frac{\partial u^2}{\partial \varphi}\right)+\left(\frac{\partial u^3}{\partial t}\right)\left(\frac{\partial u^3}{\partial \varphi}\right) + \left(\frac{\partial u^4}{\partial t}\right)\left(\frac{\partial u^4}{\partial \varphi}\right)=-\Omega^2\frac{2aMr\sin^2\theta}{\tilde{\Sigma}}, \tag{5.5.24}$$

$$\sum_{i=0}^{4}\left(\frac{\partial u^i}{\partial x^\mu}\right)\left(\frac{\partial u^i}{\partial x^\nu}\right)=0, \tag{5.5.25}$$

where $\mu,\nu=0,1,2,3$, $\mu<\nu$, with $\mu=0,\nu=3$ exclusive. We have used the metric components of Kerr spacetime in Boyer-Lindquist coordinate. It is noted that the coordinate $\phi$ in Chapter 3 has been changed to $\varphi$ in case that no confusion rises when we apply embedding map $\phi_w$. Solving the above equations gives explicit expression for an embedding of a Kerr spacetime in the 5 dimensional Euclidean space.

In equations (5.5.15)-(5.5.19) there are 10 equations and 5 unknown variables[9], and in equations (5.5.20)-(5.5.25) there are 10 equations and 5 unknown variables which both seems to be unsolvable. For a generic case, for example a binary black hole merger, the metric is more complicated and in general there are totally 16 components in the metric component matrix, while only 10 of them are independent due to the symmetry of metric between its two indices. Thus there will be 10 equations and only

[9]The conformal factor $\Omega$ leads to an extra unknown and gives us one more freedom to solve these equations.

5 unknown variables to be solved[10]. It is very likely that no solution exist for such equation set, which means that such spacetime cannot be pushed-forward in a 5 dimensional Euclidean space isometrically. This is similar to the problem that isometrically embedding a Riemannian manifold in a higher dimensional Euclidean space and existence of such embeddings is guaranteed by the Nash's theorem [147, 148, 149]. Recently, there are some mathematicians who are trying to construct similar theorems in pseudo-Riemannian space (e.g., spacetime) embedded into higher dimensional pseudo-Euclidean space and have made significant breakthrough. Nevertheless, in this project we only need to push-forward a 4 dimensional Lorentzian manifold in a 5 dimensional Euclidean space (we will prove that it is actually $\mathbb{R}^{2,3}$ pseudo-Euclidean space when we reconstruct Lorentz structure) unless otherwise specified. This specific requirement strongly constrains our choice of target space and the possibility of success. Intuitively, the most straightforward way is to prove that there exists such isometric embedding map for all types of spacetime. However, it is apparently complex and we do not know whether the theorem is true or not. In the case of embedding a 4 dimensional spacetime, which is a solution to Einstein's equation, in a flat Euclidean space, Kasner has proven that most 4 dimensional curved spacetime cannot be embedded in a flat space [150]. So a more wise procedure is to select specific spacetime and solve isometric transformation equations to work out the embeddings explicitly.

Upon construction of embedding the spacetime, the properties of embedded spacetime hypersurface need investigating in the perspective of 5 dimensional Euclidean space. Initially one needs to guarantee the causal structure within the region of spacetime hypersurface is preserved by embedding $\phi_w$. Consider a point $p \in \mathcal{M}$ and its vector space $\mathcal{T}_p$, a null vector $v^a \in \mathcal{T}_p$ satisfies

$$g_{ab}v^a v^b = 0\,. \tag{5.5.26}$$

Induced map $\phi_{w*}$ leads to

$$\begin{aligned}
\tilde{g}_{ab}\tilde{v}^a\tilde{v}^b &= \tilde{g}_{ab}(\phi_{w*}v)^a(\phi_{w*}v)^b \\
&= \tilde{g}_{ab}\phi_{w*}v^a\phi_{w*}v^b \\
&= \phi_w^*\tilde{g}_{ab}v^a v^b \\
&= (\phi_w^*\tilde{g})_{ab}v^a v^b \\
&= g_{ab}v^a v^b \\
&= 0\,,
\end{aligned} \tag{5.5.27}$$

this is true for all points as $p$ is an arbitrary point in $\mathcal{M}$, then all null curves in $\mathcal{M}$ remain null curves in $\phi_w(\mathcal{M})$ due to (A.0.54), measured by induced metric $\tilde{g}_{ab} = (\phi_{w*}g)_{ab}$. After some similar calculations, it is proven that all time-like and space-like curves are preserved. At this stage, the causal structure inside one spacetime foliation of the 5 dimensional Euclidean space is recovered, which is not restricted by our choice

[10]NB, the number of unknowns discussed herein should not be confused with the degree of freedoms of a generic manifold. The former are describing the unknown variables in the equations which need to be solved, the latter are related to the 4 coordinates in a general relativistic perspective.

of embedding maps if $\phi_w$ is a diffeomorphism[11].

Moreover, the conformal embedding relates the induced metric and the Euclidean metric in the following manner

$$(\phi_{w*}g)_{ab} = \Omega^2\delta_{ab}\,, \tag{5.5.28}$$

nevertheless, ambiguity is caused in this expression as $\phi_w$ is not a diffeomorphism from the 4 dimensional $\mathcal{M}$ to $\mathbb{R}^5$. A push-forward map is ill-defined whilst the pull-back map is sensible which leads to a correct relation

$$(\phi_w^*\delta)_{ab} = \Omega'^2 g_{ab}\,, \tag{5.5.29}$$

or another expression which is well-defined in $\phi_w(\mathcal{M}) \subsetneq \mathbb{R}^5$, given as

$$(\phi_{w*}g)_{ab} = \Omega^2 h_{ab}\,, \tag{5.5.30}$$

where $h_{ab}$ is induced by $\delta_{ab}$ as a 4 dimensional metric restricted on spacetime hypersurface $\phi_w(\mathcal{M})$, given by

$$h_{ab} := \delta_{ab} + n_a n_b\,, \tag{5.5.31}$$

where $n_a$ is a normal covector to $\phi_w(\mathcal{M})$. Apparently, a null 4 dimensional vector $v^a$ (from now on we use $v$ stand for vectors in $\mathbb{R}^5$ if no confusion arises) is null measured by $h_{ab}$ due to the conformal transformation (5.5.30). For the 5 dimensional metric $\delta_{ab}$, taking (5.5.31) into consideration, we have

$$\begin{aligned} h_{ab}v^a v^b &= (\delta_{ab} + n_a n_b)v^a v^b \\ &= \delta_{ab}v^a v^b + n_a n_b v^a v^b \\ &= \delta_{ab}v^a v^b + 0 \\ &= \delta_{ab}v^a v^b = 0\,, \end{aligned} \tag{5.5.32}$$

where we have used that the normal covector $n^a$ is orthogonal to all 4 dimensional vectors in the vector space of spacetime hypersurface. Thus, a null 4 dimensional vector $v^a$ is null measured by the 5 dimensional metric $\delta_{ab}$ and lies in the light cone of $\mathbb{R}^5$. Note that this is true regardless of the form of the 5 dimensional metric, hence we have the formula

$$h_{ab}n^a n^b = g_{ab}n^a n^b\,, \tag{5.5.33}$$

for a generic metric $g_{ab}$. Since $\phi_{w*}$ is non-degenerate, $v^a \neq 0$, indicating that there is at least one time-like dimension in $\mathbb{R}^5$, i.e., the Euclidean metric $\delta_{ab}$ becomes a pseudo-Euclidean metric $\hat{\eta}_{ab}$ with signature $(-,+,+,+,+)$. The ambient 5 dimensional space becomes $\mathbb{R}^{1,4}$.

Furthermore, it should be clarified that our aimed manifold is $\mathbb{R}^{2,3}$ with two time-like dimensions, and the metric signature is $(-,+,+,+,-)$.

[11] Thereof, an isometric embedding or a conformal embedding always preserve causal structure, as they are diffeomorphism (actually isometry group and conformal map group are subgroup of diffeomorphism group).

Detailed reasons and more explanation for introducing new time-like dimension are described in Chapter 4.5. Therefore, equation set (5.5.20)-(5.5.25) becomes

$$-\left(\frac{\partial u^0}{\partial t}\right)^2+\left(\frac{\partial u^1}{\partial t}\right)^2+\left(\frac{\partial u^2}{\partial t}\right)^2+\left(\frac{\partial u^3}{\partial t}\right)^2-\left(\frac{\partial u^4}{\partial t}\right)^2= -\Omega^2\left(1-\frac{2Mr}{\tilde{\Sigma}}\right), \tag{5.5.34}$$

$$-\left(\frac{\partial u^0}{\partial r}\right)^2+\left(\frac{\partial u^1}{\partial r}\right)^2+\left(\frac{\partial u^2}{\partial r}\right)^2+\left(\frac{\partial u^3}{\partial r}\right)^2-\left(\frac{\partial u^4}{\partial r}\right)^2=\Omega^2\left(1-\frac{\tilde{\Sigma}}{\Delta}\right), \tag{5.5.35}$$

$$-\left(\frac{\partial u^0}{\partial \varphi}\right)^2+\left(\frac{\partial u^1}{\partial \varphi}\right)^2+\left(\frac{\partial u^2}{\partial \varphi}\right)^2+\left(\frac{\partial u^3}{\partial \varphi}\right)^2-\left(\frac{\partial u^4}{\partial \varphi}\right)^2= \Omega^2\frac{\sin^2\theta}{\tilde{\Sigma}}[(r^2+a^2)^2-\tilde{\Sigma}a^2\sin^2\theta], \tag{5.5.36}$$

$$-\left(\frac{\partial u^0}{\partial \theta}\right)^2+\left(\frac{\partial u^1}{\partial \theta}\right)^2+\left(\frac{\partial u^2}{\partial \theta}\right)^2+\left(\frac{\partial u^3}{\partial \theta}\right)^2-\left(\frac{\partial u^4}{\partial \theta}\right)^2=\Omega^2\tilde{\Sigma}, \tag{5.5.37}$$

$$-\left(\frac{\partial u^0}{\partial t}\right)\left(\frac{\partial u^0}{\partial \varphi}\right)+\left(\frac{\partial u^1}{\partial t}\right)\left(\frac{\partial u^1}{\partial \varphi}\right)+\left(\frac{\partial u^2}{\partial t}\right)\left(\frac{\partial u^2}{\partial \varphi}\right)+\left(\frac{\partial u^3}{\partial t}\right)\left(\frac{\partial u^3}{\partial \varphi}\right) -\left(\frac{\partial u^4}{\partial t}\right)\left(\frac{\partial u^4}{\partial \varphi}\right)=\Omega^2\frac{2Ma\sin^2\theta}{\tilde{\Sigma}}, \tag{5.5.38}$$

$$-\left(\frac{\partial u^0}{\partial x^\mu}\right)\left(\frac{\partial u^0}{\partial x^\nu}\right)+\sum_{i=1}^{4}\left(\frac{\partial u^i}{\partial x^\mu}\right)\left(\frac{\partial u^i}{\partial x^\nu}\right)=0, \tag{5.5.39}$$

where $\mu,\nu=0,1,2,3$, and $\mu<\nu$ with $\mu=0,\nu=3$ exclusive. And it is assumed that the extra time-like dimension is denoted by the fourth coordinate $u^4$. Solving these equations to carry out the explicit transformation for Kerr spacetime into $\mathbb{R}^{2,3}$ with conformal factor being smooth everywhere on $\phi_w(\mathcal{M})$ except true singularities.

Similar to the Nash's theorem, it is natural to generalize the results from Riemannian cases to pseudo-Riemannian cases. In 1916 Cartan and Janet proved that any $n$ dimensional Riemannian manifold can be locally and isometrically embedded into a Euclidean space $\mathbb{R}^n$ with dimension dim$=n(n+1)/2$ [151, 9]. This result has been generalized on pseudo-Riemannian $\mathcal{M}$ into Minkowskian space $\mathbb{L}^n$ by Friedman in 1961. The number of difference between dimensions of $\mathcal{M}$ and $\mathbb{L}^n$ is called embedding class and denoted by $p=n(n+1)/2-n=n(n-1)/2$. In GR, dimension of spacetime is generally $n=4$, which leads to $p=10$. In the case of a spacetime with some symmetries, the embedding class might decrease. For example, for a constant curvature spacetime $p$ is 1, for a spherically symmetric spacetime, i.e., Schwarzschild spacetime, $p$ becomes 2 [152, 153].

As mentioned previously, there exist 6 locally and globally isometric embeddings of Schwarzschild spacetime, which has been carried out in a

6 dimensional Minkowskian space [144]. In the case of Kerr spacetime, there is only one local embedding in (3+6) dimensional Minkowskian space [154]. Intuitively, it is apparent that embedding a Kerr spacetime is more complicated than embedding a Schwarzschild spacetime since the symmetries of Kerr spacetime is axisymmetry resulting from one time-like Killing vector field and a spatial Killing vector field, and that of a Schwarzschild spacetime is spherical symmetry resulting from three Killing vector fields (one Killing vector field corresponds to one independent symmetry of spacetime). This situation is likely contributing to a locally and isometrically embedding of Kerr spacetime into an 8 dimensional pseudo-Euclidean space. Nevertheless, this is just a conjecture and requires further investigation. On the other hand, the embedding class for a conformal embedding is referred to as conformal embedding class which is 1 dimension less than that of an isometric embedding. Hence it is possible to locally and conformally embed a Schwarzschild spacetime into a 5 dimensional Minkowskian space as well as a 5 dimensional pseudo-Euclidean space. Suppose the ambient space is $\mathbb{R}^{2,3}$, equations (5.5.15)-(5.5.19) become

$$-\left(\frac{\partial u^0}{\partial t}\right)^2+\left(\frac{\partial u^1}{\partial t}\right)^2+\left(\frac{\partial u^2}{\partial t}\right)^2+\left(\frac{\partial u^3}{\partial t}\right)^2-\left(\frac{\partial u^4}{\partial t}\right)^2= -\Omega^2\left(1-\frac{2M}{r}\right), \tag{5.5.40}$$

$$-\left(\frac{\partial u^0}{\partial r}\right)^2+\left(\frac{\partial u^1}{\partial r}\right)^2+\left(\frac{\partial u^2}{\partial r}\right)^2+\left(\frac{\partial u^3}{\partial r}\right)^2-\left(\frac{\partial u^4}{\partial r}\right)^2= \Omega^2\left(1-\frac{2M}{r}\right)^{-1}, \tag{5.5.41}$$

$$-\left(\frac{\partial u^0}{\partial \theta}\right)^2+\left(\frac{\partial u^1}{\partial \theta}\right)^2+\left(\frac{\partial u^2}{\partial \theta}\right)^2+\left(\frac{\partial u^3}{\partial \theta}\right)^2-\left(\frac{\partial u^4}{\partial \theta}\right)^2=\Omega^2 r^2, \tag{5.5.42}$$

$$-\left(\frac{\partial u^0}{\partial \varphi}\right)^2+\left(\frac{\partial u^1}{\partial \varphi}\right)^2+\left(\frac{\partial u^2}{\partial \varphi}\right)^2+\left(\frac{\partial u^3}{\partial \varphi}\right)^2-\left(\frac{\partial u^4}{\partial \varphi}\right)^2=\Omega^2 r^2\sin\theta^2, \tag{5.5.43}$$

$$-\left(\frac{\partial u^0}{\partial x^\mu}\right)\left(\frac{\partial u^0}{\partial x^\nu}\right)+\sum_{i=1}^{4}\left(\frac{\partial u^i}{\partial x^\mu}\right)\left(\frac{\partial u^i}{\partial x^\nu}\right)=0, \tag{5.5.44}$$

for $\mu,\nu=0,1,2,3$, and $\mu<\nu$. After some algebra, we find that these coupled non-linear partial differential equations (PDE) are difficult to solve in the Schwarzschild coordinate system, even by choosing suitable conformal factor. Nevertheless, one of the advantage of GR is the freedom of choosing coordinate. In a particular Cartesian coordinate system, it is possible to split the Schwarzschild metric into the temporal section and a 3 dimensional positive definite metric which is isometric to a flat Euclidean metric [145], where the line element is given as

$$\mathrm{d}s^2=-\left(\frac{1-\frac{M}{2R}}{1+\frac{M}{2R}}\right)^2\mathrm{d}t^2+\left(1+\frac{M}{2R}\right)^4\left((\mathrm{d}x^1)^2+(\mathrm{d}x^2)^2+(\mathrm{d}x^3)^2\right). \tag{5.5.45}$$

This metric looks well organized since its spatial section is conformally flat and can be pushed-forward into $\mathbb{R}^{2,3}$ slice by slice. Nevertheless, in order to recover a Lorentzian metric via these foliations one needs to combine all 3 dimensional space-like hypersurfaces, which makes the whole process tedious and the possibility of recovering a Schwarzschild metric via space-like hypersurfaces in a 5 dimensional space remains uncertain. To seek a sensible way of reconstructing Schwarzschild metric in $\mathbb{R}^{2,3}$, observe equations (5.5.42) and (5.5.43) we can obtain a direct solution to $(u^1, u^2, u^3)$ by setting $\Omega^2 = r^{-2}$

$$\begin{cases} u^1 = \sin\theta \sin\varphi \,, \\ u^2 = \cos\theta \,, \\ u^3 = \sin\theta \cos\varphi \,. \end{cases} \tag{5.5.46}$$

Where we assume that $(u^0, u^4)$ are functions of $(t, r)$. As a result, equations (5.5.44) would be satisfied automatically. The remaining two equations need more subtle consideration. The different coefficients $g_{tt}$ and $g_{rr}$ might be converted to same expression due to (5.4.12), which yields

$$-\left(\frac{1}{r^2} - \frac{2M}{r^3}\right) \mathrm{d}t^2 + \frac{1}{r^2 - 2Mr} \mathrm{d}r^2 = \frac{1}{\Lambda^2}(-\mathrm{d}T^2 + \mathrm{d}X^2) \,. \tag{5.5.47}$$

Where $\Lambda = \Lambda(T, X)$ is a function of $T$ and $X$. This new factor could be regarded as an extra conformal factor and extract from the whole metric, which is given as

$$g^{[\mathrm{c}]}{}_{\mu\nu} \mathrm{d}x^\mu \mathrm{d}x^\nu = -\mathrm{d}T^2 + \mathrm{d}X^2 + \Lambda^2 X^2 \left(\mathrm{d}\theta^2 + \sin^2\theta \mathrm{d}\varphi^2\right) \,, \tag{5.5.48}$$

where $g^{[\mathrm{c}]}{}_{\mu\nu}$ are the components of an intermediate metric $g^{[\mathrm{c}]}{}_{ab}$ which is conformal to the Schwarzschild metric, such that

$$g^{[\mathrm{c}]}{}_{\mu\nu} = \Omega^2 \Lambda^2 g^{[\mathrm{S}]}{}_{\mu\nu} \,. \tag{5.5.49}$$

We now can consider an isometric transformation between $(T, X, \theta, \varphi)$ and $(u^0, u^1, u^2, u^3, u^4)$. The only consequence of introducing the new conformal factor is that solution (5.5.46) gains a factor $\Lambda$, e.g., $u^1 = \Lambda \sin\theta \sin\varphi$, without affecting equations (5.5.44) ($\mu = 0$ , $\nu = 1$ excluded). Note that the conformal factor becomes $\Omega\Lambda$ in terms of $g^{[\mathrm{c}]}{}_{\mu\nu}$. Equations (5.5.40), (5.5.41) and (5.5.44), after some calculation with $\mu = 0$ , $\nu = 1$, become

$$-\left(\frac{\partial u^0}{\partial T}\right)^2 + \left(\frac{\partial \Lambda}{\partial T}\right)^2 - \left(\frac{\partial u^4}{\partial T}\right)^2 = -1 \,, \tag{5.5.50}$$

$$-\left(\frac{\partial u^0}{\partial T}\right)\left(\frac{\partial u^0}{\partial X}\right) + \left(\frac{\partial \Lambda}{\partial T}\right)\left(\frac{\partial \Lambda}{\partial X}\right) - \left(\frac{\partial u^4}{\partial T}\right)\left(\frac{\partial u^4}{\partial X}\right) = 0 \,, \tag{5.5.51}$$

$$-\left(\frac{\partial u^0}{\partial X}\right)^2 + \left(\frac{\partial \Lambda}{\partial X}\right)^2 - \left(\frac{\partial u^4}{\partial X}\right)^2 = 1 \,. \tag{5.5.52}$$

There exist more than one solution to these equations, for example $u^0 = T$ , $u^4 = \sqrt{3}X$ , $\Lambda = 2X$. Nevertheless, we have to find a coordinate

transformation such that the solution $\Lambda$ satisfies the transformation rule for $(T, X)$, i.e., we must solve three coupled equations

$$-\frac{1}{\Lambda^2}\left(\frac{\partial T}{\partial t}\right)^2+\frac{1}{\Lambda^2}\left(\frac{\partial X}{\partial t}\right)^2=-\left(\frac{1}{r^2}-\frac{2M}{r^3}\right), \tag{5.5.53}$$

$$-\frac{1}{\Lambda^2}\left(\frac{\partial T}{\partial t}\right)\left(\frac{\partial T}{\partial r}\right)+\frac{1}{\Lambda^2}\left(\frac{\partial X}{\partial t}\right)\left(\frac{\partial X}{\partial r}\right)=0, \tag{5.5.54}$$

$$-\frac{1}{\Lambda^2}\left(\frac{\partial T}{\partial r}\right)^2+\frac{1}{\Lambda^2}\left(\frac{\partial X}{\partial r}\right)^2=\frac{1}{r^2-2Mr}. \tag{5.5.55}$$

We have reduced ten coupled non-linear differential equations to these three equations, but it remains a problem due to the number of unknowns are less than that of the equations, and an explicit coordinate transformation from $(t, r)$ to $(T, X)$ needs to be obtained.

It is unlikely for solutions to exist as the simplified system is still over-determined, which indicates that Schwarzschild spacetime may not be isometrically or conformally embedded in a 5 dimensional flat pseudo-Euclidean space. Additional codimensions are in general needed to solve the PDE system. This phenomenon is similar to the isometric embedding problem for isometrically embedding Riemannian manifolds in higher dimensional Euclidean spaces, which was solved in the celebrated work of John Nash [155, 156, 157]. Later on, mathematicians have resolved the isometric embedding problem in the pseudo-Riemannian setting and have made significant breakthrough [152].

In the mathematical study of isometric embedding problems, the degree of regularity on the metrics has substantial effect on the existence of solutions to the problem. More precisely, if we consider $C^k$-isometric embeddings where $k \geq 2$, then there are higher-order compatibility conditions given by the Gauss-Codazzi constraint equations which imply certain rigidity phenomena [158]. On the other hand, if we consider isometric embeddings which are only $C^1$, then the system of non-linear partial differential equations exhibit $h$-principles[12] [159] which imply that solutions are expected to exist in abundance, provided that certain topological conditions are satisfied (cf., [160]). For our embedding problem at hand, if we are only concerned about the spacetime conformal structures, only $C^1$ metrics and $C^1$ isometric embeddings will suffice and we should expect the conformal isometric embedding problem to be solvable in most cases. However, if we want our spacetime to satisfy the Einstein equation in the classical sense, then we require our metrics to be at least $C^2$ and the conformal isometric embedding problem theoretically could be harder to solve.

Nevertheless, for our particular problem at hand, we need to embed a 4 dimensional Lorentzian manifold into a 5 dimensional pseudo-Euclidean space $\mathbb{R}^{2,3}$. These specific requirements on the dimensions and signature strongly constrain the problem. However, there exist two alternative approaches of solving this resolution. Firstly, instead of looking at the general problem of isometrically embedding an arbitrary spacetime, we could focus on solving the problem for some specific spacetimes, which

[12]Throughout this thesis, we apply the notations $h$ and $h_{ab}$ to represent the induced metrics, except for the $h$-principles that is presented here, unless otherwise specified.

gives a more tractable problem. Moreover, once can solve this problem by relaxing the condition of the ambient space, e.g., the Campbell's theorem guarantees that a $D$ dimensional Riemannian manifold can be locally embedded in a $(D+1)$ dimensional Ricci flat Riemannian manifold [161, 162, 163, 164]. In the next section we will follow the second method and propose a distinct way of embedding a 4 dimensional spacetime into a 5 dimensional space, which is applicable to an arbitrary spacetime.

## 5.6 Recover the Lorentz Structure in a General 5 Dimensional Manifold

As mentioned previously, one problem must be circumvented before making progress. The local Lorentz structure is lost if the particle traverses through different spacetime foliations in the ambient space, see Fig.5.1. The basic idea to cure this problem is to rebuild a 'vertical' manifold, within which the null geodesics are cut by zero level sets and prove that the metric induced in the new manifold is isometric to that of the original spacetime. It then allows one to reconstruct local coordinate systems and a Lorentz metric $h'_{ab}$. Thereof, the causal structure can be recovered by means of the 5 dimensional metric and the coordinate systems in the 5 dimensional manifold which consists of all spacetime slices.

In the previous section I derived a reduced set of equations for the coordinate transformation of a conformal embedding into a flat pseudo-Euclidean space. Nevertheless, equations (5.5.53)-(5.5.55) are still difficult to solve since the number of equations exceeds the number of unknowns.

Although a solution can be directly determined by brute force and a conformal embedding of the Schwarzschild spacetime in a flat 5 dimensional space may exist [165], this is not a readily extendable approach when converting to a spacetime with more complicated geometric structures, e.g., the fully-dynamical spacetimes found in the gravitational wave producing systems. We instead employ a new method which relaxes the constraint on the target 5 dimensional ambient space. The target ambient space, as mentioned previously, requires the definition of a suitably-chosen metric. This metric is obtained as follows.

The basic idea is to relax the requirement that the target space is flat. We consider instead a general 5 dimensional pseudo-Riemannian manifold with a metric which remains to be defined. The metric is partially defined when embedding the 4 dimensional spacetime into the 5 dimensional manifold, since one can always obtain a specific, coordinate-dependent, isometric transformation which recovers the original metric. The form of the 5 dimensional metric is chosen such that the Lorentz structure of the original 4 dimensional spacetime is recovered from the foliations of the new 5 dimensional space.

We focus on the Schwarzschild case, with metric form $g_{\mu\nu}$ given in (5.5.12) in the Schwarzschild coordinate. A conformal embedding is replaced by a more rigorous isometric embedding. An explicit coordinate

transformation reads

$$\begin{cases} u^0 = t\,, \\ u^1 = r\,, \\ u^2 = \theta\,, \\ u^3 = \varphi\,, \end{cases} \tag{5.6.1}$$

with $u^4 = t_0$ on the slice, where $t_0$ is a constant and the slice is labelled as the zeroth slice. We re-define all coordinates as,

$$\begin{cases} u^0 = t'\,, \\ u^1 = r'\,, \\ u^2 = \theta'\,, \\ u^3 = \varphi'\,, \\ u^4 = w'\,, \end{cases} \tag{5.6.2}$$

which is a Schwarzschild-like coordinate system and $w' = w'_0$ on this slice, herein prime coordinates substitute $u^i$ coordinates throughout the following context. This transformation is definitely an isometry and the metric ${g'}_{\mu\nu}$ has the same formula as that of the original metric in the original Schwarzschild coordinate by replacing non-prime coordinates with prime ones in (5.5.12).

For the first slice, we do the same operation and the explicit coordinate transformation is given by

$$\begin{cases} t' &= t - \Delta t\,, \\ r' &= r\,, \\ \theta' &= \theta\,, \\ \varphi' &= \varphi\,, \\ {w'}_1 &= t_0 + \Delta t = t_1\,, \end{cases} \tag{5.6.3}$$

where $t_1$ and $t_0$ are constants, and $\Delta t$ is a positive finite constant.

Continue the embedding process we get a set of foliations, similar coordinate transformation applied on each of them except for the zeroth and fourth coordinates $t'$ and $w'$, which are given regularly as

$$\begin{aligned} t' &= t - n\Delta t &= t_0\,, \\ {w'}_n &= t_0 + n\Delta t = t_n\,, \end{aligned} \tag{5.6.4}$$

on the $n$-th slice. It is apparently that the whole 5 dimensional manifold has a $\mathbb{R} \times \mathcal{M} = \mathcal{M}'$ topology. Recall that one of our tasks is to recover the Lorentz structure, in the above setting we can find a 'null geodesic' $\phi_{w_n}(C)$ on each hypersurface in $\mathcal{M}'$, which is the image of a same null geodesic $C$ in the original 4 dimensional manifold. We pick out one spacetime point from each $\phi_{w_n}(C)$: $({t'}_0, {r'}_0, {\theta'}_0, {\varphi'}_0, {w'}_0)$ on $\phi_{w_0}(C)$, $({t'}_1, {r'}_1, {\theta'}_1, {\varphi'}_1, {w'}_1)$ on $\phi_{w_1}(C)$, and similar for the remaining curves. If we let $\Delta t \to 0$, and rewrite the infinitesimal quantity as $\mathrm{d}t$, this is resulting that all these points constitute a curve which is the image of $C$. By this one can recover a 3 dimensional null surface in which the embedded geodesic is inclusive within the 5 dimensional space, and furthermore one needs to recover the whole 4 dimensional manifold which consists of all

cut 4 dimensional null geodesics and prove that this new 4 dimensional manifold is isometrically embedded from $\mathcal{M}$[13].

The new constructed manifold is formed via all cut null geodesics, which is called a vertical spacetime and it turns out that $w' = t$ on this vertical slice, and the metric in this foliation is

$$h'_{\mu\nu}\mathrm{d}x^\mu\mathrm{d}x^\nu = -\left(1-\frac{2M'}{r'}\right)\mathrm{d}w'^2+\left(1-\frac{2M'}{r'}\right)^{-1}\mathrm{d}r'^2+r'^2(\mathrm{d}\theta'^2+\sin^2\theta'\mathrm{d}\varphi'^2)\,, \tag{5.6.5}$$

the full 5 dimensional metric is given by

$$\begin{aligned} g'_{\mu\nu}\mathrm{d}x^\mu\mathrm{d}x^\nu = &-\left(1-\frac{2M'}{r'}\right)\mathrm{d}w'^2-\left(1-\frac{2M'}{r'}\right)\mathrm{d}t'^2+\left(1-\frac{2M'}{r'}\right)^{-1}\mathrm{d}r'^2 \\ &+r'^2(\mathrm{d}\theta'^2+\sin^2\theta'\mathrm{d}\varphi'^2)\,, \end{aligned} \tag{5.6.6}$$

where $M' = M$ represents the Schwarzschild mass in the new 5 dimensional manifold, and both are written in the Schwarzschild-like coordinate system $(t', r', \theta', \varphi', w')$.

Note that the new dimension introduced here is a temporal one instead of a spatial one in common sense, which is atypical but can be proven its necessity. To recover the Lorentz structure, it is natural to add time-like dimension as intuitively the cut null geodesic is evolving along the extra dimension, denoted by $w'$[14].

Moreover, the 3 dimensional null surface recovery in 5 dimensional manifold is a purely mathematical process, physically only a 4 dimensional 'universe' is meaningful for an observer, which implies that one has to recover the entire 4 dimensional spacetime consisting of all 3 dimensional null geodesics. To prove that the original spacetime $\mathcal{M}$ is isometric to the recovered 4 dimensional manifold, denoted by $\Phi(\mathcal{M})$, two steps must be done: Firstly, all 4 dimensional null geodesics constitute a smooth 4 dimensional manifold with a metric denoted by $h'_{ab}$. Secondly, there exists an isometry $\Phi$ from $\mathcal{M}$ to the recovered manifold (that is why we use $\Phi(\mathcal{M})$ to denote it), satisfying $(\Phi^* g)_{ab} = h'_{ab}$.

We already obtained a series of embeddings, denoted by $\phi_{w_n}$ (in numerical simulation $w_n$ denote for discrete numerics of spacetime foliations). A congruence of null geodesics $\{C(\lambda)\}$ is selected, where the 4 dimensional spacetime is filled by these curves. Note this can always be done for a real spacetime, for example, a Minkowskian space can be filled by all 45° null geodesics and a Schwarzschild spacetime can be filled by all incoming and outgoing null geodesics of Schwarzschild spacetime (in the Eddington-Finkelstein coordinate system). Figure Fig.5.2 illustrates how we recover the Lorentz structure of 2 dimensional Minkowskian foliations in a 3 dimensional pseudo-Euclidean manifold.

[13]From now on hypersurface represents only for a 4 dimensional manifold in a 5 dimensional manifold, and we use surface to denote all other manifolds including a 3 dimensional null hypersurface of a 4 dimensional spacetime.

[14]Mathematically, it is possible to introduce a spatial dimension and recover the Lorentz structure and derive null geodesics along the original temporal direction, but this leads to uncertainty in the evolution direction of the 4 dimensional manifold, which may either flow along positive $w'$ direction or negative $w'$ direction.

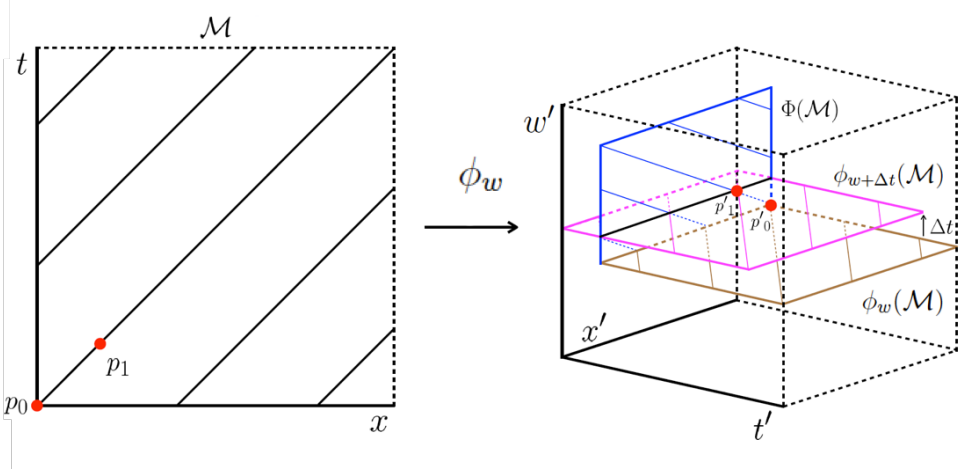


Figure 5.2: The figure illustrates the embedding of a 2 dimensional Minkowskian manifold embedded into a 3 dimensional pseudo-Euclidean manifold. The Lorentz structure is recovered along $p_0p_1$ curve. The first two foliations are plotted, where $\phi_w(\mathcal{M})$ (brown) represents the initial foliation and $\phi_{w+\Delta t}(\mathcal{M})$ (pink) represents the adjacent foliation. The blue foliation $\Phi(\mathcal{M})$ represents the vertical foliation. $p_0{}'p_1{}'$ are the image of $p_0p_1$ curve.

After embedding, with the setting from (5.6.2), (5.6.3) and (5.6.4), we pick the image of a null geodesic which travel through point $(t_0, r_0, \theta_0, \varphi_0)$ of the original manifold $\mathcal{M}$, and in the zeroth spacetime slice it is $\phi_{w_0}(C)$, and passes through $(\phi_{w_0}(t_0), \phi_{w_0}(r_0), \phi_{w_0}(\theta_0), \phi_{w_0}(\varphi_0), w'_0)$. In the first spacetime slice the image of the same null geodesic passes $(\phi_{w_1}(t_0), \phi_{w_1}(r_0), \phi_{w_1}(\theta_0), \phi_{w_1}(\varphi_0), w'_1)$ and $(\phi_{w_1}(t_1), \phi_{w_1}(r_1), \phi_{w_1}(\theta_1), \phi_{w_1}(\varphi_1), w'_1)$. It is natural to cut each spacetime slice $\phi_{w_n}(\mathcal{M})$ where the intersection are $(\phi_{w_n}(t_n), \phi_{w_n}(r_n), \phi_{w_n}(\theta_n), \phi_{w_n}(\varphi_n), w'_n)$ on each of them, where $w'_n = t + n\Delta t = t_n$ as we set in (5.6.4) and all these points in the 5 dimensional space form an image of $C$, denoted by $\Phi(C)$. Herein, we have demanded that the temporal interval between $\phi_{w_n}(t_n)$ and $\phi_{w_{n+1}}(t_{n+1})$ is equal to that between $t_n$ and $t_{n+1}$. This is true because $\Delta w = w_{n+1} - w_n = \Delta t$. Now on this individual null geodesic the Lorentz structure is physically recovered because adjacent points on $\Phi(C)$ are one to one correspondence via the following map

$$\phi_{w_{n+1}} \circ a_{n,n+1} \circ \phi_{w_n}^{-1} : \ (t'_n, r'_n, \theta'_n, \varphi'_n, w'_n) \\ \to (t'_{n+1}, r'_{n+1}, \theta'_{n+1}, \varphi'_{n+1}, w'_{n+1}) \,, \tag{5.6.7}$$

where $a_{n,n+1}$ represents the vector which drags point $(t'_n, r'_n, \theta'_n, \varphi'_n, w'_n)$ to point $(t'_{n+1}, r'_{n+1}, \theta'_{n+1}, \varphi'_{n+1}, w'_{n+1})$ on curve $C$[15]. Fig.5.3 illustrates how one recovers the Lorentz structure between two adjacent foliations in the 5 dimensional manifold. Note that in that graph, $A$ cannot traverse to any other point but the point $B'$, otherwise the causality will be violated even in principle.

Generalize this cutting construction to all null geodesics in this congruence and the images constitute a new 4 dimensional manifold $\Phi(\mathcal{M})$[16]

[15]Note that the statement is more appropriate when $\Delta t \to 0$, i.e., the dragging vector becomes the null tangent.

[16]Actually, $\Phi(\mathcal{M})$ is not covering the whole spacetime since we fix the starting point

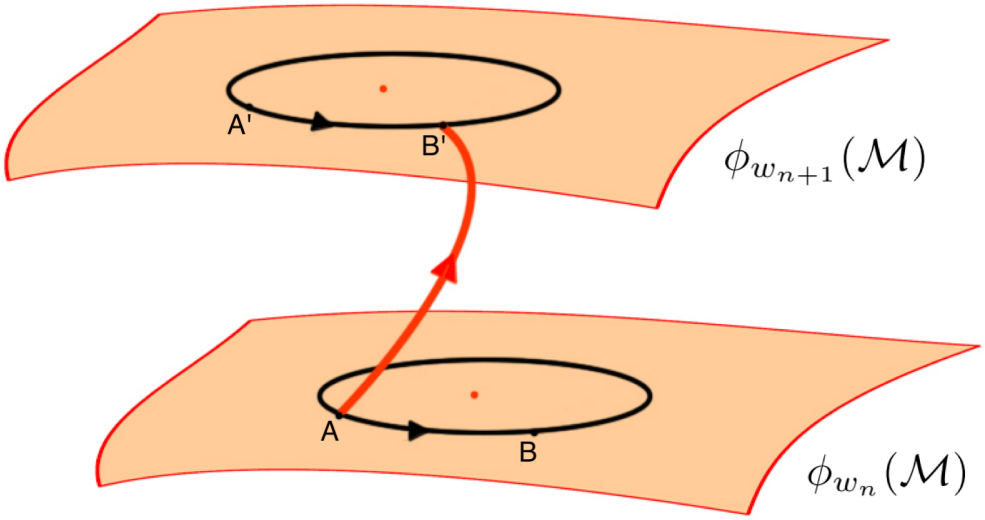


Figure 5.3: Illustration of a photon traveling from one spacetime foliation $\phi_{w_n}(\mathcal{M})$ to the adjacent foliation $\phi_{w_{n+1}}(\mathcal{M})$. The two black circles correspond to the same pre-image in $\mathcal{M}$, e.g., $A$ and $A'$ mapped from $a$. To maintain the Lorentz structure, one must let the photon travel from $A$ in $\phi_{w_n}(\mathcal{M})$ to $B'$ in $\phi_{w_{n+1}}(\mathcal{M})$, i.e., the red line. It is noted that these slices, $\phi_{w_n}(\mathcal{M})$ and $\phi_{w_{n+1}}(\mathcal{M})$ are in the 5 dimensional space. Furthermore, the interval between $A$ and $B$ (hence $A'$ and $B'$) must be equal to that between $A$ and $B'$, i.e., $\Delta w = \Delta t$.

which is an image of our original Lorentzian manifold. On this manifold coordinate $t'$ is a constant since on the $i$-th spacetime slice $t' = t_n - n\Delta t = t_0$ as given in (5.6.4), in addition formula (5.6.4) demonstrates that in the new manifold $w'$ replaces the physical time $t$ and plays a similar role provided $\Delta t \to 0$, where the map is given by

$$\Phi : \ \mathcal{M} \to \Phi(\mathcal{M}) \subset \mathcal{M}' \,, \tag{5.6.8}$$

with coordinate transformation given as

$$\begin{cases} t' &= t_0 \,, \\ r' &= r \,, \\ \theta' &= \theta \,, \\ \varphi' &= \varphi \,, \\ w' &= t \,. \end{cases} \tag{5.6.9}$$

This is a smooth manifold as all of the open sets in $\Phi(\mathcal{M})$ is mapped via the induced map $\Phi$ from the open sets in $\mathcal{M}$ and since the transition map $\psi \circ \Phi$ is smooth, where $\psi$ is the coordinate presentation of spacetime $\mathcal{M}$, a smooth coordinate presentation of $\Phi(\mathcal{M})$ is just the inverse of that particular transition map.

We then need to find out the induced metric on the vertical manifold $\Phi(\mathcal{M})$. It is supposed in (5.6.6) that the components of the 5 dimensional metric of $\mathcal{M}'$ reads

$$g_{\mu\nu} = g^{[o]}{}_{\mu\nu} + g_{44} \mathrm{d}w'^2 \,, \tag{5.6.10}$$

of spacetime slice and these null geodesics are incomplete ones in the 5 dimensional space. We need to extend these curves backward in $w'$ to recover the whole Lorentzian manifold.

where ${g^{[o]}}_{\mu\nu}$ denote the original metric components of the Schwarzschild spacetime and $g_{44} = -(1 - 2M'/r')$ is associated to $\mathrm{d}w'^2$.

There exists a map from $\Phi(\mathcal{M})$ to $\mathcal{M}'$, denoted by $\tilde{i}$. A 4 dimensional metric is induced by this map, given by

$$\tilde{i}^* : \ {g'}_{ab} \to {h'}_{ab} \,. \tag{5.6.11}$$

Consider the coordinate relation between these two spaces we can find that the coordinate transformation is given by

$$\begin{cases} T &= t' = t_0 \,, \\ R &= r' \,, \\ \Theta &= \theta' \,, \\ \Psi &= \varphi' \,, \\ W &= w' \,, \end{cases} \tag{5.6.12}$$

where capital letters are used for the coordinates of $\mathcal{M}'$ in case no confusion is caused. Note that the first row of these equations implies that $T$ is a constant for the submanifold of $\mathcal{M}'$ which means that this vertical spacetime is a hypersurface of the 5 dimensional space. Using the explicit coordinate transformation we find the induced metric on $\Phi(\mathcal{M})$ is given by

$${h'}_{\mu\nu}\mathrm{d}u^\mu \mathrm{d}u^\nu = \left(1 - \frac{2M'}{r'}\right)^{-1} \mathrm{d}r'^2 + r'^2(\mathrm{d}\theta'^2 + \sin^2\theta' \mathrm{d}\varphi'^2) - \left(1 - \frac{2M'}{r'}\right) \mathrm{d}w'^2 \,, \tag{5.6.13}$$

where, we use notation $u$ to denote the general coordinates of the 5 dimensional manifold. Moreover, the original spacetime metric can be mapped on 5 dimensional space by means of the induced map $\Phi$ and the metric is pushed-forward as $h''_{ab} = (\Phi_* g)_{ab}$, using the coordinate transformation (5.6.9), the explicit form of the induced metric is given as

$${h''}_{\mu\nu}\mathrm{d}u^\mu \mathrm{d}u^\nu = \left(1 - \frac{2M''}{r'}\right)^{-1} \mathrm{d}r'^2 + r'^2(\mathrm{d}\theta'^2 + \sin^2\theta' \mathrm{d}\varphi'^2) - \left(1 - \frac{2M''}{r'}\right) \mathrm{d}w'^2 \,, \tag{5.6.14}$$

where $M'' = M$ is the original Schwarzschild mass. By inspection, it is apparent that $h''_{ab}$ coincides with ${h'}_{ab}$, i.e., $(\Phi_* g)_{ab} = {h'}_{ab}$, which indicates that $\Phi$ is an isometric embedding. The Lorentz structure is recovered on the cut manifold $\Phi(\mathcal{M})$ in the 5 dimensional space $\mathcal{M}'$ .

This formalism can be generalized to all stationary spacetime, including Kerr spacetime. Ignoring the region enclosed by event horizon, there is always existing a coordinate system such that the metric can be expressed in a time independent way, satisfying

$$\frac{\partial g_{\mu\nu}}{\partial t} = 0 \,, \tag{5.6.15}$$

where $t$ denotes the physical time. From (5.6.9) we know that

$$\mathrm{d}w' = \mathrm{d}t \,, \tag{5.6.16}$$

$$\mathrm{d}t' \ = 0 \,. \tag{5.6.17}$$

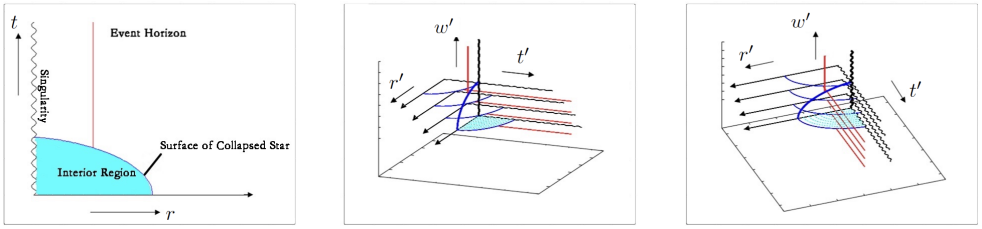


Figure 5.4: The figures illustrate the Schwarzschild spacetime (the one in the left panel) embedded in 5 dimensional space in a Schwarzschild-like coordinate in 5 dimensional space viewed from two different angels (the middle and right panels), where coordinates $\theta'$ and $\varphi'$ are suppressed. Only four of spacetime foliations $\phi(\mathcal{M})$ are drawn in the plot. Red lines represent for event horizons, wavy black lines for spacetime singularity and blue curves represent for the boundary of collapsed star which finally fall into the horizon (the dotted light blue lines represent the interior of the star, only shown on the first slice). The vertical lines represent spacetime $\Phi(\mathcal{M})$. It is apparent from the figure that the fifth coordinate $w'$ substitute the physical time $t'$.

No matter what metric form we have, we can write down an appropriately-chosen metric form which is more generic than (5.6.6), given by

$$\begin{aligned} g'_{\mu\nu}\mathrm{d}u^\mu\mathrm{d}u^\nu = \quad & g'_{00}\mathrm{d}t'^2 + g'_{44}\mathrm{d}w'^2 \\ & + g'_{0k}\mathrm{d}t'\mathrm{d}u^k + g'_{jm}\mathrm{d}u^j\mathrm{d}u^m \\ & + g'_{4i}\mathrm{d}w\mathrm{d}u^i\,, \end{aligned} \tag{5.6.18}$$

where $\mu$ and $\nu$ run from 0 to 4, $k$, $m$, $i$ and $j$ run from 1 to 3. Due to (5.6.16) and (5.6.17), all $\mathrm{d}t'$ terms in (5.6.18) vanish and are transferred to the $\mathrm{d}w'$ term on the vertical spacetime $\Phi(\mathcal{M})$, even those containing cross terms, for example the $\mathrm{d}t\mathrm{d}\varphi$ term in the Kerr metric. Due to (5.6.15), this is guaranteed even if the two coordinate origins of $\mathcal{M}$ and $\mathcal{M}'$ do not coincide, where $w' = t + \Delta t$ on $\Phi(\mathcal{M})$. However, a $\Delta t$ shift affects the result for dynamical spacetimes, i.e., the pulling-back of a 5 dimensional metric onto the 4 dimensional recovered spacetime $\Phi(\mathcal{M})$ leads to a non-isometric embedding of the original spacetime to $\Phi(\mathcal{M})$.

Consider a modified Schwarzschild metric, along with the metric form given by

$$\begin{aligned} g_{\mu\nu}\mathrm{d}x^\mu\mathrm{d}x^\nu = & -\left(1-\frac{2M(t)}{r}\right)\mathrm{d}t^2 + \left(1-\frac{2M(t)}{r}\right)^{-1}\mathrm{d}r^2 \\ & + r^2(\mathrm{d}\theta^2 + \sin^2\theta\mathrm{d}\varphi^2)\,. \end{aligned} \tag{5.6.19}$$

Where $M$ is a function of $t$, which satisfies $M(t) = t$ called the dynamical Schwarzschild mass. It is noted that the metric is a generalization of the normal Schwarzschild metric and is not necessarily a solution to the Einstein equation. Without loss of generality, the result derived here can be generalized to all analytical solutions of dynamical spacetime. We demand a similar coordinate transformation for this ideal mathematical model as is operated in formulas (5.6.2), (5.6.3) and (5.6.4). The ambient space $\mathcal{M}'$ is given as $\mathcal{M}\times\mathbb{R}$ and the topology for each hypersurface is that of the original pseudo-Schwarzschild manifold which possesses a constant coordinate $w'$ in a Schwarzschild-like coordinate. One point which is different from a stationary case should be noticed is that now the mass term $M$ is time dependent and it is only a function of the coordinate time

$t$, or a function of spacetime coordinate $x^\mu$ at most. After embedding $M$ becomes a function of $(t', w')$ on the whole 5 dimensional manifold and varies with respect to $w'$ only on the vertical manifold, otherwise it makes the 'spacetime' to be stationary on the vertical hypersurface, i.e., it is given by

$$M'_n = t' + w' \,, \tag{5.6.20}$$

for $g'_{00}$ and $g'_{11}$ on the $n$-th slice, and is given as

$$M' = w' \,, \tag{5.6.21}$$

for $g'_{44}$ on the $n$-th foliation. This result is curious because $t$ is the real physical time and could affect the black hole mass, however the extra coordinate $w'$ is not a physical dimension but an evolution parameter. The coordinate $w'$ is avoided in the final solution by pulling-back the spacetime after deriving the null geodesics. Now the full metric has the following form

$$\begin{aligned} g'_{\mu\nu}\mathrm{d}u^\mu \mathrm{d}u^\nu = &- \left(1 - \frac{2w'}{r'}\right)\mathrm{d}w'^2 - \left(1 - \frac{2(w'+t')}{r'}\right)\mathrm{d}t'^2 \\ &+ \left(1 - \frac{2(w'+t')}{r'}\right)^{-1}\mathrm{d}r'^2 + r'^2(\mathrm{d}\theta'^2 + \sin^2\theta'\mathrm{d}\varphi'^2) \,. \end{aligned} \tag{5.6.22}$$

The coordinate transformation would not produce isometric embedding if two coordinate origins locate at different positions. This issue might be cured if we set $w' = t$ to force a coincide of two origins. This operation results in converting all $t$ dependent terms in (5.6.18) to $w'$ dependent for the induced metric $h'_{ab}$.

Moreover, the physical time dependent term (mass term in this case) needs to be chosen very carefully in order to guarantee that each $\phi_{w_n}$ is an isometry. For a generic 4 dimensional spacetime, the metric $g_{ab}$ becomes

$$g_{\mu\nu}\mathrm{d}x^\mu \mathrm{d}x^\nu = g_{00}\mathrm{d}t^2 + g_{0i}\mathrm{d}t\mathrm{d}x^i + g_{jk}\mathrm{d}x^j\mathrm{d}x^k \,, \tag{5.6.23}$$

where $i$, $j$ and $k$ run from 1 to 3. After embedding, the original time dependent term $A(t)$ becomes

$$A'_n(w', t') = A'_n(t' + w') \,, \tag{5.6.24}$$

for the metric components of the first, third and fourth terms in equation (5.6.18) on the $n$-th spacetime foliation, and $A(t)$ becomes

$$A'_n(w', t') = A'_n(w') \,, \tag{5.6.25}$$

for the components of the second and fourth terms in equation (5.6.18) on the $n$-th spacetime foliation. Herein, $A'_n(t'+w')$ and $A'_n(w')$ possess the same form as that of $A(t)$. For the zeroth slice, the isometric condition is satisfied due to that $t' = t$. For the first component of equation (5.6.23), according to (5.6.4), the '00' component of a pushed-forward metric $h''$

is given by

$$\begin{aligned} h''_{00} &= \frac{\partial t}{\partial t'}\frac{\partial t}{\partial t'}g_{00} \\ &= g_{00} \\ &= g_{00}(t) \\ &= g_{00}(t' + n\Delta t)\,, \end{aligned} \tag{5.6.26}$$

on the $n$-th foliation $\phi_{w_n}(\mathcal{M})$. The '00' component of metric $h'$ induced on $\phi_{w_n}(\mathcal{M})$ by the 5 dimensional metric is given by

$$\begin{aligned} h'_{00} &= \frac{\partial T'}{\partial t'}\frac{\partial T'}{\partial t'}g'_{00} \\ &= g'_{00} \\ &= g'_{00}(t' + n\Delta t + t_0)\,, \end{aligned} \tag{5.6.27}$$

where we have used capital $T'$ for the coordinate of the 5 dimensional manifold to avoid confusion. We require that $g_{00}$ and $g'_{00}$ have the same form, hence (5.6.26) and (5.6.27) lead to $h'_{00} = h''_{00}$ provided the initial value $t_0$ (hence the initial value of $w'$) is set to be zero, i.e., $w'_0 = t_0 = 0$, which implies that $\phi_{w_n}$ is an isometric embedding.

As for the remaining of the metric components in equation (5.6.18), we can perform the same transformation and demand that the pushed-forward 4 dimensional metric $h''_{ab}$ is isometric to the pulled-back metric of the 5 dimensional metric $g'_{ab}$. Then the form of the 5 dimensional metric (5.6.18) can be rewritten as

$$\begin{aligned} g'_{\mu\nu}\mathrm{d}u^\mu\mathrm{d}u^\nu = \quad & g'_{00}\,(t' + w')\,\mathrm{d}t'^2 + g'_{44}\,(w')\,\mathrm{d}w'^2 \\ & + g'_{0k}\,(t' + w')\,\mathrm{d}t'\mathrm{d}u^k + g'_{4m}\,(w')\,\mathrm{d}w'\mathrm{d}u^m \\ & + g'_{ij}\,(t' + w')\,\mathrm{d}u^i\mathrm{d}u^j\,. \end{aligned} \tag{5.6.28}$$

## 5.7 Application and Generalization

The Oppenheimer-Snyder solution [166] is one of the most simple and famous dynamical solution to the Einstein equation, where the metric form is given by

$$g_{\mu\nu}\mathrm{d}x^\mu\mathrm{d}x^\nu = -\mathrm{d}\tilde{\tau}^2 + o(\tilde{\tau})^2(\mathrm{d}\tilde{\chi}^2 + \sin^2\tilde{\chi}\mathrm{d}\tilde{\Omega}^2)\,. \tag{5.7.1}$$

This solution describes the process of a spherical star with zero pressure and uniform density dust collapsing to a Schwarzschild black hole, where $\tilde{\tau}$ is the proper time parameter, $\tilde{\chi}$ is radial coordinate and $o$ is the scale factor, satisfying

$$\dot{o}^2 + 1 = \frac{8\pi}{3}\rho o^2\,, \tag{5.7.2}$$

if taking Einstein equation into consideration, where the overdot denotes differentiation with respect to $\tilde{\tau}$. Consider the energy-momentum conservation with zero pressure, one derives

$$\rho o^3 = con \equiv \frac{3}{8\pi}o_\mathrm{m}\,, \tag{5.7.3}$$

where $o_{\mathrm{m}}$ is the maximum value of scale factor $o$ and is a scalar (constant) under general coordinate transformation. And $o$ is related to $\tilde{\tau}$ through the conformal time $\Upsilon$ as

$$o = \frac{1}{2} o_{\mathrm{m}} (1 + \cos \Upsilon) \,, \tag{5.7.4}$$

$$\tilde{\tau} = \frac{1}{2} o_{\mathrm{m}} (\Upsilon + \sin \Upsilon) \,. \tag{5.7.5}$$

The fluid elements gather into the star as the collapse proceed, along the geodesics with fixed spatial coordinates $\tilde{\chi}$ , $\theta$ and $\varphi$, and eventually form a Schwarzschild black hole.

A similar method constructed in the last section can be implemented for the dust collapse spacetime, for which the particular coordinate transformation is given by

$$\begin{cases} \tilde{\tau}'_n = \tilde{\tau} - n\Delta\tilde{\tau} \,, \\ \tilde{\chi}'_n = \tilde{\chi} \,, \\ \theta'_n = \theta \,, \\ \varphi'_n = \varphi \,, \\ w'_n = \tilde{\tau}_0 + n\Delta\tilde{\tau} \,, \end{cases} \tag{5.7.6}$$

for the $n$-th spacetime slice, where $\tilde{\tau}_0$ is a constant and $\Delta\tilde{\tau}$ is a positive constant. The topology of the 5 dimensional manifold is given by $\mathcal{M}_{\mathrm{OS}} \times \mathbb{R}$. Then we can follow a similar route to recover the Lorentz structure by first choosing a metric for which form is expressed as

$$g'_{\mu\nu} \mathrm{d}u^\mu \mathrm{d}u^\nu = -\mathrm{d}\tilde{\tau}'^2 + o'(\tilde{\tau}', w')^2 (\mathrm{d}\tilde{\chi}'^2 + \sin^2 \tilde{\chi}' \mathrm{d}\tilde{\Omega}'^2) - \mathrm{d}w'^2 \,, \tag{5.7.7}$$

where the factor $o'$ is now a function of $\tilde{\tau}'$ and the new coordinate $w'$, given as

$$o'_n(\tilde{\tau}', w') = o_n(\tilde{\tau}' + w') \,, \tag{5.7.8}$$

on the $n$-th discrete slice. Construct the vertical 4 dimensional manifold $\Phi(\mathcal{M}_{\mathrm{OS}})$ in a similar way, we find that the metric introduced on $\Phi(\mathcal{M}_{\mathrm{OS}})$ is just that of (5.7.7) without the first $\mathrm{d}\tilde{\tau}'$ term, and in addition the factor $o'$ becomes a function of $w'$ due to that $\tilde{\tau}'$ is transferred to $w'$ on $\Phi(\mathcal{M}_{\mathrm{OS}})$ by coordinate transformation $w' = \tilde{\tau}$. The full proof of isometric relation between $\Phi(\mathcal{M}_{\mathrm{OS}})$ and $\mathcal{M}_{\mathrm{OS}}$ and the recovery of Lorentz structure on $\Phi(\mathcal{M}_{\mathrm{OS}})$ can be referred to the last section where we demonstrate an example for the Schwarzschild spacetime and an example for the pseudo-Schwarzschild spacetime.

In the case of Oppenheimer-Snyder spacetime, we deduce that the induced metric on $\Phi(\mathcal{M}_{\mathrm{OS}})$ is given as

$$h'_{\mu\nu} \mathrm{d}u^\mu \mathrm{d}u^\nu = o'(w')^2 (\mathrm{d}\tilde{\chi}'^2 + \sin^2 \tilde{\chi}' \mathrm{d}\tilde{\Omega}'^2) - \mathrm{d}w'^2 \,, \tag{5.7.9}$$

where

$$o' = \frac{1}{2} o'_{\mathrm{m}} (1 + \cos \Upsilon') \,, \tag{5.7.10}$$

$$w' = \frac{1}{2} o'_{\mathrm{m}} (\Upsilon' + \sin \Upsilon') \,, \tag{5.7.11}$$

along with the conformal time satisfies $\Upsilon' = \Upsilon$, since $w' = \tilde{\tau}$ by virtue of the coordinate transformation which leads to that $\Upsilon' = \Upsilon$ due to

(5.7.5) and (5.7.11), provided the constant maximum value of scale factor satisfies ${o'}_{\mathrm{m}} = o_{\mathrm{m}}$. Accordingly, consider (5.7.4) and (5.7.10), $o' = o$. Note that we need to set $\tilde{\tau}_0 = 0$ in (5.7.6), hence the fifth coordinate on the zeroth slice satisfies that ${w'}_0 = 0$.

# Chapter 6

# Generalization of the 4+1 Method to Brill-Lindquist Data and 3+1 Representation of a Kerr Black Hole

## 6.1 Overview

We have shown in the last Chapter that analytical metric can be embedded in a 5 dimensional manifold with the recovery of Lorentz structure between neighbouring foliations, and whether we can employ the method to a 3+1 numerical spacetime remains a question. Now we will generalize the embedding approach to the applications of 3+1 representations of dynamical spacetime before proceeding to the embedding of a real binary black hole evolution. In this Chapter, we first embed a fake evolution of a Brill-Lindquist initial slice in a 5 dimensional manifold, then we investigate application of the embedding approach to the Kerr black hole data. The implementation of the embedding method to the 3+1 representations of these spacetimes forms a bridge between the application of embedding approach to analytical and real 3+1 numerical data, which will be discussed in the 8th Chapter.

## 6.2 Numerical Method for Binary Black Hole

The spacetime around a binary black hole merger system is solved by using specific scheme from numerical relativity. The initial work for 3+1 numerical relativity originates from George Darmois in the 1920's [167], André Lichnerowicz in the 1930-40's [168, 169, 170] and then Yvonne Choquet-Bruhat (known as Yvonne Fourès-Bruhat at that time) in the 1950's [171, 172] who was able to show that the Cauchy problem arising from 3+1 decomposition has locally a unique solution [171]. Later in the late 1950's and early 1960's, a considerable impulse, serving as the foundation of GR, was contributed to the formalism by Paul Dirac [173, 174], and R. Arnowitt, S. Deser and C. Misner (the ADM formalism) [175, 176, 177, 178, 179, 180, 181, 182, 183, 184]. In the 1970's, by which time 3+1 formalism became the basic tool for nascent numerical relativity,

James York who developed a general method to solve the initial value problem [185] played a primordial role in putting the 3+1 equations in the shape which are used afterwards by the numerical community [16]. L. Smarr performed the first non-spherically symmetric simulation of the black hole spacetime [186]. It is the 1980's and 1990's when numerous authors devoted to help increase the numerical computations, both in complexity and suitable numerical implementation. Many efforts have been dedicated to such area and recently fruitful results have been carried out. Among them, Takashi Nakamura and his school, including Shibata, initiated the formulation, which was later on improved by Shapiro and Baumgarte and now becomes the popular BSSN scheme [187, 188, 189, 190]. In 2003, Alcubierre and his collaborators proposed a gauge condition which is now called the 'moving puncture' method to avoid the spacetime singularity while evolving the coordinates [191, 192]. Furthermore, the mathematical aspects of 3+1 numerical relativity are well established, and new computational algorithms are being developed (e.g. [193, 194]), aiming for improving the numerical accuracy and stability, and for extending the ranges of the physical parameters. Nowadays, most of the numerical relativity codes are based on the 3+1 formalism. Other approaches are the 2+2 formalism or characteristic formulation as reviewed by Winicour [195], the conformal field equations by Friedrich [196] as reviewed in [197], and the generalized harmonic decomposition by Pretorius [198, 199, 200].

Before proceeding, we need to demonstrate the 3+1 formalism of Einstein equation and that of spacetime metric, based on the configuration introduced in section 5.2

First of all, the induced metric $h_{ab}$ introduce in (A.0.58) can be rewritten as

$$h_{ab} = g_{ab} \mp n_a n_b \,, \tag{6.2.1}$$

where $n^a$ is the normalized normal vector[17]. The related projector tensor is given by

$$h_a{}^b = \delta_a{}^b \mp n_a n^b \,. \tag{6.2.2}$$

And the inverse of $h_{ab}$ can be deduced and is given by

$$h^{ab} = g^{ab} \mp n^a n^b \,. \tag{6.2.3}$$

We then introduce the extrinsic curvature, which is also known as the second fundamental form of hypersurface $\mathcal{W}$. More precisely, one defines the Weingarten map (sometime called the shape operator) $\tilde{\mathfrak{X}}$, which is a map on a tangent space at point $p$ of hypersurface $\mathcal{W}$ in $\mathcal{M}$

$$\tilde{\mathfrak{X}} \begin{cases} \mathcal{T}_p(\mathcal{W}) \to \mathcal{T}_p(\mathcal{W}) \,, \\ v^a \quad \mapsto v^b \nabla_b n^a \,, \end{cases} \tag{6.2.4}$$

where $n^a$ is normal to $\mathcal{W}$. Note that this definition is well-defined due to that

$$g_{ab} n^a \tilde{\mathfrak{X}}(v^b) = n_b v^c \nabla_c n^b = \frac{1}{2} v^c \nabla_c (n_b n^b) = 0 \,. \tag{6.2.5}$$

[17]Herein, a minus sign is employed if $n^a n_a = 1$, and a plus sign is employed if $n^a n_a = -1$.

The last equality is a result of (4.3.11) if $\mathcal{W}$ is not a null surface, whereas if $\mathcal{W}$ is null, then the definition of $\mathcal{X}$ depends on the choice of null normal vector $n^a$. A fundamental property of Weingarten map is that it is self-adjoint, such that

$$h_{ab}v^a\tilde{\mathcal{X}}(u^b) = h_{ab}u^a\tilde{\mathcal{X}}(v^b)\,, \tag{6.2.6}$$

given $\forall\ u^a\,,\ v^a \in \mathcal{T}_p(\mathcal{W})$. See Gourgoulhon [201] for a full mathematical proof.

The self-adjointness of $\tilde{\mathcal{X}}$ indicates that a symmetric bilinear form defined on $\mathcal{T}_p(\mathcal{W})\,,\ K$ given by

$$K\begin{cases} \mathcal{T}_p(\mathcal{W}) \times \mathcal{T}_p(\mathcal{W}) \to \quad \mathbb{R}\,, \\ \qquad (u,v) \qquad\quad \mapsto h_{ab}u^a\tilde{\mathcal{X}}(v^b)\,. \end{cases} \tag{6.2.7}$$

This is called the extrinsic curvature of hypersurface $\mathcal{W}$. Some authors, for example in [115], choose a minus sign for $K_{ab}$ in the above definition, whereas a plus sign is used here which is in agree with other authors' choice, e.g., Carroll [202], Wald [19] and Poisson [203]. More precisely, the extrinsic curvature is given by

$$\begin{aligned} K_{ab}u^av^b &= h_{ab}u^a\tilde{\mathcal{X}}(v^b) \\ &= h_{ab}u^ah_d{}^cv^d\nabla_cn^b \\ &= h_d{}^cu^av^d(g_{ab}+n_an_b)\nabla_cn^b \\ &= h_d{}^cu^av^d(g_{ab}\nabla_cn^b+n_an_b\nabla_cn^b) \\ &= h_d{}^cu^av^dg_{ab}\nabla_cn^b \\ &= h_d{}^cu^av^d\nabla_cn_a \\ &= h_b{}^cu^av^b\nabla_cn_a\,, \end{aligned} \tag{6.2.8}$$

where we use the fact that $n_b\nabla_cn^b = 0$ in the fifth equality and $\nabla_cg_{ab} = 0$ in the sixth equality, and change the dummy index $d$ to $b$. Hence we can rewrite the extrinsic curvature as

$$K_{ab} = h_b{}^c\nabla_cn_a\,, \tag{6.2.9}$$

and

$$K_{ab}u^av^b = u^av^c\nabla_cn_a\,. \tag{6.2.10}$$

The trace of $K_{ab}$ is denoted by $K$, given by

$$K = h^{ab}K_{ab}\,. \tag{6.2.11}$$

In principle, the contractions in equations (6.2.6)-(6.2.11) are measured by induced metric $h_{ab}$. Nevertheless, $n^a$ acting on a vector in $\mathcal{T}(\mathcal{W})$ leads to zero by definition. It gives the same results when we use $g_{ab}$ instead of $h_{ab}$

$$\begin{aligned} h^{ab}K_{ab} &= g^{ab}K_{ab}+n^an^bK_{ab} \\ &= g^{ab}K_{ab}+n^an^b\nabla_an_b \\ &= g^{ab}K_{ab}+\frac{1}{2}n^a\nabla_a(n^bn_b) \\ &= g^{ab}K_{ab}\,, \end{aligned} \tag{6.2.12}$$

where the inverse of $h_{ab}$ from (6.2.3) is applied in the first equality. $K_{ab}$ and $K$ are able to be related to the normal vector $n^a$ by means of the covariant derivative $\nabla_a$ according to the formula

$$\nabla_a n_b = K_{ba} - A_b n_a \,, \tag{6.2.13}$$

and

$$K = -g^{ab}\nabla_a n_b \,, \tag{6.2.14}$$

where

$$A^a = n^b \nabla_b n^a \,, \tag{6.2.15}$$

is defined as the 4 dimensional acceleration of an Eulerian observer, whose 4 dimensional velocity is $n^a$. The proof of (6.2.13) is given by virtue of (6.2.2) and (6.2.9), such that

$$\begin{aligned} K_{ab} &= h_b{}^c \nabla_c n_a \\ &= (\delta_b{}^c + n_b n^c)\nabla_c n_a \\ &= \nabla_b n_a + n_b n^c \nabla_c n_a \\ &= \nabla_b n_a + n_b A_a \,. \end{aligned} \tag{6.2.16}$$

This completes the proof of (6.2.13), where $A_a = g_{ab}A^b$.

The essential step for numerical relativity is the decomposition of metric and that of Einstein equation. Consider the 4 dimensional Riemann curvature tensor $R_{abc}{}^d$ defined in (B.0.24), the tensor is decomposed in a 3+1 manner by using the covariant derivative defined on hypersurface $\mathcal{W}$, denoted by $D_a$ and the derived 3 dimensional Riemann curvature tensor, denoted by ${}^3R_{abc}{}^d$, which is associated with induced 3 dimensional metric $h_{ab}$ on $\mathcal{W}$, where the 3 dimensional covariant derivative satisfies

$$D_a h_{bc} = 0 \,. \tag{6.2.17}$$

And the 3 dimensional Riemann tensor is given by

$$(D_a D_b - D_b D_a)v^c = -{}^3R_{abd}{}^c v^d \,, \tag{6.2.18}$$

where $v^c$ is a generic vector field tangent to $\mathcal{W}$. Given a tensor $T^{a_1\cdots a_i}{}_{b_1\cdots b_j} \in \mathfrak{T}_p(i,j)$, the 3 dimensional covariant derivative is expressible in terms of the 4 dimensional covariant derivative according to the formula

$$D_c T^{a_1\cdots a_i}{}_{b_1\cdots b_j} = h^{a_1}{}_{e_1}\cdots h^{a_i}{}_{e_i} h^{f_1}{}_{b_1}\cdots h^{f_j}{}_{b_j} h^d{}_c \nabla_d T^{e_1\cdots e_i}{}_{f_1\cdots f_j} \,. \tag{6.2.19}$$

In addition, we have another formula relates the two covariant derivatives, first let us compute the following formula

$$\begin{aligned} u^a D_a v^b &= u^a h_a{}^c h_d{}^b \nabla_c v^d \\ &= u^c(\delta_d{}^b + n_d n^b)\nabla_c v^d \\ &= u^c \nabla_c v^b + u^c n_d n^b \nabla_c v^d \\ &= u^c \nabla_c v^b + u^c n^b \nabla_c (n_d v^d) - u^c n^b v^d \nabla_c n_d \\ &= u^c \nabla_c v^b - u^c n^b v^d \nabla_c n_d \\ &= u^a \nabla_a v^b - u^a n^b v^d \nabla_a n_d \,, \end{aligned} \tag{6.2.20}$$

where the last equality is due to $n_d v^d = 0$, provided $v^d \in \mathcal{T}_p(\mathcal{W})$. Consider (6.2.10) and plug it into (6.2.20), gives

$$u^a D_a v^b = u^a \nabla_a v^b - K_{ad} v^a u^d n^b \,. \tag{6.2.21}$$

The 4 dimensional Riemann tensor is able to be decomposed with respect to the quantities relative to hypersurface $\mathcal{W}$, namely the 3 dimensional Riemann tensor ${}^3R_{abc}{}^d$ and extrinsic curvature $K_{ab}$. By using formula (6.2.19), we obtain that

$$\begin{aligned} D_a D_b v^c &= h_a{}^d h_b{}^e h_f{}^c \nabla_d (D_e v^f) \\ &= h_a{}^d h_b{}^e h_f{}^c \nabla_d (h_e{}^m h_n{}^f \nabla_m v^n) \,. \end{aligned} \tag{6.2.22}$$

After expanding and some algebra, we get the following expression

$$D_a D_b v^c = K_{ab} h_f{}^c n^e \nabla_e v^f - K_a{}^c K_{bf} v^f + h_a{}^d h_b{}^e h_f{}^c \nabla_d \nabla_e v^f \,. \tag{6.2.23}$$

Permute the indices $a$ and $b$ to get the expression for $D_b D_a v^c$, in the LHS of (6.2.18) there remains

$$D_a D_b v^c - D_b D_a v^c = (K_{ad} K_b{}^c - K_{bd} K_a{}^c) v^d + h_a{}^f h_b{}^e h_g{}^c (\nabla_f \nabla_e v^g - \nabla_e \nabla_f v^g) \,. \tag{6.2.24}$$

Consider the expression for the 4 dimensional Riemann tensor given in the appendix B, the above formula becomes

$$D_a D_b v^c - D_b D_a v^c = (K_{ad} K_b{}^c - K_{bd} K_a{}^c) v^d - h_a{}^f h_b{}^e h_g{}^c R_{fed}{}^g v^d \,, \tag{6.2.25}$$

substitute this relation into (6.2.18) results in

$${}^3R_{abd}{}^c v^d = h_a{}^f h_b{}^e h_g{}^c R_{fed}{}^g v^d - (K_{ad} K_b{}^c - K_{bd} K_a{}^c) v^d \,, \tag{6.2.26}$$

since $v^d = h_e{}^d v^e$, an equivalent formula is given by

$$h_a{}^d h_b{}^e h_c{}^f h_g{}^m R_{dem}{}^c v^g = {}^3R_{abg}{}^f v^g - (K_a{}^f K_{gb} - K_b{}^f K_{ag}) v^g \,. \tag{6.2.27}$$

Given the vector $v$ is an arbitrary tangent in $\mathcal{T}_p$, therefore we conclude

$$h_a{}^d h_b{}^e h_c{}^f h_g{}^m R_{dem}{}^c = {}^3R_{abg}{}^f - K_a{}^f K_{gb} + K_b{}^f K_{ag} \,, \tag{6.2.28}$$

which is known as the Gauss relation. Consider the contraction between two induced metrics,

$$h_a{}^b h_b{}^c = \delta_a{}^c + n_a n^c \,, \tag{6.2.29}$$

then we can contract the indices $a$ and $f$ in the Gauss relation

$$h_a{}^d h_b{}^e R_{de} + h_{ad} n^e h_b{}^c n^m R_{cme}{}^d = {}^3R_{ab} - K K_{ab} + K_{ad} K_b{}^d \,, \tag{6.2.30}$$

where $R_{de}$ and ${}^3R_{ab}$ are 4 dimensional Ricci and 3 dimensional Ricci tensors respectively. This is called the contracted Gauss relation. The scalar Gauss relation is given by

$$R + 2R_{ab} n^a n^b = {}^3R - K^2 + K_{ab} K^{ab} \,, \tag{6.2.31}$$

by taking the trace of (6.2.30) with respect to $h^{ab}$, where ${}^3R$ denotes the 3 dimensional Ricci scalar. Apply the identity (B.0.25) to normal vector $n^a$ and project it onto $\mathcal{W}$ via $h_{ab}$, gives

$$h_a{}^d h_b{}^e h_c{}^f R_{dem}{}^c n^m = h_a{}^d h_b{}^e h_c{}^f (\nabla_d \nabla_e n^c - \nabla_e \nabla_d n^c) \,. \tag{6.2.32}$$

From (6.2.13),

$$h_a{}^d h_b{}^e h_c{}^f \nabla_d \nabla_e n^c = D_a K_b{}^f - A^f K_{ab} \,, \tag{6.2.33}$$

swap the indices of $a \leftrightarrow b$ and subtraction from (6.2.33), equation (6.2.32) becomes

$$h_a{}^d h_b{}^e h_c{}^f R_{dem}{}^c n^m = D_a K_b{}^f - D_b K_a{}^f \,. \tag{6.2.34}$$

This is the Codazzi relation, or sometimes called Codazzi-Mainardi relation in the mathematical literature [204]. Contracting the Codazzi relation on the indices $a$ and $f$ yields

$$h_c{}^d n^c h_b{}^e R_{dem}{}^c = D_d K_b{}^d - D_b K \,. \tag{6.2.35}$$

Moreover,

$$\begin{aligned} h_c{}^d n^m h_b{}^e R_{dem}{}^c &= (\delta_c{}^d + n_c n^d) n^m h_b{}^e R_{dem}{}^c \\ &= n^m h_b{}^e R_{em} + h_b{}^e R_{dem}{}^c n_c n^m n^d \,. \end{aligned} \tag{6.2.36}$$

Taking the anti-symmetric property of the Riemann tensor, we conclude that

$$n^m h_b{}^e R_{em} = D_d K_b{}^d - D_b K \,, \tag{6.2.37}$$

which is known as the contracted Codazzi relation.

As mentioned in the previous context, an Eulerian observer, or called a fiducial observer [205], is defined as whose worldline's 4 dimensional velocity is the unit normal vector $n^a$ to a hypersurface $\mathcal{W} \subset \mathcal{M}$. Locally, according to Einstein's simultaneity convention, all physical events on the hypersurface can be simultaneously observed by such an observer. Furthermore, one can deduce that the 4 dimensional acceleration of an Eulerian observer satisfies

$$A_a = n^b \nabla_b n_a = D_a \ln N = \frac{1}{N} D_a N \,, \tag{6.2.38}$$

where $N$ is the lapse function. We then substituting this relation into (6.2.13), leads to

$$\nabla_a n_b = K_{ab} - D_a \ln N n_b \,. \tag{6.2.39}$$

The gradient of the time-like normal evolution vector $m^a$ is then deduced from (4.3.12) and (6.2.39), we obtain

$$\nabla_a m^b = N K^b{}_a - D^b N n_a + n^b \nabla_a N \,, \tag{6.2.40}$$

by means of this formula, we are able to derive the following expression

$$\begin{aligned} \mathcal{L}_m h_{ab} =& \; m^c \nabla_c h_{ab} + h_{cb} \nabla_a m^c + h_{ac} \nabla_b m^c \\ =& \; N n^c \nabla_c (n_a n_b) + h_{cb} (N K_b{}^c - D^b N n_c + n^c \nabla_a N) \\ & + h_{ac} (N K_b{}^c - D^c N n_a + n^c \nabla_a N) \\ =& \; N (n^c \nabla_c n_a n_b + n_a n^c \nabla_c n_b) + N K_{ba} - D_b N n_a + N K_{ab} - D_a N n_b \\ =& \; 2 N K_{ab} \,, \end{aligned} \tag{6.2.41}$$

where we have used $h_{ab} n^a = 0$ in the third equality and (6.2.38) in the last equality. It follows the simplest result

$$\mathcal{L}_m h_{ab} = 2 N K_{ab} \,. \tag{6.2.42}$$

Consider the relation $m^a = Nn^a$, after some algebra we get

$$\mathcal{L}_n h_{ab} = \frac{1}{N}\mathcal{L}_m h_{ab}\,, \tag{6.2.43}$$

this together with (6.2.42), leads to

$$K_{ab} = \frac{1}{2}\mathcal{L}_n h_{ab}\,. \tag{6.2.44}$$

Moreover, the Lie derivative of the projection tensor $h_a{}^b$ and any tensor which is in $\mathcal{T}_{\mathcal{W}}(i,j)$ along $m^a$ vanish,

$$\mathcal{L}_m h_a{}^b = 0\,, \tag{6.2.45}$$
$$\mathcal{L}_m T^{a_1\cdots a_i}{}_{b_1\cdots b_j} = 0\,. \tag{6.2.46}$$

The result implies that any tensor tangent to $\mathcal{W}$ remains a tangent tensor under the action of Lie derivative along $m^a$. Contrarily, this feature is not shared by $n^a$, for which $\mathcal{L}_n h_a{}^b \neq 0$.

Consider the expression $h_{ad}n^f h_b{}^g n^e R_{gef}{}^d = h_{ad}n^e h_b{}^g(\nabla_g\nabla_e n^d - \nabla_e\nabla_g n^d)$, by means of (6.2.39), we get successively

$$h_{ad}n^f h_b{}^g n^e R_{gef}{}^d = -K_{ae}K_b{}^e + \frac{1}{N}D_bD_aN - h_a{}^d h_b{}^g n^e \nabla_e K_{dg}\,. \tag{6.2.47}$$

And using (6.2.40), the Lie derivative of extrinsic curvature along the normal evolution vector is given by

$$\mathcal{L}_m K_{ab} = -Nn^c\nabla_c K_{ab} - 2NK_{ac}K_b{}^c + K_{ac}D^cNn_b + K_{bc}D^cNn_a\,. \tag{6.2.48}$$

Apply the projection operator $h_a{}^b$ twice to the above formula, we get

$$\mathcal{L}_m K_{ab} = -Nh_a{}^c h_b{}^e n^d \nabla_d K_{ce} - 2NK_{ac}K_b{}^c\,. \tag{6.2.49}$$

Extracting term $Nh_a{}^c h_b{}^e n^d\nabla_d K_{ce}$ and plug it into equation(6.2.47), leads to

$$h_{ad}n^f h_b{}^g n^e R_{gef}{}^d = -\frac{1}{N}\mathcal{L}_m K_{ab} + \frac{1}{N}D_aD_bN + K_{ad}K_b{}^d\,, \tag{6.2.50}$$

where the torsion free feature of the 3 dimensional covariant derivative is applied here. This relation is sometimes called the Ricci equation. Moreover, one can discard the 4 dimensional Riemann tensor by combining (6.2.30) and (6.2.50) to obtain a equation with only Ricci tensor, given by

$$h_a{}^c h_b{}^d R_{cd} = \frac{1}{N}\mathcal{L}_m K_{ab} - \frac{1}{N}D_aD_bN + {}^3R_{ab} + KK_{ab} - 2K_{ac}K_b{}^c\,. \tag{6.2.51}$$

Contracting this relation with respect to $h^{ab}$, leads to

$$\begin{aligned} h^{ab}R_{ab} &= \frac{1}{N}h^{ab}\mathcal{L}_m K_{ab} - \frac{1}{N}D_aD^aN + {}^3R + K^2 - 2K_{ab}K^{ab} \\ \Rightarrow (g^{ab}+n^an^b)R_{ab} &= \frac{1}{N}h^{ab}\mathcal{L}_m K_{ab} - \frac{1}{N}D_aD^aN + {}^3R + K^2 - 2K_{ab}K^{ab} \\ \Rightarrow R + R_{ab}n^an^b &= \frac{1}{N}h^{ab}\mathcal{L}_m K_{ab} - \frac{1}{N}D_aD^aN + {}^3R + K^2 - 2K_{ab}K^{ab}\,. \end{aligned} \tag{6.2.52}$$

From (6.2.42) and $h_{ab}h^{bc} = \delta_a{}^c$, we conclude

$$\mathcal{L}_m h^{ab} = -2NK^{ab}\,. \tag{6.2.53}$$

Consequently, (6.2.52) becomes

$$R + R_{ab}n^a n^b = {}^3R + K^2 + \frac{1}{N}\mathcal{L}_m K - \frac{1}{N}D_a D^a N\,. \tag{6.2.54}$$

Combine the relation with the scalar Gauss relation (6.2.31), we get an equation with only Ricci scalar

$$R = {}^3R + K^2 + K_{ab}K^{ab} + \frac{2}{N}\mathcal{L}_m K - \frac{2}{N}D_a D^a N\,. \tag{6.2.55}$$

Now we are at the stage to decompose the Einstein's gravitational equation. Firstly, by taking the contraction of it with respect to $g^{ab}$ on both sides, yields to the following formula

$$R = -8\pi T\,, \tag{6.2.56}$$

where $T = g^{ab}T_{ab}$ stands for the trace of energy-momentum tensor. An equivalent form of (E.0.1) is immediately derived from this

$$R_{ab} = 8\pi(T_{ab} - \frac{1}{2}T g_{ab})\,. \tag{6.2.57}$$

Focus on the right hand side of (E.0.1), from the very definition of energy-momentum tensor, energy density as measured by an Eulerian observer is given by

$$E := T_{ab}n^a n^b\,, \tag{6.2.58}$$

similarly, the 3 dimensional momentum density as measured by the Eulerian observer is given by

$$p_a := -T_{cb}n^c h^b{}_a\,. \tag{6.2.59}$$

Finally, still from the very definition of energy-momentum tensor, the stress tensor as measured by the Eulerian observer is given by

$$S_{ab} := h_a{}^c h_b{}^d T_{cd}\,. \tag{6.2.60}$$

Herein, $p^a$ and $S_{ab}$ are tangent to hypersurface $\mathcal{W}$. Denote the trace of stress tensor by $S$ with respect to $h_{ab}$

$$S = h^{ab}S_{ab}\,. \tag{6.2.61}$$

It is sufficient to reformulate $T_{ab}$ in terms of $(E, p_a, S_{ab})$

$$T_{ab} = S_{ab} + n_a p_b + E n_a n_b\,. \tag{6.2.62}$$

Take the trace with respect to $G_{ab}$ yields

$$T = S - E\,. \tag{6.2.63}$$

It is now fully equipped to perform the projection of Einstein equation onto the hypersurface and along its normal direction. A full projection

of (E.0.1) onto $\mathcal{W}$ is by taking the action of projection operator $h_a{}^b$ twice and taking the (6.2.51) into consideration, we get

$$\frac{1}{N}\mathcal{L}_m K_{ab} - \frac{1}{N} D_a D_b N + {}^3R_{ab} + K K_{ab} - 2K_{ac}K_b{}^c = 8\pi \left[ S_{ab} - \frac{1}{2}(S-E)h_{ab} \right] , \tag{6.2.64}$$

after some algebra, we have

$$\mathcal{L}_m K_{ab} = D_a D_b N - N \left\{ {}^3R_{ab} + K K_{ab} - 2K_{ac}K_b{}^c + 4\pi \left[ (S-E)h_{ab} - 2S_{ab} \right] \right\} , \tag{6.2.65}$$

the mixed projection onto $\mathcal{W}$ and along normal $n^a$ is given as

$$R_{ab} n^a h_c{}^b - \frac{1}{2} R g_{ab} n^a h_c{}^b = 8\pi T_{ab} n^a h_c{}^b . \tag{6.2.66}$$

It follows from the contracted Codazzi equation (6.2.37) and (6.2.59) that

$$D_a K - D_b K_a{}^b = 8\pi p_a . \tag{6.2.67}$$

This is called the momentum constraint.

The full projection along the normal direction to hypersurface $\mathcal{W}$, given by

$$R_{ab} n^a n^b - \frac{1}{2} R g_{ab} n^a n^b = 8\pi T_{ab} n^a n^b , \tag{6.2.68}$$

consider $g_{ab} n^a n^b = -1$ and (6.2.58), the above equation becomes

$${}^3R + K^2 - K_{ab} K^{ab} = 16\pi E . \tag{6.2.69}$$

This equation is called the Hamiltonian constraint. At the stage, equations (6.2.65), (6.2.67) and (6.2.69) consist of a 3+1 equivalent form of Einstein gravitational field equation (6.2.51).

We then introduce the adapted coordinate system, denoted by $(t, x^i)$, which is suitable for our foliation $\mathcal{W}_t$ , $\forall\ t \in \mathbb{R}$, such that the three field equations could be translated into a set of partial differential equations and are able to be carried out practically. To establish the coordinate system, let us first construct a local 3 dimensional coordinate system, denoted by $x^i$, on a single hypersurface $\mathcal{W}_0$. The local coordinates are carried out from $\mathcal{W}_0$ to the adjacent foliation $\mathcal{W}_{\delta t}$, by the Eulerian observer along its tangent direction. Accordingly, at each intersection point $p = C_{\mathrm{EO}} \cap \mathcal{W}_t$ of the Eulerian observer and the hypersurfaces, a local coordinate is well defined. Together with the global function time $t$, one can define a coordinate system $(t, x^i)$ for the manifold $\mathcal{M}$ which is adapted to the foliation that we choose. The coordinates $x^i$ are recognized as the spatial coordinates and $t$ is recognized as the temporal coordinate, although in some cases its tangent vector $(\partial_t)^a$ is not time-like according to (4.3), for which would not cause unphysical consequence.

Note that for a coordinate line of $(\partial_i)^a$, it always lies on the slice $\mathcal{W}_t$ due to a constant zeroth coordinate $t = con$ (constant), which results in that the tangent vector $(\partial_i)^a$ is tangent to $\mathcal{W}_t$.

Write down the components of metric and induced metric as follow

$$g_{ab} = g_{\mu\nu} (\mathrm{d}x^\mu)_a (\mathrm{d}x^\nu)_b , \tag{6.2.70}$$

$$h_{ab} = h_{ij} (\mathrm{d}x^i)_a (\mathrm{d}x^j)_b . \tag{6.2.71}$$

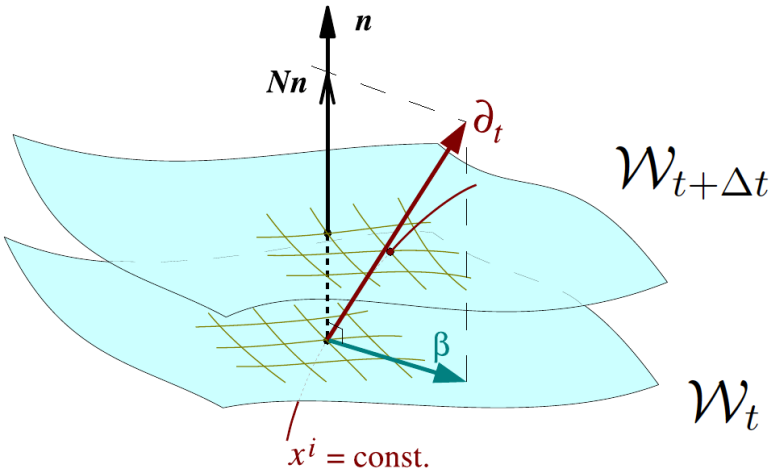


Figure 6.1: This figure illustrates the adapted coordinate system on the foliations. Credit: É. Gourgoulhon, 2012.

The components in the coordinate system constructed above are then given as

$$g_{\mu\nu} = g_{ab}(\partial_\mu)^a(\partial_\nu)^b\,, \tag{6.2.72}$$
$$h_{ij} = h_{ab}(\partial_i)^a(\partial_j)^b\,. \tag{6.2.73}$$

From definition (4.3.15), we get

$$\beta_i(\mathrm{d}x^i)_a = \beta_a = g_{ab}\beta^b = h_{ab}\beta^b\,, \tag{6.2.74}$$

where we have used that $n^a$ is normal to $\mathcal{W}_t$ and $\beta^b$ is tangent to $\mathcal{W}_t$. The '00' component of metric $g_{ab}$ is given by

$$g_{00} = g_{\mu\nu}(\partial_t)^a(\partial_t)^b = -N^2 + \beta_i\beta^i\,, \tag{6.2.75}$$

where we have used (4.3.18) in the second equality. The '$0i$' components are given by

$$\begin{aligned} g_{0i} &= g_{ab}(\partial_t)^a(\partial_i)^b \\ &= g_{ab}(m^a + \beta^a)(\partial_i)^b \\ &= g_{ab}\beta^a(\partial_i)^b \\ &= (h_{ab} - n_a n_b)\beta^a(\partial_i)^b \\ &= h_{ab}\beta^a(\partial_i)^b \\ &= \beta_j(dx^j)_b(\partial_i)^b \\ &= \beta_i\,, \end{aligned} \tag{6.2.76}$$

where (6.2.74) is applied in the second last equality. The '$ij$' components of $g_{ab}$ is given by

$$g_{ij} = g_{ab}(\partial_i)^a(\partial_j)^a = (h_{ab} - n_a n_b)(\partial_i)^a(\partial_j)^b = h_{ij}\,. \tag{6.2.77}$$

Hence, the expression (6.2.70) can be rewritten as

$$g_{\mu\nu}\mathrm{d}x^\mu\mathrm{d}x^\nu = -N^2\mathrm{d}t^2 + h_{ij}(\mathrm{d}x^i + \beta^i\mathrm{d}t)(\mathrm{d}x^j + \beta^j\mathrm{d}t)\,, \tag{6.2.78}$$

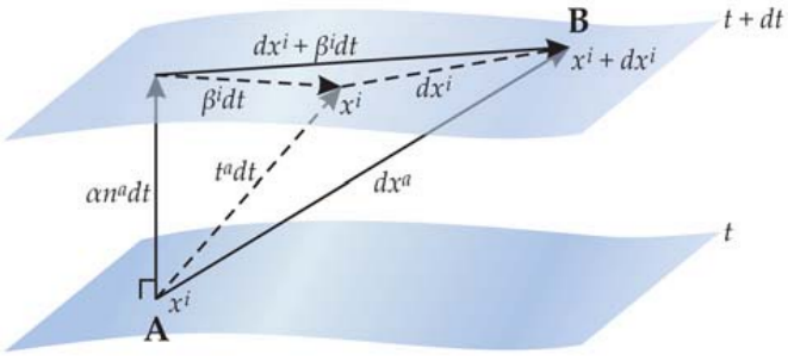


Figure 6.2: This graph illustrates how lapse function and shift vector 'propagate' the coordinate from one time slice to another. Credit: T. W. Baumgarte and S. L. Shapiro, 2010.

where we ignore the abstract indices here.

Further calculation implies that the relation between the determinants of $g_{ab}$ and $h_{ab}$ is given by

$$\sqrt{-g} = N\sqrt{h}\,, \tag{6.2.79}$$

where $g$ and $h$ denote the determinant of a 4 dimensional metric and the induced metric respectively.

Given a coordinate system $(t, x^i)$ on manifold $\mathcal{M}$ and a space-like hypersurface $\mathcal{W}_0$ uniquely determine a lapse function $N$ and a shift vector $\beta$. The converse is true in the sense that given a coordinate system $(x^i)$, a lapse function field and a shift vector field on the space-like hypersurface $\mathcal{W}_0$ uniquely determine a coordinate system $(t, x^i)$ in the neighbourhood region of $\mathcal{W}_0$, such that $t = 0$ is $\mathcal{W}_0$. Graphically, the lapse function tells us the distance between the point $p$ in $\mathcal{W}_0$ and the point $p'$ in the adjacent hypersurface $\mathcal{W}_{\delta t}$, where $p'$ is right 'above' $p$ (perpendicularly moving from $p$ to $p'$), and the shift vector tells us how to propagate the coordinate $(x^i)$ from its original location to its current location in $\mathcal{W}_{\delta t}$.

In the adapted coordinate system, $\mathcal{L}_m K_{ab}$ can be expressed as

$$\mathcal{L}_m K_{ab} = \mathcal{L}_{\partial_t} K_{ab} - \mathcal{L}_\beta K_{ab}\,, \tag{6.2.80}$$

rewrite in component form

$$\mathcal{L}_m K_{ij} = \mathcal{L}_{\partial_t} K_{ij} - \mathcal{L}_\beta K_{ij}\,, \tag{6.2.81}$$

where

$$\mathcal{L}_{\partial_t} K_{ij} = \frac{\partial K_{ij}}{\partial t} \equiv \partial_t K_{ij}\,, \tag{6.2.82}$$

and

$$\mathcal{L}_\beta K_{ij} = \beta^k \partial_k K_{ij} + K_{kj}\partial_i \beta^k + K_{ik}\partial_j \beta^k\,, \tag{6.2.83}$$

similarly, it follows from (6.2.42) that

$$2NK_{ij} = \mathcal{L}_{\partial_t} h_{ij} - \mathcal{L}_\beta h_{ij}\,, \tag{6.2.84}$$

where

$$\mathcal{L}_{\partial_t} h_{ij} = \partial_t h_{ij}\,, \tag{6.2.85}$$

and the second term on the RHS is given as

$$\begin{aligned}\mathcal{L}_\beta h_{ij} &= \beta^k D_k h_{ij} + h_{kj} D_i \beta^k + h_{ik} D_j \beta^k \\ &= D_i \beta_j + D_j \beta_i \,, \end{aligned} \tag{6.2.86}$$

by means of equations (6.2.81) and (6.2.82), as well as (6.2.84) and (6.2.85), the 3+1 form of Einstein equation (6.2.65), (6.2.67) and (6.2.69) become

$$\partial_t h_{ij} - \mathcal{L}_\beta h_{ij} = 2NK_{ij} \,, \tag{6.2.87}$$

$$\begin{aligned}\partial_t K_{ij} - \mathcal{L}_\beta K_{ij} = {} & D_i D_j N - N^3 R_{ij} - NKK_{ij} + 2NK_i{}^k K_{kj} \\ & + 4\pi N[(S-E)h_{ij} - 8\pi N S_{ij}] \,, \end{aligned} \tag{6.2.88}$$

$${}^3R + K^2 - K_{ij}K^{ij} = 16\pi E \,, \tag{6.2.89}$$

$$D_i K - D_j K_i{}^j = 8\pi p_i \,. \tag{6.2.90}$$

Furthermore, the covariant derivative terms can be expressed in terms of partial derivative with respect to the spatial coordinates $x^i$ by means of 3 dimensional Christoffel symbols ${}^3\Gamma_{ij}{}^k$ of $D_i$, where

$$D_i D_j N = \partial_i \partial_j N - {}^3\Gamma_{ij}{}^k \partial_k N \,, \tag{6.2.91}$$

$$D_j K_i{}^j = \partial_j K_i{}^j + {}^3\Gamma_{jk}{}^j K_i{}^k - {}^3\Gamma_{ji}{}^k K_k{}^j \,, \tag{6.2.92}$$

$$D_i K = \partial_i K \,. \tag{6.2.93}$$

Equations (6.2.83) and (6.2.86) then become

$$\mathcal{L}_\beta K_{ij} = \beta^k \partial_k K_{ij} + K_{kj} \partial_i \beta^k + K_{ik} \partial_j \beta^k \,, \tag{6.2.94}$$

$$\mathcal{L}_\beta h_{ij} = \partial_i \beta_j + \partial_j \beta_i - 2\Gamma_{ij}{}^k \beta_k \,. \tag{6.2.95}$$

With the 3 dimensional Ricci tensor and 3 dimensional Christoffel symbol given by

$${}^3R_{ij} = \partial_k {}^3\Gamma_{ij}{}^k - \partial_j {}^3\Gamma_{ik}{}^k + {}^3\Gamma_{ij}{}^k {}^3\Gamma_{kl}{}^l - {}^3\Gamma_{ik}{}^l {}^3\Gamma_{lj}{}^k \,, \tag{6.2.96}$$

$${}^3\Gamma_{ij}{}^k = \frac{1}{2} h^{kl} (\partial_i h_{lj} + \partial_j h_{il} - \partial_l h_{ij}) \,. \tag{6.2.97}$$

These equations, (6.2.87)-(6.2.97) complete the second-order non-linear PDEs of 3+1 Einstein equation for unknowns $(h_{ij}, N, K_{ij}, \beta^i)$, assuming that source terms $(E, p_i, S_{ij})$ are given. This is first derived by Darmois in [167], with the special case $N = 1$ and $\beta^i = 0$.

## 6.3 Embedding the 3+1 Brill-Lindquist Data in a 5 Dimensional Manifold

Follow the last section, we now have the mathematical tools to build the numerical data for binary compact star systems, such as BBH, NS-BH and NS-NS binaries. Let us start with a simple data set, derived by Brill and Lindquist, describing the initial condition of two head-on colliding non-spinning black holes [206, 207].

Another head-on collision initial value solution for black holes is given by Misner in 1960 [208].

A treatment that 2 dimensional Misner and Brill-Lindquist slices are isometrically embedded into 3 dimensional Euclidean space is discussed by Hsungrow [209].

In this section, we first study the Brill-Lindquist data. These data are helpful to us for two main justifications: The initial data is readily derived and can be easily generalized to provide discrete data on a 4 dimensional spacetime, i.e., the physical variables $(N, \beta^i, h_{ab}, K_{ab})$. Secondly, a fake evolution Brill-Lindquist metric might allow the appearance of radiation region.

A time symmetric Brill-Lindquist initial 3 dimensional metric $h_{ab}$ is given by

$$h_{ab} = \hat{\psi}^4 \delta_{ab} \,, \tag{6.3.1}$$

where $\delta_{ab}$ is the metric of a 3 dimensional Euclidean space, and this metric is apparently conformally flat. $\hat{\psi}$ is given as

$$\hat{\psi} = 1 + \sum_{i=1}^{N_{bh}} \frac{M_i}{2r_i} \,, \tag{6.3.2}$$

where $N_{bh}$ is the number of black holes which takes the value of 2 throughout the thesis, $M_i$ is the mass of the $i$-th black hole and $r_i$ are the radial distance from the centres of the black holes [210].

By using the isotropic (spherical) coordinates, the metric can be expressed as

$$h_{\mu\nu} \mathrm{d}x^\mu \mathrm{d}x^\nu = \hat{\psi}^4 \left[ \mathrm{d}r^2 + r^2 \left( \mathrm{d}\theta^2 + \sin^2\theta \mathrm{d}\varphi^2 \right) \right] \,, \tag{6.3.3}$$

with

$$r_i = \sqrt{r^2 + {d_i}^2 - 2 d_i r \cos\theta} \,, \tag{6.3.4}$$

where $d_i$ denotes the distance between the $i$-th black holes and the origin of the coordinate system. When they are far apart, each hole has a horizon radius of $M/2$ in the coordinate system.

The limitation of separation for two black holes between single and double horizons have been found by several people, including Brill and Lindquist [206], Shoemaker et al. [210], Cadez [211], Alcubierre et al. [212], and Huq [213] and others [214, 215]. Herein, we use the critical separation $1.53(5)M$ found by Shoemaker et al..

Next we can obtain an evolution from the initial data $(1, {\beta_0}^a, {\hat{\psi}_0}^4 \delta_{ab}, 0)$ with isotropic coordinates $(t_0, r_0, \theta_0, \varphi_0)$, where $\hat{\psi}_0 = 1 + M/r_1 + M/r_2$ and two equal mass black holes are assumed here and for the rest of the context. Suppose the two black holes locate on the $z$-axis and have the initial radial values of $d_0$ and $-d_0$ respectively. Let the initial separation value of binary black hole spacetime be $10M$ and at the next time point a Brill-Lindquist slice with separation smaller than that of the initial one. Repeat this procedure and effectively glue all time slices together until the slice with separation $1.5M$. This can be viewed in the following physical scenario: Let each hole possess a small initial constant speed $v$[18]. For each finite time step $\delta t$, both objects move along the $z$-axis a small distance $\delta r$, where

$$\delta r = v \delta t \,. \tag{6.3.5}$$

[18]Herein, small means that the distance that each hole moves in a finite time period is incomparable to that of the separation of two black holes.

This is a smooth manifold $\mathcal{M}$ with a 4 dimensional metric, given by

$$g_{\mu\nu}\mathrm{d}x^{\mu}\mathrm{d}x^{\nu} = -\left(N^2 - \beta^{\alpha}\beta_{\alpha}\right)\mathrm{d}t^2 + \beta_1\mathrm{d}t\mathrm{d}r + \beta_2\mathrm{d}t\mathrm{d}\theta + \beta_3\mathrm{d}t\mathrm{d}\varphi + \hat{\psi}^4\left[\mathrm{d}r^2 + r^2\left(\mathrm{d}\theta^2 + \sin^2\theta\mathrm{d}\varphi^2\right)\right], \tag{6.3.6}$$

where $d_n = d_0 - n\delta r$. In addition, a very important truth is concealed from the implicit term $\hat{\psi}$, which is a time dependent term

$$\hat{\psi} = 1 + \frac{M}{r_{b1}(t)} + \frac{M}{r_{b2}(t)}, \tag{6.3.7}$$

where $r_{b1}(t)$ and $r_{b2}(t)$ stand for the radial distance from the black hole centres, which are time dependent due to (6.3.5). This will lead to a dynamical spacetime for the 4 dimensional Brill-Lindquist metric.

Before making a progress, one should notice this type of evolution might not be allowed in the physical world. As each slice is a solution to the Hamiltonian and momentum constraint equations but the full metric is not necessarily a solution to the Einstein equations. Nevertheless, this construction is a good test for the viability of the 4+1 numerical method for a discrete data set.

The first time slice is now able to be constructed. After a short time evolving by $\delta t$, the initial data becomes $(N_1, {\beta_1}^a, \hat{\psi}_1{}^4\delta_{ab}, 0)$, where $\hat{\psi}_1$ is given by

$$\hat{\psi}_1 = 1 + \frac{M}{2r_1} + \frac{M}{2r_1} \tag{6.3.8}$$

$$= 1 + \frac{M}{r_1}, \tag{6.3.9}$$

where $r_1$ is given by

$$r_1 = \sqrt{r^2 + {d_1}^2 - 2d_1 r\cos\theta}. \tag{6.3.10}$$

Note that here we insist the fact that both black holes possess the same value of radial distance from star centre, denoted by $r_1$. We can follow a similar procedure for the rest of the slices until the critical separation is approached and a single horizon is formed. We now have achieved a 4 dimensional Brill-Lindquist data set.

Furthermore, we need to determine the value of lapse function $N_n$ and shift vector ${\beta_n}^a$. Despite the slices and a coordinate system are determined, there is freedom to choose a suitable pair of $(N, \beta^a)$ since the fake manifold feature of the dynamical Brill-Lindquist spacetime. Let the lapse function take the value of 1 and the shift vector be 0. Hence we obtain a series data

$$(1, 0, \hat{\psi}_n{}^4\delta_{ab}, 0), \tag{6.3.11}$$

for the 4 dimensional metric defined on the $n$-th slice of the Brill-Lindquist manifold.

Note that the slow decelerating motion of two black holes might give rise to a gravitational radiation in the spacetime, with a small 3 dimensional acceleration $a^{\mu}$. Such an evolution will absolutely lead to a solution of Einstein equations, but satisfy the full vacuum Hamiltonian constraint

$$D_j K^j{}_i - D_i K = 0, \tag{6.3.12}$$

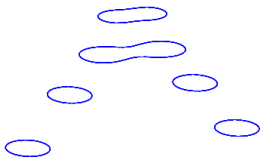

Figure 6.3: These plots illustrate the evolution of two equal mass black holes merging, derived from Brill-Lindquist initial data. 4 slices are drawn in the figure.

on each Brill-Lindquist time slice. For the case of the fake wave propagation, we have to find out other way of deriving the waveform. The gravitational wave is caused by the accelerating motion of massive bodies, and hence one intuitively wants to borrow this idea, such that the gravitational wave energy is equal to that of the energy loss of the gravitating system between two adjacent foliations.

We then apply the 4+1 method to the 4 dimensional Brill-Lindquist data that is constructed in the last section here. Firstly, we embed the 4 dimensional metric into a 5 dimensional space and obtain the coordinate transformation as below

$$\begin{cases} t' &= t\,, \\ r' &= r\,, \\ \theta' &= \theta\,, \\ \varphi' &= \varphi\,, \\ {w'}_0 &= t_0\,. \end{cases} \tag{6.3.13}$$

This is done on the zeroth 4 dimensional slice $\phi_{w_0}(\mathcal{M})$, $\mathcal{M}$ denotes the original 4 dimensional manifold generated from the Brill-Lindquist data.

On the first slice the coordinate transformation is given by

$$\begin{cases} t' &= t - \Delta t\,, \\ r' &= r\,, \\ \theta' &= \theta\,, \\ \varphi' &= \varphi\,, \\ {w'}_1 &= t_0 + \Delta t = t_1\,. \end{cases} \tag{6.3.14}$$

Repeating this operation to the rest of the 4 dimensional spacetime slices and a new manifold is formed via combining all 4 dimensional spacetime foliations, denoted by $\mathcal{M}' = \mathbb{R} \times \mathcal{M}$.

Then one needs to recover the Lorentz structure by introducing a 5 dimensional metric, which is given by

$$\begin{aligned} {g'}_{ab} = &- \left(N^2 - {\beta'}_c {\beta'}^c\right) \left(\mathrm{d}w'\right)_a \left(\mathrm{d}w'\right)_b + {\beta'}_1 \left(\mathrm{d}t'\right)_a \left(\mathrm{d}r'\right)_b + {\beta'}_2 \left(\mathrm{d}t'\right)_a \left(\mathrm{d}\theta'\right)_b \\ &+ {\beta'}_3 \left(\mathrm{d}t'\right)_a \left(\mathrm{d}\varphi'\right)_b + g_{ab}\,. \end{aligned} \tag{6.3.15}$$

The only term in the metric that needs to be concerned is the time dependent $\hat{\psi}$, which becomes $\hat{\psi}'(t', w')$, given by

$$\hat{\psi}'_n(t', w') = \hat{\psi}'_n(t' + w')\,, \tag{6.3.16}$$

for the coefficient contained in the $g_{\mu\nu}$ component, where $\hat{\psi}'$ has the same expression as that of $\hat{\psi}$. By virtue of these transformations and constructions, a Lorentz structure can be recovered and the proof is given in previous context.

We have investigated the 3 dimensional Brill-Lindquist stationary metric and made a generalization from the initial data to an evolution version of this metric. Apart from the initial slice, more time slices are added and glued to form a smooth Brill-Lindquist manifold at time $t > t_0$, where $t_0$ labels the initial time on the zeroth slice. By adjusting the separation $d_i$ one can create a fake evolution of a head-on collision of the two compact stars. The collision is requiring that the distance between two holes is decreasing as the introduced 'physical' time $t$ increases. This is by no means a real evolution, since the 4 dimensional Brill-Lindquist metric is not a solution to the full Einstein equation. Nevertheless, this treatment is still a good sample for studying the usability of a 4+1 formulation for a discrete 3+1 spacetime data.

We have, at this stage, applied the embedding process with the fake evolution Brill-Lindquist data, and successfully construct a 4+1 data from the discrete 3+1 numerical data. The Lorentz structure of the reconstructed 4 dimensional manifold $\Phi(\mathcal{M})$ is recovered outside one spacetime slice.

We have already discussed in Chapter 4 the dynamical case of a dust collapse Oppenheimer-Snyder spacetime. However, this metric is not employing 3+1 numerical relativity and only an analytical solution is studied. We then have to apply the 4+1 method to a real numerical data. Making use of the fake evolution Brill-Lindquist metric is a first step. There is no solution of this initial value to the general relativity that is singled out as two initially stationary black holes. Accordingly, it is still necessary to have a try with more generic data which has to be a solution of Einstein equation. The simplest case, two equal mass, non-spinning black holes is the best to start with. Using Einstein toolkit [216, 217] it is convenient to generate a data set from our own initial value.

In some previous papers, people have described a Brill-Lindquist data with radiation on the time slice by means of perturbation theory, in which case a gravitational radiation area is deduced and may comparable to another initial value solution given by Misner [218].

Furthermore, the study of an evolution Misner 4 dimensional spacetime has been considered [219] and it is not surprisingly that one would be able to research an extensive solution to a Brill-Lindquist initial data, satisfying the Einstein equation, for which possesses a gravitational radiation region. Nevertheless, we will not do it here in this thesis. Intuitively, there should exist some correlations between a real evolution and the fake one, in which a further investigation may take this into consideration and explain more details.

Consider the real evolution of two black holes, which undergo head-on collision, there is a numerical simulation and the data is given by the SERN/NRPY code [220, 221, 222].

## 6.4 Applications of the 4+1 Method to Kerr Spacetime

The analytical Kerr solution in the Boyer-Lindquist coordinate system is given in (3.2.1)-(3.2.9)

The embedding method has been constructed in the previous Chapter. We now apply it to the analytical Kerr spacetime. Define a 5 dimensional manifold $\mathcal{M}'$ which is given by $\mathbb{R} \times \mathcal{M}$, where $\mathcal{M}$ represents the original Kerr spacetime. A metric can be defined on this manifold, whose form is given by

$$g'_{\mu\nu}\mathrm{d}u^{\mu}\mathrm{d}u^{\nu} = g'_{00}\mathrm{d}t'^{2} + 2g'_{03}\mathrm{d}t'\mathrm{d}\varphi' + g'_{km}\mathrm{d}u^{k}\mathrm{d}u^{m} + g'_{4j}\mathrm{d}w'\mathrm{d}u^{j}\,, \quad (6.4.1)$$

where index 3 corresponds to the $\varphi'$ coordinate, 0 corresponds to the $t'$ coordinate and index 4 corresponds to the $w'$ coordinate, $k$ , $m$ and $j$ run from 1 to 3. And

$$g'_{4k}\mathrm{d}w'\mathrm{d}u^{k} = g'_{44}\mathrm{d}w'^{2} + g'_{43}\mathrm{d}w'\mathrm{d}\varphi'\,, \quad (6.4.2)$$

with

$$g'_{44} = -\left(1 - \frac{2M'r'}{\tilde{\Sigma}'}\right)\,, \quad (6.4.3)$$

$$g'_{43} = -\frac{2a'M'r'\sin^{2}\theta'}{\tilde{\Sigma}'}\,, \quad (6.4.4)$$

where

$$\tilde{\Sigma}' = r'^{2} + a'^{2}\cos^{2}\theta'\,, \quad (6.4.5)$$

$$a' = \frac{J'}{M'}\,, \quad (6.4.6)$$

and the remaining components of $g'$ have similar expressions as those given in (3.2.1)-(3.2.6).

The coordinate transformation for the 4 dimensional Kerr spacetime is given by

$$\begin{cases} t' &= t - n\Delta t\,, \\ r' &= r\,, \\ \theta' &= \theta\,, \\ \varphi' &= \varphi\,, \\ w'_{n} &= t_0 + n\Delta t = t_n\,, \end{cases} \quad (6.4.7)$$

on the $n$-th slice $\phi_{w_n}(\mathcal{M})$, $t_0$ and $t_n$ are constants. One then needs to cut the foliations in $\mathcal{M}'$ to obtain a new manifold, denoted by $\Phi(\mathcal{M})$, which is an image of $\mathcal{M}$. On this submanifold, one can recover the Lorentz structure by pulling-back the 5 dimensional metric $g'$. A pulled-back metric is given by

$$h'_{\mu\nu}\mathrm{d}u^{\mu}\mathrm{d}u^{\nu} = g'_{44}\mathrm{d}w'^{2} + 2g'_{43}\mathrm{d}w'\mathrm{d}\varphi' + g'_{km}\mathrm{d}u^{k}\mathrm{d}u^{m}\,. \quad (6.4.8)$$

The local Lorentz structure is encoded in the above 4 dimensional Lorentzian metric.

We then apply the above embedding method to a 3+1 numerical representation for the Kerr spacetime derived by the ADM formulation.

We will apply the Kerr-Schild line element, which possesses the following form

$$g_{\mu\nu} = \eta_{\mu\nu} + 2\mathcal{H} l_\mu l_\nu \,, \tag{6.4.9}$$

where $\eta_{\mu\nu}$ represents the Minkowskian metric, $l_\mu$ and $l_\nu$ are incoming null vectors, and $\mathcal{H}$ denotes a scalar function of coordinates [223]. In a Cartesian coordinate system $(t, x, y, z)$, the components of the metric read

$$\mathcal{H} = \frac{Mr^3}{r^4 + a^2 z^2} \,, \tag{6.4.10}$$

and

$$l_\mu = \left(1, \frac{rx + ay}{r^2 + a^2}, \frac{ry - ax}{r^2 + a^2}, \frac{z}{r}\right) \,, \tag{6.4.11}$$

where $r$ is given by

$$r^2 = \frac{1}{2}(\rho^2 - a^2) + \sqrt{\frac{1}{4}(\rho^2 - a^2)^2 + a^2 z^2} \,, \tag{6.4.12}$$

where $M$ denotes the mass of the black hole, $a = J/M$ is the black hole's angular momentum, and $\rho \equiv \sqrt{x^2 + y^2 + z^2}$.

A numerical decomposition of this metric is given by applying the equation (6.2.78), such that the components for Kerr metric can be represented by the lapse function, shift vector and a 3 dimensional metric defined on each hypersurface, which are given as

$$N = \frac{1}{\sqrt{1 + 2\mathcal{H} {l_t}^2}} \,, \tag{6.4.13}$$

$$\beta^k = 2\mathcal{H} l_t \delta^{kj} l_j / \left(1 + 2\mathcal{H} {l_t}^2\right) \,, \tag{6.4.14}$$

$$h_{kj} = \eta_{kj} + 2\mathcal{H} l_k l_j \,, \tag{6.4.15}$$

where $l_t$ denotes the zeroth component of $l_\mu$ , $k$ and $j$ run from 1 to 3.

We then embed these data in a 5 dimensional manifold, which is introduced as $\mathcal{M}' = \mathbb{R} \times \mathcal{M}$. First we need a coordinate transformation given in the Chapter 4, which is given as

$$\begin{cases} t' &= t \,, \\ r' &= r \,, \\ \theta' &= \theta \,, \\ \varphi' &= \varphi \,, \\ {w'}_0 &= t_0 \,, \end{cases} \tag{6.4.16}$$

on the zeroth 4 dimensional slice in the 5 dimensional manifold. On the first slice, it is

$$\begin{cases} t' &= t - \Delta t \,, \\ r' &= r \,, \\ \theta' &= \theta \,, \\ \varphi' &= \varphi \,, \\ {w'}_1 &= t_0 + \Delta t = t_1 \,. \end{cases} \tag{6.4.17}$$

As mentioned before, the 5 dimensional manifold $\mathcal{M}'$ is formed by repeating the process, for which on the $n$-th slice, the coordinate transformation is given as

$$\begin{cases} t' &= t - n\Delta t\,, \\ r' &= r\,, \\ \theta' &= \theta\,, \\ \varphi' &= \varphi\,, \\ {w'}_n &= t_0 + n\Delta t = t_n\,. \end{cases} \tag{6.4.18}$$

where $t_0$ , $t_n$ and $t_1$ are constants, $\Delta t$ is a positive constant.

An appropriate 5 dimensional metric is given by

$$\begin{aligned} {g'}_{\mu\nu}\mathrm{d}u^\mu\mathrm{d}u^\nu = &- \left(N'^2 - {\beta'}_i\beta'^i\right)\mathrm{d}w'^2 + g_{\mu\nu}\mathrm{d}u^\mu\mathrm{d}u^\nu \\ &+ {h'}_{ij}\beta'^i\mathrm{d}u^j\mathrm{d}w' \\ &+ {h'}_{ij}\beta'^j\mathrm{d}u^i\mathrm{d}w'\,. \end{aligned} \tag{6.4.19}$$

Where we have reformulated the equation (6.2.78), and $g_{\mu\nu}$ denote the components of the original Kerr metric and are now depending on the coordinates $u^\mu$. Note that none of the components of the Kerr metric depends on the temporal coordinate $t$, hence we have the following relations

$$N' = N\,, \tag{6.4.20}$$

$$\beta'^i = \beta^i\,, \tag{6.4.21}$$

$$h'_{ij} = h_{ij}\,. \tag{6.4.22}$$

Following the procedure we proposed in the Chapter 4, a vertical manifold $\Phi(\mathcal{M})$ can be constructed by cutting all spacetime foliations. One can find that the Lorentz structure is recovered by pulling-back the 5 dimensional metric on the induced 4 dimensional manifold $\Phi(\mathcal{M})$.

We can recover the local Lorentz structure by a similar way, for which a detailed derivation is ignored here.

# Chapter 7

# Isometric Embedding for a Four Dimensional Lorentzian Manifold in a Five Dimensional Pseudo-Riemannian Manifold

## 7.1 Overview

We have exploit the embedding of a 4 dimensional spacetime in a flat or a non-flat 5 dimensional manifold in Chapter 5. However, we lack a rigorous proof whether an embedding exist, and if so, whether this is the only way to embed. In this Chapter we will demonstrate that the embedding do exist and we can define a class of embeddings which allow one to recover the Lorentz structure correlating adjacent foliations.

For the former problem, we rely on the coordinate which can be chosen freely on the 4 dimensional manifold. Although this is not a purely geometrical way, it relaxes the choice of the coordinate that one can use, i.e., we can choose our preferred coordinate for the 4 dimensional manifold, and find a coordinate correlation of the two manifolds.

For the latter problem, we propose one type of different embedding which introduces an extra constant parameter $\Theta$. The result derived in here shows that we might be able to generalize the current embedding approach, from the one we found in Chapter 5 to a large family, or even a group, of embeddings characterized with parameter $\Theta \in \mathbb{R}$ (at the moment, likely to introduce new factors to describe the embedding). These mathematical discoveries are new and interesting, which are of the main findings of this research.

## 7.2 Proof on Recovering the Lorentz Structure with a Given 5 Dimensional Metric

The existence and uniqueness (aka rigid embedding) of the embedding map are the two main aspects of the aforementioned embedding problem. In this Chapter we will deal with these two topics.

For a 5 dimensional manifold $\mathcal{M}$ with a metric $g_{ab}$ defined on it (note that we will ignore the abstract indices of metric in the following context, which is true only in this Chapter), if one wants to isometrically embed a 4 dimensional manifold $\mathcal{N}$ with a Lorentzian metric $h'$ in the higher dimensional space, we need to impose certain constraints on the 5 dimensional manifold $\mathcal{M}$ and the 5 dimensional metric that we choose. Actually, such a problem can be achieved in the following two steps as mentioned: First we need to prove such an embedding(s) exist; secondly we need to prove whether this embedding is unique or not.

For the first problem, we can change our mind and think about this process. We define a 5 dimensional space $\mathcal{M}$ with a given metric $g$, and then foliate this space into a family of 4 dimensional hypersurfaces. Then we pull-back the 5 dimensional metric on the 4 dimensional hypersurfaces, and prove that each of the 4 dimensional manifold is equivalent to a solution of the Einstein's equation. Finally, we need to prove that all 4 dimensional hypersurfaces are mutually isometric, which means there exist isometric maps $\phi_{ij}$ between any two submanifolds ${}^i\mathcal{M}$ and ${}^j\mathcal{M}$ of $\mathcal{M}$.

Let us first analyze the first problem. Investigate the set of the solutions to the Einstein's equation, we can find that this set is actually a subset of the set of all the 4 dimensional Lorentzian manifolds, where the metrics are given arbitrarily, whose signatures are $(-,+,+,+)$. Hence, if one could prove that the existence of the embedding holds for all kinds of Lorentzian type of manifolds, the former would be guaranteed as a consequence.

Hence this requirement would impose constraint on the 5 dimensional metric that one can choose. In order to obtain a 4 dimensional Lorentzian metric by pulling-back a 5 dimensional metric we need at least one time-like dimension, i.e., the signature of the 5 dimensional metric should be of the type $(-,+,+,+,\pm)$. The last sign is yet to be determined by further constraints. We have the following lemma.

**Lemma 7.2.1.** *Given a 5 dimensional manifold $\mathcal{M}$ with metric $g$, a hypersurface of $\mathcal{M}$ can be a 4 dimensional Lorentzian manifold, iff the signature of the metric of $\mathcal{M}$ possesses at least one different sign.*

*Proof.* Consider a 5 dimensional manifold $\mathcal{M}$ with a metric $g$, a 4 dimensional manifold ${}^1\mathcal{M} \subset \mathcal{M}$ and is a hypersurface on $\mathcal{M}$. Let $\mathcal{M}$ be a pseudo-Riemannian manifold where its metric is given by $g$ with signature $(-,+,+,+,+)$, Given a map between the two manifolds, the 4 dimensional metric can be pulled-back from $g$, i.e.

$$\phi_1 : {}^1\mathcal{M} \to \mathcal{M}\,, \tag{7.2.1}$$

induces

$$\phi_1{}^* : \ g \to {}^1h \,, \tag{7.2.2}$$

let the normal vector to the hypersurface be ${}^1n$, we then can construct a relation between $g$ and ${}^1h$, such that

$${}^1h = g + {}^1n{}^1n \,. \tag{7.2.3}$$

Given the normal covector for which direction is along one of the 'plus' dimensions, we can prove, by means of 7.2.3, that the signature of the induced 4 dimensional metric is given by $(-,+,+,+)$, which is a Lorentzian manifold (spacetime).

If the signature of a 5 dimensional metric $g$ is given by $(-,+,+,+,-)$, then the normal vector's direction can be either 'minus' one or 'minus' two, which leads to the consequence that the signature of ${}^1h$ is given by $(+,+,+,-)$ or $(-,+,+,+)$. Hence we obtain a Lorentzian manifold $({}^1\mathcal{M}, {}^1h)$.

The results hold if we change the signs of the signature of the 5 dimensional metric, i.e., the signature of the metric is given by $(+,-,-,-,-)$ or $(+,-,-,-,+)$, which is just a different choice of convention. □

Assume that the 5 dimensional manifold $\mathcal{M}$ is endowed with a metric $g$, given a hypersurface on the 5 dimensional manifold, denoted by $\phi_i(\mathcal{N})$, there is a 4 dimensional metric ${}^ih$ induced by the 5 dimensional metric, given by

$${}^ih = g + {}^in{}^in \,, \tag{7.2.4}$$

where ${}^in$ represents for the normal covector field defined on $\phi_i(\mathcal{N})$, which satisfies ${}^in \in \mathcal{T}^*(\mathcal{M})$, where $\mathcal{T}^*(\mathcal{M})$ denotes the covector field. We need to introduce a way of foliating the 5 dimensional manifold. This will require one more constraint on the 5 dimensional manifold. i.e., the 5 dimensional manifold must be hyperbolic, such that one can define a global function, which is labelled by the parameter $w$ on it. Note that the hyperbolicity implies that the whole manifold can be decomposed as $\mathbb{R} \times {}^i\mathcal{M}$, where $\{{}^i\mathcal{M} \mid {}^i\mathcal{M},\ i \in \mathbb{N}_0\}$ denote a family of 4 dimensional hypersurfaces. We define that such a function on $\mathcal{M}$, and the whole manifold can be decomposed into a family of hypersurfaces, given by

$$\{\phi_i(\mathcal{N}) \subset \mathcal{M} \mid w(p) = con_i \,, \text{ where } con_i \in \mathbb{R} \text{ and is a constant, } p \in \phi_i(\mathcal{N}) \,, \\ i \in \mathbb{N}_0\}. \tag{7.2.5}$$

From now on, we use ${}^i\mathcal{M}$, defined in the 7.2.5, to denote the 4 dimensional hypersurface $\phi_i(\mathcal{N})$. Use equation (7.2.4), one notices that there might be a map between any two slices and an induced map between their metrics, given by

$$\phi_j \circ {\phi_i}^{-1} : \ {}^i\mathcal{M} \to {}^j\mathcal{M} \,, \tag{7.2.6}$$

$$(\phi_j \circ {\phi_i}^{-1})_* : \ {}^ih \to {}^jh \,, \tag{7.2.7}$$

where map $\phi_j \circ {\phi_i}^{-1}$ is a diffeomorphism, as both $\phi_j$ and $\phi_i$ (hence is the inverse map ${\phi_i}^{-1}$) are diffeomorphisms. Furthermore, we require that the embedding map is isometric, i.e., $\phi_i$ preserves the metric ${}^ih$, where ${}^ih$ is isometric to the metric $h$ of a 4 dimensional manifold $\mathcal{N}$, $\forall\ i \in \mathbb{N}_0$.

Herein, we use $h$ to denote the 4 dimensional metric. From this we know that $\phi_i : \mathcal{N} \to {}^i\mathcal{M}$ induces a map $\phi_{i*}$, which satisfies

$$\phi_{i*}h = {}^ih\,. \tag{7.2.8}$$

**Lemma 7.2.2.** *The mapping $\phi_j \circ {\phi_i}^{-1}$, between any two arbitrary hypersurfaces ${}^j\mathcal{M}$ and ${}^i\mathcal{M}$, is an isometry, given any two integer labels $j$ and $i$.*

*Proof.* From (7.2.4), we know that the metrics induced on ${}^j\mathcal{M}$ and ${}^i\mathcal{M}$ are give by

$${}^jh = g + {}^jn{}^jn\,, \tag{7.2.9}$$
$${}^ih = g + {}^in{}^in\,. \tag{7.2.10}$$

From (7.2.8), we have

$$h = {\phi_j}^{*j}h\,, \tag{7.2.11}$$
$$h = {\phi_i}^{*i}h\,, \tag{7.2.12}$$

hence we have

$$(\phi_j \circ {\phi_i}^{-1})_*{}^ih = {}^jh\,, \tag{7.2.13}$$

which implies that $\phi_j \circ {\phi_i}^{-1} : {}^i\mathcal{M} \to {}^j\mathcal{M}$ is an isometry, for any $i$ and $j$. □

We then give the form of the 5 dimensional metric.

Let us first consider the flat manifold case as a demo and then follow a similar approach to derive the proof. Suppose a pseudo-Euclidean 5 dimensional manifold with metric $\hat{\eta}$, such that $\hat{\eta}$ has the following diagonal component form $(-1, 1, 1, 1, \pm 1)$ in a Cartesian coordinate system $x^\mu$. In this coordinate we decompose the whole manifold in a way that each hypersurface possesses a constant fifth coordinate $x^4 = con$. Pull the metric back onto a 4 dimensional hyperplane, leading to a 4 dimensional metric $h$ with diagonal components $(-1, 1, 1, 1)$. Consider one more constraint, that on each hyperplane, the zeroth coordinate satisfies the following formula

$$x^0 = X^0 + i\Delta x\,, \tag{7.2.14}$$

for the $i$-th foliation, where the capital letter denotes the 5 dimensional zeroth coordinate. $\Delta x$ is an infinitesimal constant between two adjacent slices, which equals to the difference in the $x^4$ direction. In this setting, it is clear that the Lorentz structure can be recovered outside one spacetime foliation, shown in the Fig.7.1.

Now consider a generic 5 dimensional manifold $(\mathcal{M}, g)$ with metric signature $(-, +, +, +, -)$, and a hypersurface ${}^i\mathcal{M}$ in it. We choose a local coordinate $(x^0, x^1, x^2, x^3)$ on ${}^i\mathcal{M}$ and propagate this coordinate along the normal unit vector ${}^in$ to the next adjacent foliation ${}^{i+1}\mathcal{M}$, and translate the coordinate by a factor of $t^a\Delta t$, where $t^a$ is a unit tangent along the $x^0$ coordinate line, which forms a local coordinate in ${}^{i+1}\mathcal{M}$. From (7.2.5), we know that the difference between the neighbouring foliations is given as ${}^in\Delta t$. Hence, if we set the first foliation as ${}^0\mathcal{M}$ and the zeroth coordinate as $x^0 = t$, then the zeroth coordinate on the $i$-th foliation is given by

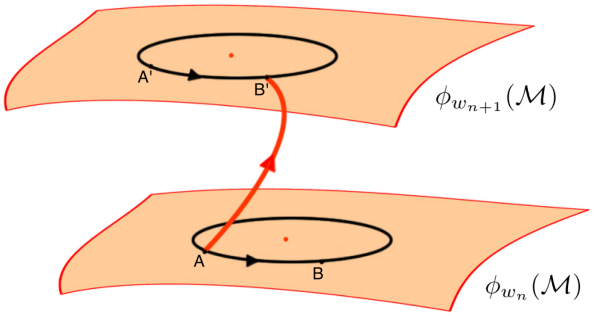


Figure 7.1: This figure illustrates that how one would recover the local Lorentz structure outside one 4 dimensional foliation.

$x^0 = t$, where $t$ is the 4 dimensional zeroth coordinate of $\mathcal{N}$. Now a local coordinate has been constructed on the 5 dimensional manifold, given as $(X^0, X^1, X^2, X^3, W)$, where $X^1 = x^1$ , $X^2 = x^2$ , $X^3 = x^3$ and the fifth coordinate $W$ is given as follow: $W$ is a constant on each hypersurface. Without loss of generality, let the $W_0 = t_0$ on the ${}^0\mathcal{M}$ hyperplane. We conclude that $W_i = t_0 + i\Delta t$ on the $i$-th foliation. And $X^0 = x^0 - i\Delta t$ on the $i$-th foliation. We then can recover the Lorentz structure which correlates adjacent foliation.

Consider a hypersurface $\mathcal{N}'$ which traverses each 4 dimensional foliations ${}^i\mathcal{M}$, a metric on $\mathcal{N}'$ can be defined as

$$h' + {}^{\mathrm{c}}n'{}^{\mathrm{c}}n' = g\,, \tag{7.2.15}$$

where ${}^{\mathrm{c}}n'$ denotes the normal covector to $\mathcal{N}'$. We set $t_0 = 0$ without loss of generality. We choose hypersurface $\mathcal{N}'$ where the normal vector satisfies the following relation

$${}^0n' = k'\frac{\partial}{\partial X^0}\,, \tag{7.2.16}$$

there always exists hypersurface $\mathcal{N}'$ which satisfies (7.2.16). For example, an $X^0 = con$ (constant) hyperplane would obey the condition. We have the following theorem.

**Lemma 7.2.3.** *The $X^0 = con$ hyperplane traverses each foliation ${}^i\mathcal{M}$.*

*Proof.* The intersection of $X^0 = con$ hyperplane and ${}^i\mathcal{M}$ is given as $\{p \mid p = (con, X^1, X^2, X^3, t_0 + i\Delta t)\}$, which is not empty, where $X^1$ , $X^2$ and $X^3$ are free coordinates. Hence, the hyperplane $X^0 = con$ correlates adjacent foliations ${}^i\mathcal{M}$ and ${}^{i+1}\mathcal{M}$. □

Now we require the $X^0 = 0$ for the $\mathcal{N}'$ without loss of generality. First, the normal vector can be derived from the normal covector, given as

$$n^a = {}^{\mathrm{c}}n_c g^{ac}\,. \tag{7.2.17}$$

We also have that the 5 dimensional metric is given by (7.2.4).

**Lemma 7.2.4.** *There exists an isometric embedding between $\mathcal{N}'$ and a hyperplane ${}^0\mathcal{M}$, if the metric takes a uniform expression in* $\mathrm{d}X^0$ *and* $\mathrm{d}W$

*coefficient, i.e.*

$$\begin{aligned} g_{\mu\nu}\mathrm{d}x^\mu\mathrm{d}x^\nu = \; & A_{00}(\mathrm{d}X^0)^2 + A_{00}\mathrm{d}W^2 \\ & + A_{11}(\mathrm{d}X^1)^2 + A_{12}\mathrm{d}X^1\mathrm{d}X^2 \\ & + A_{13}\mathrm{d}X^1\mathrm{d}X^3 + A_{22}(\mathrm{d}X^2)^2 \\ & + A_{33}(\mathrm{d}X^3)^2 + A_{23}\mathrm{d}X^2\mathrm{d}X^3 \\ & + A_{01}\mathrm{d}X^0\mathrm{d}X^1 + A_{01}\mathrm{d}W\mathrm{d}X^1 \\ & + A_{02}\mathrm{d}X^0\mathrm{d}X^2 + A_{02}\mathrm{d}W\mathrm{d}X^2 \\ & + A_{03}\mathrm{d}X^0\mathrm{d}X^3 + A_{03}\mathrm{d}W\mathrm{d}X^3 \\ & + A_{04}\mathrm{d}X^0\mathrm{d}W\,, \end{aligned} \tag{7.2.18}$$

*in the given coordinate* $(X^0, X^1, X^2, X^3, W)$.

*Proof.* First, look at the following lemma:

**Lemma 7.2.5.** *The manifold* $\mathcal{M}$ *is given as* $\mathbb{R} \times {}^i\mathcal{M}$.

*Proof.* On any given hyperplane ${}^i\mathcal{M}$, the fifth coordinate reduces to a constant, which is $W_i = i\Delta t$. Hence, $\mathrm{d}W$ terms vanish. The metric then reduces to

$$\begin{aligned} {}^ig_{\mu\nu}\mathrm{d}x^\mu\mathrm{d}x^\nu = \; & A_{00}(\mathrm{d}X^0)^2 + A_{11}(\mathrm{d}X^1)^2 + A_{12}\mathrm{d}X^1\mathrm{d}X^2 \\ & + A_{13}\mathrm{d}X^1\mathrm{d}X^3 + A_{22}(\mathrm{d}X^2)^2 + A_{33}(\mathrm{d}X^3)^2 + A_{23}\mathrm{d}X^2\mathrm{d}X^3 \\ & + A_{01}\mathrm{d}X^0\mathrm{d}X^1 + A_{03}\mathrm{d}X^0\mathrm{d}X^3\,. \end{aligned} \tag{7.2.19}$$

And the induced metric ${}^ih$ on ${}^i\mathcal{M}$ is given by

$${}^ih = {}^ig\,. \tag{7.2.20}$$

Consequently, each hyperplane possesses the same metric form given in (7.2.20), which proves that $\phi : {}^i\mathcal{M} \to {}^j\mathcal{M}$ is an isometric map, $\forall\, i$ and $j$. □

**Lemma 7.2.6.** $(\partial/\partial W)$ *is orthogonal to* $(\partial/\partial X^0)$*, hence the cross term* $A_{04}$ *is zero.*

*Proof.* The coordinate line of $W$ is given when $X^0$, $X^1$, $X^2$, $X^3$ are constants. On ${}^0\mathcal{M}$, the origin is $X^0 = X^1 = X^2 = X^3 = 0$, where $x^0 = X^0$. Propagate to foliation ${}^1\mathcal{M}$, the origin of $X^\mu$ is $0 = X^0 = x^0 - \Delta t$, i.e., we need to transform the coordinate $x^0$ by $(-t^a\Delta t)$, where $t^a$ is along the $x^0$ coordinate line. Hence, the origin of $X^0 = X^1 = X^2 = X^3 = 0$ is propagated by ${}^0n\Delta t$. We then have the following relation

$$\frac{\partial}{\partial W} = k'' \times {}^0n\,, \tag{7.2.21}$$

where $k'$ is a reparameterization factor. Furthermore, we have

$$g({}^0n, \partial/\partial X^0) = 0\,, \tag{7.2.22}$$

due to ${}^0N$ is normal to the hyperplane and $\partial/\partial X^0$ is tangent to that plane. We conclude that $g(\partial/\partial X^0, \partial/\partial W) = 0$, i.e., $A_{04} = 0$. □

The normal vector to $\mathcal{N}'$ is $n' = k'\partial/\partial X^0$. After reparameterizing we can get $k' = 1$. Hence the normal covector is given as follow

$$ {}^{\mathrm{c}}n' = g(n')\,, \tag{7.2.23} $$

the explicit form of ${}^{\mathrm{c}}n'$ is given as

$$ {}^{\mathrm{c}}n' = A_{00}\mathrm{d}X^0 + A_{01}\mathrm{d}X^1 + A_{02}\mathrm{d}X^2 + A_{03}\mathrm{d}X^3\,. \tag{7.2.24} $$

Hence, we can derive the metric induced on $\mathcal{N}'$, given as

$$ \begin{aligned} h'_{\mu\nu} =\ & g_{\mu\nu} - {}^{\mathrm{c}}n'_{\mu}\,{}^{\mathrm{c}}n'_{\nu} \\ =\ & A_{00}(\mathrm{d}X^0)^2 + A_{00}\mathrm{d}W^2 + A_{11}(\mathrm{d}X^1)^2 + A_{12}\mathrm{d}X^1\mathrm{d}X^2 \\ & + A_{13}\mathrm{d}X^1\mathrm{d}X^3 + A_{22}(\mathrm{d}X^2)^2 + A_{33}(\mathrm{d}X^3)^2 + A_{23}\mathrm{d}X^2\mathrm{d}X^3 \\ & + A_{01}\mathrm{d}X^0\mathrm{d}X^1 + A_{01}\mathrm{d}W\mathrm{d}X^1 + A_{02}\mathrm{d}X^0\mathrm{d}X^2 + A_{02}\mathrm{d}W\mathrm{d}X^2 \\ & + A_{03}\mathrm{d}X^0\mathrm{d}X^3 + A_{03}\mathrm{d}W\mathrm{d}X^3 \\ & - \left(A_{00}\mathrm{d}X^0 + A_{01}\mathrm{d}X^1 + A_{02}\mathrm{d}X^2 + A_{03}\mathrm{d}X^3\right)^2\,, \end{aligned} \tag{7.2.25} $$

which leads to

$$ \begin{aligned} h'_{\mu\nu} =\ & \left(A_{00} - (A_{00})^2\right)(\mathrm{d}X^0)^2 + A_{00}\mathrm{d}W^2 \\ & + \left(A_{11} - (A_{01})^2\right)(\mathrm{d}X^1)^2 + (A_{10} - 2A_{01}A_{00})\,\mathrm{d}X^1\mathrm{d}X^0 \\ & + \left(A_{22} - (A_{02})^2\right)(\mathrm{d}X^2)^2 + (A_{02} - 2A_{00}A_{02})\,\mathrm{d}X^0\mathrm{d}X^2 \\ & + \left(A_{33} - (A_{03})^2\right)(\mathrm{d}X^3)^2 + (A_{03} - 2A_{00}A_{03})\,\mathrm{d}X^0\mathrm{d}X^3 \\ & + (A_{12} - 2A_{01}A_{02})\,\mathrm{d}X^1\mathrm{d}X^2 \\ & + (A_{23} - 2A_{02}A_{03})\,\mathrm{d}X^2\mathrm{d}X^3 \\ & + (A_{13} - 2A_{01}A_{03})\,\mathrm{d}X^1\mathrm{d}X^3 \\ & + A_{01}\mathrm{d}W\mathrm{d}X^1 + A_{02}\mathrm{d}X^2\mathrm{d}W + A_{03}\mathrm{d}X^3\mathrm{d}W\,. \end{aligned} \tag{7.2.26} $$

For the hyperplane ${}^0\mathcal{M}$, the normal covector is given as

$$ {}^0n_{\mu} = g_{\mu\nu}\,{}^0n^{\nu} = g_{\mu\nu}\frac{\partial}{\partial W}\,, \tag{7.2.27} $$

where we have reparameterized the ${}^0n^{\nu}$ and $k'$ is now 1. Consider equations (7.2.18), (7.2.4) and (7.2.27), we have the following expression

$$ \begin{aligned} {}^0h_{\mu\nu} =\ & \left(A_{00} - (A_{00})^2\right)\mathrm{d}W^2 + A_{00}(\mathrm{d}X^0)^2 \\ & + \left(A_{11} - (A_{01})^2\right)(\mathrm{d}X^1)^2 + (A_{10} - 2A_{01}A_{00})\,\mathrm{d}X^1\mathrm{d}W \\ & + \left(A_{22} - (A_{02})^2\right)(\mathrm{d}X^2)^2 + (A_{02} - 2A_{00}A_{02})\,\mathrm{d}W\mathrm{d}X^2 \\ & + \left(A_{33} - (A_{03})^2\right)(\mathrm{d}X^3)^2 + (A_{03} - 2A_{00}A_{03})\,\mathrm{d}W\mathrm{d}X^3 \\ & + (A_{12} - 2A_{01}A_{02})\,\mathrm{d}X^1\mathrm{d}X^2 \\ & + (A_{23} - 2A_{02}A_{03})\,\mathrm{d}X^2\mathrm{d}X^3 \\ & + (A_{13} - 2A_{01}A_{03})\,\mathrm{d}X^1\mathrm{d}X^3 \\ & + A_{01}\mathrm{d}X^0\mathrm{d}X^1 + A_{02}\mathrm{d}X^2\mathrm{d}X^0 + A_{03}\mathrm{d}X^3\mathrm{d}X^0\,. \end{aligned} \tag{7.2.28} $$

In addition, we have the coordinate relation as follow

$$\begin{cases} {X^0}_0 = W_{\prime}\,, \\ {X^1}_0 = X^{1}{}_{\prime}\,, \\ {X^2}_0 = X^{2}{}_{\prime}\,, \\ {X^3}_0 = X^{3}{}_{\prime}\,, \\ X^0{}_{\prime} = W_0 = 0\,, \end{cases} \tag{7.2.29}$$

where '′' denotes the coordinate of $\mathcal{N}'$ and '0' denotes that of ${}^0\mathcal{M}$, which implies that the metric $h'$ is isometric to ${}^0h$, i.e., the mapping $\Phi:\ \mathcal{N}' \to {}^0\mathcal{M}$ is an isometric embedding. □

**Lemma 7.2.7.** *The 4 dimensional Lorentz structure can be recovered on* $\mathcal{N}'$*.*

*Proof.* The lemma is equivalent to that the mapping between $\mathcal{N}'$ and the original 4 dimensional manifold $\mathcal{N}$ is an isometric embedding. We know that an induced mapping given as $\phi' \equiv \Phi^{-1} \circ \phi_0$ relates $\mathcal{N}'$ and $\mathcal{N}$ as

$$\phi':\ \mathcal{N} \to \mathcal{N}'\,, \tag{7.2.30}$$

is an isometry due to the previous lemma. Hence, the Lorentz structure is recovered on $\mathcal{N}'$. □

**Proposition 7.2.8.** *The 4 dimensional Lorentz structure (of manifold* $\mathcal{N}$*) which correlates two adjacent foliations can be recovered, provided the 5 dimensional metric have certain constraint, and the 5 dimensional manifold is given as* $\mathbb{R} \times {}^i\mathcal{M}$*, where* $\mathcal{N}$ *is isometric to* ${}^i\mathcal{M}$*,* $\forall$ *i an integer.*

## 7.3 Proof of the Non-Uniqueness of the Embedding

The uniqueness of the embedding, is that whether this embedding mechanism is unique or not, such that the Lorentz structure is maintained when a 4 dimensional spacetime is carried into a 5 dimensional manifold with a given 5 dimensional metric where the signature is $(-,+,+,+,+)$ or $(-,+,+,+,-)$. The conclusion is that this mechanism is not unique, i.e., the isometric is not rigid, as the metric that we choose in the last section is a specific one and we impose too many constraints on it. We may relax these conditions and make new choice of the 5 dimensional metric $g$ and the embedding.

Consider only these two constraints, which are: First, we require isometric embeddings for all pull-back mappings. Moreover, we require that the Lorentz structure is maintained outside each individual 4 dimensional hypersurface (i.e., correlate two adjacent foliations). Define a 5 dimensional manifold with a pseudo-Riemannian 5 dimensional metric $g$, whose signature is, without loss of generality, given by $(-,+,+,+,-)$. The induced 4 dimensional metric, by pulling-back the 5 dimensional metric onto a 4 dimensional hypersurface, is given in (7.2.4).

First, again, consider the Minkowski case as a demonstration with coordinate $(t, r, \theta, \varphi)$. The first slice embedded in the 5 dimensional flat

manifold is locating on the $w' = 0$ hyperplane and rotated wrt the $w'$-axis by a factor of $\Theta = \arctan(\sqrt{2}/2)$. The new coordinates $(t', r', \theta', \phi')$ are given as

$$\begin{cases} t' &= t'' \,, \\ r' &= r'' \,, \\ \theta' &= \theta'' \,, \\ \varphi' &= \varphi'' \,, \\ w' &= 0 \,, \end{cases} \tag{7.3.1}$$

where $(r'', t'', \theta'', \varphi'')$ are given as

$$\begin{bmatrix} t'' \\ r'' \\ \theta'' \\ \varphi'' \end{bmatrix} = \begin{bmatrix} \cos\Theta & \sin\Theta & 0 & 0 \\ -\sin\Theta & \cos\Theta & 0 & 0 \\ 0 & 0 & 1 & 0 \\ 0 & 0 & 0 & 1 \end{bmatrix} \begin{bmatrix} t \\ r \\ \theta \\ \varphi \end{bmatrix} , \tag{7.3.2}$$

the next foliation would locate on a $w' = con$, where $con$ is a constant, plane while rotated in the following way: ${t''}_2 \to t - \Delta t$ and the fifth coordinate is given as ${w'}_2 = \Delta t/\sqrt{2}$, where $\Delta t$ is a positive constant. The full coordinate transformation of $(t', r', \theta', \varphi', w')$ is given as

$$\begin{cases} {t'}_2 &= {t''}_2 \cos\Theta + {r''}_2 \sin\Theta \,, \\ {r'}_2 &= -{t''}_2 \sin\Theta + {r''}_2 \cos\Theta \,, \\ {\theta'}_2 &= {\theta''}_2 \,, \\ {\varphi'}_2 &= {\varphi''}_2 \,, \\ {w'}_2 &= \frac{\sqrt{2}}{2}\Delta t \,, \end{cases}$$

where ${\theta''}_2 = \theta$, and ${\varphi''}_2 = \varphi$.

For the foliations after the first and second ones, we can deduce the following coordinate transformation

$$\begin{cases} {t''}_n &= t - n\Delta t \,, \\ {r''}_n &= r \,, \\ {\theta''}_n &= \theta \,, \\ {\varphi''}_n &= \varphi \,, \\ {w'}_n &= \frac{\sqrt{2}}{2} n\Delta t \,, \end{cases} \tag{7.3.3}$$

with

$$\begin{bmatrix} {t'}_n \\ {r'}_n \\ {\theta'}_n \\ {\varphi'}_n \end{bmatrix} = \begin{bmatrix} \cos\Theta & \sin\Theta & 0 & 0 \\ -\sin\Theta & \cos\Theta & 0 & 0 \\ 0 & 0 & 1 & 0 \\ 0 & 0 & 0 & 1 \end{bmatrix} \begin{bmatrix} {t''}_n \\ {r''}_n \\ {\theta''}_n \\ {\varphi''}_n \end{bmatrix} , \tag{7.3.4}$$

on the $n$-th foliation, where all the coordinates with "$''$" denote the intermediate coordinates which can be cancelled out in the final coordinate transformation from $(t, r, \theta, \varphi)$ to $(t', r', \theta', \varphi', w')$. The embedding formalism is pictured in the Fig.7.2.

We can now consider the embedding of the Schwarzschild metric given in (2.2.4). We introduce a new metric form for the 5 dimensional manifold

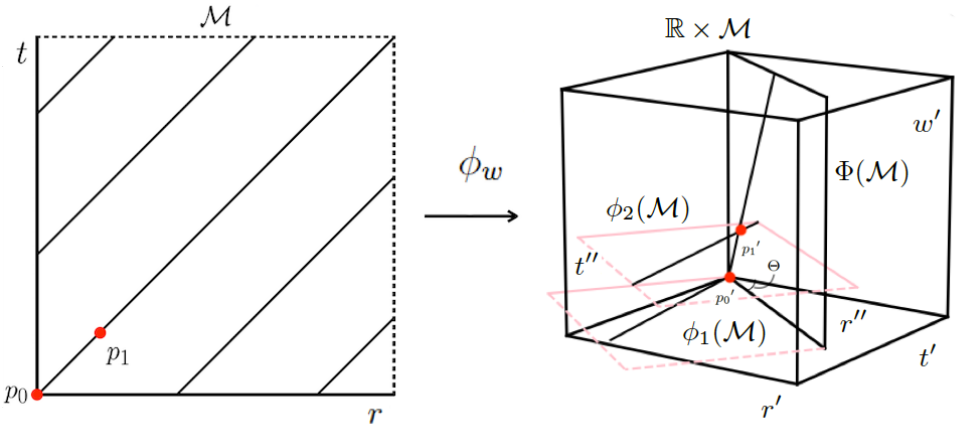


Figure 7.2: The figure illustrates the embedding of the 4 dimensional Minkowskian manifold in a 5 dimensional pseudo-Euclidean manifold. The left panel denotes the original Minkowskian manifold $\mathcal{M}$ with two spatial dimensions are suppressed. And the right panel denotes the 5 dimensional flat manifold $\mathbb{R}\times\mathcal{M}$. The 45° inclined black lines in the right panel represent the null geodesics, $t$ and $r$ are the temporal and spatial coordinates respectively. The line $p_0p_1$ denotes the null curve which traverses the origin of $\mathcal{M}$. $\phi_w$ represents the isometric embedding. For the left panel, $w'$, $r'$ and $t'$ denote the three coordinates, where $w'$ and $t'$ are time-like. $\phi_1(\mathcal{M})$ represents the initial foliation and $\phi_2(\mathcal{M})$ denotes the second slice with $w'_2 = \Delta t/\sqrt{2}$. The intermediate coordinate $(t'', r'')$ are denoted with pink colour. The can be approached by rotating the $(t', r')$ coordinate along the $w'$-axis by an angle of $\Theta$. $p_0'p_1'$ denotes the image of $p_0p_1$. Note that the upper foliation is shifted along the $-t''$ direction by a factor of $\Delta t$. The vertical manifold is denoted by $\Phi(\mathcal{M})$. The Lorentz structure of $\mathcal{M}$ can be recovered within this hyperplane.

$\mathbb{R}\times\mathcal{M}$, given as

$$
\begin{aligned}
g_{\mu\nu}\mathrm{d}x'^{\mu}\mathrm{d}x'^{\nu} = &-\left(1-\frac{2M}{t'\sin\Theta+r'\cos\Theta}\right)\cos^2\Theta\mathrm{d}t'^2\\
&+2\left(1-\frac{2M}{t'\sin\Theta+r'\cos\Theta}\right)\sin\Theta\cos\Theta\mathrm{d}t'\mathrm{d}r'\\
&-\left(1-\frac{2M}{t'\sin\Theta+r'\cos\Theta}\right)\sin^2\Theta\mathrm{d}r'^2\\
&+\left(1-\frac{2M}{t'\sin\Theta+r'\cos\Theta}\right)^{-1}\sin^2\Theta\mathrm{d}t'^2\\
&+2\left(1-\frac{2M}{t'\sin\Theta+r'\cos\Theta}\right)^{-1}\sin\Theta\cos\Theta\mathrm{d}t'\mathrm{d}r'\\
&+\left(1-\frac{2M}{t'\sin\Theta+r'\cos\Theta}\right)^{-1}\cos^2\Theta\mathrm{d}r'^2\\
&+(t'\sin\Theta+r'\cos\Theta)^2(\mathrm{d}\theta'+\sin^2\theta'\mathrm{d}\varphi'^2)\\
&-2\left(1-\frac{2M}{t'\sin\Theta+r'\cos\Theta}\right)\mathrm{d}w'^2\\
&-2\sqrt{2}\left(1-\frac{2M}{t'\sin\Theta+r'\cos\Theta}\right)\cos\Theta\mathrm{d}t'\mathrm{d}w'\\
&+2\sqrt{2}\left(1-\frac{2M}{t'\sin\Theta+r'\cos\Theta}\right)\sin\Theta\mathrm{d}r'\mathrm{d}w'\,, \qquad (7.3.5)
\end{aligned}
$$

a coordinate transformation given as

$$\begin{cases} t &= \sqrt{2}w'_n + t'_n \cos\Theta - r'_n \sin\Theta\,, \\ r &= t'_n \sin\Theta + r'_n \cos\Theta\,, \\ \theta &= \theta'_n\,, \\ \varphi &= \varphi'_n\,, \\ w'_n &= \frac{\sqrt{2}}{2} n\Delta t\,, \end{cases} \tag{7.3.6}$$

would induce an isometric embedding from the 4 dimensional Schwarzschild $\mathcal{M}$ to a foliation ($n$-th, where $w'_n = con$) in $\mathbb{R}\times\mathcal{M}$. An isometric embedding can be defined from $\mathcal{M}$ to a hypersurface $\Phi(\mathcal{M})$ of $\mathbb{R}\times\mathcal{M}$, by the following coordinate transformation

$$\begin{cases} t &= \sqrt{2}w' + \frac{\sqrt{2}}{2} r' \cos\Theta - r' \sin\Theta\,, \\ r &= \frac{\sqrt{2}}{2} r' \sin\Theta + r' \cos\Theta\,, \\ \theta &= \theta'\,, \\ \varphi &= \varphi'\,, \end{cases} \tag{7.3.7}$$

where $\Phi(\mathcal{M})$ is given as

$$\Phi(\mathcal{M}) = \begin{cases} w' = w'\,, \\ t' &= \frac{\sqrt{2}}{2} r'\,, \\ \theta' &= \theta'\,, \\ \varphi' &= \varphi'\,, \end{cases} \tag{7.3.8}$$

in the 5 dimensional manifold. Hence, we can infer that the pulled-back metric of (7.3.5) onto $\Phi(\mathcal{M})$ and the pushed-forward metric of (2.2.4) into $\Phi(\mathcal{M})$ have the same expression, given as

$$\begin{aligned} &h_{\mu\nu}\mathrm{d}x'^{\mu}\mathrm{d}x'^{\nu} = \\ &\quad\left(\sqrt{2}\sin\Theta\cos\Theta - \frac{1}{2}\cos^2\Theta - \sin^2\Theta\right)\left(1 - \frac{2M}{r'\sin\Theta/\sqrt{2} + r'\cos\Theta}\right)\mathrm{d}r'^2 \\ &+ \left(\sqrt{2}\cos\Theta\sin\Theta + \cos^2\Theta + \frac{1}{2}\sin^2\Theta\right)\left(1 - \frac{2M}{r'\sin\Theta/\sqrt{2} + r'\cos\Theta}\right)^{-1}\mathrm{d}r'^2 \\ &+ \left(\frac{\sqrt{2}}{2} r'\sin\Theta + r'\cos\Theta\right)^2 (\mathrm{d}\theta'^2 + \sin^2\theta'\mathrm{d}\varphi'^2) \\ &- 2\left(1 - \frac{2M}{r'\sin\Theta/\sqrt{2} + r'\cos\Theta}\right)\mathrm{d}w'^2 \\ &+ \left(2\sqrt{2}\sin\Theta - 2\cos\Theta\right)\left(1 - \frac{2M}{r'\sin\Theta/\sqrt{2} + r'\cos\Theta}\right)\mathrm{d}r'\mathrm{d}w'\,, \end{aligned} \tag{7.3.9}$$

which implies that the embedding $\Phi$ is an isometric embedding, where $h$ denotes the induced metric on $\Phi(\mathcal{M})$. Note that this is by no means a generic form of the 5 dimensional metric which satisfies our requirement. The constant factor $\Theta$ can be changed to give another form of the embedding. There is also a chance to introduce more variables and get a more complicated expression of the metric in the following research.

# Chapter 8

# Application of the 4+1 Level Set Approach to Spacetime around Binary Black Hole

## 8.1 Overview

In this Chapter we will be dealing with a real binary black hole spacetime and solve the Einstein's equations numerically by the powerful 3+1 numerical relativity. Having seen in the previous Chapters that the resolution to the Einstein equations amounts to solving the Cauchy problem, namely propagating a set of initial data on the initial hypersurface forward in time. Technically speaking, this means that solving the second-order non-linear Einstein's gravitational field equations reduces to computing the propagation (evolution) equations of initial data, which satisfy the Hamiltonian and momentum constrain equations, via appropriate numerical schemes. Now, depending on the formulation constructed in the Chapter 5, we can apply the embedding approach to the real numerical data of binary black hole.

We apply the approach that is proposed in Chapter 5, to a real binary black hole numerical data generated from the Einstein toolkit. We show that the discrete data can be isometrically embedded into the 5 dimensional manifold, due to the linear coordinate transformation we introduced in Chapter 5. The linearity and smoothness of coordinate transformation are critical to the embedding, which guarantees the embedded manifold maintains the original structure, regardless of the analytical or numerical metric form. In fact, the coordinate transformations that are introduced in the previous context are $C^{\infty}$ differentiable, i.e., smooth. With the help of the coordinate transformation derived in Chapter 6, we can embed the discrete data set of a 4 dimensional manifold to a 5 dimensional manifold.

## 8.2 Embedding the BBH in a 5 Dimensional Manifold

Conceptually, this initial value problem can be considered in two different ways: (i) The mathematical problem: given a hypersurface $\Sigma_0$,

find a positive definite metric $h_{ab}$, a symmetric bilinear tensor $K_{ab}$ and some matter distribution $(E, p^a)$ on $\Sigma_0$ such that the two constraints are satisfied. Note that the energy-momentum tensor components $(E, p^a)$ may have their own constraints which are independent of that derived from the Einstein equations. (ii) The astrophysical problem: it should be guaranteed that the solution to these equations is subject to certain astrophysical conditions, which implies we have to correlate the results to a specific physical system that we want to investigate.

Let us focus on an equal mass, non-spinning black hole binary merger.

The first task is to determine the initial data for the 3+1 Cauchy problem. We calculate the initial value of this spacetime evolution, satisfying the Hamiltonian constraint and momentum constrain equations, given by (6.2.89) and (6.2.90).

Looking for an appropriate set of initial data is a tough task and can be dated back to the year of 1944, under the work of Lichnerowicz [169], who has obtained a much more satisfactory split of the initial data $(h_{ab}, K_{ab})$ between its freely chosen parts and the rest parts which are given by solving the constraint equations (6.2.89) and (6.2.90) by means of the conformal decomposition, cf., appendix F for further information. Later on, this method was extended by several physicists, including Choquet-Bruhat (1956, 1971) [172, 224], York and Ó Murchadha (1972, 1974, 1979) [185, 225, 226, 16] and York and Pfeiffer (1999, 2003) [227, 228]. Alternative methods are also developed recently, cf. [229, 230, 231, 232].

At this stage, one can evolve the spatial initial foliation by solving the equations (6.2.87) and (6.2.88). The initial values on the first foliation are propagated pointwisely in the adapted coordinate system constructed in the preceding context.

Firstly, let us look at the conformal decomposition of the 3+1 Einstein equations. This mathematical tool is a decomposition of the induced 3 dimensional metric $h_{ab}$ of hypersurface $\mathcal{W}$ and was first introduced by Lichnerowicz in 1944 [169], which is of the type

$$h_{ab} = \Psi^4 \tilde{h}_{ab}\,, \tag{8.2.1}$$

where $\Psi$ is a strictly positive scalar field and $\tilde{h}_{ab}$ is an auxiliary positive definite 3 dimensional metric field on $\mathcal{W}$. The conformal decomposition method has been proven to be a fruitful technique for generating valid initial data in the simulation of dynamical spacetimes. In the follow-up research, in 1971 and 1972, York demonstrated that the conformal method is also important in the evolution scheme of the Cauchy problem [233, 234], by showing that there exist conformal equivalence classes which carry two degrees of freedom of the gravitational field, where the classes are defined via equation (8.2.1), given by

$$\left\{\hat{h}_{ab} \mid \exists \text{ Positive definite } \Psi, \text{ such that } \Psi^4 \hat{h}_{ab} = h_{ab}\right\}. \tag{8.2.2}$$

And a rank-2 tensor, called the Cotton-York tensor, was introduced by York

$$C^{ij} := -\frac{1}{2}\epsilon^{ikl}\mathcal{C}_{mkl}h^{mj} = \epsilon^{ikl}D_k\left(R^j{}_l - \frac{1}{4}R\delta^j{}_l\right), \tag{8.2.3}$$

where $\mathcal{C}_{mkl} = D_l\left(R_{mk} - Rh_{mk}/4\right) - D_k\left(R_{ml} - Rh_{ml}/4\right)$ is the Cotton tensor [235]. This tensor was used to support his argument [233]. The Cotton-York tensor exhibits the following properties

$$\text{symmetric } C^{ij} = C^{ji}\,, \tag{8.2.4}$$
$$\text{traceless } C^{ij}h_{ij} = 0\,, \tag{8.2.5}$$
$$\text{divergence-free } D_jC^{ij} = 0\,. \tag{8.2.6}$$

For an initial data one needs to solve the Hamiltonian and momentum constraints of the Einstein equation, as are given in appendix F, the conformal version of constraints have been derived in (F.0.53) and (F.0.67). Re-scaling the energy-momentum components as follow

$$\tilde{E} := \Psi^8 E\,, \tag{8.2.7}$$
$$\tilde{p}^a := \Psi^{10} p^a\,. \tag{8.2.8}$$

The equations (F.0.53) and (F.0.67) can be rewritten as

$$\tilde{D}^a\tilde{D}_a\Psi - \frac{1}{8}{}^3\tilde{R}\Psi + \frac{1}{8}\hat{\mathscr{K}}^{ab}\hat{\mathscr{K}}_{ab}\Psi^{-7} + 2\pi\tilde{E}\Psi^{-3} - \frac{1}{12}K^2\Psi^5 = 0\,, \tag{8.2.9}$$
$$\tilde{D}_b\hat{\mathscr{K}}^{ab} - \frac{2}{3}\Psi^6\tilde{D}^aK = 8\pi\tilde{p}^a\,. \tag{8.2.10}$$

Based on the work of York [185, 16, 236], by decomposing the tensor $\hat{\mathscr{K}}^{ab}$ as

$$\hat{\mathscr{K}}^{ab} = (\tilde{L}\boldsymbol{k})^{ab} + \hat{\mathscr{K}}_t{}^{ab}\,, \tag{8.2.11}$$

where $\hat{\mathscr{K}}_t{}^{ab}$ is both traceless and transverse (i.e., divergence free), such that

$$\begin{aligned}\tilde{h}_{ab}\hat{\mathscr{K}}_t{}^{ab} &= 0\,,\\ \tilde{D}_a\hat{\mathscr{K}}_t{}^{ab} &= 0\,.\end{aligned} \tag{8.2.12}$$

The $\tilde{L}^a$ denotes the conformal Killing operator associated with the metric $\tilde{h}_{ab}$ and is defined as

$$(\tilde{L}\boldsymbol{k})^{ab} := \tilde{D}^a\boldsymbol{k}^b + \tilde{D}^b\boldsymbol{k}^a - \frac{2}{3}\tilde{D}_c\boldsymbol{k}^c\tilde{h}^{ab}\,, \tag{8.2.13}$$

which is by construction traceless and symmetric. The first term in (8.2.11) is called the longitudinal part of $\hat{\mathscr{K}}^{ab}$, and the second is called the transverse part of $\hat{\mathscr{K}}^{ab}$. Consider (8.2.12), it is apparently that

$$\tilde{D}_b(\tilde{L}\boldsymbol{k})^{ab} = \tilde{D}_b\hat{\mathscr{K}}^{ab}\,. \tag{8.2.14}$$

Define the conformal vector Laplacian $\tilde{\Delta}_L$ as (using (8.2.13) and the definition of 3 dimensional Ricci tensor)

$$\tilde{\Delta}_L\boldsymbol{k}^a := \tilde{D}_b(\tilde{L}\boldsymbol{k})^{ab} = \tilde{D}_b\tilde{D}^b\boldsymbol{k}^a + \frac{1}{3}\tilde{D}^a\tilde{D}_b\boldsymbol{k}^b + {}^3\tilde{R}^a{}_b\boldsymbol{k}^b\,, \tag{8.2.15}$$

then (8.2.14) can be rewritten as

$$\tilde{\Delta}_L\boldsymbol{k}^a = \tilde{D}_b\hat{\mathscr{K}}^{ab}\,. \tag{8.2.16}$$

Insert (8.2.11) into (8.2.9) and (8.2.10), yields

$$\tilde{D}^a\tilde{D}_a\Psi - \frac{1}{8}{}^3\tilde{R}\Psi + \frac{1}{8}\left[(\tilde{L}\boldsymbol{k})^{ab} + \hat{\varkappa}_t{}^{ab}\right]\left[(\tilde{L}\boldsymbol{k})_{ab} + \hat{\varkappa}^t{}_{ab}\right]\Psi^{-7} + 2\pi\tilde{E}\Psi^{-3} - \frac{1}{12}K^2\Psi^5 = 0\,, \tag{8.2.17}$$

$$\tilde{\Delta}_L\boldsymbol{k}^a - \frac{2}{3}\Psi^6\tilde{D}^aK = 8\pi\tilde{p}^a\,, \tag{8.2.18}$$

where the indices are lowered by $\tilde{h}_{ab}$. According to the two above constraint equations, it is free to choose the quantities $(\tilde{h}_{ab}, \hat{\varkappa}^{ab}, K, \tilde{E}, \tilde{p}^a)$ and to solve equations (8.2.17) and (8.2.18) for the rest two quantities $(\Psi, \boldsymbol{k}^a)$ on the initial foliation $\mathcal{W}_0$. The original data $(h_{ab}, E, p^a, K^{ab})$ might be obtained by solving the formulas (8.2.1), (8.2.7), (8.2.8) and

$$K^{ab} = \Psi^{-10}\left((\tilde{L}\boldsymbol{k})^{ab} + \hat{\varkappa}_t{}^{ab}\right) + \frac{1}{3}\Psi^{-4}K\tilde{h}^{ab}\,. \tag{8.2.19}$$

This method is called the conformal transverse traceless (CTT) method [16].

If one chooses one of the free data to be constant, e.g., $K$ a constant scalar field on the initial slice $\mathcal{W}_0$, then constraint (8.2.18) becomes

$$\tilde{\Delta}_L\boldsymbol{k}^a = 8\pi\tilde{p}^a\,. \tag{8.2.20}$$

This leads to that the simplified constraint equation (8.2.20) is decoupled from the constraint (8.2.17). We can first solve (8.2.20) for $\boldsymbol{k}^a$, and plug it back into (8.2.17) to solve for the conformal factor $\Psi$. N.B. a hypersurface with constant $K$ is called a constant mean curvature (CMC) hypersurface. The details of proof of the uniqueness and existence of solutions to (8.2.20), a conformal vector Poisson equation, are given in [237, 238, 239].

A more tough task is to obtaining a solution to the elliptic, non-linear differential equation (8.2.18). Many attempts have been made by several people, cf. [231, 240, 241, 242, 243, 169, 170].

Some of the simplest cases of the solutions to the constraints are listed below:

A flat conformal metric $\tilde{h}_{ab} = \delta_{ab}$, a vanishing $\hat{\varkappa}^{ab} = 0$ and a vanishing mean curvature $K = 0$ in a vacuum background, where $\tilde{E} = 0$ and $\tilde{p}^a = 0$. Given these values, it is enough to solve the equations (8.2.20) and (8.2.18) with appropriate boundary conditions, obtain a flat space-like hypersurface of a 4 dimensional Minkowskian space, where $h_{ab} = \delta_{ab}$ and $K_{ab} = 0$.

A non-trivial solution is by selecting a flat conformal metric $\tilde{h}_{ab} = \delta_{ab}$, a vanishing $\hat{\varkappa}^{ab} = 0$, a vanishing mean curvature $K = 0$ and a vacuum mass-energy tensor. However, this time we obtain a different solution depends on a different boundary condition, and the 3 dimensional metric is given as

$$h_{\mu\nu} = \left(1 + \frac{2M}{r}\right)\mathrm{diag}(1, r^2, r^2\sin\theta)\,, \tag{8.2.21}$$

and the extrinsic curvature is

$$K_{ab} = 0\,. \tag{8.2.22}$$

This is just a hypersurface of a constant zeroth coordinate of a Schwarzschild spacetime in the isotropic coordinate.

Note that these types of initial data possess a conformally flat geometry and a normal evolution vector $m^a$ which is a locally Killing vector. Additionally the extrinsic curvature locally vanishes on the foliation. The feature is called the momentarily stationary.

An alternative method for calculating initial data is described in the appendix H.

Having discussed the initial data problem in the preceding section, the next logic step is to study the feature of coordinate choice, which could affect the hyperbolic or elliptic character of the system, based on the chosen lapse function and shift vector. Description of the topic can be found in review articles [244, 245, 246, 16, 247].

The simplest choice of foliation is the geodesic slicing, which leads to a unit lapse function

$$N = 1\,. \tag{8.2.23}$$

This condition leads to a consequence that the worldline of an Eulerian observer is a geodesic and coincides with the $t$ coordinate line. In addition, the proper time coincides with the coordinate time $t$. See [187, 248, 249] for examples and applications.

The maximal slicing corresponds to a vanishing mean curvature on hypersurface, i.e., $K = 0$. This fact gives rise to a maximal volume of the hypersurface (see [201] for a proof). Consider the equation (F.0.57) and the demand of $K = 0$, we obtain an elliptic equation

$$D_a D^a N = N\left[4\pi(E+S) + K_{ab}K^{ab}\right]\,, \tag{8.2.24}$$

see [250, 251, 252, 253, 254] for examples. The applications are given in [255, 256, 257, 258, 259, 260, 261, 262]. A modified maximal slicing method was proposed by Shibata [263] by changing the elliptic equation (8.2.24) to a less CPU-consuming parabolic equation, which has been made use to the binary neutron star and other numerical simulations [264, 265, 266, 267, 268, 269, 270, 271, 272, 273].

A third category of time slicing is called the harmonic slicing, deduced from the harmonic (aka De Donder) condition for the coordinates

$$\Box_g x^\mu := \nabla_\nu \nabla^\nu x^\mu = 0\,, \tag{8.2.25}$$

where $\Box_g$ is the d'Alembertian associated with the 4 dimensional metric $g_{ab}$ [274, 275, 276, 277, 238]. The harmonic slicing condition holds only for the $x^0$ coordinate, yields

$$\Box_g x^0 = 0\,, \tag{8.2.26}$$

and herein $x^0 = t$. The standard d'Alembertian leads to

$$\frac{\partial}{\partial x^\mu}\left(\sqrt{-g}g^{\mu 0}\right) = 0\,. \tag{8.2.27}$$

The components of the inverse 4 dimensional metric might be deduced

from (6.2.78), given by

$$g^{00} = \frac{1}{N^2}\,, \tag{8.2.28}$$

$$g^{0i} = \frac{\beta^i}{N^2}\,, \tag{8.2.29}$$

$$g^{i0} = \frac{\beta^i}{N^2}\,, \tag{8.2.30}$$

$$g^{ij} = h^{ij} - \frac{\beta^i\beta^j}{N^2}\,. \tag{8.2.31}$$

Consider the relation $\sqrt{-g} = N\sqrt{h}$ and the expressions (8.2.28), (8.2.30), (8.2.27) becomes

$$-\frac{\partial}{\partial t}\left(\frac{\sqrt{h}}{N}\right) + \frac{\partial}{\partial x^i}\left(\frac{\sqrt{h}}{N^2}\beta^i\right) = 0\,. \tag{8.2.32}$$

Further expansion and reordering leads to

$$\frac{\partial N}{\partial t} - \beta^i\frac{\partial N}{\partial x^i} - N\left[\frac{1}{\sqrt{h}}\frac{\partial\sqrt{h}}{\partial t} - \frac{1}{\sqrt{h}}\frac{\partial}{\partial x^i}(\sqrt{h}\beta^i)\right] = 0\,. \tag{8.2.33}$$

Introducing a formula [201]

$$\frac{1}{\sqrt{h}}\frac{\partial\sqrt{h}}{\partial t} = -NK + D_a\beta^a\,. \tag{8.2.34}$$

The (8.2.33) then becomes

$$\left(\frac{\partial}{\partial t} - \mathcal{L}_\beta\right)N = -NK\,. \tag{8.2.35}$$

The above equation is an evolution equation for the lapse function. Applications of the harmonic slicing might be referred to [276, 278].

A generalized harmonic slicing condition was deduced in 1995 [279], given by

$$\left(\frac{\partial}{\partial t} - \mathcal{L}_\beta\right)N = -KN^2 f(N)\,, \tag{8.2.36}$$

where $f(N)$ is a function of lapse $N$. Choose that $f(N) = 2N$, then

$$\left(\frac{\partial}{\partial t} - \mathcal{L}_\beta\right)N = -KN^2 N\,, \tag{8.2.37}$$

plug (8.2.34) into (8.2.37), yields

$$\left(\frac{\partial}{\partial t} - \mathcal{L}_\beta\right)N = \frac{\partial}{\partial t}\ln h - 2D_a\beta^a\,. \tag{8.2.38}$$

If the shift vector vanishes, then leading to a solution

$$N = 1 + \ln h\,. \tag{8.2.39}$$

Any foliation which is subject to the condition (8.2.37) is called a 1+log slicing. Note that the harmonic slicing and geodesic slicing are special

cases of (8.2.36) when $f(N) = 1\,,\ 0$ respectively. The $1 + \log$ slicing was introduced by Anninos et al. and Bernstein [280, 281, 282]. There have been numerous applications of the 1+log slicing, including the simulations of binary systems, e.g., black hole mergers [283, 284, 285, 286, 287, 288, 289, 290, 291, 87, 292, 293, 294, 295, 296, 297, 298].

For the details of the conformal time slicing and algebraic slicing, see [299, 247, 300].

As for the coordinate choice, we need to deal with the shift vector as it governs the movement of the coordinate from the preceding slice to the later one. The choice of normal coordinates set the condition

$$\beta^a = 0\,. \tag{8.2.40}$$

This leads to the fact that all lines with constant $x^\mu$ coordinates are orthogonal to the hypersurfaces, where $\mu$ run from 1 to 3. This condition is also know as the Eulerian coordinates [261]. For a partial review of the applications of this gauge, referred to [301].

A second coordinate choice is called the minimal distortion. First we define a distortion tensor $\boldsymbol{Q}_{ab}$, given by

$$\boldsymbol{Q}_{ab} := \mathcal{L}_{\partial_t} h_{ab} - \frac{1}{3} h^{cd} \mathcal{L}_{\partial_t} h_{cd} h_{ab}\,. \tag{8.2.41}$$

This quantity measures the evolution of the shape of spatial domain $\mathcal{V}$ from $\mathcal{W}_t$ to $\mathcal{W}_{t+\Delta t}$ [201]. One can deduce that

$$h^{ab}\mathcal{L}_{\partial_t} h_{ab} = h^{ab}\frac{\partial h_{ab}}{\partial t} = \frac{\partial \ln h}{\partial t} = \frac{\partial \Psi^{12}}{\partial t} + \frac{\partial \ln I}{\partial t} = 12\frac{\partial \Psi}{\partial t}\,, \tag{8.2.42}$$

where we have used the (F.0.7) and (F.0.1), also taking the following formula into consideration

$$\delta(\ln A) = \mathrm{tr}(A^{ab}\delta A_{ab})\,, \tag{8.2.43}$$

where $A_{ab}$ is a general matrix and $A\,,\ A^{ab}$ denote its trace and inverse form respectively. By means of (8.2.41), (8.2.43) and (F.0.6), we obtain

$$\boldsymbol{Q}_{ab} = \Psi^4 \dot{\tilde{h}}_{ab}\,. \tag{8.2.44}$$

Decompose the tensor into two parts

$$\boldsymbol{Q}_{ab} = (\tilde{L}\boldsymbol{k})_{ab} + \boldsymbol{Q}^t{}_{ab}\,, \tag{8.2.45}$$

where the action $\tilde{L}_a$ is defined previously by (8.2.13), $\boldsymbol{Q}^t{}_{ab}$ is traceless and transverse w rt $h_{ab}$. It is legitimate to attribute the first term in (8.2.45) to account for the gravitational field and the second part to account for the change of the 3 dimensional metric between two adjacent time slices due to the variation of the coordinates [201].

The minimal distortion coordinates are then defined by demanding that

$$\boldsymbol{Q}_{ab} = \boldsymbol{Q}^t{}_{ab}\,, \tag{8.2.46}$$

which leads to

$$D^a \boldsymbol{Q}_{ab} = 0\,, \tag{8.2.47}$$

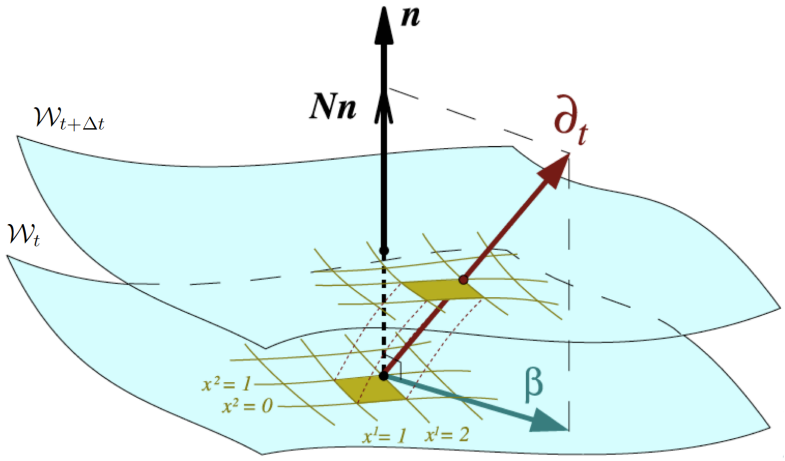


Figure 8.1: The operation of $\boldsymbol{Q}_{ab}$ is the change of the domain of fixed coordinates from foliations $\mathcal{W}_t$ to $\mathcal{W}_{t+\Delta t}$. Credit: É. Gourgoulhon, 2012.

due to the property of the transverse part of $\boldsymbol{Q}_{ab}$. Consider the equations (6.2.87), (8.2.41) and the formula $h^{ab}\partial_t h_{ab} = -2NK + 2D_a\beta^a$, we obtain

$$\boldsymbol{Q}_{ab} = -2NK_{ab} + \mathcal{L}_\beta h_{ab} + \frac{1}{3}\left(2NK - 2D_c\beta^c\right)h_{ab}\,, \tag{8.2.48}$$

i.e.

$$\boldsymbol{Q}_{ab} = -2N\varkappa_{ab} + (\tilde{L}\beta)_{ab}\,, \tag{8.2.49}$$

due to the fact $\mathcal{L}_\beta h_{ab} = 2D_{(a}\beta_{b)}$. Insert this into (8.2.47), yields

$$-2ND_b\varkappa^{ab} - 2\varkappa^{ab}D_bN + D_b(\tilde{L}\beta)^{ab} = 0\,. \tag{8.2.50}$$

The divergence of $\varkappa_{ab}$ may be rewritten by means of (6.2.90) as

$$D_b\varkappa^{ab} = 8\pi p^a + \frac{2}{3}D^aK\,. \tag{8.2.51}$$

The third term on the LHS of (8.2.50) can be rewritten as $D_b(\tilde{L}\beta)^{ab} = D_bD^b\beta^a + D^aD_b\beta^b/3 + {}^3R^a{}_b\beta^b$ [201]. Hence we get an elliptic equation about the shift vector, given by

$$D_bD^b\beta^a + \frac{1}{3}D^aD_b\beta^b + {}^3R^a{}_b\beta^b = 16\pi Np^a + \frac{4}{3}ND^aK + 2\varkappa^{ab}D_bK\,. \tag{8.2.52}$$

Consider the equation (8.2.44), minimal distortion condition (8.2.47) can be rewritten as

$$D^b(\Psi^4\dot{\tilde{h}}_{ab}) = 0\,, \tag{8.2.53}$$

or rewritten by means of $\tilde{D}_a$ as

$$\tilde{D}^b(\Psi^6\dot{\tilde{h}}_{ab}) = 0\,. \tag{8.2.54}$$

The minimal distortion was studied by Smarr and York, etc. [238, 302].

Furthermore, an alternative formula which deviates from (8.2.54) by

$$\tilde{D}^b\dot{\tilde{h}}_{ab} = 0\,, \tag{8.2.55}$$

or modified into

$$\mathcal{D}^b\dot{\tilde{h}}_{ab} = 0\,, \tag{8.2.56}$$

called the pseudo-minimal distortion coordinate [303, 188].

An alternative version of the condition was given in [304]. By (H.1.3), re-express the $\dot{\tilde{h}}_{ab}$ as

$$2N\tilde{\varkappa}_{ab} = -\dot{\tilde{h}}_{ab} + \tilde{h}_{ac}\tilde{h}_{bd}(\tilde{L}\beta)^{cd}\,, \tag{8.2.57}$$

plug into (8.2.55), yields

$$\tilde{D}^b\left[\tilde{h}_{ac}\tilde{h}_{bd}(\tilde{L}\beta)^{cd} - 2N\tilde{\varkappa}_{ab}\right] = 0\,. \tag{8.2.58}$$

Expanding this expression and taking the operation of conformal vector Laplacian, equation (F.0.68) and by replacing the conformal Laplacian associated to $\tilde{h}_{ab}$ with the conformal Laplacian associated to the flat metric $\delta_{ab}$, leads to

$$\mathcal{D}_b\mathcal{D}^b\beta^a + \frac{1}{3}\mathcal{D}^a\mathcal{D}_b\beta^b - 2\tilde{\varkappa}^{ab}\tilde{D}_b N + \left[3\tilde{\varkappa}^{ab}\tilde{D}_b\ln\Psi - \frac{1}{3}\tilde{D}^a K - 4\pi\Psi^4 p^a\right] = 0\,. \tag{8.2.59}$$

The above equation defines an elliptic equation instead of the (8.2.52), called the approximate minimal distortion [264, 270, 266, 305, 306].

A fourth prescription of the evolution equation of shift vector is the Gamma freezing, by replacing the two symbols in the (8.2.56)

$$\mathcal{D}_b\dot{\tilde{h}}^{ab} = 0\,, \tag{8.2.60}$$

where $\dot{\tilde{h}}^{ab} := \partial\tilde{h}^{ab}/\partial t$. Expanding the above equation leads to

$$\begin{aligned}\mathcal{D}_b\dot{\tilde{h}}^{ab} &= \mathcal{D}_b\frac{\partial\tilde{h}^{ab}}{\partial t}\\ &= \frac{\partial}{\partial t}\mathcal{D}_b\tilde{h}^{ab} = 0\,,\end{aligned} \tag{8.2.61}$$

due to the commutation of the two derivative operators. For the covariant derivative $\mathcal{D}_a$, we have

$$\begin{aligned}\mathcal{D}_b\tilde{h}^{ab} &= \partial_b\tilde{h}^{ab} + \bar{\Gamma}_{cb}{}^a\tilde{h}^{cb} + \bar{\Gamma}_{cb}{}^c\tilde{h}^{ab}\\ &= \tilde{h}^{cb}\left(\bar{\Gamma}_{cb}{}^a - \tilde{\Gamma}_{cb}{}^a\right)\,,\end{aligned} \tag{8.2.62}$$

where we have used $\bar{\Gamma}_{cb}{}^b = \partial_c\ln I/2$, $\tilde{\Gamma}_{cb}{}^b = \partial_c\ln\tilde{h}/2$, the relation between $\tilde{D}_a\,\tilde{h} = I$, $\tilde{\Gamma}_{ab}{}^c$ and $\tilde{D}_a\tilde{h}^{ab} = 0$. Introduce a notation

$$\tilde{\Gamma}^a := \tilde{h}^{cb}\left(\tilde{\Gamma}_{cb}{}^a - \bar{\Gamma}_{cb}{}^a\right)\,, \tag{8.2.63}$$

by applying this to (8.2.62), yields

$$\mathcal{D}_b\tilde{h}^{ab} = -\tilde{\Gamma}^a\,. \tag{8.2.64}$$

Combine the above equation with (8.2.61), we obtain

$$\partial_t\tilde{\Gamma}^a = 0\,, \tag{8.2.65}$$

which implies a non-dynamical $\Gamma$ notation [307].

The time derivative of $\tilde{h}^{ab}$ can be written in terms of the $\mathcal{D}_a$ as

$$\dot{\tilde{h}}^{ab} = 2N\tilde{\varkappa}^{ab} + \beta^c\mathcal{D}_c\tilde{h}^{ab} - \tilde{h}^{cb}\mathcal{D}_c\beta^a - \tilde{h}^{ca}\mathcal{D}_c\beta^b + \frac{2}{3}\tilde{D}_c\beta^c\tilde{h}^{ab}\,, \quad (8.2.66)$$

by means of (8.2.64) and the action of $\partial_t$, leads to

$$\begin{aligned}\partial_t\tilde{\Gamma}^a =& -2N\mathcal{D}_b\tilde{\varkappa}^{ab} - 2N\varkappa^{ab}\mathcal{D}_bN + \beta^c\mathcal{D}_c\tilde{\Gamma}^a - \tilde{\Gamma}^c\mathcal{D}_c\beta^a + \frac{2}{3}\tilde{\Gamma}^a\mathcal{D}_c\beta^c \\ &+ \tilde{h}^{bc}\mathcal{D}_c\mathcal{D}_b\beta^a + \frac{1}{3}\tilde{h}^{ab}\mathcal{D}_c\mathcal{D}_b\beta^c\,. \end{aligned} \quad (8.2.67)$$

The term $\mathcal{D}_b\tilde{\varkappa}^{ab}$ can be re-expressed by the momentum constraint equation, such that the above equation becomes

$$\begin{aligned}\partial_t\tilde{\Gamma}^a =& \ \tilde{h}^{bc}\mathcal{D}_c\mathcal{D}_b\beta^a + \frac{1}{3}\tilde{h}^{ab}\mathcal{D}_c\mathcal{D}_b\beta^c + \frac{2}{3}\tilde{\Gamma}^a\mathcal{D}_c\beta^c - \tilde{\Gamma}^c\mathcal{D}_c\beta^a + \beta^c\mathcal{D}_c\tilde{\Gamma}^a \\ &- 2N\left[8\pi\Psi^4p^a - \tilde{\varkappa}^{cb}\left(\tilde{\Gamma}_{cb}{}^a - \bar{\Gamma}_{cb}{}^a\right) - 6\tilde{\varkappa}^{ab}\mathcal{D}_b\ln\Psi + \frac{2}{3}\tilde{h}^{ab}\mathcal{D}_bK\right] \\ &- 2\tilde{\varkappa}^{ab}\mathcal{D}_bN\,, \end{aligned} \quad (8.2.68)$$

hence the condition (8.2.65) is equivalent to the following elliptic equation

$$\begin{aligned}&\tilde{h}^{bc}\mathcal{D}_c\mathcal{D}_b\beta^a + \frac{1}{3}\tilde{h}^{ab}\mathcal{D}_c\mathcal{D}_b\beta^c + \frac{2}{3}\tilde{\Gamma}^a\mathcal{D}_c\beta^c - \tilde{\Gamma}^c\mathcal{D}_c\beta^a + \beta^c\mathcal{D}_c\tilde{\Gamma}^a = \\ &-2N\left[8\pi\Psi^4p^a - \tilde{\varkappa}^{cb}\left(\tilde{\Gamma}_{cb}{}^a - \bar{\Gamma}_{cb}{}^a\right) - 6\tilde{\varkappa}^{ab}\mathcal{D}_b\ln\Psi + \frac{2}{3}\tilde{h}^{ab}\mathcal{D}_bK\right] - 2\tilde{\varkappa}^{ab}\mathcal{D}_bN\,. \end{aligned} \quad (8.2.69)$$

A fifth condition is called the Gamma driver coordinate. Consider, instead the relation

$$\partial_t\beta^a = f\partial\tilde{\Gamma}^a\,, \quad (8.2.70)$$

with a positive function $f$. Injecting this relation back to equation (8.2.68) will result in a parabolic equation for $\beta^a$. Alternatively, in [191], the authors require that

$$\frac{\partial^2\beta^a}{\partial t^2} = f\frac{\partial\tilde{\Gamma}^a}{\partial t} - \left(f_1 - \frac{\partial\ln f}{\partial t}\right)\frac{\partial\beta^a}{\partial t}\,, \quad (8.2.71)$$

where $f_1$ is a positive function, cf. [308, 309, 310]. This prescription indeed produces a hyperbolic evolution equation for $\beta^a$, given as

$$\begin{aligned}&\frac{\partial^2\beta^a}{\partial t^2} + \left(f_1 - \frac{\partial\ln f}{\partial t}\right)\frac{\partial\beta^a}{\partial t} = \\ &f\left(\tilde{h}^{bc}\mathcal{D}_c\mathcal{D}_b\beta^a + \frac{1}{3}\tilde{h}^{ab}\mathcal{D}_c\mathcal{D}_b\beta^c + \frac{2}{3}\tilde{\Gamma}^a\mathcal{D}_c\beta^c - \tilde{\Gamma}^c\mathcal{D}_c\beta^a + \beta^c\mathcal{D}_c\tilde{\Gamma}^a\right) \\ &-2Nf\left[8\pi\Psi^4p^a - \tilde{\varkappa}^{cb}\left(\tilde{\Gamma}_{cb}{}^a - \bar{\Gamma}_{cb}{}^a\right) - 6\tilde{\varkappa}^{ab}\mathcal{D}_b\ln\Psi + \frac{2}{3}\tilde{h}^{ab}\mathcal{D}_bK\right] \\ &-2f\tilde{\varkappa}^{ab}\mathcal{D}_bN\,. \end{aligned} \quad (8.2.72)$$

The hyperbolic Gamma driver has been utilized in many contemporary numerical computations, referred to [311, 297]. Other dynamical gauge may be found in various articles and reviews, see [271, 272, 273]. Appendix I contains further discussion on gauging, regarding the coordinate evolution.

We are now in the position to discuss the full completion of integrating the Einstein equations, by introducing the free scheme and constrained scheme of the evolutionary equations [312, 313, 314, 315, 316].

For the constrained schemes, there exist two branches, one is called the partially constrained scheme, the other is the full constrained scheme. Such a scheme requires the code to re-calculate the constraint equations on each time slice (corresponding to each time step). Herein, we focus on the free scheme whereas ignore the constrained scheme. Further discussion on this approach may refer to [317, 318, 319, 320].

A free scheme implies that one only needs to solve the constraint equations once on the initial slice for the initial value, the rest of the calculation would emphasis on looking for solutions to the evolution equations rather than computing the constraints slice by slice [321]. We will justify the statement hereafter in the following text.

The general relativity is a well-posed initial value problem [322], which indicates that given a initial condition $(h_{ab}, K_{ab})$ defined on a 3 dimensional hypersurface, such that they satisfy the vacuum Einstein constraint equations

$$
\begin{aligned}
&{}^3R - K_{ab}K^{ab} + K^2 = 0\,, && (8.2.73)\\
&D_a K_b{}^a - D_b K = 0\,. && (8.2.74)
\end{aligned}
$$

And the original Einstein equation can be derived from the evolution equations

$$
\begin{aligned}
&\left(\frac{\partial}{\partial t} - \mathcal{L}_\beta\right) h_{ab} \;=\; 2NK_{ab}\,, && (8.2.75)\\
&\left(\frac{\partial}{\partial t} - \mathcal{L}_\beta\right) K_{ab} = -N^3 R_{ab} + 2NK_a{}^c K_{cb} - NKK_{ab} + D_a D_b N\,, && (8.2.76)
\end{aligned}
$$

where for a vacuum spacetime it is assumed $T_{ab}$ vanishes. Compare the equation (6.2.51), which is in general satisfied by the extrinsic curvature, to equation (8.2.76), they are differed by a term $R_{cd}h_a{}^c h_b{}^d$. Now for a vacuum configuration, this term is equal to zero. When the equations (8.2.73) and (8.2.74) are satisfied, we have the following relation

$$
\begin{aligned}
&G_{ab}n^a h^b{}_c = D_a K_c{}^a - D_c K = 0\,, && (8.2.77)\\
&G_{ab}n^a n^b \;= {}^3R - K_{ab}K^{ab} + K^2 = 0\,. && (8.2.78)
\end{aligned}
$$

For (8.2.78), one can conclude that

$$
R_{ab}n^a n^b = -\frac{1}{2}R\,, \tag{8.2.79}
$$

due to that $g_{ab}n^a n^b = -1$. For (8.2.77), there is a natural consequence

$$
R_{ab}n^a n^b n_c = -\frac{1}{2}R_{ac}n^a\,. \tag{8.2.80}
$$

Note that $g_{ab}n^a h_c{}^b = n_b h_c{}^b = 0$. $G_{ab}n^a h_c{}^b = 0$ leads to

$$\begin{aligned} 0 &= R_{ab}n^a h_c{}^b - \frac{1}{2}R g_{ab}n^a h_c{}^b \\ \Rightarrow 0 &= R_{ab}n^a(\delta_c{}^b + n_c n^b) \\ \Rightarrow 0 &= R_{ac}n^a + R_{ab}n^a n_c n^b \\ \Rightarrow R_{ac}n^a &= -R_{ab}n^a n_c n^b \,. \end{aligned} \tag{8.2.81}$$

Hence the equation (8.2.80). Combine (8.2.80) and (8.2.79), one can immediately obtain

$$R_{ac}n^a = R n_c \,, \tag{8.2.82}$$

by means of (8.2.82), (8.2.80) and $R_{ab}h_c{}^a h_d{}^b = 0$, we conclude that

$$R_{cd} + \frac{1}{2}R n_c n_d = 0 \,, \tag{8.2.83}$$

which implies that

$$0 = R_{cd}g^{cd} + \frac{1}{2}R n_c n_d g^{cd} = R - \frac{1}{2}R = \frac{1}{2}R \,, \tag{8.2.84}$$

i.e., $R = 0$. Consequently, this leads to

$$G_{ab}h^a{}_c h^b{}_d = R_{ab}h^a{}_c h^b{}_d = 0 \,. \tag{8.2.85}$$

This recovers the remaining part of Einstein equations. To conclude, we have recovered the full system of vacuum Einstein equations, consisting of (8.2.73), (8.2.74), (8.2.75) and (8.2.76), which reflect the dynamics of spacetime geometry, i.e., the evolution of an initial 3 dimensional space-like hypersurface in the foliations, for which we sometimes call it geometrodynamics.

Moreover, with the help of equations (8.2.75) and (8.2.76), the Lie derivatives of the LHS of (8.2.73) and (8.2.74) along the $\partial_t$ coordinate line vanish, i.e.,

$$\mathcal{L}_{\partial_t}\left({}^3R - K_{ab}K^{ab}\right) = 0 \,, \tag{8.2.86}$$

$$\mathcal{L}_{\partial_t}\left(-N^3 R_{ab} + nK_a{}^c K_{cb} - NKK_{ab} + D_a D_b N\right) = 0 \,. \tag{8.2.87}$$

We ignore the proof here, for details see [201]. The equations (8.2.86) and (8.2.87) demonstrate that any quantities $(h^0{}_{ab}, K^0{}_{ab})$ can be regarded as the initial condition on some hypersurface, if they obey the equations (8.2.73) and (8.2.74). Furthermore, the constraints (8.2.73) and (8.2.74) are preserved by the data which satisfy the evolution equations (8.2.75) and (8.2.76) based on the initial values $(h^0{}_{ab}, K^0{}_{ab})$. Note that we assume the vacuum condition in the proof here, in general the mass-energy tensor must satisfy the conservation law $\nabla^a T_{ab} = 0$ to guarantee a generic satisfaction of (8.2.86) and (8.2.87).

The well-established mathematical formulation of the constraint preservation property does not imply that any numerical procedure and algorithms would obey the same rule. Indeed, people have struggled with constructing a formalism which preserves the constraint equations in most

of the early time simulations. Many work has been done and devoted to this field, referred to [315, 323, 324, 313, 325, 326, 327, 328].

The most successful and well-behaved free evolution scheme must be the BSSN formalism, founded by Baumgarte, Shapiro, Shibata and Nakamura in 1990s, which demonstrated strong hyperbolicity of the Einstein equations [329]. We describe the basics for this evolution formalism and its applications to practical algorithms, then it will be applied in the thesis to model the binary black hole spacetime with two equal mass, non-spinning compact objects.

To continue, let us begin with considering the conformal 3 dimensional Ricci tensor ${}^3\tilde{R}_{ab}$ appears in the appendix F. Rewrite it in the following pattern

$$ {}^3\tilde{R}_{ab} = \partial_c \tilde{\Gamma}_{ab}{}^c - \partial_b \tilde{\Gamma}_{ac}{}^c + \tilde{\Gamma}_{ab}{}^c \tilde{\Gamma}_{cd}{}^d - \tilde{\Gamma}_{ad}{}^c \tilde{\Gamma}_{cb}{}^d \,. \tag{8.2.88} $$

Introduce a tensor

$$ \Delta_{ab}{}^c := \tilde{\Gamma}_{ab}{}^c - \bar{\Gamma}_{ab}{}^c \,, \tag{8.2.89} $$

where $\Delta_{ab}{}^c$ is an auxiliary tensor of type $(1,2)$. An equivalent form of (8.2.89) is given by

$$ \Delta_{ab}{}^c = \frac{1}{2}\tilde{h}^{cd}\left(\mathcal{D}_a \tilde{h}_{bd} + \mathcal{D}_b \tilde{h}_{ad} - \mathcal{D}_d \tilde{h}_{ab}\right) . \tag{8.2.90} $$

One can then deduce the following result

$$ \Delta_{ac}{}^c = 0 \,, \tag{8.2.91} $$

by contracting indices $c$ and $b$ of $\Delta_{ab}{}^c$, where we have considered $\tilde{h} = I$. Replace $\tilde{\Gamma}_{ab}{}^c$ in (8.2.88) by means of $\Delta_{ab}{}^c$, yields

$$ \begin{aligned} {}^3\tilde{R}_{ab} = \;& \partial_c \Delta_{ab}{}^c + \partial_c \bar{\Gamma}_{ab}{}^c - \partial_b \Delta_{ac}{}^c - \partial_b \bar{\Gamma}_{ac}{}^c + \Delta_{cd}{}^d \Delta_{ab}{}^c + \Delta_{cd}{}^d \bar{\Gamma}_{ab}{}^c \\ & + \Delta_{cd}{}^d \bar{\Gamma}_{ab}{}^c + \bar{\Gamma}_{cd}{}^d \bar{\Gamma}_{ab}{}^c - \Delta_{cd}{}^d \Delta_{ab}{}^c - \bar{\Gamma}_{cb}{}^d \Delta_{ad}{}^c - \bar{\Gamma}_{ad}{}^c \Delta_{cb}{}^d - \bar{\Gamma}_{ad}{}^c \bar{\Gamma}_{cb}{}^d \,. \end{aligned} \tag{8.2.92} $$

If we consider the flat feature of $I_{ab}$, which leads to a vanishing Ricci tensor, we then can obtain the reduced expression for ${}^3\tilde{R}_{ab}$ as

$$ \begin{aligned} {}^3\tilde{R}_{ab} = \;& \partial_c \Delta_{ab}{}^c - \partial_b \Delta_{ac}{}^c + \Delta_{cd}{}^d \Delta_{ab}{}^c + \Delta_{cd}{}^d \bar{\Gamma}_{ab}{}^c + \Delta_{cd}{}^d \bar{\Gamma}_{ab}{}^c \\ & - \Delta_{cb}{}^d \Delta_{ad}{}^c - \bar{\Gamma}_{cb}{}^d \Delta_{ad}{}^c - \bar{\Gamma}_{ad}{}^c \Delta_{cb}{}^d \,. \end{aligned} \tag{8.2.93} $$

Formula (8.2.91) enables us to simplify the above equation to

$$ \begin{aligned} {}^3\tilde{R}_{ab} &= \partial_c \Delta_{ab}{}^c + \bar{\Gamma}_{cd}{}^d \Delta_{ab}{}^c - \bar{\Gamma}_{ca}{}^d \Delta_{bd}{}^c - \bar{\Gamma}_{cb}{}^d \Delta_{ad}{}^c - \Delta_{cb}{}^d \Delta_{ad}{}^c \\ &= \mathcal{D}_c \Delta_{ab}{}^c - \Delta_{cb}{}^d \Delta_{ad}{}^c \,. \end{aligned} \tag{8.2.94} $$

Consider the alternative expression of $\Delta_{ab}{}^c$ given in (8.2.90), plug it into (8.2.94) yields

$$ {}^3\tilde{R}_{ab} = -\frac{1}{2}\left(\tilde{h}^{cd}\mathcal{D}_c\mathcal{D}_d\tilde{h}_{ab} + \tilde{h}_{ca}\mathcal{D}_b\mathcal{D}_d\tilde{h}^{cd} + \tilde{h}_{cb}\mathcal{D}_a\mathcal{D}_d\tilde{h}^{cd}\right) + \mathcal{R}_{ab}(\tilde{h}, \mathcal{D}\tilde{h}) \,, \tag{8.2.95} $$

where

$$\mathcal{R}_{ab}(\tilde{h}, \mathcal{D}\tilde{h}) := \frac{1}{2}\left(\mathcal{D}_c\tilde{h}_{bd}\mathcal{D}_a\tilde{h}^{cd} + \mathcal{D}_c\tilde{h}_{ad}\mathcal{D}_b\tilde{h}^{cd} + \mathcal{D}_c\tilde{h}^{cd}\mathcal{D}_d\tilde{h}_{ab}\right) - \Delta_{ad}{}^{c}\Delta_{bc}{}^{d}\,. \tag{8.2.96}$$

Consider the equation (8.2.64), (8.2.95) becomes

$${}^{3}\tilde{R}_{ab} = -\frac{1}{2}\left(\tilde{h}^{cd}\mathcal{D}_c\mathcal{D}_d\tilde{h}_{ab} - \tilde{h}_{ac}\mathcal{D}_b\tilde{\Gamma}^{c} - \tilde{h}_{bc}\mathcal{D}_a\tilde{\Gamma}^{c}\right) + \mathcal{R}_{ab}(\tilde{h}, \mathcal{D}\tilde{h})\,. \tag{8.2.97}$$

The 3 dimensional Ricci scalar is then given by contracting the indices of 3 dimensional Ricci tensor as

$${}^{3}\tilde{R} = \frac{1}{2}\left[\tilde{h}^{cd}\mathcal{D}_c(\tilde{h}^{ab}\mathcal{D}_d\tilde{h}_{ab}) + \tilde{h}^{cd}\mathcal{D}_c\tilde{h}^{ab}\mathcal{D}_d\tilde{h}_{ab} + 2\mathcal{D}_c\tilde{\Gamma}^{c}\right] + \tilde{h}^{ab}\mathcal{R}_{ab}(\tilde{h}, \mathcal{D}\tilde{h})\,. \tag{8.2.98}$$

From (8.2.90), we have $2\Delta_{cd}{}^{d} = \tilde{h}^{ab}\mathcal{D}_c\tilde{h}_{ab}$, and from (8.2.91), we obtain

$${}^{3}\tilde{R} = \mathcal{D}_c\tilde{\Gamma}^{c} + \mathcal{R}(\tilde{h}, \mathcal{D}\tilde{h})\,, \tag{8.2.99}$$

where

$$\mathcal{R}(\tilde{h}, \mathcal{D}\tilde{h}) := \frac{1}{2}\tilde{h}^{cd}\mathcal{D}_c\tilde{h}^{ab}\mathcal{D}_d\tilde{h}_{ab} + \tilde{h}^{ab}\mathcal{R}_{ab}(\tilde{h}, \mathcal{D}\tilde{h})\,. \tag{8.2.100}$$

The motivation of introducing an auxiliary variable $\tilde{\Gamma}^{a}$ was first investigated by de Donder [274] with a different formalism in the 4 dimensional case, and then formally proposed by Nakamura et al. [187]. Additional references about this topic might be found in [330, 331, 86, 200, 332, 333, 334].

Hence, the complete BSSN scheme is given by gathering evolution equations (F.0.44), (F.0.45), (F.0.62) and (F.0.63) and constraints (F.0.66) and (F.0.68) (or (F.0.54) and (F.0.67)), and equations (8.2.97) and (8.2.96), and equations (8.2.99) and (8.2.100), and (8.2.68) [292].

## 8.3 Null Geodesics Finder for BBH Spacetime Using the 4+1 Formulation

Applying the 4+1 method to the derived data set in the last section. Firstly, we embed the 4 dimensional metric into a 5 dimensional manifold where the coordinate transformation is given as

$$\begin{cases} t' &= t\,, \\ r' &= r\,, \\ \theta' &= \theta\,, \\ \varphi' &= \varphi\,, \\ w'_0 &= t_0\,. \end{cases} \tag{8.3.1}$$

This is done on the zeroth slice $\phi_{w_0}(\mathcal{M})$, where $\mathcal{M}$ denotes the original 4 dimensional manifold generated from the initial data by solving the 3+1 Einstein equations, and $t_0$ is a constant.

On the first slice the coordinate transformation is given by

$$\begin{cases} t' &= t - \Delta t\,, \\ r' &= r\,, \\ \theta' &= \theta\,, \\ \varphi' &= \varphi\,, \\ {w'}_1 &= t_0 + \Delta t = t_1\,. \end{cases} \tag{8.3.2}$$

Where $\Delta t$ is a positive constant. Repeating this operation to the remaining of the spacetime slices and a new 5 dimensional manifold is formed via combining all 4 dimensional spacetime foliations, denoted by $\mathcal{M}' = \mathbb{R} \times \mathcal{M}$.

Then one needs to recover the Lorentz structure by introducing a 5 dimensional metric, which is given by

$$\begin{aligned} {g'}_{\mu\nu}\mathrm{d}u^\mu \mathrm{d}u^\nu = \quad & \left(-N'^2 + {h'}_{ij}\beta'^i\beta'^j\right)\mathrm{d}w'^2 \\ & + {h'}_{ij}\beta'^j \mathrm{d}w'\mathrm{d}u^i + {h'}_{ij}\beta'^i \mathrm{d}w'\mathrm{d}u^j \\ & + g_{\mu\nu}\mathrm{d}u^\mu \mathrm{d}u^\nu\,. \end{aligned} \tag{8.3.3}$$

Where the notation $u$ represents the coordinate of 5 dimensional manifold as before, $i$ and $j$ are concrete indices, and $g_{\mu\nu}$ represent the components of the original 4 dimensional metric. Follow the similar procedure that has been constructed in the fourth Chapter, we may choose a congruence of light rays in the original spacetime $\mathcal{M}$, denoted by $\{C_i\}$. Find their images in each spacetime slice of the 5 dimensional space $\mathcal{M}'$. We recover one of the curves in $\{C_i\}$, by choosing a point in the zeroth slice $\phi_{w_0}(\mathcal{M})$ and track it to the successive point located at a point which has a shifted zeroth coordinate, by a value of $\Delta t$. Follow this operation we can track the third and more points to recover an image of this curve, travelling through all spacetime foliations $\phi_{w_n}(\mathcal{M})$ in the chronological order in terms of coordinate $w$. Repeating this procedure for the remaining null curves of $\{C_i\}$ and gathering all the images, we can recover a vertical (at least locally) manifold, denoted by $\Phi(\mathcal{M})$.

Moreover, it is natural to obtain an isometric transformation between $\Phi(\mathcal{M})$ and the original 4 dimensional spacetime $\mathcal{M}$, by pulling-back the 5 dimensional metric given in (8.3.3) to $\Phi(\mathcal{M})$, then it is apparently that the pulled-back metric on $\Phi(\mathcal{M})$ is isometric to the original 4 dimensional metric of $\mathcal{M}$, for a detailed proof see Chapter 5.

We will analyze the data[19] and demonstrate how one can apply the data as a 5 dimensional quantity. This is a necessary step before we can make a further progress. We will first focus on the lapse function as a concise demonstration, which is nonetheless, an appropriate example to explain how we can work with the discrete data and what kind of extra information we need for further numerical calculation.

It is noted that we do not need the whole data set hence the only embedded data would be part of the huge data set, which will consist of

[19]Three are more than one package for manipulating the results of Einstein toolkit, e.g., SimulationTools, PostCactus, and kuibit. One can use any of these to illustrate the plots and movies, or transform file format of the output data files.

the lapse function, shift vector, 3 dimensional metric and the extrinsic curvature.

We can first focus on one of the files which contains (partially) the information of lapse function $N$ on each time foliation. The data can be generated from the code of the Einstein toolkit web page [17]. We would produce an equal mass, non-spinning binary black hole merger dataas we have discussed in the previous context. The data file might look like: [lapse.xz.asc] or [lapse.h5]. These files contain all information that is required to reconstruct the physical quantity and the coordinates. We need to embed the values into the 5 dimensional coordinate system, where the detailed procedure has been given in Chapter 6. However, unlike what we have done in the that Chapter, we cannot straightforwardly perform the embedding and obtain the values on the corresponding 5 dimensional grid points. This is mainly because that the data of a real numerical spacetime has a more complicated structure than the data of a symmetric head-on collision spacetime, where each quantity, including scalar and tensor is decomposed into various components, which are labeled by .xx, .xz etc., In particular, those variables which depend on the temporal coordinate demand extra attention due to a more complex transformation law (Chapter 4). Herein, we propose a sensible and convenient way of constructing the 5 dimensional data. We read the 3 dimensional physical quantities from the HDF file (.h5 file in the output directory) on each foliation [335, 336], and use one of the above processing tools to convert the HDF file into a Fortran readable format. We then can embed all the variables in the 5 dimensional manifold and their values are assigned on the 5 dimensional grid points. Note that the 5 dimensional data take the same values as their counterparts due to the isometric embedding $\phi_w$, provided they are correctly locating at the corresponding grid points. We need then to store the 5 dimensional data in the Fortran code for further computation.

We can find that in the following chart how one practically manipulates the numbers given in file.h5. First we need to recover the lapse function via the data from files: admbase-lapse.h5. For example, for the value at grid point (0,-6,-124,-6), the lapse function is given by $N = 9.961815 \times 10^{-1}$, hence, a transformation is given as follow

$$\begin{aligned} &(9.961815 \times 10^{-1}) \text{ at } (0, -6, -124, -6) \rightarrow \\ &(9.961815 \times 10^{-1}) \text{ at } (0, -6, -124, -6, 0)\,, \end{aligned} \tag{8.3.4}$$

on the first spacetime foliation $\phi_{w_0}(\mathcal{M})$. We can perform the similar operation for the remaining HDF files and recover the whole 3+1 metric on each 4 dimensional foliation in the 5 dimensional manifold. For the time-dependent metric components, we follow the rule and calculate the original 4 dimensional quantity first by equations (5.6.24) and (5.6.25), and embed them in the 5 dimensional manifold.

For the full and comprehensive analysis of the data generated from Einstein toolkit, check with the kuibit platform [337].

Furthermore, a generic level set equation given by (4.5.3), requires a propagation speed factor which control the evolution of propagating interface. Hence, we have to know more geometrical quantities than just the 3+1 metric components. For example, for the mean curvature

flow, we will need to derive the mean curvature $\kappa$ as the propagation parameter, where the level set equation would be modified to acquire an alternative term $H' = |\nabla u|\mathrm{div}(\nabla u/|\nabla u|)$ [338] instead of the second term of equation (4.5.3). For the general relativity, we need to determine the local values of null tangent, metric tensor and probably further quantities which might be demanded in deriving the null geodesic.

We will hereafter derive the 5 dimensional null tangents on certain grid point, at which we first decide the embedded 4 dimensional metric components and then derive the 5 dimensional metric components using (8.3.3). Then one can calculate the 5 dimensional geometric quantities via the 5 dimensional metric. Furthermore, we can decide the 5 dimensional Riemann curvature in terms of the 4 dimensional Riemann curvature if necessary, like what we have done for the relation between the 4 dimensional Riemann curvature and the 3 dimensional Riemann curvature in the 3+1 formalism [339].

Given a null tangent $n^a$, it satisfies

$$g_{ab}n^a n^b = 0\,, \tag{8.3.5}$$

consider the equation (6.2.78), we have the following expression

$$(-N^2 + h_{ij}\beta^i\beta^j)n^0 n^0 + h_{ij}n^i n^j = 0\,, \tag{8.3.6}$$

where $n^\mu$ denote the components of $n^a$ in the given coordinate, $i$ and $j$ run from 1 to 3. Apparently, there exist numerous solutions to this equation, which also justifies that at a given spacetime point we have more than one vector on the light cone. To pick out a specific null tangent, let us first set that

$$n^\mu = (1, n^1, n^2, n^3)\,, \tag{8.3.7}$$

hence (8.3.6) reduces to

$$-N^2 + h_{ij}\beta^i\beta^j + h_{ij}n^i n^j = 0\,, \tag{8.3.8}$$

furthermore, we are free to choose $n^1$ and $n^3$, which left us only one degree of freedom (DOF), the $n^2$. Without loss of generality, let $n^1 = n^3 = 0$, leads to that

$$-N^2 + h_{ij}\beta^i\beta^j + h_{22}n^2 n^2 = 0\,, \tag{8.3.9}$$

from (8.3.8). We can now proceed by plugging the values of $h_{ij}$ , $\beta^i$ and $N$ at a grid point $(0, 0, 0, 0)$ into (8.3.9) and compute $n^2$, which is

$$n^2 = 0.96770429508\,, \tag{8.3.10}$$

hence the null tangent is given as $n^\mu = (1, 0, 0.96770429508, 0)$. And a 5 dimensional null tangent can be derived from this, given as $n'^\mu = (1, 0, 0.96770429508, 0, 0)$ at grid $(0, 0, 0, 0, 0)$. This is guaranteed due to (5.5.33).

We need first to propose the level set equation that governs the propagation of the photons. One equation that we can use is given by

$$\frac{\partial}{\partial\tau}\phi\,(\tau, x^\mu) + n^a\nabla_a\phi\,(\tau, x^\mu) = 0\,, \tag{8.3.11}$$

where $\phi$ is a function defined on the manifold, $\tau$ is an evolution parameter, $x^\mu$ is the coordinates of the manifold, $n^a$ is a vector field and $\nabla_a$ is the 5 dimensional covariant derivative. We can now proceed by first explaining the terms in equation (8.3.11). Let the $\tau$ denote the parameter of the null geodesic, $n^a$ is the tangent vector to the null geodesic which do not depend on the parameter $\tau$, and $\nabla_a$ denote the covariant derivative which is adapted to the 5 dimensional metric, where $x^\mu$ is the 5 dimensional coordinate. The $\phi$ is denoting the level set hypersurface which propagates under the control of equation (8.3.11).

In addition, we need also to apply extra constraint to control the evolution to make it remain on the correct path — null geodesic. A practical algorithm for calculating the null geodesic is ongoing and numerical implementation will be carried out in a further detailed research.

# Chapter 9

# Summary, Discussions and Additional Remarks

## 9.1 Summary of the Thesis

The core physics of this project is to construct the covariant formulation of radiative transfer in dynamical spacetime, in particular two coalescing black holes, and seek solution schemes of the radiative transfer equations. In order to achieve this goal, one needs to find the photons' trajectories in a BBH spacetime. Specifically, the null geodesics, i.e., worldlines of free falling massless particles (including photons) are constructed by combining 3+1 numerical relativity and the level set method in a 4+1 formulation, by embedding the original 4 dimensional spacetime in a 5 dimensional ambient space and solving the level set equations (evolution equations), and the covariant radiative transfer equations are constructed along the derived geodesics. General relativistic radiative transfer formulation in Kerr black hole system has been constructed previously [2, 340] (cf., the article [341] for the most original research).

In the Chapter 1, which is the introductory Chapter, the general relativity background and the radiation transport are discussed. Motivations for constructing a covariant formulation of radiative transfer in dynamical spacetime is introduced. And an alternative covariant formulation for constructing an appropriate radiation transport equation in dynamical spacetime is given.

In the Chapter 2, the basics of GR is introduced and the GWs development and its EM counterpart are discussed.

The previous ray-tracing algorithm and covariant formulation of radiative transfer are reviewed in Chapter 3. I derived the photons' trajectories using Euler-Lagrange equations in the stationary Kerr spacetime.

We discussed the fundamental knowledge of the level set method in Chapter 4. The non-constrained geodesic formulation has been introduced with level set equation given in (4.4.3). Currently, we used both first-order accurate finite difference method and third-order accurate ENO method to solve the equations for a demo case and results will be compared with precise solutions. The higher-order TVD RK has been applied to a generic equation and will be modified to match specific equations. Nevertheless, the precision of numerical integrators must be improved and then be tested. This can be done via the implementation

of different computational algorithms, e.g., the symplectic integrator for Hamilton-Jacobi equations.

Furthermore, the new method should be generalized to any type of geodesic in an arbitrary spacetime, including null and time-like geodesics in the Kerr spacetime and those in the binary black hole systems. Nevertheless, the method that is currently used is designed for a shortest geodesic in space with a Riemannian metric. In a manifold with pseudo-Riemannian metric, where it could be completely different, the space-like geodesic is locally shortest curve and time-like geodesic is locally longest curve, while null geodesic is indefinite due to the indefinite property of the metric. As mentioned, we must overcome this problem and seek appropriate technique to obtain null geodesics. And a final geodesic equation is also strongly affected by the spacetime embeddings, in which the evolution pattern could be simplified by an appropriate selection of embedding.

In Chapter 5 we look at the problems arising when the 4 dimensional spacetime is embedded in a 5 dimensional pseudo-Euclidean space $\mathbb{R}^{2,3}$. Embedding of the causal relation has been discussed and the solution scheme is proposed. We use conformal embedding instead of isometric embedding to reduce the difficulty of seeking proper transformation and absorb the geometric structure of the black hole spacetime. In addition, the causal structure and null geodesics are preserved by the conformal map as expected. Local and global embeddings are working in this project but the map selected in either approach should cover at least the region outside the event horizon for an astrophysical problem including radiative transfer in the dynamical spacetime. We investigate the embeddings for both Schwarzschild and Kerr spacetimes and briefly analyze the difference between them, where the latter one is more difficult to carry out due to lack of symmetry. In the case of the Schwarzschild spacetime, it is promising to find an explicit embedding into $\mathbb{R}^{2,3}$. We work out, in partial, an implicit embedding and convert all information into a conformal function $\Lambda$ and reduce the number of PDEs. Nevertheless, the results are not completed, particularly in mapping selection. Apparently we need further mathematical techniques, which are to complement the whole procedure of construction. Causal structure recovery is critical as otherwise one cannot prove that a null geodesic is a null geodesic even if it is derived from the calculations. This is one of the core schemes in the whole process (the other one is the geodesic derivation). The trivial case of Minkowskian spacetime can be borrowed to make a simple demonstration which is an embedding from $\mathbb{L}^4$ in $\mathbb{R}^{2,3}$. This method leads to some interesting consequences, one of which is the property of extra coordinate. Intuitively, as discussed in the main context, it is a time-like coordinate since one expects that null geodesics evolve along that direction, and the extra coordinate is treated as a dummy parameter even if it is a time-like coordinate. Nevertheless, the idea of this method could be an open field and may have applications in other areas for future research.

In the sixth Chapter, we investigate the Brill-Lindquist initial data obtained by solving the constraint equations from the Hamiltonian formulation of the general relativity. The 4+1 method that is constructed previously in the fourth Chapter is applied to a generalized fake evolution

Brill-Lindquist data. The 3+1 fake Brill-Lindquist spacetime is embedded in a 5 dimensional space with a given 5 dimensional metric. The Lorentz structure is recovered for the discrete spacetime within the vertical spacetime $\Phi(\mathcal{M})$. It is proven that this method is applicable to any of the spacetime described by the discrete data, including those derived from the 3+1 numerical relativity approach.

The 7th Chapter demonstrates how we can embed the 4 dimensional manifold in a 5 dimensional manifold with the Lorentz structure being maintained, which correlates adjacent foliations. The proofs of the existence and non-uniqueness of the embedding are given.

In the Chapter 8, we briefly reviewed the fundamental knowledge of the numerical relativity developed in the last few decades. We start from the conformal decomposition and then discuss the construction of the initial condition. The choice of adapted coordinate is given and finally the BSSN evolution scheme is introduced. Equipped with the mathematical tool, we calculate the metric of the equal-mass non-spinning binary black hole spacetime and embed it in a 5 dimensional manifold with an appropriately-chosen 5 dimensional metric. Lorentz structure is recovered by the method introduced in the fourth Chapter. We show in detail how to manipulate the discrete data from the 3+1 numerical relativity and how one can derive corresponding 5 dimensional quantities. The null geodesics can be derived by obtaining a level set equation and resolving it, using a specific algorithm. We then define the level set equation and assign different implications for the terms in that equation, which is now an equation governing the propagation of the wave-front of photon in the 5 dimensional manifold. The photon goes through each 4 dimensional slice. We will have to find out a specific numerical method to solve the equation and the appropriate algorithm may require extra conditions. Currently we are working on this. A plausible research plan to achieve this goal would be: We will demonstrate with the Minkowskian manifold first and then generalize to a more complicated case, the Schwarzschild spacetime. The results are carried out and compared to that derived by the normal 4 dimensional way. Finally, we will work with the binary black hole merger and derive a null geodesic where the photon is emitted from the near field region of a binary black hole merger (while they are coalescing) to the distant observer on earth.

## 9.2 Discussions

We in the thesis do not aim to enhance or develop the mature formulation of the numerical relativity, whereas we are trying to overcome certain problems that are encountered in deriving the null geodesics in the strong gravitational field regime, and constructing a more appropriate way of solving for the null path, hence is appropriate for a covariant radiative transfer formulation in dynamical spacetime. The discovery of the gravitational waves in 2015 opens a new era for astrophysics, it also leads to the demanding of the reception of EM counterpart from the gravitational source. Hence, the construction of a covariant formulation of radiation transport in dynamical spacetime is necessary for the field. However, as we have discussed in the previous context, the 3+1 numerical relativ-

ity is incapable of obtaining an accurate enough null geodesic emitting from the rapidly changing gravitational area, where information would lost during the numerical calculation. The level set method would be a good aid for maintaining the spacetime structure while propagating the photon, by solving the level set equation which governs the wave-front evolution in the higher dimensional manifold.

With the help of this formulation, one can propagate the photon wave-front along the extra dimension without losing information of geometry and particle. All these constructions are based on the 3+1 formulation of relativity, the isometric embedding and the level set approach. We might be able to generalize the formulation to other physical theory.

# Chapter 10

# Directions for Future Work

## 10.1 Mathematical Completion of the Embedding Process

As we have shown in the main context, the embedding formalism is not completed (Chapter 5). We need further to consider the possibility of embedding a 4 dimensional Lorentzian manifold in a higher dimensional manifold.

As is discussed in the thesis, an embedding of the Schwarzschild spacetime in a higher dimensional flat manifold is carried out, the isometric embedding for the Kerr metric has not developed good enough. Currently, we only know a 9 dimensional embedding for the Kerr spacetime. However, consider the axisymmetry feature, this condition might be reduced to lower dimensional manifold, which will remain as a potential question and requires further investigation.

The embedding process for a 4 dimensional Lorentzian manifold in a 5 dimensional generic pseudo-Riemannian manifold is proposed in this thesis, where the Lorenz structure correlating adjacent foliations is recovered. The metric form given in the main context is highly specific and by no means the generic form of an expectation metric. Hence, the following proof which depends on this fact should be generalized. We might want to ask if this is doable? The answer at the moment is not clear enough. Nevertheless, based on the non-uniqueness of the embedding formalism, we might hypothetically hold a positive perspective on this, which leads to a yes answer. Furthermore, the extension of embedding for a specific type of dynamical spacetime (e.g., binary black hole) might be considered as well. Finally, the non-uniqueness of the embedding is not completed (if the large family of embeddings can form a group? How many parameters we can introduce to this family, except for the $\Theta$?) and a more general form of the 5 dimensional metric and its generalization to the time-dependent metric components should be derived in the future. Nevertheless, the embeddings together with their generalisation found in this research are new and important, which have not been found in other research.

## 10.2 Direct Quantitative Comparison of Results Computed by the 4+1 Method and the 3+1 Numerical Relativity

We compare the difference of the 3+1 numerical relativity and the newly proposed 4+1 formulation. It should be noted that the purpose of the thesis is not to replace the original 3+1 method in manipulating the complicated structure of dynamical spacetime. Whereas to find an appropriate computational algorithm for propagating photons in the highly dynamical spacetimes when the 3+1 numerical relativity is incapable of this work.

As mentioned in the main text, lacking of enough Killing vector may lead to non-integrability of the geodesic equation [342, 343]. Furthermore, the discreteness feature of 3+1 method results in its own defect (e.g., the interpolation of data might lead to inaccurate in photon trajectory). The chaos problem can either from the physical theory or the numerical calculation, where further investigation is required.

## 10.3 Extension of the Formulation to Other Physical Theories

We have not discussed this topic in the main context. However, the possibility of generalizing the 4+1 method to other physical fields. For example, the unification of the electromagnetic field and the gravitational filed might be worked out in the background of the $\mathbb{R}^{2,3}$ Euclidean space, or a more generic Riemannian manifold where two dimensions are time-like, where the Maxwell tensor can be unified with the metric tensor in one matrix form.

As is discussed by Kaluza and Klein, the magnetic and gravitational fields can be reconciled in a unified formulation within a 5 dimensional theory. In their proposal, the two fundamental forces (interactions) are rewritten in a single metric form. However, in their initial paper, the extra dimensional was introduced as a spatial one, in this project we demand a different temporal dimensional instead, which leads to different physical consequence and mathematical formulation.

An extra time-like dimension might be of physical interest and currently most research are dedicated to building up higher dimensional theories with extra space-like rather than time-like dimensions. Nevertheless, a time-like dimensional has more significance than just a physical 'time'. Mathematician has discovered that when people are trying to isometrically embed a Riemannian manifold into a higher dimensional space, a time-like dimension might be able to help absorb the curved geometric structure and do better work than a space-like dimension [344, 345]. This remains an open question to the physical and mathematical communities.

# Appendix A

# Differential Geometry

Differential geometry [346] is one of the main mathematical tools throughout the whole project. This is foundation for general relativity so will be applied frequently in this thesis [347]. In addition to the basic aspects introduced in the appendix, more advanced topics are involved, including 3+1 foliation of a pseudo-Riemannian manifold [19] and geometric flow [348]. The former one is one of the core techniques to derive null geodesics, and the second one can be used to rebuild local Lorentz structure, i.e., the local causal structure in higher dimensional space (5 dimensional pseudo-Euclidean space and 5 dimensional pseudo-Riemannian manifold).

The topology of a non-empty set $\mathcal{X}$, denoted by $\hat{\mathcal{T}}$, consists of a certain number of subsets of $\mathcal{X}$, such that

$$
\begin{aligned}
&(a)\ \mathcal{X}\,, \varnothing \in \hat{\mathcal{T}}\,,\\
&(b)\ \text{If } \mathcal{O}_i \in \hat{\mathcal{T}}\,,\ i = 1\,, 2\,, \cdots, n\,,\ \text{then } \bigcap_{i=1}^{n} \mathcal{O}_i \in \hat{\mathcal{T}}\,,\\
&(c)\ \text{If } \mathcal{O}_\alpha \in \hat{\mathcal{T}}\,,\ \forall\ \alpha\,,\ \text{then } \bigcup_{\alpha} \mathcal{O}_\alpha \in \hat{\mathcal{T}}\,.
\end{aligned}
$$

Given the topology $\hat{\mathcal{T}}$, set $\mathcal{X}$ is called a topological space, denoted by $(\mathcal{X}, \hat{\mathcal{T}})$. A subset $\mathcal{O}$ of $\mathcal{X}$ is called an open subset (or open set), if $\mathcal{O} \in \hat{\mathcal{T}}$.

A subset $Nei \subset \mathcal{X}$ is said to a neighbourhood of $x$, if $\exists\ \mathcal{O} \in \hat{\mathcal{T}}$ such that $x \in \mathcal{O} \subset Nei$. $Nei$ is called an open set if $Nei \in \hat{\mathcal{T}}$.

A set $\mathcal{C} \subset \mathcal{X}$ is called a closed set if $\mathcal{X} - \mathcal{C}$ is an open set. A closed set satisfies the following properties

$$
\begin{aligned}
&(a)\ \mathcal{X}\,,\ \varnothing \in \text{ closed sets},\\
&(b)\ \text{If } \mathcal{C}_i \text{ are closed sets, } i = 1\,,\ 2\,,\ \cdots\,,\ n\,,\ \text{then } \bigcup_{i=1}^{n} \mathcal{C}_i \text{ is closed set},\\
&(c)\ \text{If } \mathcal{C}_\alpha \text{ are closed sets, then } \bigcap_{\alpha} \mathcal{C} \text{ is closed set.}
\end{aligned}
$$

Suppose $(\mathcal{X}, \hat{\mathcal{T}})$ is a topological space, $\mathcal{A} \subset \mathcal{X}$. The closure of $\mathcal{A}$ is defined as

$$
\bar{\mathcal{A}} := \bigcap_{\alpha} \mathcal{C}_\alpha\,, \tag{A.0.1}
$$

where $\mathcal{A} \subset \mathcal{C}_\alpha$, and $\mathcal{C}_\alpha$ are closed sets.

The interior of $\mathcal{A}$ is

$$i(\mathcal{A}) := \bigcup_{\alpha} \mathcal{O}_\alpha \,, \tag{A.0.2}$$

where $\mathcal{O}_\alpha \subset \mathcal{A}$, and $\mathcal{O}_\alpha \subset \hat{\mathcal{T}}$.

The boundary of $\mathcal{A}$ is defined as

$$\dot{\mathcal{A}} := \bar{\mathcal{A}} - i(\mathcal{A}) \,. \tag{A.0.3}$$

A point $x \in \dot{\mathcal{A}}$ is called a boundary point. $\dot{\mathcal{A}}$ can also be denoted by $\partial\mathcal{A}$.

Some useful corollaries are given here without proof,

$$\begin{aligned} &① \ \bar{\mathcal{A}} \text{ is closed. } \mathcal{A} \subset \bar{\mathcal{A}} \,.\, \mathcal{A} = \bar{\mathcal{A}} \iff \mathcal{A} \text{ is closed.} \\ &② \ i(\mathcal{A}) \in \hat{\mathcal{T}} \,.\, i(\mathcal{A}) \subset \mathcal{A} \,.\, i(\mathcal{A}) = \mathcal{A} \iff \mathcal{A} \subset \hat{\mathcal{T}} \,. \\ &③ \ \partial\mathcal{A} \text{ is closed.} \end{aligned} \tag{A.0.4}$$

A homeomorphism is a map between two topological spaces $(\mathcal{X}, \hat{\mathcal{T}})$ and $(\mathcal{Y}, \mathcal{P})$, $f : \mathcal{X} \to \mathcal{Y}$, such that $f$ is one-to-one and onto, the inverse $f^{-1}$ and $f$ are continuous maps. Herein, we denote differentiability by $C^r$, i.e., $C^0$ represents continuity, $C^\infty$ represents infinitely differentiable and continuous (referred to as smooth), similar rules hold for $C^r$.

A set $\{\mathcal{O}_\alpha\}$, consists of some open sets of $\mathcal{X}$, is called an open cover for $A \subset \mathcal{X}$, if $A \subset \bigcup_{\alpha} \mathcal{O}_\alpha$.

An $n$ dimensional smooth manifold $\mathcal{M}$ is a topological space, abbreviated as $n$ dimensional manifold, if $\mathcal{M} \subset \{\mathcal{O}_\alpha\}$, such that

$$(a) \ \forall \ \mathcal{O}_\alpha \,, \ \exists \text{ homeomorphisms } \psi_\alpha : \ \mathcal{O}_\alpha \to \mathcal{O'}_\alpha \,, \tag{A.0.5}$$

$$(b) \text{ If } \mathcal{O}_\alpha \cap \mathcal{O}_\beta \neq \varnothing \,, \text{ then the composition } \psi_\beta \circ {\psi_\alpha}^{-1} \text{ is } C^\infty, \tag{A.0.6}$$

where $\mathcal{O'}_\alpha$ is an open ball in $\mathbb{R}^n$. $(\mathcal{O}_\alpha, \psi_\alpha)$ constitute the coordinate systems, $\mathcal{O}_\alpha$ are the coordinate patches. The coordinate system is referred to as $x^\mu$ in the main and following context unless otherwise specified. The transition function $\psi_\beta \circ {\psi_\alpha}^{-1}$ is given by

$$(x^1, \cdots, x^n) = \psi_\beta \circ {\psi_\alpha}^{-1}(y^1, \cdots, y^n) \,, \tag{A.0.7}$$

where $x^\mu$ and $y^\mu$ are coordinates of $(\mathcal{O}_\beta, \psi_\beta)$ and $(\mathcal{O}_\alpha, \psi_\alpha)$ respectively. Equation (A.0.7) implies that transition function actually consists of n $n$ dimensional real functions $x^\mu = (\psi_\beta \circ {\psi_\alpha}^{-1})^\mu(y^1, \cdots, y^n)$, where $\forall \ \mu \in \mathbb{N}, \ 1 \leqslant \mu \leqslant n$. The $C^\infty$ property requires that these functions are infinitely differentiable with respect to $y^\nu$, $\forall \ \nu \in \mathbb{N}, \ 1 \leqslant \nu \leqslant n$. For simplicity, $(x^\mu)$ denotes coordinate system for most cases throughout this thesis.

A manifold $\mathcal{M}$ is said to be diffeomorphic to manifold $\mathcal{N}$, if $\exists \ \phi : \mathcal{M} \to \mathcal{N}$, such that $\phi$ is one-to-one and onto, $\phi^{-1}$ and $\phi$ are $C^\infty$. $\phi$ is a diffeomorphism map (or diffeomorphism) from $\mathcal{M}$ to $\mathcal{N}$. Two manifolds which are diffeomorphic to each other can be regarded as equivalent in geometrical perspective. Furthermore, $\mathcal{M}$ is diffeomorphic to $\mathcal{N} \iff \dim\mathcal{M} = \dim\mathcal{N}$. In (A.0.6) the requirement in $(a)$ is actually diffeomorphism instead of homeomorphism, since diffeomorphism is a relation between manifolds whereas at that time the concept has not been introduced.

A function, or a scalar field, on $\mathcal{M}$ is a map $f:\ \mathcal{M}\to\mathbb{R}$. In general, one wants that $f$ is a smooth function. The set of all smooth functions is denoted by $\mathcal{F}_{\mathcal{M}}$.

A map $v:\ \mathcal{F}_{\mathcal{M}}\to\mathbb{R}$ is defined as a vector at $p\in\mathcal{M}\,,\ \forall\ f\,,\ g\in\mathcal{F}_{\mathcal{M}},$ and $\zeta_1\,,\ \zeta_2\in\mathbb{R}$, such that

$$(a)\ \text{Linearity}:\ v(\zeta_1 f+\zeta_2 g)=\zeta_1 v(f)+\zeta_2 v(g)\,, \tag{A.0.8}$$

$$(b)\ \text{Leibniz rule}:\ v(fg)=f|_p\cdot v(g)+v(f)\cdot g|_p\,, \tag{A.0.9}$$

where $f|_p$ is the value of $f(p)\,,\ fg$ is the product of $f|_p$ and $g|_p$. The set of all vectors at $p$ forms a vector space (or tangent space) at $p$, denoted by $\mathcal{T}_p$. Note that $\dim\mathcal{T}_p=\dim\mathcal{M}$.

Assigning a vector to each point of a manifold $\mathcal{M}$ will define a vector field $\mathcal{T}(\mathcal{M})$ on $\mathcal{M}$. $\mathcal{T}(\mathcal{M})$ is $C^\infty$ if $\forall\ v\in\mathcal{T}(\mathcal{M})$ acts on $C^\infty$ functions yielding $C^\infty$ functions, $\mathcal{T}(\mathcal{M})$ is $C^r$ if $\forall\ v\in\mathcal{T}(\mathcal{M})$ acts on $C^\infty$ functions yielding $C^r$ functions.

The union of vector spaces at all points of a manifold is called the tangent bundle, denoted by $\mathcal{T}_{\mathcal{M}}=\cup_{p\in\mathcal{M}}\mathcal{T}_p$.

Given a coordinate system $x^\mu$ and a point $p$, a vector $v\in\mathcal{T}_p$ can be decomposed in the following way

$$v=v^\mu(x)\frac{\partial}{\partial x^\mu}\Big|_p\,, \tag{A.0.10}$$

where $v^\mu$ is the $\mu$-th component of $v$, depending on $x^\mu$. $\partial/\partial x^\mu$ constitute a basis for the vector space. Herein, Einstein summation convention is adopted, i.e., any two repeated upper and lower indices trigger contraction. We will apply this convention throughout this thesis unless otherwise specified.

The transformation law of vector components between any two coordinate systems $x^\mu$ and $x'^\mu$ is given by

$$v^\mu(x)=\frac{\partial x^\mu}{\partial x'^\nu}v'^\nu(x')\,, \tag{A.0.11}$$

where $\forall\ x\,,\ x'\in\mathcal{O}_\mu\cap\mathcal{O}_\nu\,,\ v^\mu$ and $v'^\nu$ are components of a vector $v$ in vector field $\mathcal{T}(\mathcal{O}_\mu\cap\mathcal{O}_\nu)$ in coordinate systems $x^\mu$ and $x'^\nu$ respectively. Equation (A.0.11) is also known as the general coordinate transformation in general relativity.

A dual vector (or covector) at $p$ is a linear map $w:\ \mathcal{T}_p\to\mathbb{R}$, such that

$$w(\zeta_1 v+\zeta_2 u)=\zeta_1 w(v)+\zeta_2 w(v)\,, \tag{A.0.12}$$
$$\forall\ v\,,\ u\in\mathcal{T}_p\,,\quad \zeta_1\,,\ \zeta_2\in\mathbb{R}\,.$$

The covector space $\mathcal{T}^*{}_p$, covector field $\mathcal{T}^*(\mathcal{M})$ and the cotangent bundle $\mathcal{T}^*{}_{\mathcal{M}}$ can be defined in a similar manner as what we have done for vectors. Similarly, the general coordinate transformation for covector is given by

$$w_\mu(x)=\frac{\partial x'^\nu}{\partial x^\mu}w'{}_\nu(x')\,, \tag{A.0.13}$$

where $w_\mu$ and $w'{}_\nu$ are components of $w$ in $x^\mu$ and $x'^\nu$ respectively.

Suppose $I \subset \mathbb{R}$ is an interval, a $C^r$ map $C: I \to \mathcal{M}$ is defined as a $C^r$ curve on $\mathcal{M}$. For any $t \in I$, there exists a unique point $p$ on $\mathcal{M}$, such that $C(t) = p$, $t$ is the parameter of the curve $C$.

Consider a $C^1$ curve $C(t)$ on $\mathcal{M}$, a vector $T$ at $C(t_0)$ is a tangent vector to $C(t)$, defined as

$$T(f) := \left.\frac{\mathrm{d}(f \circ C)}{\mathrm{d}t}\right|_{t_0}, \quad \forall\ f \in \mathcal{F}_{\mathcal{M}}\,. \tag{A.0.14}$$

In this thesis, we use notation $\mathrm{d}/\mathrm{d}t$ to denote the tangent $T$. In a given coordinate system $x^\mu$, $T$ can be rewritten as

$$T = \frac{\mathrm{d}}{\mathrm{d}t} = \frac{\mathrm{d}x^\mu}{\mathrm{d}t}\frac{\partial}{\partial x^\mu}\,. \tag{A.0.15}$$

More explicitly, $\mathrm{d}x^\mu/\mathrm{d}t$ is $\mathrm{d}x^\mu(t)/\mathrm{d}t$, where the n $x^\mu(t) = \psi^\mu \circ C(t)$ are maps from $I \in \mathbb{R}$ to $\mathbb{R}$.

If the tangent to a curve coincides with $v^a$ of a vector field at every point on that curve, then the curve is called the integral curve of the vector field $v^a$, such that

$$\frac{\partial x^\mu}{\partial \tau} = v^\mu\,. \tag{A.0.16}$$

Suppose $(\mathcal{O}, \psi)$ is a coordinate system with coordinate $x^\mu$, the subset of $\mathcal{O}$

$$\{p \in \mathcal{O} \mid x^\nu(p) = \psi^\nu(p)\,,\ x^1(p) = c_1\,,\ \cdots,\ x^n(p) = c_n\}\,, \tag{A.0.17}$$

where $\nu$ is an integer, running from 1 to $n$, and $c_1\,, \cdots, c_n$ are constants. This subset can be considered as a curve parameterized by coordinate $x^\nu$ (here $x^\nu$ only represents one coordinate, not the whole system), called the coordinate line, $\partial/\partial x^\nu$ is the tangent to this curve.

A tensor of type $(k, l)$ at $p$ is a multi-linear map acting on $k$ covectors and $l$ vectors

$$T: \underbrace{\mathcal{T}^* \times \cdots \times \mathcal{T}^*}_{k} \times \overbrace{\mathcal{T} \times \cdots \times \mathcal{T}}^{l} \to \mathbb{R}\,. \tag{A.0.18}$$

The tensor space of type $(k, l)$ is denoted by $\mathcal{T}_p(k, l)$, $\dim\mathcal{T}_p(k, l) = n^{k+l}$, where $n$ is the dimension of $\mathcal{M}$. $\mathcal{T}_{\mathcal{M}}(k, l)$ is the tensor field on $\mathcal{M}$, note that this is different from the tangent bundle $\mathcal{T}_{\mathcal{M}}$.

With (A.0.11) and (A.0.13), one can construct the general coordinate transformation of a type $(k, l)$ tensor $T$, yielding

$$\begin{aligned} T^{\mu_1\cdots\mu_k}{}_{\nu_1\cdots\nu_l}(x) = \\ \frac{\partial x^{\mu_1}}{\partial x'^{\mu'_1}}\cdots\frac{\partial x^{\mu_k}}{\partial x'^{\mu'_k}}\frac{\partial x'^{\nu'_1}}{\partial x^{\nu_1}}\cdots\frac{\partial x'^{\nu'_l}}{\partial x^{\nu_l}} T'^{\mu'_1\cdots\mu'_k}{}_{\nu'_1\cdots\nu'_l}(x')\,, \end{aligned} \tag{A.0.19}$$

where $T^{\mu_1\cdots\mu_k}{}_{\nu_1\cdots\nu_l}$ and $T'^{\mu'_1\cdots\mu'_k}{}_{\nu'_1\cdots\nu'_l}$ are components of $T$ in coordinate systems $x$ and $x'$ respectively.

The symmetric part and anti-symmetric part of a tensor $T_{\mu_1\cdots\mu_l}$ are given by

$$T_{(\mu_1\cdots\mu_l)} := \frac{1}{l!}\sum_{\pi} T_{\mu_{\pi(1)}\cdots\mu_{\pi(l)}}\,, \tag{A.0.20}$$

$$T_{[\mu_1\cdots\mu_l]} := \frac{1}{l!}\sum_{\pi} \delta_\pi T_{\mu_{\pi(1)}\cdots\mu_{\pi(l)}}\,, \tag{A.0.21}$$

where $\pi$ represents a permutation of $(1,\cdots,l)$. $\delta_\pi = \pm 1$ ($+$ for even permutation, $-$ for odd permutation).

A covariant derivative $\nabla$ on manifold $\mathcal{M}$ is a map, $\nabla : \mathcal{T}_{\mathcal{M}}(k,l) \to \mathcal{T}_{\mathcal{M}}(k,l+1)$, which satisfies properties given as follow

($a$) Linearity :

$$\nabla_\mu(\zeta_1 T^{\sigma_1\cdots\sigma_k}{}_{\nu_1\cdots\nu_l} + \zeta_2 R^{\sigma_1\cdots\sigma_k}{}_{\nu_1\cdots\nu_l}) = \zeta_1\nabla_\mu T^{\sigma_1\cdots\sigma_k}{}_{\nu_1\cdots\nu_l} + \zeta_2\nabla_\mu R^{\sigma_1\cdots\sigma_k}{}_{\nu_1\cdots\nu_l}\,, \tag{A.0.22}$$

$$\forall\ T^{\sigma_1\cdots\sigma_k}{}_{\nu_1\cdots\nu_l}\,,\ R^{\sigma_1\cdots\sigma_k}{}_{\nu_1\cdots\nu_l} \in \mathcal{T}_{\mathcal{M}}(k,l)\,,\quad \zeta_1\,,\ \zeta_2 \in \mathbb{R}\,,$$

($b$) Leibnitz rule :

$$\nabla_\mu(TR) = T\nabla_\mu R + R\nabla_\mu T\,, \tag{A.0.23}$$

$$\forall\ T \in \mathcal{T}_{\mathcal{M}}(k,l)\,,\ R \in \mathcal{T}_{\mathcal{M}}(k',l')\,,$$

($c$) Commutative with contraction,

($d$) $v^\mu\nabla_\mu f = v(f)\,,\ \forall\ v \in \mathcal{T}(\mathcal{M})\,,\ \forall\ f \in \mathcal{F}_{\mathcal{M}}\,,$ (A.0.24)

($e$) Torsion free :

$$\nabla_\mu\nabla_\nu f = \nabla_\nu\nabla_\mu f\,,\ \forall\ f \in \mathcal{F}_{\mathcal{M}}\,. \tag{A.0.25}$$

Property ($c$) implies $\nabla_\nu(T^\mu R_\mu) = T^\mu\nabla_\nu R_\mu + \nabla_\nu T^\mu R_\mu$. Property ($d$) leads to $\nabla_a f = (\mathrm{d}f)_a$ ($a$ is an abstract index, see the abstract index part). The covariant derivative is not unique on a manifold, any two of them, $\nabla$ and $\nabla'$, can be correlated in the following coordinate-independent manner

$$\nabla_\mu w_\nu = \nabla'_\mu w_\nu - C_{\mu\nu}{}^\sigma w_\sigma\,, \tag{A.0.26}$$

where $C_{\mu\nu}{}^\sigma$ is a type $(1,2)$ tensor, symmetric between two lower indices $\mu$ and $\nu$, $\forall\ w \in \mathcal{T}^*(\mathcal{M})$. We also have

$$\nabla_\mu v^\nu = \nabla'_\mu v^\nu + C_{\mu\gamma}{}^\nu v^\gamma\,, \tag{A.0.27}$$

where $\forall\ v \in \mathcal{T}(\mathcal{M})$. Hence one can obtain the action of $\nabla$ on an arbitrary type $(k,l)$ tensor, such that

$$\nabla_\gamma T^{\mu_1\cdots\mu_k}{}_{\sigma_1\cdots\sigma_l} = \nabla'_\gamma T^{\mu_1\cdots\mu_k}{}_{\sigma_1\cdots\sigma_l} - \sum_i C_{\gamma\nu}{}^{\mu_i} T^{\mu_1\cdots\nu\cdots\mu_k}{}_{\sigma_1\cdots\sigma_l} + \sum_j C_{\gamma\sigma_j}{}^{\nu} T^{\mu_1\cdots\mu_k}{}_{\sigma_1\cdots\nu\cdots\sigma_l}\,, \tag{A.0.28}$$

where $i\,,\ j$ are integers, running from 1 to $k$ and 1 to $l$ respectively.

A very important tensor in general relativity is the metric tensor, which is a symmetric non-degenerate type $(0,2)$ tensor $g$. Consider its components $g_{\mu\nu}$ in a coordinate system, symmetric property implies that $g_{\mu\nu} = g_{\nu\mu}$, and non-degenerate property implies that $g_{\mu\nu}$ has a non-zero determinant. Two vectors are said to be orthogonal to each other if $g_{\mu\nu}v^\mu u^\nu = 0$. A non-coordinate basis $e_\mu$ is said to be orthonormal (this is true at least in a sufficiently small region), if $g(e_\mu, e_\mu) = 0$, and

$g(e_\mu, e_\nu) = \pm 1$ for any $\mu \neq \nu$. In this sense, $g(u, v)$ can be treated as the inner product of vectors $u$ and $v$ under the action of $g$.

Given an orthonormal basis, the components of $g$ can be expressed readily by a diagonal matrix. The diagonal elements for a positive (negative) definite metric are all $+1$, the rest are indefinite metrics with r $+1$ elements and n-r $-1$ elements. A Lorentzian metric has only one $-1$ diagonal element. The signature of a metric is the value of sum of all diagonal elements, for a positive definite metric it is $n$, for a Lorentzian metric it is $n - 2$. This is sometimes represented by means of the signs of diagonal elements in a row vector, for example $(-, +, +, +)$ for a 4 dimensional Lorentzian metric.

With the Lorentzian metric, all vectors in a vector space $\mathcal{T}_p$ can be divided into three categories, given by

$$\text{(1) } v^\mu \text{ is space-like} \iff g_{\mu\nu} v^\mu v^\nu > 0\,, \tag{A.0.29}$$

$$\text{(2) } v^\mu \text{ is null} \iff g_{\mu\nu} v^\mu v^\nu = 0\,, \tag{A.0.30}$$

$$\text{(3) } v^\mu \text{ is time-like} \iff g_{\mu\nu} v^\mu v^\nu < 0\,, \tag{A.0.31}$$

where $\forall\ v^\mu\,,\ v^\nu \in \mathcal{T}_p$.

The inverse of metric $g$ is defined as

$$g^{\mu\nu} g_{\nu\gamma} = \delta^\mu{}_\gamma\,. \tag{A.0.32}$$

A manifold $\mathcal{M}$ with a positive definite metric $g$ is called a Riemannian space, whilst a manifold with a Lorentzian metric is called a pseudo-Riemannian space or spacetime in physics (4 dimension in general), written as $(\mathcal{M}, g)$.

In general relativity, we are interested in metric adapted covariant derivative, such that

$$\nabla_\mu g_{\nu\sigma} = 0\,. \tag{A.0.33}$$

This relation is adopted throughout this thesis unless otherwise specified.

The metric may also be expressed as

$$\mathrm{d}s^2 = g = g_{\mu\nu} \mathrm{d}x^\mu \mathrm{d}x^\nu\,, \tag{A.0.34}$$

where $\mathrm{d}s^2$ is called the line element. The length of a line on a manifold $\mathcal{M}$ with metric $g$ is defined as

$$l := \int_{\tau_0}^{\tau} \sqrt{|g(T, T)|}\mathrm{d}\tau = \int \sqrt{|\mathrm{d}s^2|}\,, \tag{A.0.35}$$

where $\tau$ denotes parameter of that line and $T$ denotes the tangent vector. Specifically, for a time-like wordline in spacetime $(\mathcal{M}, g)$, the length of a time-like curve is given as

$$l = \int \sqrt{-\mathrm{d}s^2}\,. \tag{A.0.36}$$

For a null wordline, $l$ always vanishes due to $g(T_{null}, T_{null}) = 0$.

The proper time $\tau$ of a particle or an observer is given by

$$\tau_1 - \tau_2 = \int_{p_2}^{p_2} \sqrt{-\mathrm{d}s^2}\,, \tag{A.0.37}$$

where $\tau_1$ and $\tau_2$ are values of proper time at point $p_1$ and $p_2$ on the worldline. An observer's worldline is a time-like curve with unity tangent.

The 4 dimensional velocity $U^\mu$ of a particle or an observer is defined as the tangent vector to the worldline, with parameter being the proper time

$$U^\mu = \frac{\partial}{\partial \tau}\,, \qquad g(U,U) = -1\,. \tag{A.0.38}$$

We denote an observer by $(p, \tilde{Z}^\mu)$ where $p$ is the point on the observer's worldline, and $\tilde{Z}^\mu$ is the 4 dimensional velocity. We can decompose a series of 4 dimensional vector by means of an observer's 4 dimensional velocity.

A 1+3 decomposition of a particle's 4 dimensional velocity $U^\mu$ with respect to observer $(p, \tilde{Z}^\nu)$ is given by

$$U^\mu = -U^\nu \tilde{Z}_\nu(\tilde{Z}^\mu + u^\mu)\,, \tag{A.0.39}$$

where $u^\mu$ denotes the 3 dimensional velocity of the particle measured by observer.

The 4 dimensional acceleration of a particle with 4 dimensional velocity $U^\mu$ is defined as

$$A^\mu := U^\nu \nabla_\nu U^\mu\,. \tag{A.0.40}$$

$A^\mu$ is orthogonal to $U^\mu$ since $U_\mu U^\nu \nabla_\nu U^\mu = U^\nu \nabla_\nu (U_\mu U^\mu)/2 = 0$. $A^\mu = 0$ yields geodesic motion. A 1+3 decomposition of the 4 dimensional acceleration is complicated and is less likely to be used in this thesis, thereof we neglect it here.

The 4 dimensional momentum of a particle with rest mass $m$ and 4 dimensional velocity $U^\mu$ is

$$P^\mu := mU^\mu\,. \tag{A.0.41}$$

The $3+1$ decomposition of $P^\mu$ with respect to $(p, \tilde{Z}^\nu)$ is given by

$$P^\mu = E\tilde{Z}^\mu + {p_3}^\mu\,, \tag{A.0.42}$$

where $E = -P^\mu \tilde{Z}_\mu = mU^\mu \tilde{Z}_\mu$ denotes the energy of a particle in the observer's frame, ${p_3}^\mu := \vec{p}$ is the 3 dimensional momentum of a particle in the observer's frame.

In order to illustrate an abstract tensor by its indices, Penrose introduced the abstract index notation, such that

1. The abstract indices only appears with abstract tensors, not tensor components, denoted by lower-case Latin letters $a\,,\ b\,,\ c\,,\ \cdots$. This implies that the abstract indices only represent the type of the tensors. A type $(k,l)$ tensor has k upper indices and l lower indices.
2. Repeated abstract indices lead to contraction.
3. Lower-case Greek letters $\mu\,,\ \nu\,,\ \cdots$ are used for components of the tensors, these indices are the common indices we used in calculation, one can use concrete number to replace them, for example ${T_2}^1$ accordingly they are called the concrete indices[20].

[20]Note that the $t\,,\ r$ notations for Kerr metric represent concrete coordinates.

With abstract indices notation, a tensor of type $(k, l)$ can be readily written as

$$T^{a_1 a_2 \cdots a_k}{}_{b_1 b_2 \cdots b_l} = T^{\mu_1 \mu_2 \cdots \mu_k}{}_{\sigma_1 \sigma_2 \cdots \sigma_l} (e_{\mu_1})^{a_1} (e_{\mu_2})^{a_2} \cdots (e_{\mu_k})^{a_k} (e^{\sigma_1})_{b_1} (e^{\sigma_2})_{b_2} \cdots (e^{\sigma_l})_{b_l} , \tag{A.0.43}$$

where $(e_{\mu_i})^{a_i}$ and $(e^{\sigma_j})_{b_j}$ denote the bases of vector and covector spaces respectively. The coordinate-dependent bases read $(\partial/\partial x^\mu)^a$ and $(\mathrm{d}x^\mu)_a$. Note that only tensors with the same abstract indices can be added or subtracted, for example $v^a + u^a$ is correct. The contraction of tensors is given by

$$R^a T_a = R^\mu T_\mu \, . \tag{A.0.44}$$

The components of $T$ are given by

$$T^{\mu_1 \cdots \mu_k}{}_{\nu_1 \cdots \nu_l} = T^{a_1 \cdots a_k}{}_{b_1 \cdots b_l} (e^{\mu_1})_{a_1} \cdots (e^{\mu_k})_{a_k} (e_{\nu_1})^{b_1} \cdots (e_{\nu_l})^{b_l} \, . \tag{A.0.45}$$

Particularly, the action of a metric $g_{ab}$ on vectors reads

$$g(v, u) = g_{ab} v^a u^b \, . \tag{A.0.46}$$

Moreover, $g_{ab}$ can be considered as an isomorphic map (one-to-one and onto, preserving the vector space action), $g : \mathcal{T}_p \to \mathcal{T}^*{}_p \ \forall \ p \in \mathcal{M}$, hence one can identify the elements in $\mathcal{T}$ and $\mathcal{T}^*{}_p$ by

$$v_a = g_{ab} v^b \, , \tag{A.0.47}$$

where $v_a \in \mathcal{T}^* \, , \ v^b \in \mathcal{T}_p \, , \ \forall \ p \in \mathcal{M}$. This corresponding relation is one-to-one and onto, guaranteed by isomorphism.

A symmetric or anti-symmetric tensor $T_{ab}$ satisfies

$$\begin{aligned} T_{ab} &= T_{ba} \text{ for symmetric,} \\ T_{ab} &= -T_{ba} \text{ for anti-symmetric.} \end{aligned} \tag{A.0.48}$$

The induced mappings come along with the mappings $\phi$ between manifolds and are induced by these maps $\phi$. Firstly, a pull-back map is defined as $\phi^* : \ \mathcal{F}_\mathcal{M} \ \to \ \mathcal{F}_\mathcal{N}$, such that

$$(\phi^* f)|_p := f|_{\phi(p)} \, , \quad \forall \ f \in \mathcal{F}_\mathcal{N} \, , \ p \in \mathcal{M} \, , \tag{A.0.49}$$

abbreviated as $\phi^* f = f \circ \phi$, where $\phi$ is a map between manifolds $\mathcal{M}$ and $\mathcal{N}$, $f$ is a function on $\mathcal{M}$. $\phi^*$ is a linear map such that

$$\phi^*(\zeta_1 f + \zeta_2 g) = \zeta_1 \phi^*(f) + \zeta_2 \phi^*(g) \, , \ \forall \ f \, , \ g \in \mathcal{F}_\mathcal{N} \, , \ \ \zeta_1 \, , \ \zeta_2 \in \mathbb{R} \, , \tag{A.0.50}$$

and satisfies

$$\phi^*(fg) = \phi^*(f) \phi^*(g) \, , \ \ \forall \ f \, , \ g \in \mathcal{F}_\mathcal{N} \, . \tag{A.0.51}$$

A push-forward map is defined as $\phi_* : \ \mathcal{T}_p \ \to \ \mathcal{T}_{\phi(p)}$, such that

$$(\phi_* v)(f) := v(\phi^* f) \, , \quad \forall \ f \in \mathcal{F}_\mathcal{N} \, , \ p \in \mathcal{M} \, , \tag{A.0.52}$$

where $\forall \ v^a \in \mathcal{T}_p$, its image is $(\phi_* v)^a \in \mathcal{T}_{\phi(p)}$. $\phi_*$ is a linear map, such that

$$\phi_*(\zeta_1 u^a + \zeta_2 v^a) = \zeta_1 (\phi_* u)^a + \zeta_2 (\phi_* v)^a \, , \ \ \forall \ u^a \, , \ v^a \in \mathcal{T}_p \, , \ \ \zeta_1 \, , \ \zeta_2 \in \mathbb{R} \, . \tag{A.0.53}$$

A very useful corollary is that

The image of a tangent to a curve is the tangent to the image of the curve, i.e., $(\phi_* T)^a \in \mathfrak{T}(\phi(C(t_0)))$, where $T^a \in \mathfrak{T}(C(t_0))$, $C$ is a curve parameterized by $t$, $t_0 \in I \subset \mathbb{R}$, $I$ is the interval of curve $C$.

(A.0.54)

If the map $\phi$ is a diffeomorphism [158], for which its inverse map $\phi^{-1}$ exists, the push-forward (as well as the pull-back) map can be generalized to any type of tensors in the following manner, $\phi_* : \mathfrak{T}_{\mathcal{M}}(k,l) \to \mathfrak{T}_{\mathcal{N}}(k,l)$, such that

$$(\phi_* T)^{a_1 \cdots a_k}{}_{b_1 \cdots b_l}|_q v_1{}^{b_1} \cdots v_l{}^{b_l} w^1{}_{a_1} \cdots w^k{}_{a_k} = T^{a_1 \cdots a_k}{}_{b_1 \cdots b_l}|_{\phi^{-1}(q)} (\phi^* v_1)^{b_1} \cdots (\phi^* v_l)^{b_l} (\phi^* w^1)_{a_1} \cdots (\phi^* w^k)_{a_k} , \tag{A.0.55}$$

$$\forall\ q \in \mathcal{N}\,,\ w^i \in \mathfrak{T}^*{}_q\,,\ v_j \in \mathfrak{T}_q\,,$$

where the subscripts of $v$ and superscripts of $w$ are dummy labels, indicating they are distinct tensors. In (A.0.55), $(\phi^* v_j)^{b_j}$ is equivalent to $(\phi^{-1}{}_* v_j)^{b_j}$. Similarly, pull-back maps can be generalized to $\mathfrak{T}(k,l)$ by virtue of $\phi^{-1}$. The pull-back and push-forward maps are known as induced maps which play significant roles in spacetime embedding as well as numerical relativity.

Suppose $\mathcal{W}$ and $\mathcal{M}$ are manifolds, let $\dim\mathcal{W} \leqslant \dim\mathcal{M}$[21]. A map $\phi : \mathcal{W} \to \mathcal{M}$ is called an embedding, such that $\phi$ is one-to-one and $C^\infty$, and $\forall\ p \in \mathcal{W}$, the push-forward map $\phi_*$ is non-degenerate, i.e., $(\phi_* v)^a = 0 \ \Rightarrow\ v^a = 0$, $v^a \in \mathfrak{T}_p$. These properties carry the topological structure of $\mathcal{W}$ onto manifold $\mathcal{M}$, such that $\phi$ is a diffeomorphism. $\phi(\mathcal{W})$ is a submanifold of $\mathcal{M}$, if $\dim\mathcal{W} = n-1$, then $\phi(\mathcal{W}) \subset \mathcal{M}$ is also known as a hypersurface of $\mathcal{M}$.

Suppose $\mathcal{W} \subset \mathcal{M}$ is a hypersurface, $p \in \mathcal{W}$, there exists an $(n-1)$ dimensional vector space $U_p$ at $p$ which is a tangent space in $\mathcal{W}$. With this, one can define the non-zero normal covector $n_a$, such that

$$n_a u^a = 0\,,\quad \forall\ u^a \in U_p\,, \tag{A.0.56}$$

where $n_a \in \mathfrak{T}^*{}_p$, $\mathfrak{T}^*{}_p$ is the cotangent space in $\mathcal{M}$. From the definition we find that a normal covector is orthogonal to any vector in $U_p$.

Given a metric $g_{ab}$ on $\mathcal{M}$, the normal vector can be defined as

$$n^a = g^{ab} n_b\,, \tag{A.0.57}$$

where $n^a \in \mathfrak{T}_p$, $n_b$ is a normal covector to the hypersurface. It can be shown that $n^a$ is orthogonal to all vectors in $U_p$, since $g_{ab} n^a u^b = n_b u^b = 0$, where we have used (A.0.56) in the second equality.

Suppose $f$ is a function on, without loss of generality, a three dimensional manifold $\mathcal{M}$, given different constant values to $f(x,y,z)$ (with $x$, $y$, $z$ the coordinates on $\mathcal{M}$) gives rise to distinct hypersurfaces, denoted by $\mathcal{W}$. We then can prove that $\nabla_a f$ is a normal vector to the surface determined by $f(x,y,z) = con$, where $con$ is a constant.

[21] $\dim\mathcal{W}$ denotes the dimension of manifold $\mathcal{W}$.

The induced metric $h_{ab}$ can be defined by virtue of an embedding map $\phi:\ \mathcal{W}\to\mathcal{M}$, $\mathcal{W}$ is a hypersurface on $\mathcal{M}$, such that

$$h=\phi^{*}g\,, \tag{A.0.58}$$

where $g$ is the metric on $\mathcal{M}$. Induced metric is also known as the first fundamental form of $\mathcal{W}$, or the short-hand name the 3 dimensional metric. Note that

$$g_{ab}u^{a}v^{b}=h_{ab}u^{a}v^{b}\,,\qquad \forall\ u^{a}\,,\ v^{b}\in\mathcal{T}_{p}(\mathcal{W})\,, \tag{A.0.59}$$

where $\forall\ p\in\mathcal{W}\subset\mathcal{M}$. From now on we use $\mathcal{W}$ to denote the hypersurface of $\mathcal{M}$ if this does not cause confusion.

A hypersurface $\mathcal{W}$ is said to be

- space-like if $h$ is positive definite, i.e., has signature $(+,+,+)$, (A.0.60)
- null if $h$ is degenerate, i.e., has signature $(0,+,+)$, (A.0.61)
- time-like if $h$ is Lorentzian, i.e., has signature $(-,+,+)$. (A.0.62)

The Lie derivative of a tensor $T^{a_1\cdots a_k}{}_{b_1\cdots b_l}$ along the vector field $v$ is a linear map $\mathcal{L}_v:\ \mathcal{T}_{\mathcal{M}}(k,l)\to\mathcal{T}_{\mathcal{M}}(k,l)$, given by

$$\mathcal{L}_vT^{a_1\cdots a_k}{}_{b_1\cdots b_l}:=\lim_{t\to0}\frac{1}{t}(\phi_t{}^{*}T^{a_1\cdots a_k}{}_{b_1\cdots b_l}-T^{a_1\cdots a_k}{}_{b_1\cdots b_l})\,, \tag{A.0.63}$$

where $\phi_t{}^{*}$ is a diffeomorphism induced by $v^a$. A theorem states that $\mathcal{L}_vf=v(f)\,,\ \forall\ f\in\mathcal{F}$.

Given a vector field $v^a$ on a manifold $\mathcal{M}$, choose its integral curve as the $x^1$ coordinate line. Then randomly choose a group of lines traverse $x^1$ lines, regard these lines as $x^2$ coordinate line if two tangent vectors at the same intersection point are different. It is natural to generalize this procedure to $n$ dimension, such that they form an $n$ dimensional coordinate system $(x^1,x^2,\cdots,x^n)$, called the adapted coordinate system of $v^a$.

The components of the Lie derivative of $T^{a_1\cdots a_k}{}_{b_1\cdots b_l}$ along $v^a$ in the adapted coordinate system of $v^a$ are given as

$$\mathcal{L}_vT^{\mu_1\cdots\mu_k}{}_{\nu_1\cdots\nu_l}=\frac{\partial T^{\mu_1\cdots\mu_k}{}_{\nu_1\cdots\nu_l}}{\partial x^1}\,. \tag{A.0.64}$$

The explicit expression of the Lie derivative is given by

$$\mathcal{L}_vT^{a_1\cdots a_k}{}_{b_1\cdots b_l}=v^c\nabla_cT^{a_1\cdots a_k}{}_{b_1\cdots b_l}-\sum_{i=1}^{k}T^{a_1\cdots c\cdots a_k}{}_{b_1\cdots b_l}\nabla_cv^{a_i}+\sum_{j=1}^{l}T^{a_1\cdots a_k}{}_{b_1\cdots c\cdots b_l}\nabla_{b_j}v^c\,, \tag{A.0.65}$$

where $\forall\ T\in\mathcal{T}(k,l)\,,\ v\in\mathcal{T}(1,0)$. The Lie derivative is a linear operator, for which satisfies

$$\mathcal{L}_{\zeta_1v+\zeta_2u}T^{a_1\cdots a_k}{}_{b_1\cdots b_l}=\zeta_1\mathcal{L}_vT^{a_1\cdots a_k}{}_{b_1\cdots b_l}+\zeta_2\mathcal{L}_uT^{a_1\cdots a_k}{}_{b_1\cdots b_l}\,, \tag{A.0.66}$$

where $\zeta_1\,,\ \zeta_2\in\mathbb{R}$.

A vector field $\xi^a$ on spacetime $(\mathcal{M},g_{ab})$ is called a Killing vector field, if $\mathcal{L}_\xi g_{ab}=0$. $\xi^a$ satisfies the following equation

$$\nabla_a\xi_b+\nabla_b\xi_a=0\,. \tag{A.0.67}$$

# Appendix B

# Curvature and Christoffel Symbols

Given a coordinate system $x^\mu$, the Christoffel symbol is defined as

$$\nabla_a T_{c_1\cdots c_l}{}^{b_1\cdots b_k} = \partial_a T_{c_1\cdots c_l}{}^{b_1\cdots b_k} + \sum_i \Gamma_{ad}{}^{b_i} T_{c_1\cdots c_l}{}^{b_1\cdots d\cdots b_k} - \sum_j \Gamma_{ac_j}{}^{d} T_{c_1\cdots d\cdots c_l}{}^{b_1\cdots b_k}\,, \tag{B.0.1}$$

where $T$ is a tensor of type $(k,l)$, $\partial_a$ denotes $(\partial/\partial x^\mu)(\mathrm{d}x^\mu)^a$. It is apparently that $\Gamma_{ac}{}^{d}$ is a coordinate-dependent quantity which is referred to as a coordinate-dependent tensor (i.e., not a tensor). Substituting $g_{ab}$ into (B.0.1) and note that covariant derivative is metric adapted, yields

$$\partial_a g_{bc} = \Gamma_{cab} + \Gamma_{bac}\,. \tag{B.0.2}$$

Permuting the three indices, yields

$$\partial_b g_{ac} = \Gamma_{cba} + \Gamma_{abc}\,, \tag{B.0.3}$$

$$\partial_c g_{ab} = \Gamma_{bca} + \Gamma_{abc}\,, \tag{B.0.4}$$

where the upper index of $\Gamma$ has been lowered by $g$. (B.0.3) plus (B.0.2) minus (B.0.4) gives rise to

$$\Gamma_{abc} = \frac{1}{2}(\partial_a g_{bc} + \partial_b g_{ac} - \partial_c g_{ab})\,. \tag{B.0.5}$$

Raising the index with $g^{cd}$, yields

$$\Gamma_{ab}{}^{c} = \frac{1}{2} g^{cd}(\partial_a g_{db} + \partial_b g_{ad} - \partial_d g_{ab})\,. \tag{B.0.6}$$

Christoffel symbol is a symmetric coordinate-dependent tensor between its two lower indices, i.e., $\Gamma_{ab}{}^{c} = \Gamma_{ba}{}^{c}$.

The non-vanishing components of Christoffel symbol for the Kerr met-

ric are given as follow

$$\Gamma_{tr}{}^{t} = \frac{M(r^2+a^2)(2r^2-\Sigma)}{\Sigma^2\Delta}\,, \tag{B.0.7}$$

$$\Gamma_{t\theta}{}^{t} = -\frac{a^2 Mr\sin 2\theta}{\Sigma^2}\,, \tag{B.0.8}$$

$$\Gamma_{r\theta}{}^{t} = -\frac{aM[4r^4-(r^2-a^2)\Sigma]\sin^2\theta}{\Sigma^2\Delta}\,, \tag{B.0.9}$$

$$\Gamma_{\theta\varphi}{}^{t} = \frac{2a^3 Mr\sin^3\theta\cos\theta}{\Sigma^2}\,, \tag{B.0.10}$$

$$\Gamma_{tt}{}^{r} = \frac{M\Delta(2r^2-\Sigma)}{\Sigma^3}\,, \tag{B.0.11}$$

$$\Gamma_{t\varphi}{}^{r} = -\frac{aM\Delta(2r^2-\Delta)\sin^2\theta}{\Sigma^3}\,, \tag{B.0.12}$$

$$\Gamma_{rr}{}^{r} = \frac{\left(1+\frac{\Delta}{\Sigma}\right)r - M}{\Delta}, \tag{B.0.13}$$

$$\Gamma_{r\theta}{}^{r} = -\frac{a^2\sin 2\theta}{2\Sigma} = \Gamma^{\theta}{}_{\theta\theta} = -\frac{\Gamma^{\theta}{}_{rr}}{\Delta}\,, \tag{B.0.14}$$

$$\Gamma_{\theta\theta}{}^{r} = -\frac{r\Delta}{\Sigma} = \Delta\Gamma^{\theta}{}_{r\theta}\,, \tag{B.0.15}$$

$$\Gamma_{\varphi\varphi}{}^{r} = -\frac{\Delta[r\Sigma^2 - a^2M(2r^2-\Sigma)]\sin^2\theta}{\Sigma^3}\,, \tag{B.0.16}$$

$$\Gamma_{tt}{}^{\theta} = -\frac{a^2 Mr\sin 2\theta}{\Sigma^3}\,, \tag{B.0.17}$$

$$\Gamma_{t\varphi}{}^{\theta} = \frac{aMr(r^2+a^2)\sin 2\theta}{\Sigma^3}\,, \tag{B.0.18}$$

$$\Gamma^{\theta}{}_{\varphi\varphi} = -\frac{\sin 2\theta}{2\Sigma^3}\{(r^2+a^2)\Sigma^2 + 2a^2Mr[\Sigma+(r^2+a^2)]\sin^2\theta\}\,, \tag{B.0.19}$$

$$\Gamma_{tr}{}^{\varphi} = \frac{aM(2r^2-\Sigma)}{\Delta\Sigma^2}\,, \tag{B.0.20}$$

$$\Gamma_{t\theta}{}^{\varphi} = -\frac{2aMr\cot\theta}{\Sigma^2}\,, \tag{B.0.21}$$

$$\Gamma_{r\varphi}{}^{\varphi} = \frac{r\Sigma^2 - M[2r^2\Sigma - (2r^2-\Sigma)a^2\sin^2\theta]}{\Delta\Sigma^2}\,, \tag{B.0.22}$$

$$\Gamma_{\theta\varphi}{}^{\varphi} = \cot\theta + \frac{a^2 Mr\sin 2\theta}{\Sigma^2}\,. \tag{B.0.23}$$

All these components reduce to the components of the Schwarzschild metric in the limit of non-rotating object, i.e., $a = 0$, and to the Minkowskian metric in the limit of $a = 0$ and $M = 0$.

The Riemann curvature tensor $R_{abc}{}^{d}$ of $\nabla_a$ is defined as

$$(\nabla_a\nabla_b - \nabla_b\nabla_a)w_c = R_{abc}{}^{d}w_d\,, \tag{B.0.24}$$

or

$$(\nabla_a\nabla_b - \nabla_b\nabla_a)v^c = -R_{abd}{}^{c}v^d\,, \tag{B.0.25}$$

where $w_c \in \mathcal{T}(0,1)$ and $v^c \in \mathcal{T}(1,0)$. Given a coordinate system $x^\mu$, the Riemann curvature can be written as

$$R_{abc}{}^{d} = \partial_b\Gamma_{ac}{}^{d} - \partial_a\Gamma_{bc}{}^{d} + \Gamma_{ca}{}^{e}\Gamma_{be}{}^{d} - \Gamma_{cb}{}^{e}\Gamma_{ae}{}^{d}\,. \tag{B.0.26}$$

There are only two independent contractions of different indices in Riemann curvature tensor. One of them is the Ricci tensor

$$R_{ac} := R_{abc}{}^{b} \,. \tag{B.0.27}$$

The other one is scalar curvature

$$R := g^{ac} R_{ac} \,. \tag{B.0.28}$$

It can be proven that a Riemann tensor satisfies the following identities

$$\begin{aligned}
&(1)\ R_{abc}{}^{d} = -R_{bac}{}^{d} \,, && \text{(B.0.29)}\\
&(2)\ R_{abcd} = -R_{abdc} \,, && \text{(B.0.30)}\\
&(3)\ R_{abcd} = \ \ R_{cdab} \,, && \text{(B.0.31)}\\
&(4)\ \text{Cyclic identity } R_{[abc]}{}^{d} = 0 \,, && \text{(B.0.32)}\\
&(5)\ \text{Bianchi identity } \nabla_{[a} R_{bc]d}{}^{e} = 0 \,. && \text{(B.0.33)}
\end{aligned}$$

The indices are lowered by $g_{ab}$.

When $\dim\mathcal{M} \geq 3$, the Weyl curvature tensor is defined as

$$C_{abcd} := R_{abcd} - \frac{2}{n-2}(g_{a[c} R_{d]b} - g_{b[c} R_{d]a}) + \frac{2}{(n-2)(n-1)} R g_{a[c} g_{d]b} \,. \tag{B.0.34}$$

A Wely tensor has the following properties

$$\begin{aligned}
&(1)\ C_{abcd} = -C_{bacd} = -C_{abdc} = C_{cdab} \,, && \text{(B.0.35)}\\
&(2)\ C_{[abc]d} = 0 \,, && \text{(B.0.36)}\\
&(3)\ \text{Wely tensor is traceless, i.e., } g^{ab} C_{abcd} = C_{cd} = 0 \,,\ g^{ab} C_{ab} = 0 \,. && \text{(B.0.37)}
\end{aligned}$$

Any manifold with a vanishing Weyl tensor is conformally flat, which means that in a specific coordinate system the metric is proportional to a constant tensor.

# Appendix C

# Higher-Order Numerical Schemes

In this section the first-order accurate method described in the main context is improved by high-order schemes. The essentially non-oscillatory method (ENO) [349] for spatial terms and the total variation diminishing Runge-Kutta [135] for temporal terms are introduced.

## C.1 Essentially Non-Oscillatory Method

The idea of ENO is firstly proposed by Harten et al. [350]. The actual implementation was improved by Shu and Osher in [134] and [10]. Furthermore, in [14], Sethian and Osher borrowed this ENO method and extended it for the numerical discretization of Hamilton-Jacobi equation, e.g., the level set equation (4.4.3). This Hamilton-Jacobi ENO (HJ ENO) allows one to promote the spatial precision of first-order upwind scheme by providing better numerical approximations of $\phi^+_{x_i}$ and $\phi^-_{x_i}$, where $x_i$ represent the spatial coordinates $x$ , $y$ , $z$ , .... in the $n$ dimensional space.

We use the smoothest polynomial interpolation to find $\phi$ and differentiate it to derive $\phi_x$ in one dimensional space [15]. The zeroth divided differences of $\phi$ are given by

$$D^0_i\phi = \phi_i \,, \tag{C.1.1}$$

located at $x_i$. By means of this definition, the

$$D^1_{i+\frac{1}{2}}\phi = \frac{D^0_{i+1}\phi - D^0_i\phi}{\Delta x} \,, \tag{C.1.2}$$

denote the first divided differences of $\phi$ and are defined at the midpoint between grid node $i$ (located at $x_i$) and $i+1$ (located at $x_{i+1}$). Note that the forward and backward differences are given by $(D^+\phi)_i = D^1_{i+1/2}\phi$ and $(D^-\phi)_i = D^1_{i-1/2}\phi$ respectively. The second divided differences, located at $x_i$, are given by

$$D^2_i\phi = \frac{D^1_{i+\frac{1}{2}} - D^1_{i-\frac{1}{2}}}{2\Delta x} \,, \tag{C.1.3}$$

and the third divided differences are defined at midway between grid node, given as

$$D^3_{i+\frac{1}{2}}\phi = \frac{D^2_{i+\frac{1}{2}} - D^2_{i-\frac{1}{2}}}{3\Delta x} \,. \tag{C.1.4}$$

These divided differences can be used to reconstruct the polynomial form of the derivatives of $\phi(x) = Q_0(x)+Q_1(x)+Q_2(x)+Q_3(x)$, the first term $Q_0$ is zero, which vanishes upon differentiation. Accordingly, differentiating $\phi$ leads to

$$\phi_x(x_i) = Q_1{}'(x_i) + Q_2{}'(x_i) + Q_3{}'(x_i)\,, \tag{C.1.5}$$

where '′' denote derivatives. Note that $x_i$ in this equation denote $x$ at grid nodes $i$, not the coordinates.

Next we introduce parameters $c$, $c^\star$, $k^\star$ and $k$ to distinguish $\phi^+$ and $\phi^-$. We start with $k = i$ for $\phi^+$, and $k = i-1$ for $\phi^-$. Then define

$$Q_1(x) = (D^1_{k+\frac{1}{2}}\phi)(x - x_i)\,, \tag{C.1.6}$$

such that

$$Q_1{}'(x_i) = D^1_{k+\frac{1}{2}}\,, \tag{C.1.7}$$

which implies that the contribution of the $Q_1$ term in (C.1.5) is exactly the same as the first-order upwind scheme, i.e., the $\phi^\pm$. We can improve the accuracy to second- and third-orders by adding $Q_2$ and $Q_3$ terms.

For the second-order accurate correction, if $|D^2_k\phi| < |D^2_{k+1}\phi|$, $c = D^2_k\phi$ and $k^\star = k-1$; otherwise, $c = D^2_{k+1/2}\phi$ and $k^\star = k$. Then we define

$$Q_2(x) = c(x - x_k)(x - x_{k-1})\,, \tag{C.1.8}$$

upon differentiating leads to

$$Q_2{}'(x_i) = c(2(i-k)-1)\Delta x\,. \tag{C.1.9}$$

Similarly, for the third-order accurate correction, if $|D^3_{k^\star+1/2}\phi| < |D^3_{k^\star+3/2}\phi|$, then $c^\star = D^3_{k^\star+1/2}\phi$; otherwise $c^\star = D^3_{k^\star+3/2}\phi$. Then we define

$$Q_3(x) = c^\star(x - x_{k^\star})(x - x_{k^\star+1})(x - x_{k^\star+2})\,, \tag{C.1.10}$$

upon differentiating yields

$$Q_3{}'(x_i) = c^\star(3(i-k^\star)^2 - 6(i-k^\star) + 2)(\Delta x)^2\,, \tag{C.1.11}$$

which is the third-order correction in equation (C.1.5).

## C.2 Total Variation Diminishing RK

HJ ENO allows one to discretize the spatial terms to third-order. Comparing with the first-order upwind scheme for spatial terms, the first-order Euler forward method for temporal discretization produces less deterioration of numerical solutions.

But in some cases, a higher-order scheme in temporal terms is necessary. The total variation diminishing Runge-Kutta approach was used in [134] to increase the temporal numerical approximation accuracy. This method assumes that the spatial discretization can be separated from the temporal discretization, such that the temporal discretization of a partial differential equation can be treated independently as an ordinary differential equation (ODE).

The basic first-order accurate TVD RK is just the Euler forward method. The second-order accurate scheme is identical to the standard second-order accurate RK scheme. We focus on the third-order accurate scheme.

Firstly, an Euler step is taken to forward the solution to time $t^n + \Delta t$,

$$\frac{\phi^{n+1} - \phi^n}{\Delta t} + H(\phi^n) = 0\,, \tag{C.2.1}$$

where $H(\phi^n)$ is a function of $\phi$ at time $t^n$. Then we forward the solution to $t^n + 2\Delta t$,

$$\frac{\phi^{n+2} - \phi^{n+1}}{\Delta t} + H(\phi^{n+1}) = 0\,, \tag{C.2.2}$$

taking the average of $\phi^n$ and $\phi^{n+2}$ produces

$$\phi^{n+\frac{1}{2}} = \frac{3}{4}\phi^n + \frac{1}{4}\phi^{n+2}\,, \tag{C.2.3}$$

which produces an approximation solution at time $t^n + \frac{1}{2}\Delta t$. Taking another Euler step to forward the solution to $t^n + \frac{3}{2}\Delta t$, leads to

$$\frac{\phi^{n+\frac{3}{2}} - \phi^{n+\frac{1}{2}}}{\Delta t} + H(\phi^{n+\frac{1}{2}}) = 0\,, \tag{C.2.4}$$

followed by another averaging step, given as follow

$$\phi^{n+1} = \frac{1}{3}\phi^n + \frac{2}{3}\phi^{n+\frac{3}{2}}\,, \tag{C.2.5}$$

which produces a third-order accurate solution to $\phi$ at time $t^n + \Delta t$.

# Appendix D

# Numerical Schemes for Hamiltonian $\hat{H}$

There are several numerical approximation methods to $\hat{H}$. For simplicity, we suppress the dimensions to two. The numerical approximation can be generalized to the other dimensions in a similar manner.

## D.1 Lax-Friedrichs Schemes

The $\hat{H}$ in Lax-Friedrichs (LF) scheme [351] is given by

$$\hat{H} = H\left(\frac{\phi_x^+ + \phi_x^-}{2}, \frac{\phi_y^+ + \phi_y^-}{2}\right) - \alpha^x\left(\frac{\phi_x^+ - \phi_x^-}{2}\right) - \alpha^y\left(\frac{\phi_y^+ - \phi_y^-}{2}\right), \tag{D.1.1}$$

where the dissipation coefficients $\alpha^x$ and $\alpha^y$ are given by

$$\alpha^x = \max|H_1(\phi_x, \phi_y)|\,, \tag{D.1.2}$$

$$\alpha^y = \max|H_2(\phi_x, \phi_y)|\,. \tag{D.1.3}$$

The dissipation coefficients $\alpha^x$ and $\alpha^y$ are calculated through the whole computational domain. The maximum and minimum values of $\phi_x^+$, $\phi_x^-$, $\phi_y^+$, $\phi_y^-$ are chosen, denoted by $\phi_x^{\max}$, $\phi_x^{\min}$, $\phi_y^{\max}$ and $\phi_y^{\min}$, then the interval of $\phi_x$ and $\phi_y$ are defined as

$$I^x = [\phi_x^{\min}, \phi_x^{\max}]\,, \tag{D.1.4}$$

$$I^y = [\phi_y^{\min}, \phi_y^{\max}]\,. \tag{D.1.5}$$

The $\alpha^x$ are set to be the maximum possible values of $H_1(\phi_x, \phi_y)$ with $\phi_x^{\pm} \in I^x$ and $\phi_y^{\pm} \in I^y$, a similar procedure can be applied to find $\alpha^y$. Occasionally, it is rather difficult to calculate $\alpha^x$ and $\alpha^y$ when $H_1$ and $H_2$ depend on $\phi_x$ and $\phi_y$.

In order to decrease the complexity of searching dissipation coefficients, mathematicians have proposed new approach, the Local Lax-Friedrichs (LLF) scheme and Local Local Lax-Friedrichs (LLLF) scheme, where only the local values of $\phi_x^{\pm}$ and $\phi_y^{\pm}$ are required to compute $H_1$ and $H_2$ [131, 10]. In LLF, we evaluate $\phi_x^{\pm}$ at specific grid point to determine $I^x$ and $\phi_y^{\pm}$ is still selected from all grid nodes to determine $I^y$ for $\alpha^x$. For $\alpha^y$, $\phi_y^{\pm}$ is evaluated at specific point to determine $I^y$ and $\phi_x^{\pm}$ is selected from all grid nodes to determine $I^x$. While in LLLF, all coefficients $\alpha^x$ and $\alpha^y$ are determined with the local values of $\phi_x^{\pm}$ and $\phi_y^{\pm}$ at specific point.

## D.2 Roe-Fix Scheme

From last subsection we recognize that it can be rather tricky to find appropriate values of dissipation coefficients. We then introduce another method, dubbed Roe-Fix (RF) scheme [131, 10]. The numerical Hamiltonian is given as bellow

$$\hat{H} = H(\phi_x^\star, \phi_y^\star) - \alpha^x \left( \frac{\phi_x^+ - \phi_x^-}{2} \right) - \alpha^y \left( \frac{\phi_y^+ - \phi_y^-}{2} \right) . \tag{D.2.1}$$

In RF scheme, if $H_1$ does not change sign for all $\phi_x \in I^x$ and $\phi_y \in I^y$: then if $H_1 < 0$, we set $\phi_x^\star = \phi_x^-$; otherwise if $H_1 > 0$, we set $\phi_x^\star = \phi_x^+$. Similar for $H_2$ and $\phi_y^\star$. The $\alpha^x$ and $\alpha^y$ are set identically to zero.

If either $H_1$ or $H_2$ changes sign, we need to modify RF scheme by LLF. When $H_1$ does not change its sign for all $\phi_x \in I^x_{\text{LLF}}$ and $\phi_y \in I^y_{\text{LLF}}$, we set $\phi_x^\star$ equal to either $\phi_x^+$ or $\phi_x^-$, depending on the sign of $H_1$. And $\alpha^x$ is set to be zero. We use the LLF method on the $y$-direction to compute $\alpha^y$ and set $\phi_y^\star = (\phi_y^+ + \phi_y^-)/2$. A similar algorithm is executed, if $H_2$ does not change sign for all $\phi_x \in I^x_{\text{LLF}}$ and $\phi_y \in I^y_{\text{LLF}}$, setting $\phi_y^\star$ equal to either $\phi_y^+$ or $\phi_y^-$ depending on the sign of $H_2$. $\alpha^y$ is zero. Choosing $\alpha^y$ as dictated by LLF and set $\phi_x^\star = (\phi_x^+ + \phi_x^-)/2$ on the $x$-direction.

If both $H_1$ and $H_2$ change signs, we switch to standard LLF scheme at the grid point.

## D.3 Godunov's Scheme

Another scheme, called the Godunov's scheme [352], was pointed out in [353] by Osher and Bardi, that the numerical Hamiltonian is written as

$$\hat{H} = \text{ext}_x \text{ext}_y H(\phi_x, \phi_y) . \tag{D.3.1}$$

In the Godunov's scheme, the intervals $I^x$ and $I^y$ are defined in the LLLF manner with $\phi_x$ and $\phi_y$ determined only on the local grid points. Then if $\phi_x^+ > \phi_x^-$ , $\text{ext}_x H$ takes on the minimum value of $H$ for all $\phi_x \in I^x$. If $\phi^+ < \phi_x^+$, then $\text{ext}_x H$ takes on the maximum value of $H$ for all $\phi_x \in I^x$. Otherwise, if $\phi_x^+ = \phi_x^-$, simply plug $\phi_x^+ (= \phi_x^-)$ into $H$ for $\phi_x$. Similarly, if $\phi_y^+ > \phi_y^-$, then $\text{ext}_y H$ takes on the minimum value of $H$ for all $\phi_y \in I^y$. If $\phi_y^+ < \phi_y^-$, then $\text{ext}_y H$ takes on the maximum value of $H$ for all $\phi_y \in I^y$. Otherwise, if $\phi_y^+ = \phi_y^-$, plug $\phi_y^+ (= \phi_y^-)$ into $H$ for $\phi_y$. Normally, $\text{ext}_x \text{ext}_y H \neq \text{ext}_y \text{ext}_x H$. Nevertheless, this is not the case if $H$ is separable, which can be written as $H = H(\phi_x) + H(\phi_y)$.

# Appendix E

# Linearized Gravitational Equation

The Einstein's gravitational equation is

$$G_{ab} = 8\pi T_{ab}\,, \tag{E.0.1}$$

where $G_{ab} \equiv R_{ab} - Rg_{ab}/2$ called the Einstein tensor, $T_{ab}$ is the energy-momentum tensor. This is a second-order non-linear equation. It can be simplified to linearized version in the weak-field limit. In GR, the physical interpretation of weak-field is that the metric is perturbed from Minkowskian metric by an infinitesimal term, yielding

$$g_{ab} = \eta_{ab} + \gamma_{ab}\,, \tag{E.0.2}$$

where the components of $\gamma_{ab}$ satisfy that $|\gamma_{\mu\nu}| \ll 1$ in some Lorentz coordinate system of $\eta_{ab}$. Note that in the limit of weak-field, raising and lowering of indices are operated by $\eta^{ab}$ and $\eta_{ab}$. Nevertheless, there is one exception, that the inverse of $g_{ab}$ is not $g_{cd}\eta^{ca}\eta^{db}$, whereas it is given by

$$g^{ab} = \eta^{ab} - \gamma^{ab}\,. \tag{E.0.3}$$

Substituting (E.0.2) and (E.0.3) into (B.0.6) and ignoring higher-order terms in $\gamma^{ab}$ (higher than second-order), yields

$$\Gamma^{(1)}{}^{c}{}_{ab} = \frac{1}{2}\eta^{cd}(\partial_a\eta_{bd} + \partial_b\eta_{ad} - \partial_d\eta_{ab})\,. \tag{E.0.4}$$

The Riemann curvature to the first-order is given by

$$R^{(1)}{}_{abcd} = \partial_d\partial_{[a}\gamma_{c]b} - \partial_b\partial_{[a}\gamma_{c]d}\,. \tag{E.0.5}$$

The first-order accurate Ricci tensor is given by

$$R^{(1)}{}_{ab} = \partial^c\partial_{(a}\gamma_{b)c} - \frac{1}{2}\partial^c\partial_c\gamma_{ab} - \frac{1}{2}\partial_a\partial_b\gamma\,, \tag{E.0.6}$$

where $\gamma \equiv \gamma^a{}_a = \eta^{ab}\gamma_{ab}$. Then the Einstein tensor is given by

$$G^{(1)}{}_{ab} = \partial^c\partial_{(b}\gamma_{a)c} - \frac{1}{2}\partial^c\partial_c\gamma_{ab} - \frac{1}{2}\partial_a\partial_b\gamma - \frac{1}{2}\eta_{ab}(\partial^c\partial^d\gamma_{cd} - \partial^c\partial_c\gamma)\,, \tag{E.0.7}$$

such that

$$\partial^c\partial_{(b}\gamma_{a)c} - \frac{1}{2}\partial^c\partial_c\gamma_{ab} - \frac{1}{2}\partial_a\partial_b\gamma - \frac{1}{2}\eta_{ab}(\partial^c\partial^d\gamma_{cd} - \partial^c\partial_c\gamma) = 8\pi T_{ab}\,, \tag{E.0.8}$$

called the linearized Einstein equation. Defining $\bar{\gamma}_{ab} \equiv \gamma_{ab} - \frac{1}{2}\eta_{ab}\gamma$, then equation (E.0.8) can be simplified to

$$-\frac{1}{2}\partial^c\partial_c\bar{\gamma}_{ab} + \partial^c\partial_{(a}\bar{\gamma}_{b)c} - \frac{1}{2}\eta_{ab}\partial^c\partial^d\bar{\gamma}_{cd} = 8\pi T_{ab}\,. \tag{E.0.9}$$

Consider the transformation

$$\tilde{\gamma}_{ab} = \gamma_{ab} + \partial_a\epsilon_b + \partial_b\epsilon_a\,, \tag{E.0.10}$$

by another infinitesimal covector field $\epsilon_a$. After some algebra, we obtain

$$\partial^b\tilde{\bar{\gamma}}_{ab} = \partial^b\bar{\gamma}_{ab} + \partial^b\partial_b\epsilon_a\,. \tag{E.0.11}$$

If $\epsilon_a$ satisfies that $\partial^b\partial_b\epsilon_a = -\partial^b\bar{\gamma}_{ab}$, it is thus guaranteed the Lorentz gauge condition

$$\partial^b\tilde{\bar{\gamma}}_{ab} = 0\,. \tag{E.0.12}$$

Then linearized Einstein equation becomes

$$\partial^c\partial_c\tilde{\bar{\gamma}}_{ab} = -16\pi T_{ab}\,. \tag{E.0.13}$$

In addition to the Lorentz gauge, there is another gauge condition called the radiation gauge, given by

$$\tilde{\bar{\gamma}} \;\; = 0\,, \tag{E.0.14}$$
$$\tilde{\bar{\gamma}}_{00} = 0\,, \tag{E.0.15}$$
$$\tilde{\bar{\gamma}}_{0i} \;= 0\,. \tag{E.0.16}$$

# Appendix F

# Conformal Decomposition

As is given in the main context, a conformal decomposition of the 3 dimensional metric is given by equation (8.2.1). Follow the steps to derive the decompositions of 3 dimensional metric tensor, Ricci tensor, extrinsic curvature tensor and finally the 3+1 Einstein equation.

Introduce a positive definite background 3 dimensional metric $I_{ab}$ [354] on the hypersurface $\mathcal{W}$, such that in the adapted coordinate system $x^\mu$ that we choose, it satisfies

$$\mathcal{L}_{\partial_t} I_{ij} = \frac{\partial I_{ij}}{\partial t} = 0\,. \tag{F.0.1}$$

The inverse background metric satisfies

$$I^{ik} I_{kj} = \delta^i{}_j\,, \tag{F.0.2}$$

and

$$I^{ij} \neq h^{ik} h^{jl} i_{kl}\,. \tag{F.0.3}$$

We denote $\mathcal{D}_a$ as the Levi-Civita connection associated with $I_{ab}$, such that

$$D_a I_{bc} = 0\,. \tag{F.0.4}$$

The Christoffel symbols of $\mathcal{D}_a$ are given by

$$\hat{\Gamma}_{ab}{}^c = \frac{1}{2} I^{cd} \left(\partial_a I_{db} + \partial_b I_{ad} - \partial_d I_{ab}\right)\,. \tag{F.0.5}$$

Define a tensor $\tilde{h}_{ab}$ on $\mathcal{W}$

$$\tilde{h}_{ab} := \Psi^{-4} h_{ab}\,, \tag{F.0.6}$$

where

$$\Psi := \left(\frac{h}{I}\right)^{\frac{1}{12}}\,, \tag{F.0.7}$$

$$h := \det(h_{ij})\,, \tag{F.0.8}$$

$$I := \det(I_{ij})\,. \tag{F.0.9}$$

I shall call tensor $\tilde{h}_{ab}$ the conformal metric tensor. By construction, we have

$$\tilde{h} := \det(\tilde{h}_{ij}) = I\,. \tag{F.0.10}$$

Define the inverse conformal metric by

$$\tilde{h}^{ik}\tilde{h}_{kj} = \delta^{i}{}_{j}\,, \tag{F.0.11}$$

or equivalently

$$\tilde{h}^{ab} = \Psi^4 h^{ab}\,. \tag{F.0.12}$$

Define the Levi-Civita connection associated with the conformal metric as $\tilde{D}_a$, the Christoffel symbols are given by

$$\tilde{\Gamma}_{ab}{}^{c} = \frac{1}{2}\tilde{h}^{cd}\left(\partial_a\tilde{h}_{db} + \partial_b\tilde{h}_{ad} - \partial_d\tilde{h}_{ab}\right)\,. \tag{F.0.13}$$

The difference between two covariant derivatives $D_a$ and $\tilde{D}_a$ with respect to a tensor $T_{a_1a_2\cdots a_p}^{\quad b_1b_2\cdots b_q}$ is evaluated by a tensor $C_{ab}{}^{c}$, given by

$$D_cT_{a_1a_2\cdots a_p}^{\quad b_1b_2\cdots b_q} = \tilde{D}_cT_{a_1a_2\cdots a_p}^{\quad b_1b_2\cdots b_q} - \sum_{r=1}^{p} C_{ca_r}{}^{d}T_{a_1a_2\cdots d\cdots a_p}^{\quad b_1b_2\cdots b_q} + \sum_{r=1}^{q} C_{cd}{}^{b_r}T_{a_1a_2\cdots a_p}^{\quad b_1b_2\cdots d\cdots b_q}\,, \tag{F.0.14}$$

where

$$C_{ab}{}^{c} := \Gamma_{ab}{}^{c} - \tilde{\Gamma}_{ab}{}^{c}\,, \tag{F.0.15}$$

similar to the Christoffel symbol, the tensor $C_{ab}{}^{c}$ satisfies

$$C_{ab}{}^{c} = \frac{1}{2}h^{cd}\left(\tilde{D}_ah_{db} + \tilde{D}_bh_{ad} - \tilde{D}_dh_{ab}\right)\,. \tag{F.0.16}$$

Substitute the equations (F.0.6) and (F.0.12) into the above equation (F.0.16), and after some algebra we obtain

$$C_{ab}{}^{c} = 2\left(\delta_a{}^{c}\tilde{D}_b\ln\Psi + \delta_b{}^{c}\tilde{D}_a\ln\Psi - \tilde{D}^c\ln\Psi\tilde{h}_{ab}\right)\,. \tag{F.0.17}$$

From the definition of the 3 dimensional curvature tensor and the 3 dimensional Ricci tensor, we can derive that

$${}^{3}R_{ab}v^b = D_bD_av^b - D_aD_bv^b\,, \tag{F.0.18}$$

where $v^b$ is a vector on hypersurface $\mathcal{W}$. Using the equation (F.0.14), the 3 dimensional Ricci tensor becomes

$${}^{3}R_{ab}v^b = \tilde{D}_b\tilde{D}_av^b - \tilde{D}_a\tilde{D}_bv^b + \tilde{D}_bC_{ac}{}^{b}v^c - \tilde{D}_aC_{bc}{}^{b}v^c - C_{ab}{}^{c}C_{cd}{}^{b}v^d + C_{bc}{}^{b}C_{ad}{}^{c}v^d\,. \tag{F.0.19}$$

Consider a similar relation for the conformal 3 dimensional Ricci tensor

$${}^{3}\tilde{R}_{ab}v^b = \tilde{D}_b\tilde{D}_av^b - \tilde{D}_a\tilde{D}_bv^b\,, \tag{F.0.20}$$

then after some algebra from (F.0.19), we obtain

$${}^{3}R_{ab}v^b = {}^{3}\tilde{R}_{ab}v^b + \tilde{D}_cC_{ab}{}^{c}v^b - \tilde{D}_aC_{cb}{}^{c}v^b + C_{cd}{}^{d}C_{ab}{}^{c}v^b - C_{ad}{}^{c}C_{cb}{}^{d}v^b\,. \tag{F.0.21}$$

Note that $v^a$ is an arbitrary vector, it is concluded that

$${}^{3}R_{ab} = {}^{3}\tilde{R}_{ab} + \tilde{D}_cC_{ab}{}^{c} - \tilde{D}_aC_{cb}{}^{c} + C_{cd}{}^{d}C_{ab}{}^{c} - C_{ad}{}^{c}C_{cb}{}^{d}\,. \tag{F.0.22}$$

Contracting the indices $c$ and $b$ in (F.0.17), we obtain

$$\begin{aligned} C_{ac}{}^{c} &= 2\left(\tilde{D}_a\ln\Psi + 3\tilde{D}_a\ln\Psi - \tilde{D}_a\ln\Psi\right) \\ &= 6\tilde{D}_a\ln\Psi\,, \end{aligned} \tag{F.0.23}$$

hence

$$\tilde{D}_a C_{bc}{}^{c} = 6\tilde{D}_a\tilde{D}_b \ln\Psi\,, \tag{F.0.24}$$

and

$$\tilde{D}_c C_{ab}{}^{c} = 4\tilde{D}_a\tilde{D}_b \ln\Psi - 2\tilde{D}_c\tilde{D}^c \ln\Psi\tilde{h}_{ab}\,. \tag{F.0.25}$$

Taking the equations (F.0.24) and (F.0.25) into consideration, the expression (F.0.22) becomes

$$\begin{aligned} {}^3R_{ab} = {}& {}^3\tilde{R}_{ab} - 2\tilde{D}_a\tilde{D}_b \ln\Psi - 2\tilde{D}_c\tilde{D}^c \ln\Psi\tilde{h}_{ab} + 4\tilde{D}_a \ln\Psi\tilde{D}_b \ln\Psi \\ & - 4\tilde{D}_c \ln\Psi\tilde{D}^c \ln\Psi\tilde{h}_{ab}\,. \end{aligned} \tag{F.0.26}$$

Taking the trace of (F.0.26), leads to an expression for the scalar curvature, which is given by

$${}^3R = \Psi^{-4}\left[{}^3\tilde{R} - 8\left(\tilde{D}_a\tilde{D}^a \ln\Psi + \tilde{D}_a \ln\Psi\tilde{D}^a \ln\Psi\right)\right]\,, \tag{F.0.27}$$

where ${}^3\tilde{R} := {}^3\tilde{R}_{ab}\tilde{h}^{ab}$. Equation (F.0.27) can be readily rewritten as

$${}^3R = (\Psi^{-4}){}^3\tilde{R} - 8\Psi^{-5}\tilde{D}_a\tilde{D}^a\Psi\,. \tag{F.0.28}$$

For the extrinsic curvature, one can first divide it into traceless and trace parts. Define a tensor $\varkappa_{ab}$, such that

$$\varkappa_{ab} := K_{ab} - \frac{1}{3}Kh_{ab}\,, \tag{F.0.29}$$

where $K$ is the trace of $K_{ab}$ with respect to the 3 dimensional metric. And $\varkappa_{ab}$ is traceless. Define two rank-two contravariant tensors $K^{ab}$ and $\varkappa^{ab}$, given by

$$K^{ab} := h^{ac}h^{bd}K_{cd}\,, \tag{F.0.30}$$

$$\varkappa^{ab} := h^{ac}h^{bd}\varkappa_{cd}\,. \tag{F.0.31}$$

Consequently the traceless decomposition of extrinsic curvatures are given by

$$K^{ab} = \varkappa^{ab} + \frac{1}{3}Kh^{ab}\,, \tag{F.0.32}$$

$$K_{ab} = \varkappa_{ab} - \frac{1}{3}Kh_{ab}\,. \tag{F.0.33}$$

Consider the traceless part of $K_{ab}$, write

$$\varkappa^{ab} = \Psi^{\alpha}\tilde{\varkappa}^{ab}\,, \tag{F.0.34}$$

for some power $\alpha$, aka the scaling factor, to be determined. By means of equations (F.0.6), (F.0.33), the equation (6.2.41) becomes

$$\mathcal{L}_m\left(\Psi^4\tilde{h}_{ab}\right) = 2N\varkappa_{ab} + \frac{2}{3}NKh_{ab}\,, \tag{F.0.35}$$

simplifying the expression leads to

$$\mathcal{L}_m\tilde{h}_{ab} = 2N\varkappa_{ab}\Psi^{-4} + \frac{2}{3}\left(NK - 6\mathcal{L}_m \ln\Psi\right)\tilde{h}_{ab}\,. \tag{F.0.36}$$

Taking the trace of the above equation gives

$$\tilde{h}^{ab}\mathcal{L}_m\tilde{h}_{ab} = 2NK - 12\mathcal{L}_m \ln\Psi\,. \tag{F.0.37}$$

Consider the law of variation of the determinant of an invertible matrix, we have

$$\tilde{h}^{ab}\mathcal{L}_m\tilde{h}_{ab} = \mathcal{L}_m \ln\tilde{h}\,. \tag{F.0.38}$$

By means of equations (4.3.15) and (F.0.10), (F.0.38) becomes

$$\mathcal{L}_m \ln\tilde{h} = (\mathcal{L}_{\partial_t} - \mathcal{L}_\beta)\ln I\,, \tag{F.0.39}$$

and due to (F.0.1), this becomes

$$\mathcal{L}_m \ln\tilde{h} = -\mathcal{L}_\beta \ln I = \mathcal{L}_\beta\tilde{h}\,. \tag{F.0.40}$$

After some calculation, we obtain

$$\mathcal{L}_m \ln\tilde{h} = -\tilde{h}^{ab}\mathcal{L}_\beta\tilde{h}_{ab} = -2\tilde{D}_a\beta^a\,. \tag{F.0.41}$$

Combine with (F.0.38), yields

$$\tilde{h}^{ab}\mathcal{L}_m\tilde{h}_{ab} = -2\tilde{D}_a\beta^a\,, \tag{F.0.42}$$

substitute the above equation into (F.0.37), yields

$$6\mathcal{L}_m \ln\Psi - NK = \tilde{D}_a\beta^a\,, \tag{F.0.43}$$

i.e.

$$(\mathcal{L}_{\partial_t} - \mathcal{L}_\beta)\ln\Psi = \frac{1}{6}\left(\tilde{D}_a\beta^a + NK\right)\,. \tag{F.0.44}$$

An evolution equation for the conformal metric may be obtained by plugging equation (F.0.43) into (F.0.36)

$$(\mathcal{L}_{\partial_t} - \mathcal{L}_\beta)\,\tilde{h}_{ab} = 2N\tilde{\varkappa}_{ab} - \frac{2}{3}\tilde{D}_c\beta^c\tilde{h}_{ab}\,, \tag{F.0.45}$$

where $\tilde{\varkappa}_{ab} := \Psi^{-4}\varkappa_{ab}$, which possesses the following properties

$$\tilde{h}^{ab}\tilde{\varkappa}_{ab} = 0\,, \tag{F.0.46}$$

$$\tilde{\varkappa}^{ab} = \Psi^4\varkappa^{ab}\,. \tag{F.0.47}$$

where $\tilde{\varkappa}^{ab} = \tilde{h}^{ac}\tilde{h}^{bd}\tilde{\varkappa}_{cd}$. This corresponds to the case of a scaling factor $\alpha = -4$, which is introduced by Nakamura [188].

The equation (F.0.45) may lead to the following expression

$$(\mathcal{L}_{\partial_t} - \mathcal{L}_\beta)\,\tilde{h}^{ab} = -2N\tilde{\varkappa}^{ab} + \frac{2}{3}\tilde{D}_c\beta^c\tilde{h}^{ab}\,. \tag{F.0.48}$$

From (F.0.32), we have

$$D_bK^{ab} = D_b\varkappa^{ab} + \frac{1}{3}D^aK\,, \tag{F.0.49}$$

by means of (F.0.14), (F.0.17) and (F.0.23), the first term on the RHS of this equation becomes

$$D_b\varkappa^{ab} = \tilde{D}_b\varkappa^{ab} + 10\varkappa^{ab}\tilde{D}_b \ln\Psi - 2\tilde{D}^a \ln\Psi\tilde{h}_{bc}\varkappa^{bc}\,. \tag{F.0.50}$$

Note that $0 = \tilde{h}_{bc}\varkappa^{bc} = \Psi^{-4}h_{bc}\varkappa^{bc}$, (F.0.50) thus reduces to

$$D_b\varkappa^{ab} = \Psi^{-10}\tilde{D}_b\hat{\varkappa}^{ab}\,, \tag{F.0.51}$$

where $\hat{\varkappa}^{ab} = \Psi^{10}\varkappa^{ab}$, which corresponds to a scaling factor of $\alpha = -10$. This is found by Lichnerowicz [169]. The inverse tensor is given by

$$\hat{\varkappa}_{ab} := \tilde{h}_{ac}\tilde{h}_{bd}\hat{\varkappa}^{cd}\,, \tag{F.0.52}$$

which satisfies

$$\hat{\varkappa}_{ab} = \Psi^2\varkappa_{ab}\,. \tag{F.0.53}$$

Accordingly, the momentum constraint can be rewritten as

$$\tilde{D}_b\hat{\varkappa}^{ab} - \frac{2}{3}\Psi^6\tilde{D}^aK = 8\pi\Psi^{10}p^a\,. \tag{F.0.54}$$

Substitute (F.0.33) into the LHS of (6.2.65), and taking the contraction of indices $a$ and $b$ on both sides of the equation (6.2.65), yields

$$\mathcal{L}_mK_{ab} = \mathcal{L}_m\varkappa_{ab} + \frac{1}{3}\mathcal{L}_mKh_{ab} + \frac{1}{3}\mathcal{L}_mh_{ab}K\,, \tag{F.0.55}$$

$$\mathcal{L}_mK = D_aD^aN - N\left[{}^3R + K^2 + 4\pi(S-3E)\right]\,, \tag{F.0.56}$$

this can be rewritten by means of the Hamiltonian constraint, leads to

$$\left(\frac{\partial}{\partial t} - \mathcal{L}_\beta\right)K = D_aD^aN - N\left[4\pi(E+S) + K_{ab}K^{ab}\right]\,. \tag{F.0.57}$$

By applying the equations (F.0.56) and (6.2.65) into (F.0.55), and considering the expression of $K_{ab}$ in terms of $\varkappa_{ab}$, yields

$$\begin{aligned}\mathcal{L}_m\varkappa_{ab} =& -D_aD_bN + N\left[{}^3R_{ab} - \frac{1}{3}K\varkappa_{ab} - 2\varkappa_{ac}\varkappa_b{}^c - 8\pi\left(S_{ab} - \frac{1}{3}Sh_{ab}\right)\right]\\ &- \frac{1}{3}\left(D_cD^cN - {}^3RN\right)h_{ab}\,.\end{aligned} \tag{F.0.58}$$

Next step is to perform the conformal decomposition of the 3+1 equations. Consider the case where the scaling factor is given by $\alpha = -4$, i.e., $\tilde{\varkappa}_{ab}$. First, consider the relation between two Levi-Civita connections, from (F.0.14) and take the trace of the equation, we obtain

$$D_av^a = \Psi^{-6}\tilde{D}_a\left(\Psi^6v^a\right)\,. \tag{F.0.59}$$

Apply the above formula to a vector $D^aN$, yields

$$D_aD^aN = \Psi^{-4}\left(\tilde{D}_a\tilde{D}^aN + 2\tilde{D}_a\ln\Psi\tilde{D}^aN\right)\,. \tag{F.0.60}$$

From (F.0.32) and (F.0.33), we have

$$K_{ab}K^{ab} = \tilde{\varkappa}_{ab}\tilde{\varkappa}^{ab} + \frac{K^2}{3}\,. \tag{F.0.61}$$

In view of (F.0.60), (F.0.61) and (F.0.57), yields

$$\begin{aligned}\left(\frac{\partial}{\partial t} - \mathcal{L}_\beta\right)K =\ & \Psi^{-4}\left(\tilde{D}_a\tilde{D}^aN + 2\tilde{D}_a\ln\Psi\tilde{D}^aN\right)\\ & - N\left[4\pi\left(E+S\right) + \tilde{\varkappa}_{ab}\tilde{\varkappa}^{ab} + \frac{K^2}{3}\right]\,.\end{aligned} \tag{F.0.62}$$

Making use of (F.0.44), (F.0.14), (F.0.17), (F.0.22), (F.0.27) and (F.0.58), after some algebra and rearrangements, we obtain the following expression

$$\begin{aligned}\left(\frac{\partial}{\partial t}-\mathcal{L}_\beta\right)\tilde{\varkappa}_{ab} = & \\ & -\frac{2}{3}\tilde{D}_c\beta^c\tilde{\varkappa}_{ab}+N\left[K\tilde{\varkappa}_{ab}-2\tilde{h}^{cd}\tilde{\varkappa}_{ac}\tilde{\varkappa}_{bd}-8\pi\left(\Psi^{-4}S_{ab}-\frac{1}{3}S\tilde{h}_{ab}\right)\right] \\ & +\Psi^{-4}\left\{-\tilde{D}_a\tilde{D}_bN+2\tilde{D}_a\ln\Psi\tilde{D}_bN+2\tilde{D}_b\ln\Psi\tilde{D}_aN\right\} \\ & +\frac{1}{3}\left(\tilde{D}_c\tilde{D}^cN-4\tilde{D}_c\ln\Psi\tilde{D}^cN\right)\tilde{h}_{ab} \\ & +N[{}^3\tilde{R}_{ab}-\frac{1}{3}{}^3\tilde{R}\tilde{h}_{ab}-2\tilde{D}_a\tilde{D}_b\ln\Psi+4\tilde{D}_a\ln\Psi\tilde{D}_b\ln\Psi \\ & +\frac{2}{3}\left(\tilde{D}_c\tilde{D}^c\ln\Psi-2\tilde{D}_c\ln\Psi\tilde{D}^c\ln\Psi\right)\tilde{h}_{ab}]\,. \end{aligned} \tag{F.0.63}$$

We can deduce that

$$\hat{\varkappa}_{ab}=\Psi^6\tilde{\varkappa}_{ab}\,, \tag{F.0.64}$$

$$\hat{\varkappa}^{ab}=\Psi^6\tilde{\varkappa}^{ab}\,. \tag{F.0.65}$$

Then by means of the equations (F.0.28) and (F.0.61), the Hamiltonian constraint becomes

$$\tilde{D}_a\tilde{D}^a\Psi-\frac{1}{8}{}^3\tilde{R}\Psi+\left(\frac{1}{8}\tilde{\varkappa}_{ab}\tilde{\varkappa}^{ab}-\frac{1}{12}K^2+2\pi E\right)\Psi^5=0\,, \tag{F.0.66}$$

$$\tilde{D}_a\tilde{D}^a\Psi-\frac{1}{8}{}^3\tilde{R}\Psi+\frac{1}{8}\hat{\varkappa}_{ab}\hat{\varkappa}^{ab}\Psi^{-7}+\left(2\pi E-\frac{1}{12}K^2\right)\Psi^5=0\,. \tag{F.0.67}$$

This is the Lichnerowicz equation and was first derived in 1944 by Lichnerowicz [169, 170].

Consider (F.0.64) and (F.0.65), the equation (F.0.54) can be rewritten as

$$\tilde{D}_b\tilde{\varkappa}^{ab}+6\tilde{\varkappa}^{ab}\tilde{D}_b\ln\Psi-\frac{2}{3}\tilde{D}^aK=8\pi\Psi^4p^a\,. \tag{F.0.68}$$

Now the equations (F.0.44), (F.0.45), (F.0.62), (F.0.63), (F.0.66),(F.0.68), (F.0.54) and (F.0.67) constitute the conformal version of the 3+1 Einstein equations. To recover the original 3 dimensional metric $h_{ab}$ and the extrinsic curvature $K_{ab}$, we need to use (F.0.6) and (F.0.33).

# Appendix G

# Symplectic Integrator

The symplectic method is designed for integrating the system with a Hamiltonian function $H(p, q)$ [355, 356, 357, 358]. Consider the Hamiltonian system $H(p_1, p_2, \cdots, p_n, q_1, q_2, \cdots, q_n)$, and the tangent vectors to the curve in phase space are given by

$$\frac{\mathrm{d}q_i}{\mathrm{d}t} = H_{p_i}\,, \tag{G.0.1}$$

$$\frac{\mathrm{d}p_i}{\mathrm{d}t} = -H_{q_i}\,, \tag{G.0.2}$$

which are also known as the Hamiltonian equations in classical mechanics, $\forall\ i$, where $1 < i < n$. Introduce a matrix $\boldsymbol{X} = \left(\begin{smallmatrix} 0 & X_n \\ -X_n & 0 \end{smallmatrix}\right)$, and a column vector $\boldsymbol{z} = \left(\begin{smallmatrix} q \\ p \end{smallmatrix}\right)$. We can then rewrite the Hamiltonian equations as

$$\frac{\mathrm{d}}{\mathrm{d}t}\boldsymbol{z} = \boldsymbol{X}\nabla H(\boldsymbol{z})\,, \tag{G.0.3}$$

where the $\nabla$ denotes the derivative with respect to the variables $p_i$ and $q_i$.

A typical first-order accurate method is given by

$$q_{i+1} = q_i + \Delta\boldsymbol{t}\nabla_p H(p_{i+1}, q_i)\,, \tag{G.0.4}$$

$$p_{i+1} = p_i - \Delta\boldsymbol{t}\nabla_q H(p_{i+1}, q_i)\,, \tag{G.0.5}$$

or

$$q_{i+1} = q_i + \Delta\boldsymbol{t}\nabla_p H(p_i, q_{i+1})\,, \tag{G.0.6}$$

$$p_{i+1} = p_i - \Delta\boldsymbol{t}\nabla_q H(p_i, q_{i+1})\,. \tag{G.0.7}$$

This is known as the symplectic Euler method of order 1.

A second-order symplectic method is

$$q_{i+1/2} = q_i + \frac{\Delta\boldsymbol{t}}{2}\nabla_p H(p_i, q_{i+\frac{1}{2}})\,, \tag{G.0.8}$$

$$p_{i+1} = p_i - \frac{\Delta\boldsymbol{t}}{2}\left(\nabla_q H(p_i, q_{i+\frac{1}{2}}) + \nabla_q H(p_{i+1}, q_{i+\frac{1}{2}})\right)\,, \tag{G.0.9}$$

$$q_{i+1} = q_{i+\frac{1}{2}} + \frac{\Delta\boldsymbol{t}}{2}\nabla_p H(p_{i+1}, q_{i+\frac{1}{2}})\,, \tag{G.0.10}$$

$$p_{i+1/2} = p_i - \frac{\Delta\boldsymbol{t}}{2}\nabla_q H(p_i, q_{i+\frac{1}{2}})\,, \tag{G.0.11}$$

$$q_{i+1} = q_i + \frac{\Delta\boldsymbol{t}}{2}\left(\nabla_p H(p_{i+\frac{1}{2}}, q_i) + \nabla_p H(p_{i+1}, q_{i+\frac{1}{2}})\right)\,, \tag{G.0.12}$$

$$p_{i+1} = p_{i+\frac{1}{2}} - \frac{\Delta\boldsymbol{t}}{2}\nabla_q H(p_{i+\frac{1}{2}}, q_{i+1})\,, \tag{G.0.13}$$

which is also known as the Störmer-Verlet schemes.

Another second-order symplectic approach is given by

$$\boldsymbol{z}_{i+1} = \boldsymbol{z}_i + \Delta \boldsymbol{t} \boldsymbol{X} \nabla H \left( \frac{\boldsymbol{z}_{i+1} + \boldsymbol{z}_i}{2} \right) . \tag{G.0.14}$$

A general Runge-Kutta method is given by

$$k_i = f \left( \boldsymbol{t}_0 + c_i \Delta \boldsymbol{t}, Y_0 + \Delta \boldsymbol{t} \sum_{j=1}^{n} A_{ij} k_j \right) , \tag{G.0.15}$$

$$Y_1 = Y_0 + \Delta \boldsymbol{t} \sum_{i=1}^{n} b_i k_i \, , \tag{G.0.16}$$

based on the initial value

$$\frac{\mathrm{d}Y}{\mathrm{d}\boldsymbol{t}} = f(\boldsymbol{t}, Y) \, , \tag{G.0.17}$$

$$Y(\boldsymbol{t}_0) = Y_0 \, . \tag{G.0.18}$$

A symplectic Runge-Kutta [359] relates the symplecticity to the conservation of the quadratic first integrals. If a Runge-Kutta method conserves quadratic first integrals, i.e., $I(Y_1) = I(Y_0)$ whenever $I(Y) = Y^T \boldsymbol{C} Y$ with $\boldsymbol{C}$ a symmetric matrix, is a first integral of $\mathrm{d}Y/\mathrm{d}\boldsymbol{t} = f(Y)$, then it is a symplectic Runge-Kutta.

The Gauss collection method is defined as: Let $c_1 \, , \; c_2 \, , \; \cdots \, , \; c_n$ be the zeroth of the shifted Legendre polynomial $\mathrm{d}^n \left( x^n (1-x)^n \right) / \mathrm{d}x^n$, and $u(\boldsymbol{t})$ be the polynomial of degree of $n$ satisfying

$$u(\boldsymbol{t}_0) = Y_0 \, , \tag{G.0.19}$$

$$\dot{u}(\boldsymbol{t}_0 + c_i \Delta \boldsymbol{t}) = f \left( \boldsymbol{t}_0 + c_i \Delta \boldsymbol{t}, u(\boldsymbol{t}_0 + c_i \Delta \boldsymbol{t}) \right) , \tag{G.0.20}$$

the numerical solution is then given by $Y_1 = u(\boldsymbol{t}_0 + \Delta \boldsymbol{t})$ for Gauss collection method. The Gauss collection method is symplectic as it conserves quadratic first integrals.

If the coefficients of Runge-Kutta method satisfy

$$b_i a_{ij} + b_j a_{ji} = b_i b_j \, , \tag{G.0.21}$$

for all $i \, , \; j = 1 \, , \; 2 \, , \; \cdots \, , \; n$, it then conserves quadratic first integrals and is thus symplectic [360, 361, 362, 363].

Consider the following mapping

$$q_{i+1} = q_i + \nabla_p G(p_{i+1}, q_i) \, , \tag{G.0.22}$$

$$p_{i+1} = p_i - \nabla_q G(p_i, q_{i+1}) \, , \tag{G.0.23}$$

if $G(p, q)$ satisfies

$$G(p, q, \boldsymbol{t}) = \Delta \boldsymbol{t} G_1(p, q) + \Delta \boldsymbol{t}^2 G_2(p, q) + \Delta \boldsymbol{t}^3 G_3(p, q) + \cdots \, , \tag{G.0.24}$$

where

$$G_1 = H \, , \tag{G.0.25}$$

$$G_2 = \frac{1}{2} \frac{\partial H}{\partial q} \frac{\partial H}{\partial p} \, , \tag{G.0.26}$$

$$G_3 = \frac{1}{6} \left( \frac{\partial^2 H}{\partial q^2} + \left( \frac{\partial H}{\partial p} \right)^2 + \frac{\partial^2 H}{\partial q \partial p} \frac{\partial H}{\partial q} \frac{\partial H}{\partial p} + \frac{\partial^2 H}{\partial p^2} \left( \frac{\partial H}{\partial q} \right)^2 \right) . \tag{G.0.27}$$

Then (G.0.22) and (G.0.23) produce an exact solution to the Hamiltonian equations. If we apply a truncate series of $G(p,q) = \Delta \boldsymbol{t} G_1(p,q) + \Delta \boldsymbol{t}^2 G_2(p,q) + \cdots + \Delta \boldsymbol{t}^i G_i(p,q)$ to that solution, it will produce a symplectic one-step method of order 1. For $i \geq 2$, the method requires a higher-order of $H(p,q)$ [364, 365].

Consider the approximation expression

$$G_{\boldsymbol{t}}(\{q_i\}_0^n) \quad = \sum_{i=0}^{n-1} L_{\boldsymbol{t}}(q_i, q_{i+1})\,, \tag{G.0.28}$$

$$L_{\boldsymbol{t}}(q_i, q_{i+1}) \approx \int_{\boldsymbol{t}_i}^{\boldsymbol{t}_{i+1}} L(q(\boldsymbol{t}), \dot{q}(\boldsymbol{t}), \boldsymbol{t}) \mathrm{d}\boldsymbol{t}\,. \tag{G.0.29}$$

Where $L_{\boldsymbol{t}}(q_i, q_{i+1})$ denotes the discrete Lagrangian. The requirement of extremum of (G.0.28) yields the Euler-Lagrange equation

$$\partial_{e_1} L_{\boldsymbol{t}}(q_i, q_{i+1}) + \partial_{e_2} L_{\boldsymbol{t}}(q_{i-1}, q_i) = 0\,, \tag{G.0.30}$$

where the derivatives refer to $L_{\boldsymbol{t}} = L_{\boldsymbol{t}}(e_1, e_2)$, for $i = 1\,,\ 2\,,\ \cdots,\ n$. Introduce momenta via the Legendre transformation

$$p_i = -\frac{\partial L_{\boldsymbol{t}}}{\partial e_1}(q_i, q_{i+1})\,, \tag{G.0.31}$$

if one substitutes $i$ for $i+1$ in (G.0.30), it is then derived from (G.0.31) that

$$p_{i+1} = \frac{\partial L_{\boldsymbol{t}}}{\partial e_2}(q_i, q_{i+1})\,. \tag{G.0.32}$$

Producing a mapping $(p_i, q_i) \mapsto (p_{i+1}, q_{i+1})$, which defines a symplectic integrator.

# Appendix H

# Conformal Thin Sandwich Method

## H.1 Basics of Conformal Thin Sandwich (CTS) Method

In appendix F, we have derived the equation (F.0.48), hence for the traceless part $\tilde{\varkappa}^{ab}$, we obtain

$$\tilde{\varkappa}^{ab} = \frac{1}{2N}\left[(\mathcal{L}_{\partial_t} - \mathcal{L}_\beta)\,\tilde{h}^{ab} - \frac{2}{3}\tilde{D}_c\beta^c\tilde{h}^{ab}\right]. \tag{H.1.1}$$

And

$$-\mathcal{L}_\beta\tilde{h}^{ab} = (\tilde{L}\beta)^{ab} + \frac{2}{3}\tilde{D}_c\beta^c\tilde{h}^{ab}\,. \tag{H.1.2}$$

The (H.1.1) can be then rewritten as

$$\tilde{\varkappa}^{ab} = \frac{1}{2N}\left[\dot{\tilde{h}}^{ab} + (\tilde{L}\beta)^{ab}\right], \tag{H.1.3}$$

where

$$\dot{\tilde{h}}^{ab} := \frac{\partial}{\partial t}\tilde{h}^{ab}\,. \tag{H.1.4}$$

Consider (F.0.65), the formula (H.1.3) becomes

$$\hat{\varkappa}^{ab} = \frac{1}{2\tilde{N}}\left[\dot{\tilde{h}}^{ab} + (\tilde{L}\beta)^{ab}\right], \tag{H.1.5}$$

where

$$\tilde{N} := \Psi^{-6}N\,, \tag{H.1.6}$$

this denotes the conformal lapse function. We now have a new form of decomposition of the $\hat{\varkappa}^{ab}$ in terms of $\tilde{N}$, $\beta$ and $\dot{\tilde{h}}^{ab}$. Hence the constraints of Einstein equation become

$$\tilde{D}^a\tilde{D}_a\Psi - \frac{1}{8}{}^3\tilde{R}\Psi + \frac{1}{8}\hat{\varkappa}^{ab}\hat{\varkappa}_{ab}\Psi^{-7} + 2\pi\tilde{E}\Psi^{-3} - \frac{1}{12}K^2\Psi^5 = 0\,, \tag{H.1.7}$$

$$\tilde{D}_b\left(\frac{1}{\tilde{N}}(\tilde{L}\beta)^{ab}\right) + \tilde{D}_b\left(\frac{1}{\tilde{N}}\dot{\tilde{h}}^{ab}\right) - \frac{4}{3}\Psi^6\tilde{D}^aK = 16\pi\tilde{p}^a\,. \tag{H.1.8}$$

The Hamiltonian constraint which takes the same form as (8.2.9), expressed with (H.1.5). Now the freely-chosen data are $(\tilde{h}_{ab}, \dot{\tilde{h}}^{ab}, K, \tilde{N}, \tilde{E}, \tilde{p}^a)$, and solve for the $(\Psi, \beta^a)$ via (H.1.7) and (H.1.8). This method is called the conformal thin sandwich method [366, 367, 239, 368, 227]. The equation (H.1.8) can be decoupled from (H.1.7) on a CMC hypersurface.

## H.2 Extended Conformal Thin Sandwich (XCTS) Method

Consider the identity

$$\tilde{D}_a\tilde{D}^aN + 2\tilde{D}_a \ln\Psi \tilde{D}^aN = \Psi\left[4\pi(E+S) + \tilde{\varkappa}_{ab}\tilde{\varkappa}^{ab} + \frac{K^2}{3}\right], \quad \text{(H.2.1)}$$

plug (F.0.62) and (H.1.7) into the LHS and RHS of the above equation, yields,

$$\tilde{D}_a\tilde{D}^a(\tilde{N}\Psi^7) - (\tilde{N}\Psi^7) + \left[\frac{1}{8}{}^3R + \frac{5}{12}K^2\Psi^4 + \frac{7}{8}\hat{\varkappa}_{ab}\hat{\varkappa}^{ab}\Psi^{-8} + 2\pi(\tilde{E}+2\tilde{S})\Psi^{-4}\right] + \left(\dot{K} - \beta^a\tilde{D}_aK\right)\Psi^5 = 0\,, \quad \text{(H.2.2)}$$

where

$$\dot{K} := \frac{\partial K}{\partial t}\,, \quad \text{(H.2.3)}$$

$$\tilde{S} := \Psi^8 S\,. \quad \text{(H.2.4)}$$

Then the three equations (H.1.7), (H.1.8) and (H.2.4) constitute a constraint system of Einstein equation. Now the constrained data become the $\tilde{N}$, $\beta^a$ and $\Psi$. Contrary to the CTT method, it is not allowed to decouple these equations from one another even if on a CMC hypersurface. The uniqueness of the solution to the system is discussed by different people [369, 370, 371] and has been proven to be false by Walsh [372].

The two methods, CTT and CTS are both well constructed effective approach to the initial value problem for the Cauchy problem. The former is considered as a method in the Hamiltonian representation, whereas the latter is considered in the Lagrangian representation [373]. Comparison of the two approaches has been made [374, 375], cf., the [376].

# Appendix I

# Full Spatial Coordinate Fixing Choices

In the Chapter 8, we introduce a series of gauge conditions which govern the evolution of the shift vector. Therein, the coordinates on the initial slice are not fixed. In this appendix section we will describe a few prescriptions which are subject to such restrictions.

## I.1 Spatial Harmonic Coordinates

The spatial harmonic coordinate [377, 378, 379] is defined as

$$D_j D^j x^i = 0\,, \tag{I.1.1}$$

which is equivalent to

$$\partial_a(\sqrt{h}h^{ab}) = 0\,. \tag{I.1.2}$$

Rewrite the condition in terms of $\mathcal{D}_a$ and background metric $I_{ab}$, given by

$$\mathcal{D}_a\left[\left(\frac{h}{I}\right)^{1/2} h^{ab}\right] = 0\,. \tag{I.1.3}$$

## I.2 Dirac Gauge

A condition given by

$$\frac{\partial(h^{1/3}h^{ij})}{\partial x^j} = 0\,, \tag{I.2.1}$$

was introduced by Dirac in 1959 for a canonical quantization of the general relativity in a Hamiltonian formulation [174], where $i$ and $j$ run from 1 to 3. A more covariant form of the formula is given by [354]

$$\mathcal{D}_b\left[\left(\frac{h}{I}\right)^{1/3} h^{ab}\right] = 0\,, \tag{I.2.2}$$

where $\mathcal{D}_b$ denotes the 3 dimensional covariant derivative associated to the background 3 dimensional metric and $I$ denotes the determinant of the background 3 dimensional metric in the coordinate system $x^i$. It is

recognized that the term in bracket may be substituted by the inverse of conformal 3 dimensional metric, yields

$$\mathcal{D}_b \tilde{h}^{ab} = 0\,. \tag{I.2.3}$$

This is called the Dirac gauge [238]. Due to (8.2.64) and (I.2.3), we know that

$$\tilde{\Gamma}^a = 0\,, \tag{I.2.4}$$

hence the shift vector which satisfies the Dirac gauge must satisfy the equation (8.2.69) with a vanishing $\tilde{\Gamma}^a$, given by

$$\begin{aligned}\tilde{h}^{bc}\mathcal{D}_c\mathcal{D}_b\beta^a + \frac{1}{3}\tilde{h}^{bc}\mathcal{D}_c\mathcal{D}_b\beta^c = \\ - 2N\left[8\pi\Psi^4 p^a - \tilde{\varkappa}^{cb}\left(\tilde{\Gamma}_{cb}{}^a - \bar{\Gamma}_{cb}{}^a\right) - 6\tilde{\varkappa}^{ab}\mathcal{D}_b \ln\Psi + \frac{2}{3}\tilde{h}^{ab}\mathcal{D}_b K\right] \\ - 2\tilde{\varkappa}^{ab}\mathcal{D}_b N\,.\end{aligned} \tag{I.2.5}$$

Applications of the Dirac gauge has been made to various problems in the numerical relativity computation, cf. [380, 381, 382].

# Appendix J

# The Infinity and Asymptotic Flatness

We apply here the definition given by Ashtekar [383]. First we introduce the definition of spacetime infinity. There are three types of infinity: Time-like infinity, space-like infinity and light-like infinity, denoted by $\mathcal{I}^{\pm}$, $i^0$ and $\mathcal{J}^{\pm}$ respectively, where the + and − denote future and past Fig.J.2. In physics, time-like infinity implies infinitely long time, space-like infinity implies infinite distance, and null infinity implies the region (3 dimensional hypersurface) where a free photon can approach [384, 385, 386]. For the Minkowskian manifold, its metric is given as

$$\eta_{\mu\nu}\mathrm{d}x^{\mu}\mathrm{d}x^{\nu} = -\mathrm{d}t^2 + \mathrm{d}r^2 + r^2\left(\mathrm{d}\theta^2 + \sin^2\theta\mathrm{d}\varphi^2\right), \tag{J.0.1}$$

in a spherical coordinate $x^{\mu}$. Define the coordinate transformation as follow

$$u_1 = t + r\,, \tag{J.0.2}$$
$$u_2 = t - r\,, \tag{J.0.3}$$

where $-\infty < u_1 < \infty$, $-\infty < u_2 < \infty$. And another transformation given as

$$T = \arctan(u_1) + \arctan(u_2)\,, \tag{J.0.4}$$
$$R = \arctan(u_1) - \arctan(u_2)\,, \tag{J.0.5}$$

now equation (J.0.1) has the following form

$$\eta_{\mu\nu}\mathrm{d}x'^{\mu}\mathrm{d}x'^{\nu} = \frac{-\mathrm{d}T^2 + \mathrm{d}R^2 + \sin^2 R\,(\mathrm{d}\theta^2 + \sin^2\theta\mathrm{d}\varphi^2)}{4\cos^2[(T+R)/2]\cos^2[(T-R)/2]}\,, \tag{J.0.6}$$

where $-\pi < T + R < \pi$, $-\pi < T - R < \pi$ and $R \geq 0$. We need to expand the domain of $\eta$. Let a new metric $g$ given as

$$g_{\mu\nu}\mathrm{d}x'^{\mu}\mathrm{d}x'^{\nu} = -\mathrm{d}T^2 + \mathrm{d}R^2 + \sin^2 R\left(\mathrm{d}\theta^2 + \sin^2\theta\mathrm{d}\varphi^2\right), \tag{J.0.7}$$

and

$$\Omega = 2\cos[(T+R)/2]\cos[(T-R)]/2]\,, \tag{J.0.8}$$

we have

$$\Omega^2\eta_{\mu\nu} = g_{\mu\nu}\,. \tag{J.0.9}$$

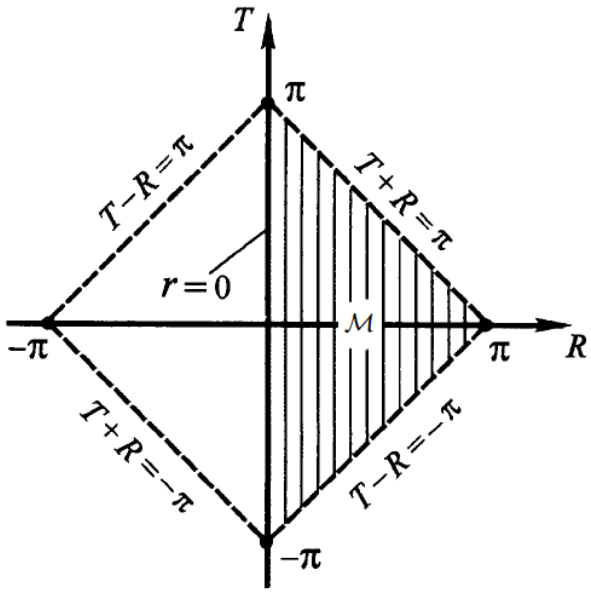


Figure J.1: The figure illustrates the embedding of a Minkowskian manifold in a $\mathbb{R}\times S^3$ manifold, the infinity region of Minkowskian manifold is conformally transformed to finite location in the ambient manifold, and $\mathcal{M}$ represents the region of the Minkowskian manifold. Credit [346].

For $g_{\mu\nu}$, we deduce that $T+R=\pi \Rightarrow |u_1|=\infty$ and $T-R=-\pi \Rightarrow |u_2|=\infty$. Now the original manifold $\mathbb{R}^{1,3}$ has been embedded in a 4 dimensional manifold Fig.J.1, given as

$$\phi:\ \mathbb{R}^{1,3}\to \mathbb{R}\times S^3\,, \tag{J.0.10}$$

the infinity region of Minkowskian manifold is now dragged to finite place, which are given as: The future time-like infinity $\mathcal{I}^+$ is $T=\pi$, $R=0$; the space-like infinity $i^0$ is $T=0$, $R=\pi$; the future light-like infinity $\mathcal{J}^+$ is $T+R=\pi$, $0<R<\pi$; the past time-like infinity $\mathcal{I}^-$ is $T=-\pi$, $R=0$; the past light-like infinity $\mathcal{J}^-$ is $T-R=-\pi$, $0<R<\pi$.

The asymptotically flat spacetime is considered along with the isolated system [387]. A definition proposed by Ashtekar is:

(a) For $(\mathcal{M}, g_{ab})$, there exists a spacetime $(\tilde{\mathcal{M}}, \tilde{g}_{ab})$, satisfies:
(a1) $\mathcal{M}\subset\tilde{\mathcal{M}}$.
(a2) $\exists\ i^0\in\tilde{\mathcal{M}}$, where $\bar{\mathrm{J}}^+(i^0)\cup\bar{\mathrm{J}}^-(i^0)=\tilde{\mathcal{M}}-\mathcal{M}$.
(a3) The metric $\tilde{g}_{ab}$ is $C^\infty$ in $\tilde{\mathcal{M}}-i^0$, and is $C^{>0}$ (cf. [346, 388]) at $i^0$.

(b) There exists a function $\Omega$ on $\tilde{\mathcal{M}}$, satisfies:
(b1) $\tilde{g}_{ab}=\Omega^2 g_{ab}$ on $\mathcal{M}$.
(b2) $\Omega$ is $C^\infty$ on $\tilde{\mathcal{M}}-i^0$, and is $C^2$ at $i^0$.
(b3) $\Omega|_{\mathcal{M}}>0$, $\Omega|_{\dot{\mathcal{M}}}=0$.
(b4) $\tilde{\nabla}_a\Omega|\mathcal{J}^\pm\neq 0$, $\lim_{p\to i^0}\tilde{\nabla}_a\Omega=0$.
(b5) $\lim_{p\to i^0}\tilde{\nabla}_a\tilde{\nabla}_c\Omega=2\tilde{g}_{ac}|_{i^0}$.

(c) $\partial\mathcal{M}$ has an open neighbourhood $Nei$, where $(Nei, \tilde{g}_{ab})$ satisfies the strongly causal condition.

where $\dot{\mathcal{M}}=\mathcal{J}^+\cup i^0\cup\mathcal{J}^-$, with $\mathcal{J}^\pm=\dot{\mathrm{J}}^\pm(i^0)-i^0$.

Further detail of the infinity and asymptotic flatness, refer to [19, 389].

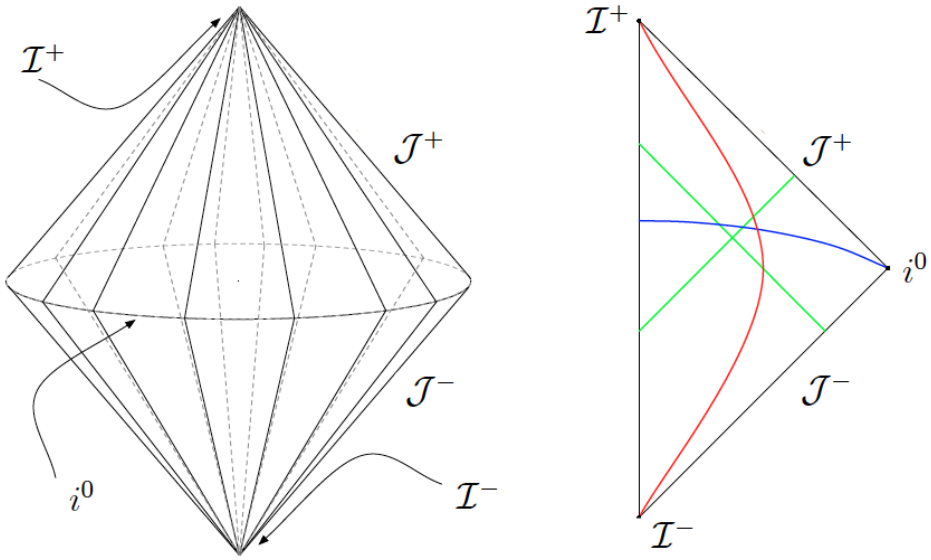


Figure J.2: The figure illustrates the Penrose diagram [390] of the conformal compactified Minkowskian manifold, where $\mathcal{I}^{\pm}$, $i^0$ and $\mathcal{J}^{\pm}$ represent the future (past) time-like infinity, spacelike-infinity and future (past) light-like infinity respectively. Red line denotes the time-like curve, blue line denotes space-like curve, and green lines denote null curve. Credit [391].

# Bibliography


[1] B. P. Abbott et al. (LIGO Scientific Collaboration and VIRGO Collaboration). "Observation of Gravitational Waves from a Binary Black Hole Merger". In: *Phys. Rev. D* **116**.061102 (2016).

[2] Z. Younsi, K. Wu, and S. V. Fuerst. "General Relativistic Radiative Transfer: Formulation and Emission from Structured Tori around Black Holes". In: *Astron. Astrophys.* **545**.A13 (2012).

[3] B. P. Abbott et al. (LIGO Scientific Collaboration and VIRGO Collaboration). "GW170817: Observation of Gravitational Waves from a Binary Neutron Star Inspiral". In: *Phys. Rev. D* **119**.161101 (2017).

[4] *LISA mission L3 proposal*. URL: `https://www.elisascience.org/files/publications/LISA%5C_L3%5C_20170120.pdf`.

[5] *The Next Generation Event Horizon Telescope Homepage*. URL: `https://www.ngeht.org`.

[6] R. Arnowitt, S. Deser, and C. W. Misner. "The Dynamics of General Relativity". In: *Gravitation: An Introduction to Current Research, edited by L. Witten, Wiley* (1962).

[7] F. H. Vincent, É. Gourgoulhon, and J. Novak. "3+1 Geodesic Equation and Images in Numerical Spacetimes". In: *Class. Quantum Grav.* **29**.245005 (2012).

[8] Z. Younsi. "General Relativistic Radiative Transfer in Black Hole Systems". In: *Ph.D Thesis, UCL* (2013).

[9] M. Janet. "Sur la Possibilité de Plonger un Espace Riemannien Donné Dans un Espace Euclidien". In: *Ann. Soc. Polon. Math.* **6**.1-7 (1927).

[10] C.-W. Shu and S. Osher. "Efficient Implementation of Essentially Non-Oscillatory Shock-Capturing Schemes II". In: *J. Comput. Phys.* **83**.32-78 (1989).

[11] K. P. Rauch and R. D. Blandford. "Optical Caustics in a Kerr Spacetime and the Origin of Rapid X-Ray Variability in Active Galactic Nuclei". In: *Astrophys. J.* **421**.46 (1994).

[12] V. Bozza. "Optical austics of Kerr Spacetime: The Full Structure". In: *Phys. Rev. D* **63**.063014 (2008).

[13] M. Patil, P. Mishra, and D. Narasimha. "Curious Case of Gravitational Lensing by Binary Black Holes: A Tale of Two Photon Spheres, New Relativistic Images, and Caustics". In: *Phys. Rev. D* **95**.024026 (2017).

[14] S. Osher and J. A. Sethian. “Fronts Propagating with Curvature Dependent Speed: Algorithms Based on Hamilton-Jacobi Formulations”. In: *J. Comput. Phys.* **79**.12-49 (1988).

[15] S. Osher and R. P. Fedkiw. “Level Set Methods and Dynamic Implicit Surfaces”. In: *Springer* (2003).

[16] J. W. York Jr. “Kinematics and Dynamics of General Relativity”. In: *Sources of Gravitational Radiation, edited by L. L. Smarr, Cambridge University Press* (1979).

[17] *Homepage of Einstein Toolkit*. URL: `https://einsteintoolkit.org/`.

[18] R. Penrose and W. Rindler. “Spinors and Space-Time Volume 1, Two-Spinor Calculus and Relativistic Fields”. In: *Cambridge Monographs on Math. Phys.* (2008).

[19] R. W. Wald. *General Relativity*. The University of Chicago Press, 1984.

[20] K. Schwarzschild. In: *Sitzungsber. K. Preuss. Akad. Wiss.* **1**.189 (1916).

[21] E. Newman and A. Janis. “Note on the Kerr Spinning-Particle Metric”. In: *J. Math.* **6**.915-917 (1965).

[22] E. Newman et al. “Metric of a Rotating, Charged Mass”. In: *J. Math.* **6**.918-919 (1965).

[23] H. Reissner. “Aber die Eigengravitation des Elektrischen Feldes nach der Einsteinschen Theorie”. In: *Annalen der Physik (in German)* **50**.106-120 (1916).

[24] H. Weyl. “Zur Gravitationstheorie”. In: *Annalen der Physik (in German)* **54**.117-154 (1917).

[25] G. Nordström. “On the Energy of the Gravitational Field in Einstein’s Theory”. In: *Verhandl. Koninkl. Ned. Akad. Wetenschap., Afdel. Natuurk.* **26**.1201-1208 (1918).

[26] G. B. Jeffery. “The Field of an Electron on Einstein’s Theory of Gravitation”. In: *Proc. R. Soc. Lond. A* **99**.123-134 (1921).

[27] R. Penrose. “Gravitational Collapse and Space-Time Singularities”. In: *Phys. Rev. Lett.* **14**.57-59 (1965).

[28] S. W. Hawking. “The Occurrence of Singularities in Cosmology”. In: *Proc. R. Soc. Lond. A* **294**.511-521 (1966).

[29] S. W. Hawking. “The Occurrence of Singularities in Cosmology. II”. In: *Proc. R. Soc. Lond. A* **295**.490-493 (1966).

[30] R. Penrose. “Gravitational Collapse: The Role of General Relativity”. In: *Riv. Nuovo Cim.* **1**.252-276 (1969).

[31] S. W. Hawking. “The Occurrence of Singularities in Cosmology. III. Causality and Singularities”. In: *Proc. R. Soc. Lond. A* **300**.187-201 (1967).

[32] S. W. Hawking and R. Penrose. “The Singularities of Gravitational Collapse and Cosmology”. In: *Proc. R. Soc. Lond. A* **314**.529-548 (1970).

[33] The Event Horizon Telescope Collaboration et al. “First M87 Event Horizon Telescope Results. I. The Shadow of the Supermassive Black Hole”. In: *Astrophys. J. Lett.* **875**.L1 (2019).

[34] The Event Horizon Telescope Collaboration et al. “First M87 Event Horizon Telescope Results. II. Array and Instrumentation”. In: *Astrophys. J. Lett.* **875**.L2 (2019).

[35] The Event Horizon Telescope Collaboration et al. “First M87 Event Horizon Telescope Results. III. Data Processing and Calibration”. In: *Astrophys. J. Lett.* **875**.L3 (2019).

[36] The Event Horizon Telescope Collaboration et al. “First M87 Event Horizon Telescope Results. IV. Imaging the Central Supermassive Black Hole”. In: *Astrophys. J. Lett.* **875**.L4 (2019).

[37] The Event Horizon Telescope Collaboration et al. “First M87 Event Horizon Telescope Results. V. Physical Origin of the Asymmetric Ring”. In: *Astrophys. J. Lett.* **875**.L5 (2019).

[38] The Event Horizon Telescope Collaboration et al. “First M87 Event Horizon Telescope Results. VI. The Shadow and Mass of the Central Black Hole”. In: *Astrophys. J. Lett.* **875**.L6 (2019).

[39] The Event Horizon Telescope Collaboration et al. “First M87 Event Horizon Telescope Results. VII. Polarization of the Ring”. In: *Astrophys. J. Lett.* **910**.L12 (2021).

[40] The Event Horizon Telescope Collaboration et al. “First M87 Event Horizon Telescope Results. VIII. Magnetic Field Structure near The Event Horizon”. In: *Astrophys. J. Lett.* **910**.L13 (2021).

[41] The Event Horizon Telescope Collaboration et al. “First Sagittarius A* Event Horizon Telescope Results. I. The Shadow of the Supermassive Black Hole in the Center of the Milky Way”. In: *Astrophys. J. Lett.* **930**.L12 (2022).

[42] The Event Horizon Telescope Collaboration et al. “First Sagittarius A* Event Horizon Telescope Results. II. EHT and Multiwavelength Observations, Data Processing, and Calibration”. In: *Astrophys. J. Lett.* **930**.L13 (2022).

[43] The Event Horizon Telescope Collaboration et al. “First Sagittarius A* Event Horizon Telescope Results. III. Imaging of the Galactic Center Supermassive Black Hole”. In: *Astrophys. J. Lett.* **930**.L14 (2022).

[44] The Event Horizon Telescope Collaboration et al. “First Sagittarius A* Event Horizon Telescope Results. IV. Variability, Morphology, and Black Hole Mass”. In: *Astrophys. J. Lett.* **930**.L15 (2022).

[45] The Event Horizon Telescope Collaboration et al. “First Sagittarius A* Event Horizon Telescope Results. V. Testing Astrophysical Models of the Galactic Center Black Hole”. In: *Astrophys. J. Lett.* **930**.L16 (2022).

[46] The Event Horizon Telescope Collaboration et al. “First Sagittarius A* Event Horizon Telescope Results. VI. Testing the Black Hole Metric”. In: *Astrophys. J. Lett.* **930**.L17 (2022).

[47] L. Medeiros et al. “The Image of the M87 Black Hole Reconstructed with PRIMO”. In: *Astrophys. J. Lett.* **947**.L7 (2023).

[48] A. Einstein and N. Rosen. “On Gravitational Waves”. In: *J. of the Franklin Institute* **223**.1 (1937).

[49] P. C. Peters and J. Mathews. “Gravitational Radiation from Point Masses in a Keplerian Orbit”. In: *Phys. Rev.* **131**.435-440 (1963).

[50] P. C. Peters. “Gravitational Radiation and the Motion of Two Point Masses”. In: *Phys. Rev.* **136**.B1224-B1232 (1964).

[51] M. Alcubierre. “Introduction to 3+1 Numerical Relativity”. In: *Oxford Science Publications* (2008).

[52] B. P. Abbott et al. (LIGO Scientific Collaboration and VIRGO Collaboration). “GW151226: Observation of Gravitational Waves from a 22-Solar-Mass Binary Black Hole Coalescence”. In: *Phys. Rev. Lett.* **116**.241103 (2016).

[53] B. P. Abbott et al. (LIGO Scientific Collaboration and VIRGO Collaboration). “GW170104: Observation of a 50-Solar-Mass Binary Black Hole Coalescence at Redshift 0.2”. In: *Phys. Rev. Lett.* **118**.221101 (2017).

[54] B. P. Abbott et al. (LIGO Scientific Collaboration and VIRGO Collaboration). “GW170814: A Three-Detector Observation of Gravitational Waves from a Binary Black Hole Coalescence”. In: *Phys. Rev. Lett.* **119**.141101 (2017).

[55] B. P. Abbott et al. (LIGO Scientific Collaboration and VIRGO Collaboration). “GW170608: Observation of a 19-Solar-Mass Binary Black Hole Coalescence”. In: *Astrophys. J. Lett.* **851**.L35 (2017).

[56] B. P. Abbott et al. (LIGO Scientific Collaboration and VIRGO Collaboration). “GWTC-1: A Gravitational-Wave Transient Catalog of Compact Binary Mergers Observed by LIGO and Virgo during the First and Second Observing Runs”. In: *Phys. Rev. X* **9**.031040 (2019).

[57] B. P. Abbott et al. (LIGO Scientific Collaboration and VIRGO Collaboration). “GW190425: Observation of a Compact Binary Coalescence with Total Mass $\sim 3.4 M_{\odot}$”. In: *Astrophys. J. Lett.* **892**.L3 (2020).

[58] R. Abbott et al. (LIGO Scientific Collaboration and VIRGO Collaboration). “GW190412: Observation of a Binary-Black-Hole Coalescence with Asymmetric Masses”. In: *Phys. Rev. D* **102**.043015 (2020).

[59] R. Abbott et al. (LIGO Scientific Collaboration and VIRGO Collaboration). “GW190814: Gravitational Waves from the Coalescence of a 23 Solar Mass Black Hole with a 2.6 Solar Mass Compact Object”. In: *Astrophys. J. Lett.* **896**.2 (2020).

[60] R. Abbott et al. (LIGO Scientific Collaboration and VIRGO Collaboration). “GW190521: A Binary Black Hole Merger with a Total Mass of $150 M_{\odot}$”. In: *Phys. Rev. Lett.* **125**.101102 (2020).

[61] R. Abbott et al. (LIGO Scientific Collaboration and VIRGO Collaboration). "Observations of Gravitational Waves from Two Neutron Star-Black Hole Coalescences". In: *Astrophys. J. Lett.* **915**.L5 (2021).

[62] R. Abbott et al. (LIGO Scientific Collaboration and VIRGO Collaboration). "Population of Merging Compact Binaries Inferred Using Gravitational Waves through GWTC-3". In: *Phys. Rev. X* **13**.011048 (2022).

[63] A. A. Abramovici et al. "LIGO: The Laser Interferometer Gravitational-Wave Observatory". In: *Sci.* **256**.325-333 (1992).

[64] T. Accadia et al. "Status of the Virgo Project". In: *Class. Quantum Grav.* **28**.114002 (2011).

[65] K. Kurado and the LCGT Collaboration. "Status of LCGT". In: *Class. Quantum Grav.* **27**.084004 (2010).

[66] Y. Aso et al. "Interferometer Design of the KAGRA Gravitational Wave Detector". In: *Phys. Rev. D* **88**.043007 (2013).

[67] Y.-Z. Zhang et al. "Taiji Program: Gravitational-Wave Sources". In: *Int. J. Mod. Phys. A* **35**.2050075 (2020).

[68] D. E. Mcclelland et al. "Second-Generation Laser Interferometry for Gravitational Wave Detection: ACIGA Progress". In: *Class. Quantum Grav.* **18**.4121-4126 (2001).

[69] J. Luo et al. "TianQin: A Space-Borne Gravitational Wave Detector". In: *Class. Quantum Grav.* **33**.035010 (2016).

[70] S. Kawamura et al. "The Japanese Space Gravitational Wave Antenna-DECIGO". In: *J. Phys.: Conf. Ser.* **33**.035010 (2008).

[71] M. Punturo et al. "The Einstein Telescope: A Third-Generation Gravitational Wave Observatory". In: *Class. Quantum Grav.* **27**.194002 (2010).

[72] K. Danzmann et al. "LISA: Laser Interferometer Space Antenna for Gravitational Wave Measurements". In: *Class. Quantum Grav.* **13**.A247-A250 (1996).

[73] S. Hild. "Beyond the Second Generation of Laser-Interferometric Gravitational Wave Observatories". In: *Class. Quantum Grav.* **29**.124006 (2011).

[74] M. Punturo et al. "The Third Generation of Gravitational Wave Observatories and Their Science Reach". In: *Class. Quantum Grav.* **27**.084007 (2010).

[75] A. Einstein. "Näherungsweise Integration der Feldglerchungen der Gravitation". In: *Sitzungsberichte der Königlich Preussischen Akademie der Wissenschaften Berlin, part 1* 688-696 (1916).

[76] A. Einstein. "Über Gravitationswellen". In: *Sitzungsberichte der Königlich Preussischen Akademie der Wissenschaften Berlin, part 1* 154-167 (1918).

[77] A. Einstein. In: *Sitzungsber. K. Preuss. Akad. Wiss.* **1**.688 (1916).

[78] P. R. Saulson. “Josh Goldberg and the Physical Reality of Gravitational Waves”. In: *Gen. Rel. Grav.* **43**.3289-3299 (2011).

[79] R. P. Kerr. “Gravitational Field of a Spinning Mass as an Example of Algebraically Special Metrics”. In: *Phys. Rev. Lett.* **11**.237-238 (1963).

[80] C. V. Vishveshwara. “Scattering of Gravitational Radiation by a Schwarzschild Black-Hole”. In: *Nat.* **227**.936-938 (1970).

[81] W. H. Press. “Long Wave Trains of Gravitational Waves from a Vibrating Black Hole”. In: *Astrophys. J.* **170**.L105 (1971).

[82] S. Chandrasekhar and S. L. Detweiler. “The Quasi-Normal Modes of the Schwarzschild Black Hole”. In: *Proc. R. Soc. Lond. A* **344**.441-452 (1975).

[83] L. Blanchet et al. “Gravitational-Radiation Damping of Compact Binary Systems to Second Post-Newtonian Order”. In: *Phys. Rev. Lett.* **74**.3515-3518 (1995).

[84] L. Blanchet. “Gravitational Radiation from Post-Newtonian Sources and Inspiralling Compact Binaries”. In: *Living Rev. Rel.* **17**.2 (2014).

[85] A. Buonanno and T. Damour. “Effective One-Body Approach to General Relativistic Two-Body Dynamics”. In: *Phys. Rev. D* **59**.084006 (1999).

[86] F. Pretorius. “Evolution of Binary Black-Hole Spacetimes”. In: *Phys. Rev. Lett.* **95**.121101 (2005).

[87] M. Campanelli et al. “Accurate Evolutions of Orbiting Black-Hole Binaries without Excision”. In: *Phys. Rev. Lett.* **96**.111101 (2006).

[88] J. Weber. “Detection and Generation of Gravitational Waves”. In: *Phys. Rev.* **117**.306-313 (1960).

[89] M. E. Gertsenshtein and V. I. Pustovoit. “On the Detection of Low Frequency Gravitational Waves”. In: *Sov. Phys. JETP* **16**.433 (1962).

[90] G. E. Moss, L. R. Miller, and R. L. Forward. “Photon-Noise-Limited Laser Transducer for Gravitational Antenna”. In: *Appl. Opt.* **10**.2495 (1971).

[91] J. Aasi et al. “The LIGO Scientific Collaboration”. In: *Class. Quantum Grav.* **32**.074001 (2015).

[92] F. Acernese et al. “Advanced Virgo: A Second-Generation Interferometric Gravitational Wave Detector”. In: *Class. Quantum Grav.* **32**.024001 (2015).

[93] C. Affeldt et al. “Advanced Techniques in GEO 600”. In: *Class. Quantum Grav.* **31**.224002 (2014).

[94] P. Amaro-Seoan et al. “Astrophysics with the Laser Interferometer Space Antenna”. In: *Living Rev. Rel.* **26**.2 (2023).

[95] K. G. Arun et al. “New Horizon for Fundamental Physics with LISA”. In: *Living Rev. Rel.* **25**.4 (2022).

[96] M. Branchesi. “Multi-Messenger Astronomy: Gravitational Waves, Neutrinos, Photons, and Cosmic Rays”. In: *J. Phys.: Conf. Ser.* **718**.022004 (2016).

[97] A. Ricciardone. “Primordial Gravitational Waves with LISA”. In: *J. Phys.: Conf. Ser.* **840**.012030 (2016).

[98] D. Espriu and M. Rodoreda. “Effects of the Cosmological Parameters on Gravitational Waves: General Analysis”. In: *Class. Quantum Grav.* **39**.015012 (2022).

[99] H. Poincaré. “Sur la Dynamique de l’électron”. In: *Comptes Rendus de l’Académie des Sciences* **140**.1504-1508 (1905).

[100] S. A. Eddington. “The Propagation of Gravitational Waves”. In: *Proc. R. Soc. Lond.* **102**.262-282 (1922).

[101] H. Bondi, M. G. J. Van der Burg, and A. W. K. Metzner. “Gravitational Waves in General Relativity, VII. Waves from Axi-Symmetric Isolated System”. In: *Proc. R. Soc. A* **269**.21-52 (1962).

[102] L. Marochnik. “Dark Energy and Inflation in a Gravitational Wave Dominated Universe”. In: *Grav. Cosmol.* **22**.10-19 (2016).

[103] M. C. Guzzetti et al. “Gravitational Waves from Inflation”. In: *Rivista del Nuovo Cim.* **39**.399-495 (2016).

[104] B. P. Abbott et al. (LIGO Scientific Collaboration and Virgo Collaboration). “Multi-Messenger Observations of a Binary Neutron Star Merger”. In: *Astrophys. J. Lett.* **848**.L12 (2017).

[105] Y.-C. Pan et al. “The Old Host-Galaxy Environment of SSS17a, the First Electromagnetic Counterpart to a Gravitational-Wave Source”. In: *Astrophys. J.* **848**.L30 (2017).

[106] B. Vaishnav et al. “Matched Filtering of Numerical Relativity Templates of Spinning Binary Black Holes”. In: *Phys. Rev. D* **76**.084020 (2007).

[107] S. V. Fuerst and K. Wu. “Radiative Transfer of Emission Lines in Curved Space-Time”. In: *Astron. Astrophys.* **424**.733-746 (2004).

[108] S. Ronchini et al. “Perspectives for Multi-Messenger Astronomy with the Next Generation of Gravitational-Wave Detectors and High-Energy Satellites”. In: *Astron. Astrophys.* **665**.A97 (2022).

[109] H.-Y. Pu et al. “Odyssey: A Public GPU-Based Code for General Relativistic Radiative Transfer in Kerr Spacetime”. In: *Astrophys. J.* **820**.105 (2016).

[110] R. C. Tolman. “Static Solutions of Einstein’s Field Equations for Spheres of Fluid”. In: *Phys. Rev.* **55**.364-373 (1939).

[111] J. R. Oppenheimer and G. M. Volkoff. “On Massive Neutron Cores”. In: *Phys. Rev.* **55**.374-381 (1939).

[112] S. V. Fuerst. “General Relativistic Radiative Transfer”. In: *Ph.D Thesis, UCL* (2007).

[113] S. Chandrasekhar. “Radiative Transfer”. In: *New York: Dover* (1963).

[114] G. B. Rubichi and A. P. Lightman. “Radiative Processes in Astrophysics”. In: *Wiley-Interscience: New York* (1979).

[115] C. W. Misner, K. S. Thorne, and J. A. Wheeler. “Gravitation”. In: *W. H. Freeman and Company* (1973).

[116] B. Carter. “Global Structure of the Kerr Family of Gravitational Fields”. In: *Phys. Rev.* **174**.1559-1571 (1968).

[117] A. Friedmann. “Über die Krümmung des Raumes”. In: *Z. Physik* **10**.377-386 (1922).

[118] A. Friedmann. “Über die Möglichkeit einer Welt Mit Konstanter Negativer Krümmung des Raumes”. In: *Z. Physik* **21**.326-332 (1924).

[119] G. Lemaître. “Expansion of the Universe, A Homogeneous Universe of Constant Mass and Increasing Radius Accounting for the Radial Velocity of Extra-Galactic Nebulæ”. In: *Mon. Not. R. Astron. Soc.* **91**.483-490 (1931).

[120] G. Lemaître. “L’Univers en Expansion”. In: *Annales de la Société Scientifique de Bruxelles A* **53**.51-58 (1924).

[121] H. P. Robertson. “Kinematics and World Structure”. In: *Astrophys. J.* **82**.284-301 (1935).

[122] H. P. Robertson. “Kinematics and World Structure II”. In: *Astrophys. J.* **83**.187-201 (1936).

[123] H. P. Robertson. “Kinematics and World Structure III”. In: *Astrophys. J.* **83**.257-271 (1936).

[124] A. G. Walker. “On Milne’s Theory of World-Structure”. In: *Proc. Lond. Math. Soc.* **42**.90-127 (1937).

[125] A. G. Lemaître and A. S. Eddington. “The Expanding Universe”. In: *Mon. Not. R. Astron. Soc.* **91**.490-501 (1931).

[126] A. G. Lemaître. “The Expanding Universe”. In: *Gen. Rel. Grav.* **29**.641-680 (1997).

[127] J. Thornburg. “Event and Apparent Horizon Finders for 3+1 Numerical Relativity”. In: *Living Rev. Rel.* **10**.3 (2007).

[128] K. Destounis, A. G. Suvorov, and K. D. Kokkotas. “Gravitational Wave Glitches in Chaotic Extreme-Mass-Ratio Inspirals”. In: *Phys. Rev. D* **126**.141102 (2021).

[129] K. Hashimoto and K. Sugiura. “Causality Bounds Chaos in Geodesic Motion”. In: *Phys. Rev. D* **107**.066005 (2023).

[130] X. Wu et al. “Explicit Symplectic Methods in Black Hole Spacetimes”. In: *Astrophys. J.* **940**.166 (2022).

[131] S. Osher and C.-W. Shu. “High-Order Essentially NonOscillatory Schemes for Hamilton-Jacobi Equations”. In: *J. Numer. Anal.* **28**.907-922 (1991).

[132] Y. L. Zhang et al. “3D Jet Impact and Toroidal Bubbles”. In: *J. Comput. Phys.* **166**.336-360 (2001).

[133] R. Kimmel, A. Amir, and A. M. Bruckstein. "Finding Shortest Paths on Surfaces Using Level Sets Propagation". In: *IEEE-PAMI* **17**.635-640 (1995).

[134] C.-W. Shu and S. Osher. "Efficient Implementation of Essentially Non-Oscillatory Shock-Capturing Schemes". In: *J. Comput. Phys.* **77**.439-471 (1988).

[135] S. Gottlieb and C.-W. Shu. "Total Variation Diminishing Runge-Kutta Schemes". In: *Math. Comput.* **67**.73-85 (1998).

[136] C. L. Epstein and M. Gage. "The Curve Shortening Flow". In: *Wave Motion: Theor. Mo. Comput., edited by A. J. Chorin and A. J. Majda* **7**.15-59 (1987).

[137] R. Kimmel, A. Amir, and A. M. Bruckstein. "Finding Shortest Paths on Graph Surfaces". In: *CIS Rep. #9301, Technion-Israel Institute of Technology, Israel* (1993).

[138] C. Stöcker and A. Voigt. "Geodesic Evolution LawsA Level-Set Approach". In: *J. Imaging Sci.* **1**.379-399 (2008).

[139] F. Dowker. "Causal Sets and the Deep Structure of Spacetime". In: *A. Ashtekar (edited) 100 Years of Relativity: space-time structure: Einstein and beyond, World Scientific* (2005).

[140] J. Henson. "Constructing an Interval of Minkowski Space from a Causal Set". In: *Class. Quantum Grav.* **23**.4 (2006).

[141] P. Wallden. "Causal Sets Dynamics: Review & Outlook". In: *J. Phys.: Con. Ser.* **453**.012023 (2013).

[142] F. Dowker, J. Henson, and R. D. Sorkin. "Quantum Gravity Phenomenology, Lorentz Invariance and Discreteness". In: *Mod. Phys. Lett. A* **19**.1829-1840 (2004).

[143] A. A. Sheykin, D. A. Grad, and S. A. Paston. "Embeddings of the Black Holes in a Flat Space". In: *Proc. Sci.* **QFTHEP2013**.091 (2014).

[144] S. A. Paston and A. A. Sheykin. "Embeddings for Schwarzschild Metric: Classification and New Results". In: *Class. Quantum Grav.* **29**.095022 (2012).

[145] H. L. Bray. "On the Positive Mass, Penrose, an ZAS Inequalities in General Dimension". In: *Surv. Geom. Anal. Rel. ALM* **20** (2011).

[146] L.-H. Huang and D. Wu. "The Equality Case of the Penrose Inequality for Asymptotically Flat Graphs". In: *Trans. Amer. Math. Soc.* **367**.31-47 (2015).

[147] J. F. Nash. "$C^1$-Isometric Imbeddings". In: *Ann. Math.* **60**.383-396 (1954).

[148] J. F. Nash. "The Imbedding Problems for Riemannian Manifolds". In: *Ann. Math.* **63**.20-63 (1965).

[149] J. F. Nash. "Analyticity of the Solutions of Implicit Function Problem with Analytic Data". In: *Ann. Math.* **84**.345-355 (1966).

[150] E. Kasner. "The Impossibility of Einstein Fields Immersed in Flat Space of Five Dimensions". In: *Amer. J. Math.* **48**.126-129 (1921).

[151] E. Cartan. “Sur la Possibilité de Plonger un Espace Riemannien Donné Dans un Espace Euclidéen”. In: *Ann. Soc. Polon. Math.* **5**.38-43 (1926).

[152] A. Friedman. “Local Isometric Embedding of Riemannian Manifolds with Indefinite Metrics”. In: *J. Math. Mech.* **10**.625-649 (1961).

[153] H. Stephani et al. “Exact Solutions of Einstein’s Field Equations”. In: *2nd Edition, Cambridge University Press* (2003).

[154] R. R. Kuzeev. “Gravitatsiya i Teoriya Otnositelnosti”. In: *Ann. Soc. Polon. Math.* **18**.75 (1981).

[155] N. J. Hicks. “Notes on Differential Geometry”. In: *Van Norstrand Math. Studies* 3 (1965).

[156] C.-B. Liang and B. Zhou. “Introduction to Differential Geometry and General Relativity”. In: *Second Edition, Volume 1, NFAPST, Science Press of China* (2006).

[157] S. W. Hawking and G. F. R. Ellis. “The Large Scale Structure of Space-Time”. In: *Cambridge University Press* (1973).

[158] M. D. Spivak. “A Comprehensive Introduction to Differential Geometry. Vol. I, II, III, IV and V”. In: *2nd Edition Publish or Perish, Inc.* (1979).

[159] M. L. Gromov. “Partial Differential Relations”. In: *Ergebnisse der Mathematik und ihrer Grenzgebiete 3, Results in Mathematics and Related Areas 3* **9** (1986).

[160] C. De Lellis and L. Székelyhidi Jr. “High Dimensionality and h-Principle in PDE”. In: *Bull. Amer. Math. Soc.* **54**.247-282 (2017).

[161] J. E. Campbell. “A Course of Differential Geometry”. In: *Clarendon Press, Oxford* (1926).

[162] L. Magaard. “Zur Einbettung Riemannscher Räume in Einstein-Räume und Konform-Euclidische Räume”. In: *Ph.D Thesis, University of Kiel* (1963).

[163] C. Romero, R. K. Tavakol, and R. Zalaletdinov. “The Embedding of General Relativity in Five Dimensions”. In: *Gen. Rel. Grav.* **28**.265-276 (1996).

[164] J. E. Lidsey et al. “On Applications of Campbell’s Embedding Theorem”. In: *Class. Quantum Grav.* **14**.865-879 (1997).

[165] M. Dunajski and P. Tod. “Conformally Isometric Embeddings and Hawking Temperature”. In: *Class. Quantum Grav.* **36**.125005 (2019).

[166] J. R. Oppenheimer and H. Snyder. “On Continued Gravitational Contraction”. In: *Phys. Rev.* **56**.455-459 (1939).

[167] G. Darmois. “Les Équations de la Gravitation Einsteinienne”. In: *Mémorial des Sciences Mathématiques **25**, Gauthier-Villars, Paris* (1927).

[168] A. Lichnerowicz. “Sur Certains Problèmes Globaux Relatifs au Système des Équations d’Einstein”. In: *Hermann, Paris, Actual. Sci. Ind.* **833** (1939).

[169] A. Lichnerowicz. “L’intégration des Équations de la Gravitation Relativiste et le Problème des n Corp”. In: *J. Math. Pures Appl.* 23.37 (1944).

[170] A. Lichnerowicz. “Sur les Équations Relativistes de la Gravitation”. In: *Bulletin de la S.M.F.* 80.237 (1952).

[171] Y. Fourès-Bruhat (Y. Choquet-Bruhat). “Théorème d’Existence pour Certains Systèms d’Équations aux Dérivées Partielles non Linéaires”. In: *Acta Mathematica* 88.141 (1952).

[172] Y. Fourès-Bruhat (Y. Choquet-Bruhat). “Sur l’Intégration des Équations de la Relativité Générale”. In: *J. Rational Mech. Anal.* 5.951 (1956).

[173] P. A. M. Dirac. “The Theory of Gravitation in Hamiltonian Form”. In: *Proc. R. Soc. Lond. A* 246.333-343 (1958).

[174] P. A. M. Dirac. “Fixation of Coordinates in the Hamiltonian Theory of Gravitation”. In: *Phys. Rev.* 114.924-930 (1959).

[175] R. Arnowitt, S. Deser, and C. W. Misner. “Dynamical Structure and Definition of Energy in General Relativity”. In: *Phys. Rev.* 116.1322-1330 (1959).

[176] R. Arnowitt and S. Deser. “Quantum Theory of Gravity: General Formulation and Linearized Theory”. In: *Phys. Rev.* 113.745-750 (1959).

[177] R. Arnowitt, S. Deser, and C. W. Misner. “Canonical Variables for General Relativity”. In: *Phys. Rev.* 117.1595-1602 (1960).

[178] R. Arnowitt, S. Deser, and C. W. Misner. “Finite Self-Energy of Classical Point Particles”. In: *Phys. Rev. Lett.* 4.375-377 (1960).

[179] R. Arnowitt, S. Deser, and C. W. Misner. “Energy and the Criteria for Radiation in General Relativity”. In: *Phys. Rev.* 118.1100-1104 (1960).

[180] R. Arnowitt, S. Deser, and C. W. Misner. “Gravitational-Electromagnetic Coupling and the Classical Self-Energy Problem”. In: *Phys. Rev.* 120.313-320 (1960).

[181] R. Arnowitt, S. Deser, and C. W. Misner. “Interior Schwarzschild Solutions and Interpretation of Source Terms”. In: *Phys. Rev.* 120.321-324 (1960).

[182] R. Arnowitt, S. Deser, and C. W. Misner. “Wave Zone in General Relativity”. In: *Phys. Rev.* 121.1556-1566 (1961).

[183] R. Arnowitt, S. Deser, and C. W. Misner. “Coordinate Invariance and Energy Expressions in General Relativity”. In: *Phys. Rev.* 122.997-1006 (1961).

[184] R. Arnowitt, S. Deser, and C. W. Misner. “epublication of: The Dynamics of General Relativity”. In: *Gen. Rel. Grav.* 40.1997 (2008).

[185] J. W. York Jr. “Conformally Invariant Orthogonal Decomposition of Symmetric Tensors on Riemannian Manifolds and the Initial-Value Problem of General Relativity”. In: *J. Math. Phys.* 14.456-464 (1973).

[186] L. Smarr. “Space-Times Generated by Computers: Black Holes with Gravitational Radiation”. In: *Ann. New York Acad. Sci.* 302.569-604 (1977).

[187] T. Nakamura, K. Oohara, and Y. Kojima. “General Relativistic Collapse to Black Holes and Gravitational Waves from Black Holes”. In: *Prog. Theor. Phys. Suppl.* 90.1-218 (1987).

[188] T. Nakamura. “3D Numerical Relativity”. In: *Relativistic Cosmology, Proc. of the 8th Nishinomiya-Yukawa Memorial Symposium, edited by M. Sasaki, Universal Acad. Press* 155 (1994).

[189] M. Shibata and T. Nakamura. “Evolution of Three-Dimensional Gravitational Waves: Harmonic Slicing Case”. In: *Phys. Rev. D* 52.5428-5444 (1995).

[190] T. W. Baumgarte and S. L. Shapiro. “Numerical Integration of Einstein’s Field Equations”. In: *Phys. Rev. D* 59.024007 (1999).

[191] M. Alcubierre et al. “Gauge Conditions for Long-Term Numerical Black Hole Evolutions without Excision”. In: *Phys. Rev. D* 67.084023 (2003).

[192] B. Brügmann M. Ansorg and W. Tichy. “Single-Domain Spectral Method for Black Hole Puncture Data”. In: *Phys. Rev. D* 70.064011 (2004).

[193] S. A. Teukolsky. “Formulation of Discontinuous Galerkin Methods for Relativistic Astrophysics”. In: *J. Comput. Phys.* 312.333-356 (2016).

[194] M. Dumbser et al. “Conformal and Covariant Z4 Formulation of the Einstein Equations: Strongly Hyperbolic First-Order Reduction and Solution with Discontinuous Galerkin Schemes”. In: *Phys. Rev. D* 97.084053 (2018).

[195] J. Winicour. “Characteristic Evolution and Matching”. In: *Living Rev. Rel.* 15.2 (2012).

[196] J. Frauendiener and H. Friedrich. “The Conformal Structure of Space-Time: Geometry, Analysis, Numerics”. In: *Lect. Notes Phys.* 604.Heidelberg (2002).

[197] J. Frauendiener. “Conformal Infinity”. In: *Living Rev. Rel.* 7.1 Original paper [392] (2004).

[198] F. Pretorius. “Numerical Relativity Using a Generalized Harmonic Decomposition”. In: *Class. Quantum Grav.* 2.425-451 (2005).

[199] F. Pretorius. “Evolution of Binary Black-Hole Spacetimes”. In: *Phys. Rev. Lett.* 95.121101 (2005).

[200] F. Pretorius. “Simulation of Binary Black Hole Spacetimes with a Harmonic Evolution Scheme”. In: *Class. Quantum Grav.* 24.S529-S552 (2006).

[201] É. Gourgoulhon. "3+1 Formalism in General Relativity: Bases of Numerical Relativity". In: *Springer* (2012).

[202] S. M. Carroll. "Spacetime and Geometry: An Introduction to General Relativity". In: *Addison Wesley (Pearson Education), San Fransisco* (2004).

[203] E. Poisson. "A Relativist's Toolkit, The Mathematics of Black-Hole Mechanics". In: *Cambridge University Press* (2004).

[204] M. Berger. "A Panoramic View of Riemannian Geometry". In: *Springer* (2003).

[205] K. S. Thorne and D. Macdonald. "Electrodynamics in Curved Spacetime: 3+1 Formulation". In: *Mon. Not. R. Astron. Soc.* 198.339-343 (1982).

[206] D. R. Brill and R. W. Lindquist. "Interaction Energy in Geometrostatics". In: *Phys. Rev.* 131.471-476 (1963).

[207] R. A. Matzner et al. "Geometry of a Black Hole Collision". In: *Sci.* 270.941-947 (1995).

[208] C. W. Misner. "Wormhole Initial Conditions". In: *Phys. Rev.* 118.1110-1111 (1960).

[209] H. Chan. "Embedding Misner and Brill-Lindquist Initial Data for Black-Hole Collisions". In: *Math. Phys., Anal. Geom.* 6.9-27 (2003).

[210] D. M. Shoemaker et al. "Generic Tracking of Multiple Apparent Horizons with Level Flow". In: *Phys. Rev. D* 62.124005 (2000).

[211] A. Cadez. "Apparent Horizons in the Two-Black-Hole Problem". In: *Ann. Phys.* 83.449-457 (1974).

[212] M. Alcubierre et al. "Test-Beds and Applications for Apparent Horizon Finders in Numerical Relativity". In: *Class. Quantum Grav.* **17**.2159-2190 (2000).

[213] M. F. Huq. "Apparent Horizons in Numerical Spacetimes". In: *Ph.D Thesis, University of Texas* (1996).

[214] J. Thornburg. "A Fast Apparent Horizon Finder for Three-Dimensional Cartesian Grids in Numerical Relativity". In: *Class. Quantum Grav.* **21**.743-766 (2004).

[215] L.-M. Lin and J. Novak. "A New Spectral Apparent Horizon Finder for 3D Numerical Relativity". In: *Class. Quantum Grav.* **24**.2665-2676 (2007).

[216] F. Löffler et al. "The Einstein Toolkit: A Community Computational Infrastructure for Relativistic Astrophysics". In: *Class. Quantum Grav.* **29**.115001 (2012).

[217] M. Zilhão and F. Löffler. "An Introduction to the Einstein Toolkit". In: *Int. J. Mod. Phys. A* **28**.1340014 (2013).

[218] A. M. Abrhams and R. H. Price. "Black-Hole Collisions from Brill-Lindquist Initial Data: Predictions of Perturbation Theory". In: *Phys. Rev. D* **53**.1972-1976 (1996).

[219] P. Anninos et al. “The Head-on Collision of Two Equal Mass Black Holes: Numerical Methods”. In: *arXiv: 9408042 [gr-qc]* (1994).

[220] Z. B. Etienne and I. Ruchlin. “NRPy+: Code Generator for Numerical Relativity”. In: *Astrophys. Source Code Library* ascl.1807.025 (2018).

[221] I. Ruchlin, Z. B. Etiennie, and T. W. Baumgarte. “SENR/NRPy+: Numerical Relativity in Singular Curvilinear Coordinate Systems”. In: *Phys. Rev. D* **97**.064036 (2018).

[222] I. Ruchlin, Z. B. Etiennie, and T. W. Baumgarte. “SENR: Simple, Efficient Numerical Relativity”. In: *Astrophys. Source Code Library* ascl.1807.026 (2018).

[223] M. F. Huq, M. W. Choptuik, and R. A. Matzner. “Locating Boosted Kerr and Schwarzschild Apparent Horizons”. In: *Phys. Rev. D* **66**.084024 (2002).

[224] Y. Fourès-Bruhat (Y. Choquet-Bruhat). “New Elliptic System and Global Solutions for the Constraints Equations in General Relativity”. In: *Commun. Math. Phys.* **21**.211-218 (1971).

[225] J. W. York Jr. “Mapping onto Solutions of the Gravitational Initial Value Problem”. In: *J. Math. Phys.* **13**.125-130 (1972).

[226] N. Ó Murchadha and J. W. York Jr. “Initial-Value Problem of General Relativity. I. General Formulation and Physical Interpretation”. In: *Phys. Rev. D* **10**.428-436 (1974).

[227] J. W. York Jr. “Conformal “Thin-Sandwich" Data for the Initial-Value Problem of General Relativity”. In: *Phys. Rev. Lett.* **82**.1350-1353 (1999).

[228] H. P. Pfeiffer and J. W. York Jr. “Extrinsic Curvature and the Einstein Constraints”. In: *Phys. Rev. D* **67**.044022 (2003).

[229] G. B. Cook. “Initial Data for Numerical Relativity”. In: *Living Rev. Rel.* **3**.5 (2000).

[230] H. P. Pfeiffer. “The Initial Value Problem in Numerical Relativity”. In: *Proc. Miami Waves Conf.* (2004).

[231] R. Bartnik and J. Isenberg. “The Constraint Equations”. In: *50 Years of the Cauchy Problem, in honour of Y. Choquet-Bruhat* 1 [232] (2004).

[232] P. T. Chruciel and H. Friedrich. “The Einstein Equations and the Large Scale Behaviour of Gravitational Fields-50 Years of the Cauchy Problem in General Relativity”. In: *Birkhäuser Verlag, Basel* (2004).

[233] J. W. York Jr. “Gravitational Degrees of Freedom and the Initial-Value Problem”. In: *Phys. Rev. Lett.* **26**.1656-1658 (1971).

[234] J. W. York Jr. “Role of Conformal Three-Geometry in the Dynamics of Gravitation”. In: *Phys. Rev. Lett.* **28**.1082-1085 (1972).

[235] E. Cotton. “Sur Les Variétés à Trois Dimensions”. In: *Annales de la Faculté des Sciences de Toulouse Sèr. 2* **1**.385 (1899).

[236] J. W. York Jr. "Covariant Decompositions of Symmetric Tensors in the Theory of Gravitation". In: *Ann. Inst. Henri Poincaré A* **21**.319-332 (1974).

[237] M. Cantor. "Some Problems of Global Analysis on Asymptotically Simple Manifolds". In: *Composition Mathematica* **38**.3-35 (1979).

[238] L. Smarr and J. W. York Jr. "Radiation Gauge in General Relativity". In: *Phys. Rev. D* **17**.1945-1956 (1978).

[239] Y. Choquet-Bruhat, J. Isenberg, and J. W. York Jr. "Einstein Constraints on Asymptotically Euclidean Manifolds". In: *Phys. Rev. D* **61**.084034 (2000).

[240] M. Cantor. "The Existence of Non-Trivial Asymptotically Flat Initial Data for Vacuum Spacetimes". In: *Commun. Math. Phys.* **57**.83-96 (1977).

[241] J. Isenberg. "Constant Mean Curvature Solutions of the Einstein Constraint Equations on Closed Manifolds". In: *Class. Quantum Grav.* **12**.2249-2274 (1995).

[242] Y. Choquet-Bruhat and J. W. York Jr. "The Cauchy Problem". In: *General Relativity and Gravitation, One Hundred Years after the Birth of Albert Einstein, edited by A. Held, Plenum Press* **1**.88 (1980).

[243] D. Maxwell. "Solutions of the Einstein Constraint Equations with Apparent Horizon Boundaries". In: *Commun. Math. Phys.* **253**.561-583 (2004).

[244] M. Alcubierre. "The Status of Numerical Relativity". In: *Gen. Rel. Grav., Proc. 17th Int. Conf., World Scientific* (2005).

[245] L. Smarr and J. W. York Jr. "Kinematical Conditions in the Construction of Spacetime". In: *Phys. Rev. D* **17**.2529-2551 (1978).

[246] L. Lehner. "Numerical Relativity: A Review". In: *Class. Quantum Grav.* **18**.R25-R86 (2001).

[247] T. W. Baumgarte and S. L. Shapiro. "Numerical Relativity and Compact Binaries". In: *Phys. Rep.* **376**.41-131 (2003).

[248] K. Martel and E. Poisson. "Regular Coordinate Systems for Schwarzschild and Other Spherical Spacetimes". In: *Amer. J. Phys.* **69**.476-480 (2001).

[249] S. L. Shapiro and S. A. Teukolsky. "Collisions of Relativistic Clusters and the Formation of Black Holes". In: *Phys. Rev. D* **45**.2739-2750 (1992).

[250] R. Beig and N. Ó Murchadha. "Late Time Behaviour of the Maximal Slicing the Schwarzschild Black Hole". In: *Phys. Rev. D* **57**.4728-4737 (1998).

[251] B. L. Reinhat. "Maximal Foliations of Extended Schwarzschild Space". In: *J. Math. Phys.* **14**.719 (1973).

[252] F. Estabrook et al. "Maximally Slicing a Black Hole". In: *Phys. Rev. D* **7**.2814-2817 (1973).

[253] B. Reimann and B. Brügmann. “Maximal Slicing for Puncture Evolutions of Schwarzschild and Reissner-Nordström Black Holes”. In: *Phys. Rev. D* **69**.044006 (2004).

[254] R. Beig. “The Maximal Slicing of a Schwarzschild Black Hole”. In: *Ann. Phys.* **11**.507-510 (2000).

[255] C. R. Evans. “An Approach for Calculating Axisymmetric Gravitational Collapse”. In: *Dynamical Spacetime and Numerical Relativity, Cambridge University Press* **3** (1986).

[256] L. Smarr. “Gauge Conditions, Radiation Formulae and the Two Black Hole Collision”. In: *Sources of Gravitational Radiation, Cambridge University Press* (1979).

[257] R. F. Stark and T. Piran. “Gravitational-Wave Emission from Rotating Gravitational Collapse”. In: *Phys. Rev. Lett.* **55**.891-894 Erratum [393] (1985).

[258] B. DeWitt L. Smarr A. Čadež and K. Eppley. “Collision of Two Black Holes: Theoretical Framework”. In: *Phys. Rev. D* **14**.2443-2452 (1976).

[259] T. Nakamura. “General Relativistic Collapse of Axially Symmetric Stars Leading to the Formation of Rotating Black Holes”. In: *Prog. Theor. Phys.* **65**.1876-1890 (1981).

[260] T. Nakamura and H. Sato. “General Relativistic Collapse of Rotating Supermassive Stars”. In: *Prog. Theor. Phys.* **66**.2038-2051 (1981).

[261] J. M. Bardeen and T. Piran. “General Relativistic Axisymmetric Rotating Systems: Coordinates and Equations”. In: *Phys. Rep.* **96**.205-250 (1983).

[262] B. Brügmann. “Binary Black Hole Mergers in 3D Numerical Relativity”. In: *Int. J. Mod. Phys. D* **8**.85-100 (1999).

[263] M. Shibata. “3D Numerical Simulations of Black Hole Formation Using Collisionless Particles: Triplane Symmetric Case”. In: *Prog. Theor. Phys.* **101**.251-282 (1999).

[264] M. Shibata and K. Uryū. “Simulation of Merging Binary Neutron Stars in Full General Relativity: $\Gamma = 2$ Case”. In: *Phys. Rev. D* **61**.064001 (2000).

[265] M. Shibata. “Fully General Relativistic Simulation of Coalescing Binary Neutron Stars: Preparatory Tests”. In: *Phys. Rev. D* **60**.104052 (1999).

[266] M. Shibata. “Axisymmetric General Relativistic Hydrodynamics: Long-Term Evolution of Neutron Stars and Stellar Collapse to Neutron Stars and Black Holes”. In: *Phys. Rev. D* **67**.024033 (2003).

[267] M. Shibata, K. Taniguchi, and K. Uryū. “Merger of Binary Neutron Stars of Unequal Mass in Full General Relativity”. In: *Phys. Rev. D* **68**.084020 (2003).

[268] Y. Sekiguchi and M. Shibata. "Axisymmetric Collapse Simulations of Rotating Massive Stellar Cores in Full General Relativity: Numerical Study for Prompt Black Hole Formation". In: *Phys. Rev. D* **71**.084013 (2005).

[269] M. Shibata, K. Taniguchi, and K. Uryū. "Merger of Binary Neutron Stars with Realistic Equations of State in Full General Relativity". In: *Phys. Rev. D* **71**.084021 (2005).

[270] M. Shibata and K. Uryū. "Gravitational Waves from the Merger of Binary Neutron Stars in a Fully General Relativistic Simulation". In: *Prog. Theor. Phys.* **107**.265-303 (2002).

[271] M. Shibata. "Collapse of Rotating Supermassive Neutron Stars to Black Holes: Fully General Relativistic Simulations". In: *Astrophys. J.* **595**.992-999 (2003).

[272] M. Shibata and K. Taniguchi. "Merger of Binary Neutron Stars to a Black Hole: Disk Mass, Short Gamma-Ray Bursts, and Quasinormal Mode Ringing". In: *Phys. Rev. D* **73**.064027 (2006).

[273] M. Shibata and Y. Sekiguchi. "Three-Dimensional Simulations of Stellar Core Collapse in Full General Relativity: Nonaxisymmetric Dynamical Instabilities". In: *Phys. Rev. D* **71**.024014 (2005).

[274] T. De Donder. "La Gravifique Einsteinienne". In: *Gauthier-Villars, Paris* (1921).

[275] Y. Choquet-Bruhat and T. Ruggeri. "Hyperbolicity of the 3+1 System of Einstein Equations". In: *Commun. Math. Phys.* **89**.269-275 (1983).

[276] C. Bona and J. Massó. "Harmonic Synchronizations of Spacetime". In: *Phys. Rev. D* **38**.2419-2422 (1988).

[277] O. A. Reula. "Hyperbolic Methods for Einstein's Equations". In: *Living Rev. Rel.* **1**.3 (1998).

[278] G. B. Cook and M. A. Scheel. "Well-Behaved Harmonic Time Slices of a Charged, Rotating, Boosted Black Hole". In: *Phys. Rev. D* **56**.4775-4781 (1997).

[279] G. B. Cook et al. "New Formalism for Numerical Relativity". In: *Phys. Rev. Lett.* **75**.600-603 (1995).

[280] P. Anninos et al. "Three-Dimensional Numerical Relativity: The Evolution of Black Holes". In: *Phys. Rev. D* **52**.2059-2082 (1995).

[281] C. Bona et al. "First Order Hyperbolic Formalism for Numerical Relativity". In: *Phys. Rev. D* **56**.3405-3415 (1997).

[282] D. H. Bernstein. "A Numerical Study of the Black Hole Plus Brill Wave Spacetime". In: *Ph.D Thesis, University of Illinois at Urbana-Champaign* (1993).

[283] F. Herrmann et al. "Unequal Mass Binary Black Hole Plunges and Gravitational Recoil". In: *Class. Quantum Grav.* **24**.S33-S42 (2007).

[284] M. Campanelli, C. O. Lousto, and Y. Zlochower. "Last Orbit of Binary Black Holes". In: *Phys. Rev. D* **73**.061501(R) (2006).

[285] M. Campanelli, C. O. Lousto, and Y. Zlochower. "Spin-Orbit Interactions in Black-Hole Binaries". In: *Phys. Rev. D* **74**.084023 (2006).

[286] B. Brügmann et al. "Calibration of Moving Puncture Simulations". In: *Phys. Rev. D* **77**.024027 (2008).

[287] J. G. Baker et al. "Binary Black Hole Merger Dynamics and Waveforms". In: *Phys. Rev. D* **73**.104002 (2006).

[288] J. R. van Meter et al. "How to Move a Black Hole without Excision: Gauge Conditions for the Numerical Evolution of a Moving Puncture". In: *Phys. Rev. D* **73**.124011 (2006).

[289] P. Diener et al. "Accurate Evolution of Orbiting Binary Black Holes". In: *Phys. Rev. Lett.* **96**.121101 (2006).

[290] J. A. Font et al. "Three-Dimensional Numerical General Relativistic Hydrodynamics. II. Long-Term Dynamics of Single Relativistic Stars". In: *Phys. Rev. D* **65**.084024 (2002).

[291] F. Herrmann et al. "Gravitational Recoil from Spinning Binary Black Hole Mergers". In: *Astrophys. J.* **661**.430-436 (2007).

[292] U. Sperhake. "Binary Black-Hole Evolutions of Excision and Puncture Data". In: *Phys. Rev. D* **76**.104015 (2007).

[293] J. G. Baker et al. "Gravitational-Wave Extraction from an Inspiraling Configuration of Merging Black Holes". In: *Phys. Rev. Lett.* **96**.111102 (2006).

[294] M. Campanelli, C. O. Lousto, and Y. Zlochower. "Spinning-Black-Hole Binaries: The Orbital Hang-up". In: *Phys. Rev. D* **74**.041501(R) (2006).

[295] P. Marronetti et al. "Binary Black Holes on a Budget: Simulations Using Workstations". In: *Class. Quantum Grav.* **24**.S43-S58 (2007).

[296] L. Baiotti and L. Rezzolla. "Challenging the Paradigm of Singularity Excision in Gravitational Collapse". In: *Phys. Rev. Lett.* **97**.141101 (2006).

[297] L. Baiotti et al. "Three-Dimensional Relativistic Simulations of Rotating Neutron-Star Collapse to a Kerr Black Hole". In: *Phys. Rev. D* **71**.024035 (2005).

[298] L. Baiotti et al. "Gravitational-Wave Emission from Rotating Gravitational Collapse in Three Dimensions". In: *Phys. Rev. Lett.* **94**.131101 (2005).

[299] M. Shibata and T. Nakamura. "Conformal Time Slicing Condition in Three Dimensional Numerical Relativity". In: *Prog. Theor. Phys.* **88**.317 (1992).

[300] T. Piran. "Methods of Numerical Relativity". In: *Rayonnement gravitationnel/Gravitation Radiation, edited by N. Deruelle and T. Piran, North Holland, Amsterdam* **203** (1983).

[301] M. Alcubierre et al. "3D Grazing Collision of Two Black Holes". In: *Phys. Rev. Lett.* **87**.271103 (2001).

[302] É. Gourgoulhon and J. L. Jaramillo. "A 3+1 Perspective on Null Hypersurfaces and Isolated Horizons". In: *Phys. Rep.* **423**.159-294 (2006).

[303] K. Oohara, T. Nakamura, and M. Shibata. "A Way to 3D Numerical Relativity". In: *Prog. Theor. Phys. Suppl.* **128**.183-249 (1997).

[304] M. Shibata. "Fully General Relativistic Simulation of Merging Binary Clusters: Spatial Gauge Condition". In: *Prog. Theor. Phys.* **101**.1199-1233 (1999).

[305] M. Shibata, T. W. Baumgarte, and S. L. Shapiro. "Stability and Collapse of Rapidly Rotating, Supermassive Neutron Stars: 3D Simulations in General Relativity". In: *Phys. Rev. D* **61**.044012 (2000).

[306] M. Shibata, T. W. Baumgarte, and S. L. Shapiro. "The Bar-Mode Instability in Differentially Rotating Neutron Stars: Simulations in Full General Relativity". In: *Astrophys. J.* **542**.453-463 (2000).

[307] M. Alcubierre and B. Brügmann. "Simple Excision of a Black Hole in 3+1 Numerical Relativity". In: *Phys. Rev. D* **63**.104006 (2001).

[308] L. Lindblom and M. A. Scheel. "Dynamical Gauge Conditions for the Einstein Evolution Equations". In: *Phys. Rev. D* **67**.124005 (2003).

[309] C. Bona, L. Lehner, and C. Palenzuela-Luque. "Geometrically Motivated Hyperbolic Coordinate Conditions for Numerical Relativity: Analysis, Issues and Implementations". In: *Phys. Rev. D* **72**.104009 (2005).

[310] M. Alcubierre et al. "Black Hole Excision for Dynamic Black Holes". In: *Phys. Rev. D* **64**.061501(R) (2001).

[311] B. Brügmann, W. Tichy, and N. Jansen. "Numerical Simulation of Orbiting Black Holes". In: *Phys. Rev. D* **92**.211101 (2004).

[312] L. Lehner and O. Reula. "Status Quo and Open Problems in the Numerical Construction of Spacetimes". In: *The Einstein Equations and the Large Scale Behavior of Gravitational Fields* [232].205-229 (2004).

[313] J. M. Stewart. "The Cauchy Problem and the Initial Boundary Value Problem in Numerical Relativity". In: *Class. Quantum Grav.* **15**.2865-2889 (1998).

[314] H. Friedrich and A. D. Rendall. "The Cauchy Problem for the Einstein Equations". In: *Einstein's Field Equations and Their Physical Implications: Selected Essays in Honour of Jürgen Ehlers, Lect. Notes Phys.* **540**.127-224 (2000).

[315] H. Shinkai and G. Yoneda. "Re-Formulating the Einstein Equations for Stable Numerical Simulations: Formulation Problem in Numerical Relativity". In: *Part of Prog. Astron. Astrophys., Nova Science Publication* (2003).

[316] H. Shinkai. "Introduction to Numerical Relativity". In: *Lect. Notes for APCTP Winter School on Gravitation and Cosmology, Korea* (2003).

[317] A. M. Abrahams et al. “Solving Einstein’s Equations for Rotating Spacetimes: Evolution of Relativistic Star Clusters”. In: *Phys. Rev. D* **49**.5153 (1994).

[318] C. R. Evans. “Enforcing the Momentum Constraints during Axisymmetric Spacelike Simulations”. In: *Frontiers in Numerical Relativity, edited by C. R. Evans, L. S. Finn, and D. W. Hobill, Cambridge University Press* (1989).

[319] M. Anderson and R. A. Matzner. “Extended Lifetime in Computational Evolution of Isolated Black Holes”. In: *Found. Phys.* **35**.1477-1495 (2005).

[320] M. W. Choptuik et al. “An Axisymmetric Gravitational Collapse Code”. In: *Class. Quantum Grav.* **20**.1857-1878 (2003).

[321] S. Frittelli. “Note on the Propagation of the Constraints in Standard 3+1 General Relativity”. In: *Phys. Rev. D* **55**.5992-5996 (1997).

[322] H. Beyer and O. Sarbach. “Well-Posedness of the Baumgarte-Shapiro-Shibata-Nakamura Formulation of Einstein’s field Equations”. In: *Phys. Rev. D* **70**.104004 (2004).

[323] L. E. Kidder et al. “Boundary Conditions for the Einstein Evolution System”. In: *Phys. Rev. D* **71**.064020 (2005).

[324] O. Sarbach and M. Tiglio. “Boundary Conditions for Einstein’s Field Equations: Mathematical and Numerical Analysis”. In: *J. Hyper. Diff. Equ.* **2**.839-883 (2005).

[325] O. Reula. “Strong Hyperbolicity”. In: *Lect. at the VII Mexican School on Grav. and Math. Phys.* (2006).

[326] L. E. Kidder, M. A. Scheel, and S. A. Teukolsky. “Extending the Lifetime of 3D Black Hole Computations with a New Hyperbolic System of Evolution Equations”. In: *Phys. Rev. D* **64**.064017 (2001).

[327] S. Frittelli and O. A. Reula. “First-Order Symmetric Hyperbolic Einstein Equations with Arbitrary Fixed Gauge”. In: *Phys. Rev. Lett.* **76**.4667-4670 (1996).

[328] A. Anderson and J. W. York Jr. “Fixing Einstein’s Equations”. In: *Phys. Rev. Lett.* **82**.4384-4387 (1999).

[329] C. Gundlach and J. M. Martín-García. “Well-Posedness of Formulations of the Einstein Equations with Dynamical Lapse and Shift Conditions”. In: *Phys. Rev. D* **74**.024061 (2006).

[330] H. Friedrich. “On the Hyperbolicity of Einstein’s and Other Gauge Field Equations”. In: *Commun. Math. Phys.* **100**.525-543 (1985).

[331] F. Pretorius. “Numerical Relativity Using a Generalized Harmonic Decomposition”. In: *Class. Quantum Grav.* **22**.425-451 (2005).

[332] D. Garfinkle. “Harmonic Coordinate Method for Simulating Generic Singularities”. In: *Phys. Rev. D* **65**.044029 (2002).

[333] C. Gundlach et al. “Constraint Damping in the Z4 Formulation and Harmonic Gauge”. In: *Class. Quantum Grav.* **22**.3767-3773 (2005).

[334] L. Lindblom et al. “A New Generalized Harmonic Evolution System”. In: *Class. Quantum Grav.* **23**.S447-S462 (2006).

[335] *A. Collette*. URL: `https://www.h5py.org/`.

[336] URL: `https://www.hdfgroup.org/downloads/hdfview/`.

[337] G. Bozzola. “Kuibit: Analyzing Einstein Toolkit Simulations with Python”. In: *J. Open Source Sof.* **6**.60 (2021).

[338] T. H. Colding and W. P. Minicozzi II. “Level Set Method for Motion by Mean Curvature”. In: *Not. Amer. Math. Soc.* **63**.1148-1153 (2016).

[339] T. W. Baumgarte and S. L Shapiro. “Numerical Relativity: Solving Einstein’s Equations on the Computer”. In: *Cambrdge University Press* (2013).

[340] Z. Younsi and K. Wu. “Covariant Compton Scattering Kernel in General Relativistic Radiative Transfer”. In: *Mon. Not. R. Astron. Soc.* **433**.1054-1081 (2013).

[341] R. W. Lindquist. “Relativistic Transport Theory”. In: *Ann. Phys.* **37**.487-518 (1966).

[342] K. Destounis, A. G. Suvorov, and K. D. Kokkotas. “Gravitational Wave Glitches in Chaotic Extreme-Mass-Ratio Inspirals”. In: *Phys. Rev. D* **126**.141102 (2021).

[343] K. Hashimoto and K. Sugiura. “Causality Bounds Chaos in Geodesic Motion”. In: *Phys. Rev. D* **107**.066005 (2023).

[344] J. R. Clough and T. S. Evans. “Embedding Graphs in Lorentzian Spacetime”. In: *PLoS ONE* **12**.e0187301 (2017).

[345] A. Sim et al. “Directed Graph Embeddings in Pseudo-Riemannian Manifolds”. In: *Proc. of the 38th Int. Conf. on Machine Learning* **139** (2021).

[346] C. Liang and B. Zhou. “Introduction to Differential Geometry and General Relativity”. In: *Second Edition, Volume 2, NFAPST, Science Press of China* (2006).

[347] B. O’Neill. “Semi-Riemannian Geometry with Applications to Relativity”. In: *Pure Appl. Math.* **103** (1983).

[348] H. L. Bray. “Black Holes, Geometric Flow, and the Penrose Inequality in General Relativity”. In: *Not. Amer. Math. Soc.* **49**.1372-1381 (2002).

[349] A. Harten et al. “Uniformly High Order Accurate Essentially Non-Oscillatory Schemes, III”. In: *J. Comput. Phys.* **71**.231-303 (1987).

[350] A. Harten et al. “Uniformly High Order Accurate Essentially Non-Oscillatory Schemes, III”. In: *J. Comput. Phys.* **131**.3-47 (1997).

[351] M. G. Crandall and P. L. Lions. “Two Approximations of Solutions of Hamilton-Jacobi Equations”. In: *Math. Comput.* **43**.1-19 (1984).

[352] S. K. Godunov and I. O. Bohachevsky. “Finite Difference Method for Numerical Computation of Discontinuous Solutions of the Equations of Fluid Dynamics”. In: *Mat. Sb.* **47**.357-393 (1959).

[353] M. Bardi and S. Osher. “The Nonconvex Multidimensional Riemann Problem for Hamilton-Jacobi Equations”. In: *J. Math. Anal.* **22**.344-351 (1991).

[354] É. Gourgoulhon S. Bonazzola and, P. Grandclément, and J. Novak. “Constrained Schemes for the Einstein Equations Based on the Dirac Gauge and Spherical Coordinates”. In: *Phys. Rev. D* **70**.104007 (2004).

[355] R. De Vogelaere. “Methods of Integration Which Preserve the Contact Transformation Property of the Hamiltonian Equations”. In: *Rep. No. 4, Dept. Math., University of Notre Dame* (1956).

[356] R. D. Ruth. “A Canonical Integration Technique”. In: *Trans. Nucl. Sci.* **30**.2669-2671 (1983).

[357] K. Feng. “On Difference Schemes and Symplectic Geometry”. In: *Proc. 5th Int., Symposium on the Differential Geometry & Differential Equations, Beijing* 42-58 (1985).

[358] Y. Nambu. “Quark Model and the Factorization of the Veneziano Amplitude”. In: *Symmetries and Quark Models: Proc. Int. Conf., Wayne State University, Detroit, Michigan, World Scientific* 269-277 (1970).

[359] P. B. Bochev and C. Scovel. “On Quadratic Invariants and Symplectic Structure”. In: *BIT Numer. Math.* **34**.337-345 (1994).

[360] G. J. Cooper. “Stability of Runge-Kutta Methods for Trajectory Problems”. In: *J. Numer. Anal.* **7**.1-13 (1987).

[361] F. M. Lasagne. “Canonical Runge-Kutta Methods”. In: *Z. Angew. Math. Phys.* **39**.952-953 (1988).

[362] J. M. Sanz-Serna. “Runge-Kutta Schemes for Hamiltonian Systems”. In: *BIT Numer. Math.* **28**.877-883 (1987).

[363] Y. B. Suris. “On the Conservation of the Symplectic Structure in the Numerical Solution of Hamiltonian Systems”. In: *Numerical Solution of Ordinary Differential Equations, edited by S. S. Filippov, Keldysh Inst. Appl. Math., USSR Acad. of Sci., Moscow, Russia* 148-160 (1988).

[364] K. Feng. “Difference Schemes for Hamiltonian Formalism and Symplectic Geometry”. In: *J. Comput. Math.* **4**.279-289 (1986).

[365] P. J. Channell and J. C. Scovel. “Symplectic Integration of Hamiltonian Systems”. In: *Nonlinearity* **3**.231-259 (1990).

[366] R. F. Baierlein, D. H. Sharp, and J. A. Wheeler. “Three-Dimensional Geometry as Carrier of Information about Time”. In: *Phys. Rev.* **126**.1864-1865 (1962).

[367] J. A. Wheeler. “Geometrodynamics and the Issue of the Final State”. In: *Rel., Groups and Topology, edited by C. DeWitt and B. S. DeWitt, Gordon and Breach, New York* **126**.317-522 (1964).

[368] R. Bartnik and G. Fodor. “On the Restricted Validity of the Thin Sandwich Conjecture”. In: *Phys. Rev. D* **48**.3596-3599 (1993).

[369] H. P. Pfeiffer and J. W. York Jr. “Uniqueness and Nonuniqueness in the Einstein Constraints”. In: *Phys. Rev. Lett.* **95**.091101 (2005).

[370] T. W. Baumgarte, N. Ó Murchadha, and H. P. Pfeiffer. “Einstein Constraints: Uniqueness and Nonuniqueness in the Conformal Thin Sandwich Approach”. In: *Phys. Rev. D* **75**.044009 (2007).

[371] S. A. Teukolsky. “Linearized Quadrupole Waves in General Relativity and the Motion of Test Particles”. In: *Phys. Rev. D* **26**.745-750 (1982).

[372] D. M. Walsh. “Non-Uniqueness in Conformal Formulations of the Einstein Constraints”. In: *Class. Quantum Grav.* **24**.1911-1926 (2007).

[373] J. W. York Jr. “Velocities and Momenta in an Extended Elliptic Form of the Initial Value Conditions”. In: *Il Nuovo Cim. B* **119**.823-837 (2004).

[374] P. Grandclément, É. Gourgoulhon, and S. Bonazzola. “Binary Black Holes in Circular Orbits. II. Numerical Methods and First Results”. In: *Phys. Rev. D* **65**.044021 (2002).

[375] T. Damour, É. Gopurgoulhon, and P. Grandclément. “Circular Orbits of Coratating Binary Black Holes: Comparison between Analytical and Numerical Results”. In: *Phys. Rev. D* **66**.024007 (2002).

[376] P. Laguna. “Conformal-Thin-Sandwich Initial Data for a Single Boosted or Spinning Black Hole Puncture”. In: *Phys. Rev. D* **69**.104020 (2004).

[377] L. Andersson and V. Moncrief. “Elliptic-Hyperbolic Systems and the Einstein Equations”. In: *Ann. Henri Poincaré* **4**.1-34 (2003).

[378] A. Čadež. “Some Remarks on the Two-Body-Problem in Geometrodynamics”. In: *Ann. Phys.* **91**.58-74 (1975).

[379] M. Alcubierre et al. “Generalized Harmonic Spatial Coordinates and Hyperbolic Shift Conditions”. In: *Phys. Rev. D* **72**.124018 (2005).

[380] M. Shibata, K. Uryū, and J. L. Friedman. “Deriving Formulations for Numerical Computation of Binary Neutron Stars in Quasicircular Orbits”. In: *Phys. Rev. D* **70**.044044 Erratum [394] (2004).

[381] L.-M. Lin and J. Novak. “Rotating Star Initial Data for a Constrained Scheme in Numerical Relativity”. In: *Class. Quantum Grav.* **23**.4545-4561 (2006).

[382] K. Uryū et al. “Binary Neutron Stars: Equilibrium Models beyond Spatial Conformal Flatness”. In: *Phys. Rev. Lett.* **97**.171101 (2006).

[383] A. Ashtekar. “Asymptotic Structure of the Gravitational Field at Spatial Infinity”. In: *Gen. Rel. Grav.* **2**.37, edited by A. Held (1980).

[384] J. Haantjes. "Conformal Representations for an $n$-Dimensional Euclidean Space with a Non-Definite Fundamental Form on Itself". In: *Proc. Kon. Ned. Akad.* **40**.700 (1937).

[385] R. Penrose. "Asymptotic Properties of Fields and Space-Times". In: *Phys. Rev. Lett.* **10**.66-68 (1963).

[386] T. Fulton, F. Rohrlich, and L. Witten. "Conformal Invariance in Physics". In: *Rev. Mod. Phys.* **34**.442-457 (1962).

[387] J. Ehlers. "Isolated Systems in General Relativity". In: *Texas Symposium on Relativistic Astrophysics, 9th, Munich, West Germany, December 14-19, 1978, Proc.* **A80**.279-294 (1980).

[388] A. Ashtekar and R. O. Hansen. "A Unified Treatment of Null and Spatial Infinity in General Relativity. I. Universal Structure, Asymptotic Symmetries, and Conserved Quantities at Spatial Infinity". In: *J. Math. Phys.* **19**.1542-1566 (1978).

[389] C.-B. Liang and B. Zhou. "Introduction to Differential Geometry and General Relativity". In: *Second Edition, Volume 3, NFAPST, Science Press of China* (2006).

[390] R. Penrose. "Zero Rest-Mass Fields Including Gravitation: Asymptotic Behaviour". In: *Proc. R. Soc. Lond. A* **284**.159 (1965).

[391] J.-P. Nicolas. "The Conformal Approach to Asymptotic Analysis". In: *arXiv: 1508.02592 [gr-qc]* (2015).

[392] J. Frauendiener. "Conformal Infinity". In: *Living Rev. Rel.* **3**.4 (2000).

[393] R. F. Stark and T. Piran. "Gravitational-Wave Emission from Rotating Gravitational Collapse". In: *Phys. Rev. Lett.* **56**.97-97 (1986).

[394] M. Shibata, K. Uryū, and J. L. Friedman. "Deriving Formulations for Numerical Computation of Binary Neutron Stars in Quasicircular Orbits". In: *Phys. Rev. D* **70**.129901 (2004).